ISSN — 0132 — 1447

BULLETIN

OF THE GEORGIAN ACADEMY
OF SCIENCES

საქართველოს
მეცნიერებათა აკადემიის

მოამბე

VOLUME 159, NUMBER 2
MARCH-APRIL
1999

TBILISI
თბილისი

The Journal is founded in 1940

BULLETIN

OF THE GEORGIAN ACADEMY OF SCIENCES

is a scientific journal, issued bimonthly in
Georgian and English languages

Editorial Office:
Georgian Academy of Sciences
52, Rustaveli Avenue,
Tbilisi, 380008,
Republic of Georgia

Telephone : **+ 995 32 99.75.93**
Fax : **+ 995 32 99.88.23**
E-mail : **BULLETIN@PRESID.ACNET.GE**

CONTENTS

MATHEMATICS

MECHANICS

PHYSICS

საქართველოს მეცნიერებათა აკადემიის მოამბე, 159, №2, 1999
BULLETIN OF THE GEORGIAN ACADEMY OF SCIENCES, 159, №2, 1999

MATHEMATICS

Corr. Member of the Academy V. Kokilashvili, V. Paatashvili

On the Dirichlet and Neumann Problems in the Domains with Piecewise Smooth Boundaries

Presented March 9, 1998

ABSTRACT. **The Dirichlet and Neumann problems are investigated in the domains with piecewise smooth boundaries involving the cusps. The complete picture of solvability in certain setting of the problem is given and explicit formulas for the solutions are presented.**

Key words: Dirichlet and Neumann problems, piecewise smooth boundaries, Smirnov class, singular integral, Cauchy type integral, conformal mapping.

In our recent papers the Dirichlet and Neumann problems were investigated for certain classes of harmonic functions in the domains with piecewise Liapunov boundaries without zero cusps [1,2]. Now we present the results in more general case in which the above mentioned problems are solved in the domains with arbitrary piecewise smooth boundaries. The whole picture of solvability is drawn, the explicit formulas for the solution by means of the Cauchy type integrals, and conformal mapping functions are deduced. When the boundary involves arbitrary cusps there arise new difficulties. Nevertheless, here we show a comprehensive influence of the boundary geometry on the solvability.

Let G be a simply connected, finite domain in the complex plane C. Let $z = z(w)$ be a conformal mapping of $U = \{w : |w| < 1\}$ onto G such that $z(0) = z_0$, $z_0 \in G$, $z'(0) > 0$. Let $w = w(z)$ be an inverse to $z = z(w)$ function. The boundary Γ of G is assumed to be represented in the form $\Gamma = \bigcup_k \Gamma_k$, where Γ_k are non-intersecting smooth arcs meeting at the points t_k ($k = 1, 2,\ldots,n$) and forming (inner with respect to G) angles with values $\nu_k\pi$, $0 \le \nu_k \le 2$. We denote a set of such curves by $C^{1,\nu_1,\ldots,\nu_n}_{t_1,t_2,\ldots,t_n}$.

In [3] it was stated that if $\Gamma \in C^{1,\nu_1,\ldots,\nu_n}_{t_1,t_2,\ldots,t_n}$, then

$$z'(w) = \prod_{k=1}^{n} (w - w(t_k))^{\nu_k - 1} z_0(w), \qquad z_0(w) = \exp\left(\frac{1}{\pi}\int_\gamma \frac{\beta(\tau)d\tau}{\tau - w}\right), \tag{1}$$

$\gamma = \{\tau : |\tau| = 1\}$ and β is a function continuous on γ.

By $E^p(G)$, ($p > 0$) we denote the Smirnov class of analytic functions. It is clear that $E^p(U)$ coincides with the Hardy H^p class.

Consider the following classes of harmonic functions:

$$e_p(G)=\{u: u=\operatorname{Re}\Phi, \Phi\in E^p(G)\},$$

$$e'_p(G)=\{n: \Delta u=0,\ \sup_{\rho<r<1}\int_{\Gamma_r}\left(\left|\frac{\partial u}{\partial x}\right|^p+\left|\frac{\partial u}{\partial y}\right|^p\right)|dz|<\infty,\ z=x+iy\}. \tag{2}$$

It is well-known that any function $u\in e^p(G)$ possesses almost everywhere on Γ angular boundary values u^+ belonging to $L^p(\Gamma)$. The functions from $e'_p(G)$ are continuous on the closure of G, absolutely continuous on Γ and the functions $\frac{\partial u}{\partial x}$, $\frac{\partial u}{\partial y}$ have angular boundary values $\left(\frac{\partial u}{\partial x}\right)^+$, $\left(\frac{\partial u}{\partial y}\right)^+$ belonging to $L^p(\Gamma)$.

Let

$$\left(\frac{\partial u}{\partial n}\right)_\Gamma=\left(\frac{\partial u}{\partial x}\right)^+\cos(n,x)+\left(\frac{\partial u}{\partial y}\right)^+\cos(n,y)=\left(\frac{\partial u}{\partial x}\right)^+(-\sin\alpha(t))+\left(\frac{\partial u}{\partial y}\right)^+\cos\alpha(t),$$

where (n, x) and (n, y) are the angles between the normal to Γ at the point t and the coordinate axis, $\alpha(t)$ is the angle between the tangent line at t and the real axis.

Let us introduce the following notations

$$\alpha(\tau)=\exp\left(-\frac{\pi i}{p}\right)\exp\left(-2i\left(\frac{\nu}{p}+\frac{\alpha(ze^{i\theta})}{p'}\right)\right),\ \theta\in[0,2\pi],\ \tau=\exp i\theta,\ p>1,$$

$$p'=\frac{p}{p-1},\ \varphi_1(\tau)=\frac{\nu-1}{p}\vartheta_{c_0}(\tau),\ \varphi_2(\tau)=2\vartheta_{\tau_0}(\tau),\ \varphi_0=\varphi_1-\varphi_2,\ \tau_0\in\gamma,$$

where ϑ_{c_0} and ϑ_{τ_0} are continuous branches of $arg\,\tau$ on the sets $\gamma\backslash\{c_0\}$ and $\gamma\backslash\{\tau_0\}$, respectively, and $c_0=\omega(t_0)$, t_0 is a fixed point on Γ and $\tau_0\neq c_0$.

Let us consider the following problems: the Dirichlet problem

$$\Delta u=0,\ u\in e_p(G),\ p>1,\ u^+=f,\ f\in L^p(\Gamma) \tag{D}$$

and the Neumann problem

$$\Delta u=0,\ u\in e'_p(G),\ p>1,\ \left(\frac{\partial u}{\partial n}\right)_\Gamma=f,\ f\in L^p(\Gamma) \tag{N}$$

When $f\equiv 0$, these problems will be called the (D_0) and (N_0) problems, respectively.

Theorem 1. *If a finite simply connected domain G bounded by the curve Γ from the class $C^{1,\nu_1,\dots,\nu_n}_{t_1,t_2,\dots,t_n}$, then the solutions of the (D_0) problem are expressed by the formula*

$$u_0(z)=\sum_{k,\nu_k\in(p,2]}N_k\operatorname{Re}\frac{w(t_k)+w(z)}{w(t_k)-w(z)}+\sum_{k,\nu_k=p}M_k(p)\operatorname{Re}\frac{w(t_k)+w(z)}{w(t_k)-w(z)}, \tag{3}$$

where N_k are arbitrary constants and

$$M_k(p)=\begin{cases}0, \ if \ \ \chi_k \notin H^p, \ \ \chi_k(w)=(w-w(t_k))^{-1}\sqrt[p]{z_0(w)} \\ arbitrary \ \ real \ constant \ if \ \ \chi_k \in H^p\end{cases}, \tag{4}$$

In general, the (D) problem is nonsolvable if Γ has the corner points from the set $\{0,p\}$. If

$$f(t)\ln\left|\prod_{k,\nu_k\in\{0,p\}}(w(t)-w(t_k))\right|\in L^p(\Gamma), \tag{5}$$

then the (D) problem is solvable. In all cases of solvability of the (D) problem the solution is given by the equality

$$u(z)=u_0(z)+u_f(z), \tag{6}$$

where u_0 is defined by formula (3), and

$$u_f(z)=\mathrm{Re}\left[\left(\frac{1}{2\pi}\int_\gamma\frac{f(z(\xi))p(\xi)}{\xi(\xi-w(z))}d\xi+\frac{(-1)^{n_1-n_2}}{2\pi i}\times\frac{\prod_{\nu_k\in(p,2]}t_k}{\prod_{k,\nu_k=0}t_k}\int_\gamma\frac{f(z(\xi))\overline{p}(\xi)}{\xi(\xi-w(z))}d\xi\right)\frac{1}{\rho(w(z))}\right] \tag{7}$$

$$\rho(w)=\prod_{k,\nu_k\in(p,2]}(w-w(t_k))\prod_{k,\nu_k=0}(w-w(t_k))^{-1}, \ \ \rho(w)\equiv 1,$$

if $\{\nu_k:\nu_k\in\{0\}\bigcup(p,2]\}=\varnothing$.

Theorem 2. *Let a finite simply connected domain G be bounded by the curve from the class $C^{1,\nu}_{t_0}$, $0\le\nu\le 2$, and*

$$\chi_{t_0}(w)=(w-\tau_0)^2\rho_p(w)\prod_{k=0}^{2}\exp\left(\frac{1}{2\pi i}\int_\gamma\frac{\varphi_k(\tau)}{\tau-w}d\tau\right), \ \ \tau_0\ne w(t_0), \ \tau_0\in\gamma, \tag{8}$$

$$\rho_p(w)=\begin{cases}1, & for \ \nu<p', \\ w-w(t_0), & for \ \nu\ge p'.\end{cases} \tag{9}$$

Then for the solvability of the (N) problem, it is necessary that

$$\int_\Gamma f(t)z_{t_0}(t)\omega^k(t)dt=0, \ \ k=0, \ k_p \tag{10}$$

where

$$z_{t_0} = \exp\left(\frac{1}{2\pi i}\int_\gamma \frac{\alpha(z(\tau))d\tau}{\tau - w(t)}\right)(w(t)-w(t_0))^{-\mu_p}(w(t)-\tau_0)^2 w'(t), \tag{11}$$

$$k_p = \begin{cases} 0 & if \quad \nu < p', \\ 1, & if \quad \nu \geq p'. \end{cases} \qquad \mu_p = \begin{cases} 0 & if \quad \nu < p', \\ 1, & if \quad \nu \geq p'. \end{cases}$$

If conditions (10) are satisfied, then the (N) problem is solvable for $\nu \notin \{0,2,p'\}$ or $\nu = 2$ and $p < 2$. When $\nu \in \{0,p'\}$ or $\nu = 2$ and $p \geq 2$, then this problem is in general nonsolvable. If together with (10) the condition

$$f(t)\ln|t - t_0| \in L^p(\Gamma)$$

is satisfied, then the (*N*) problem is solvable.

In the cases of solvability of the (N) problem the solution has the form

$$u(z) = \mathrm{Re}\left[\int_0^{w(z)} \Omega(\xi)d\xi\right] + M, \tag{12}$$

where the integral is taken over an arbitrary curve lying in U and connecting $w = 0$ with the point $w(z)$, M is an arbitrary constant, and

$$\Omega(w) = \frac{\chi_{t_0}(w)}{2\pi i}\int_\gamma \frac{g(\tau)}{\chi^+_{t_0}(\tau)}\frac{d\tau}{\tau - w}, \quad g(\tau) = -i\sqrt[p]{z'(\tau)}\exp(-i\alpha(z(\tau)))2f(z(\tau)). \tag{13}$$

the above investigated problem in the other setting has been considered in [4,5].

This work was supported by Grant 1.7/1998 of the Georgian Academy of Sciences.

Georgian Academy of Sciences
A. Razmadze Mathematical Institute

REFERENCES

1. *V. Kokilashvili, V. Paatashvili*. Georgian Math. J. **4**, 3, 1997, 279-302.
2. *V. Kokilashvili, V. Paatashvili*. Mem. Differential Equations Math.Phys. **12** ,1997, 114-121.
3. *G. Khuskivadze, V. Paatashvili*. Proc. A.Razmadze Math. Inst. **116**, 1998, 123-132.
4. *V. G. Mazy'a, A. A. Soloviev*. Atti della Acad. Naz. de Lincei, Mat. and Appl. Ser. IX, **6** ,1995, 4, 211-236.
5. *V. G. Mazy'a*, A. Soloviev. Math. Sb. **180**,1989, 1211-1233.

საქართველოს მეცნიერებათა აკადემიის მოამბე, 159, №2, 1999
BULLETIN OF THE GEORGIAN ACADEMY OF SCIENCES, 159, №2, 1999

MATHEMATICS

Z. Khechinashvili

Mean Square Optimal Hedging Strategies for (B,S) Financial Market

Presented by Corr. Member of the Academy N. Vakhania, March 9, 1998

ABSTRACT. **We defined financial (B,S) - market in the following way: the stock price $S_n = S_0 \exp\{M_n - \frac{1}{2} < M > n\}$ $n \geq 0$ and interest rate $r = 0$, where M is the Gaussian martingale with compensator $< M >$. For the European contingent claim $f(S_N)$ we constructed hedging strategies optimal in the sense of the following square criterion $\inf_{\pi \in SF} E(f(S_N) - X_N^{\pi})^2$, where X_N^{π} is the wealth process.**

Key words: Gaussian martingale, mean square optimal hedging strategy, contingent claim, convolution of distribution.

On the stochastic basis $(\Omega, \mathcal{F}, (\mathcal{F}_n)_{n\geq 0}, P)$ we consider financial (B, S)-market and assume, that the stock price is given by the following stochastic sequence:

$$S_n = S_0 e^{M_n - \frac{1}{2} < M > n}, \; S_0 > 0, \; n \geq 0, \tag{1}$$

where $M = (M_n, \mathcal{F}_n)_{n \geq 0}$, with $M_0 = 0$ is the Gaussian martingale with the compensator $< M >$. Let the interest rate be $r = 0$, i.e, for any $n \geq 0$

$$B_n = B_0, \qquad B_0 > 0. \tag{2}$$

The stock price $S = (S_n)_{n\geq 0}$, is also the martingale with respect to measure P.

1. In this model we consider European option with terminal date N and contingent claim $f(S_N)$, where $f = f(s)$, $s \in (0, \infty)$ is the integrable function. For the self-financing strategies $\gamma \in SF$ (see [1]) the wealth process has the following form

$$X_n^{\pi} = X_0^{\pi} + \sum_{k=1}^{n} \gamma_k \Delta S_k, \qquad \gamma \in SF. \tag{3}$$

Let us consider conditional expectation $E(f(S_N)|\mathcal{F}_n^S)$, where $\mathcal{F}_n^S = \sigma\{S_k, k \leq n\}$. From (1)

$$E(f(S_N)\,|\,\mathcal{F}_n^S) = E(f(S_n e^{M_N - M_n - \frac{1}{2}(< M >_N - < M >_n)})\,|\,\mathcal{F}_n^S) \equiv F_n. \tag{4}$$

It is clear that $$F_N = f(S_N) = F_0 + \sum_{n=1}^{N} \Delta F_n, \qquad F_0 = Ef(S_N). \tag{5}$$

The financial market defined by formulas (1), (2) is not complete and we can't construct hedging strategies as those of Black-Shouls model. We'll find optimal strategies in

the sense of the following square criterion

$$inf_{\pi\in SF} E(f(S_N) - X_N^{\pi})^2. \tag{6}$$

Such approach was developed in [2] and [3]. Denote $E(f(S_N) - X_N^{\pi})^2 \equiv R^N{}_0$. From (3) we have $EX_N^{\pi} = X_0^{\pi}$. It is easy to see

$$R^N{}_0 = (Ef(S_N) - X_0^{\pi})^2 + Ef(S_N) - X_N^{\pi} - (Ef(S_N) - X_0^{\pi}))^2. \tag{7}$$

When $X_0^{\pi} = Ef(S_N) = F_0$ the first term in (7) is minimal and equals zero. Using (3) and (5) for second term of (7) we'll receive

$$R^N{}_0 = \sum_{n=1}^{N} E(\Delta F_n - \gamma_n \Delta S_n)^2. \tag{8}$$

It is easy to check that the optimal strategy in the sense of criterion (6)

$$\gamma_n^* = \frac{E(\Delta F_n \Delta S_n \mid \mathcal{F}_{n-1}^S)}{E((\Delta S_n)^2 \mid \mathcal{F}_{n-1}^S)} = \frac{E(\Delta(F_n S_n) \mid \mathcal{F}_{n-1}^S)}{E((\Delta S_n)^2 \mid \mathcal{F}_{n-1}^S)}, \quad n \in 1,\ldots,N \tag{9}$$

(see also [6]). Therefore we prove the following

Theorem 1. *Let financial (B,S)-market given by the formulas* (1), (2) *and* $f(S_N)$ *be the European contingent claim, where* $f(s)$, $s \in [0,\infty)$ *is the integrable function, the optimal in the sense of criterion* (6) *self-financing hedging strategy* γ_n^*, $n \in 1,N$ *determine from* (9).

2. Now we consider the European standard call option with contingent claim $f(S_N) = (S_N - K)^+$, where K is the exercise price ([4]). In this case from (4)

$$\begin{aligned} F_n &= E((S_n e^{M_N - M_n - \frac{1}{2}(<M>_N - <M>_n)} - K)^+ \mid S_n) = \\ &= S_n \Phi(\sqrt{<M>_N - <M>_n} - z_n) - K\Phi(-z_n), \end{aligned} \tag{10}$$

where

$$z_n = \frac{\ln\frac{K}{s} + \frac{1}{2}(<M>_N - <M>_n)}{\sqrt{<M>_N - <M>_n}}. \tag{11}$$

$\Phi(x)$ is the standard normal distribution function. Using (10) and (11) we shall receive

$$F_n = S_n \Phi\left(\frac{\ln\frac{S_n}{K} + \frac{1}{2}(<M>_N - <M>_n)}{\sqrt{<M>_N - <M>_n}}\right) - K\Phi\left(\frac{\ln\frac{S_n}{K} + \frac{1}{2}(<M>_N - <M>_n)}{\sqrt{<M>_N - <M>_n}}\right) \tag{12}$$

Therefore the following is proved

Theorem 2. *Let financial (B,S)-market be defined by* (1), (2). *For the European standard call option with contingent claim* $f(S_N) = (S_N - K)^+$, *the optimal in the sense of criterion* (6) *self-financing strategy* $(\gamma^*)_{n\geq 0}$ *is determined from* (9), *where* F_n *is defined by* (12).

3. In this section we'll receive the final representation for the optimal strategy using (10)

$$E(\Delta(F_n S_n)\,|\,\mathcal{F}_{n-1}^S) = \frac{S_{n-1}^2 e^{\Delta<M>n}}{\sqrt{2\pi}} \int_R e^{\frac{-\left[z - a_n(\ln\frac{K}{S_{n-1}} + l_n^{(1)})\right]^2}{2\sigma_n^2}} \Phi(-z)dz -$$

$$- \frac{KS_{n-1}}{\sqrt{2\pi}} \int_R e^{\frac{-\left[z - a_n(\ln\frac{K}{S_{n-1}} + l_n^{(2)})\right]^2}{2\sigma_n^2}} \Phi(-z)dz - F_{n-1}S_{n-1}, \qquad (13)$$

where $a_n = (\sqrt{<M>_N - <M>_n})^{-1}$, $l_n^{(1)} = -\frac{3}{2}\Delta <M>_n - <M>_N - <M>_n$,

$\sigma_n^2 = \Delta <M>_n a_n^2$, $l_n^{(2)} = -\frac{3}{2}\Delta <M>_n + <M>_N + <M>_n$, [5].

Futher we have the following

$$\gamma_n^* = \frac{e^{\Delta<M>n}}{\sqrt{2\pi}(e^{\Delta<M>n} - 1)} \int_R e^{\frac{-\left[z - a_n(\ln\frac{K}{S_{n-1}} + l_n^{(1)})\right]^2}{2\sigma_n^2}} \Phi(-z)dz -$$

$$- \frac{K}{S_{n-1}\sqrt{2\pi}(e^{\Delta<M>n} - 1)} \int_R e^{\frac{-\left[z - a_n(\ln\frac{K}{S_{n-1}} + l_n^{(2)})\right]^2}{2\sigma_n^2}} \Phi(-z)dz - \frac{K}{S_{n-1}(e^{\Delta<M>n} - 1)} \qquad (14)$$

$$\cdot \left[S_{n-1}\Phi\left(\frac{\ln\frac{S_{n-1}}{K} + \frac{1}{2}(<M>_N - <M>_n)}{\sqrt{<M>_N - <M>_n}} \right) - K\Phi\left(\frac{\ln\frac{S_{n-1}}{K} - \frac{1}{2}(<M>_N - <M>_n)}{\sqrt{<M>_N - <M>_n}} \right) \right]$$

We denote $a_n\left(\ln\frac{K}{S_{n-1}} + l_n^{(1)}\right) \equiv a_n^{(1)}$, $a_n\left(\ln\frac{K}{S_{n-1}} + l_n^{(2)}\right) \equiv a_n^{(2)}$,

and consider $$\frac{1}{\sqrt{2\pi}}\int_R e^{\frac{-(z-a_n^{(1)})^2}{2\sigma_n^2}}\Phi(-z)dz. \tag{15}$$

This is the convolution of two normal distributions $F_1(z)=\frac{1}{\sqrt{2\pi}}\int_{-\infty}^{z} e^{-\frac{y^2}{2}}dy$,

$F_2(z)=\frac{1}{\sqrt{2\pi}}\int_{-\infty}^{z} e^{\frac{(y-a_n^{(1)})^2}{2\sigma_n^2}}dy$, which is also normal with mean and variance $a_n^{(1)}$, σ_n^2+1,respectively. Therefore, for (15) the following equality is true

$$\frac{1}{\sqrt{2\pi}}\int_R e^{\frac{-(z-a_n^{(1)})^2}{2\sigma_n^2}}\Phi(-z)dz=\sqrt{\sigma_n^2+1}\Phi\left(\frac{-a_n^{(1)}}{\sqrt{\sigma_n^2+1}}\right). \tag{16}$$

Analogously

$$\frac{1}{\sqrt{2\pi}}\int_R e^{\frac{-(z-a_n^{(2)})^2}{2\sigma_n^2}}\Phi(-z)dz=\sqrt{\sigma_n^2+1}\Phi\left(\frac{-a_n^{(2)}}{\sqrt{\sigma_n^2+1}}\right). \tag{17}$$

Finally from (14), (16) and (17) we'll receive

$$\gamma^*=\frac{e^{\Delta<M>_n}\sqrt{\sigma_n^2+1}}{e^{\Delta<M>_n}-1}\Phi\left(\frac{-a_n^{(1)}}{\sqrt{\sigma_n^2+1}}\right)-\frac{K\sqrt{\sigma_n^2+1}}{S_{n-1}(e^{\Delta<M>_n}-1)}\Phi\left(\frac{-a_n^{(2)}}{\sqrt{\sigma_n^2+1}}\right)-\frac{1}{S_{n-1}(e^{\Delta<M>_n}-1)}\cdot$$

$$\left[S_{n-1}\Phi\left(\frac{\ln\frac{S_{n-1}}{K}+\frac{1}{2}(<M>_N-<M>_n)}{\sqrt{<M>_N-<M>_n}}\right)-K\Phi\left(\frac{\ln\frac{S_{n-1}}{K}-\frac{1}{2}(<M>_N-<M>_n)}{\sqrt{<M>_N-<M>_n}}\right)\right].$$

Tbilisi I. Javakhishvili State University

REFERENCES

1. *A. V. Melnikov, A. N. Shiryaev.* Preprint N1, M, 1994 (Russian).
2. *D. Lamberton, B. Lapeyere.* Math. and Applications, **9**, Paris, 1992.
3. *M. Musela, M. Rutkovski.* Applications of Mathematics. 1997.
4. *F. Black, M. Sholes.* Journal of Political Economy, May/June, 1973, 637-657.
5. *R.Sh. Liptser, A. N. Shiryaev.* Theory of Martingales. Kluwer, 1987.
6. *O. Glonti, Z. Khechinashvili.* Proc. A. Rasmadze Math. Inst., **116**, Tbilisi, 1997, 33-43.

საქართველოს მეცნიერებათა აკადემიის მოამბე, 159, №2, 1999
BULLETIN OF THE GEORGIAN ACADEMY OF SCIENCES, 159, №2, 1999

MATHEMATICS

S. Kemkhadze

The Embedding Theorem for Modular Δ-Complemented Lattices

Presented by Corr. Member of the Academy H. Inassaridze, March 16, 1998

ABSTRACT. **The present paper is an attempt to generalize the well-known theorem of Frink and Johnson, i. e. to study the embedding problem for Δ-complemented modular lattices.**

Key words: lattice, modular lattice, D-point, D-geometric lattice, Δ-complement.

Definition 1. Let $\langle A, ^- \rangle$ be a pair consisting of the set A and mapping $X \mapsto \overline{X}$, $X, \overline{X} \subseteq A$ and satisfying the following two conditions:

(i) $X \subseteq \overline{X}$; $X \subseteq Y$ implies $\overline{X} \subseteq \overline{Y}$; $\overline{\overline{X}} = \overline{X}$.

(ii) $\overline{\varnothing} = \varnothing$; $\{\overline{x}\} = \{x\}$ for every $x \in A$.

We define partially ordered relation on the set A as follows: for $x, y \in A$ we consider that $x \leq y$ if and only if there exists such $U \in P(A)$ that $\overline{x \cup U} \subseteq \overline{y \cup U}$.

Definition 2. Let $\langle A, ^- \rangle$ be a given pair which satisfies the conditions from the definition 1. Let L be the collection of subsets of A. We say that the pair $\langle A, L \rangle$ is a projective space, if the following conditions are held:

(i) The set of all elements less than $p \in A$ is the infinitive distributive lattice with maximum condition for every $p \in A$.

(ii) Every $l \in L$ contains at least two elements.

(iii) For every pair of distinct elements p and q of A there exists at least one line $l \in \mathfrak{R}$ such that $p, q \in l$ and such l generally isn't unique.

(iv) The Pash axiom holds, that is to say:

If $p, q, r, x, y \in A$, $p, q, x, \in l_1$, $r, x, y \in l_2$, then there exists such elements $z \in A$ and $p_1, q_1, r_1, x_1, y_1 \in A$ that $p_1, r_1, x \in l_3$ and $x_1, y_1, z \in l_4$, $p_1 \leq p$, $q_1 \leq q$, $r_1 \leq r$.

The elements of the set A are called the points and the elements of are called the lines.

A set of elements of a projective space S is called a subspace of S if it contains all points collinear with any two of its points.

It follows that any subspace of a projective space is a projective space itself. In particular, a set consisting of a single point is always a subspace.

If X and Y are two distinct and non-empty subspaces of projective spaces, then by $X \vee Y$ we define the set consisting of all points on lines of S which contain two distinct points, one from X and one from Y [1]. It can be proved, that $X \vee Y$ is a subspace.

Theorem 3. *The collection of all subspaces of a projective space is a modular D-geometric lattice if the lattice order relation is taken to be the relation of set inclusion between subspaces and the operation of lattice meet is taken to be the operation of set intersection.*

Lemma 4. *The representative sets of a Δ-complemented modular D-pointwise lattice* $\mathfrak{N}$ *forms a lattice isomorphic to* $\mathfrak{N}$, *with set inclusion as the lattice order relation and set intersection as the operation of lattice meet.*

By a dual ideal I of a lattice $\mathfrak{N}$ is meant a non-empty set of elements of $\mathfrak{N}$ such that the lattice meet $a \wedge b$ of two elements of $\mathfrak{N}$ is in I if and only if both a and b are in I. (see [2], [3]).

Definition 5. We say that a dual ideal I is Δ-maximal if it isn't the entire lattice and for every dual ideal J, which satisfies $I \subset \mathrm{J} \subset \mathfrak{N}$, the following holds: $[I,1] \equiv [\mathrm{J},1]$ is an infinite distributive lattice with maximum condition and $[I,1] \equiv [\mathrm{J},1]$.

Theorem 6. ([1]). *The collection* $D(\mathfrak{N})$ *of all dual ideals of a lattice* $\mathfrak{N}$ *is a complete lattice, which is modular when* $\mathfrak{N}$ *is modular, provided the operation of lattice join* $I \vee \mathrm{J}$ *in* $D(\mathfrak{N})$ *is taken to mean set intersection, and the relation of lattice inclusion* $I \leq \mathrm{J}$ *is taken to be the superset relation* $I \supset \mathrm{J}$.

If a is an element of a lattice $\mathfrak{N}$, then the set of all elements b of $\mathfrak{N}$ such that $a \leq b$ is a dual ideal which is called a principal dual ideal and is denoted by [a) (see [1], [2]).

Theorem 7. [1]. *The collection of all principal dual ideals of a lattice* $\mathfrak{N}$ *is a sublattice of the lattice of all dual ideals of L, and is isomorphic to* $\mathfrak{N}$.

With the use of Zorn's lemma we can prove that every dual ideal of a lattice with a zero element which isn't Δ-maximal can be extended to be Δ-maximal [2].

Lemma 8. *The lattice of all dual ideals of a Δ-complemented modular lattice is complete, D-pointed and modular.*

Note, that the lattice of all dual ideals of a Δ-complemented modular lattice is not necessarily Δ-complemented.

Definition 9. If P and Q are two distinct Δ-maximal dual ideals of a Δ-complemented modular lattice $\mathfrak{N}$, then

(i) the join (that is, the set intersection) $P \vee Q$ of P and Q in the lattice of all dual ideals of $\mathfrak{N}$ will be called the linear ideal determined by P and Q.

(ii) By the line PQ determined by P and q will be meant the set of all Δ-maximal dual ideals R of $\mathfrak{N}$ such that $R \leq P \vee Q$ (i.e. $R \supset P \cap Q$).

(iii) Δ-Maximal dual ideals will be called collinear if they are on the same line.

Theorem 10. *The maximal dual ideals of any Δ-complemented lattice are the points of a projective space.*

If a is any element of the Δ-complemented modular lattice $\mathfrak{N}$ then by the representative set $r(a)$ of a will be meant the set of all Δ-maximal ideals P of $\mathfrak{N}$ such that a is an element of P. This is related to the notion of representative set $r(a)$ for D-pointed lattices. In fact, if we pass from the original lattice $\mathfrak{N}$ to the lattice $D(\mathfrak{N})$ of all dual ideals, which is D-pointed with Δ-maximal dual ideals for D-points, then the representative set of an element a of $\mathfrak{N}$ according to the definition just given $r(a)$ is identcial with the representative set of the principal dual ideal $[a)$ of $D(\mathfrak{N})$ $r([a))$. Note that by theorem 7 the lattice of all principal dual ideals of $\mathfrak{N}$ is isomorphic to $\mathfrak{N}$.

Theorem 11. *The representative sets* $r(a)$ *of a Δ-complemented modular lattice* $\mathfrak{N}$ *form a lattice isomorphic to* $\mathfrak{N}$. *This lattice is a substlattice of the lattice of all subspaces of the plojective space S determined by* $\mathfrak{N}$.

Proof. Note that any representative set $r(a)$ is a subspace of the projective space S, the

points of which are the [Δ-maximal dual ideals of the lattice $\mathfrak{M}$. For if P and Q are any two distinct points (Δ- maximal dual ideals) of $\mathfrak{r}(a)$, then the linear ideal $P \vee Q$ is the set intersection of ideals P and Q, and the lattice element a, since it is a member of both P and Q, is also a member of $P \vee Q$. Hence, if R is any point collinear with P and Q, then $P \vee Q$ is a subset of R. Hence, a is a member of R, and R is a member of $\mathfrak{r}(a)$. Therefore $\mathfrak{r}(a)$ is a subspace, since it contains all points collinear with two of its points.

Since representative sets are subspaces of the projective space S, the lattice operations of meet and join are defined for them. It will now be shown that the correspondence between elements a of $\mathfrak{M}$ and their representative sets $\mathfrak{r}(a)$ preserve the lattice operations of meet and join. It can be seen that $\mathfrak{r}(a) \wedge \mathfrak{r}(b) = \mathfrak{r}(a \wedge b)$. For the Δ-maximal dual ideal P is an element of the representative set $\mathfrak{r}(a \wedge b)$ if and only if P is an element of both $\mathfrak{r}(a)$ and $\mathfrak{r}(b)$, since by definition of reperesentative set, this is equivalent to saying that $a \wedge b$ is a member of P if and and only if both a and b are membersof P, which follows from the definition of dual ideal. This is because the lattice meet of the subspaces $\mathfrak{r}(a)$ and $\mathfrak{r}(b)$ is their intersection.

To show that the correspondence preserves the operation of lattice join is more difficult. First note that $\mathfrak{r}(a) \vee \mathfrak{r}(b) \leq \mathfrak{r}(a \vee b)$. For if P is a point of $\mathfrak{r}(a) \vee \mathfrak{r}(b)$, then P is collinear with points Q and R of $\mathfrak{r}(a)$ and $\mathfrak{r}(b)$ respectively. Hence the linear ideal $P \vee Q$ is a subset of P. It follows that $a \vee b$ is an element of P, and P is a member of $\mathfrak{r}(a \vee b)$.

Next it must be shown that $\mathfrak{r}(a \vee b) \leq \mathfrak{r}(a) \vee \mathfrak{r}(b)$. This means, that if the point P is a member of the representative set $\mathfrak{r}(a \vee b)$, then P is collinear with points Q and R of the representative sets $\mathfrak{r}(a)$ and $\mathfrak{r}(b)$ respectively. It may be assumed that neither a nor b is member of P, for in that case the conclusion follows. We may further assume that $a \vee b = 0$, since otherwise a may be replaced by the relative Δ-complement a' of b in $a \vee b$.

Since P, as well as the points Q and R which we seek is a member of the lattice of all dual ideals $D(\mathfrak{M})$, we now consider the principal dual ideals $[a)$, $[b)$, and $[a \vee b)$, which are also in $D(\mathfrak{M})$, rather than the elements a, b and $a \vee b$, which are in $\mathfrak{M}$. Since $P \leq [a \vee b)$, it follows that the dual ideal $([b) \vee P) \wedge [a)$ is not the zero element of $D(\mathfrak{M})$, since otherwise both $[b)$ and $[b) \vee P$, would be distinct relative complements of $[a)$ in $[a \vee b)$, which is impossible in a modular lattice. For we have

$[a) \vee ([b) \vee P) = [a \vee b)$, $[a) \vee [b) = [a \vee b)$ and $[a) \wedge [b) = 0$.

Hence the ideal $([b) \vee P) \wedge [a)$ may be extended to be a Δ-maximal dual ideal Q. It follows that a is a member of Q, and $Q \leq [b) \vee P$. Let us consider the ideal $(P \vee Q) \wedge [b)$. If this were the zero element of $D(\mathfrak{M})$, then both P and $P \vee Q$ would be distinct relative Δ-complements of $[b)$ in $[b) \vee P$, since we would have $[b) \vee (P \vee Q) = [b) \vee P$, and $[b) \wedge (P \vee Q) = [b \wedge P = 0$. But this is impossible in a modular lattice since $[b)$ and $[b) \vee P$ are distinct. Hence $[b) \wedge (P \vee Q)$, since it is not zero, it is a Δ-maximal dual ideal which we may call R, such that $R \leq [b)$. Hence R is a member of $\mathfrak{r}(b)$ and P is collinear with points Q and R of $\mathfrak{r}(a)$ and $\mathfrak{r}(b)$, respectively, which was to be proved, since it can be seen that P, Q, and R are collinear.

This completes the proof that the lattice operations correspond to the original lattice $\mathfrak{M}$ and to the lattice of representententative sets. It remains to show that the correspondence is one-to-one and hence an isomorphism, or in other words that if a and b are distinct,

then their representative sets $F(a)$ and $F(b)$ are distinct. Suppose a and b are distinct; then either $a \neq a \wedge b$, or $b \neq \alpha \wedge b$. By symmetry we may suppose the former, that is, $a \neq a \wedge b$. Since $\mathfrak{M}$ is Δ-complemented and modular, there exists in $\mathfrak{M}$ an element a' which is a relative Δ-complement of $a \wedge b$ in a, that is, such that $a' \vee (a \wedge b) = a$, while $a' \wedge (a \wedge b) = a' \wedge 0$. This element a' is not the zero element of $\mathfrak{M}$, since otherwise $a = a' \vee (a \wedge b) = a \wedge b$, contrary to assumption. Hence it follows that a' is an elemnt of some maximal dual ideal P. Then P is a member of $F(a)$, but not of $F(b)$, since otherwise $a' \wedge b = 0$ would be an element of P, which is impossible since the zero element is never a member of a Δ-maximal dual ideal. It follows that $F(a)$ and $F(b)$ are distinct, which was to be proved. This completes the proof of Theorem 11.

According to the statements, given above, Theorem 11 can be formed in this way too:

Theorem 11'. *Every Δ-complemented modular lattice can be embedded in modular Δ-geometric lattice.*

Georgian Technical University

REFERENCES

1. *O. Frink*. Trans. Amer. Math. Soc. **60**, 1946, 452-467.
2. *G. Gratzer*. General lattice theory. Academie-Verlag Berlin, 1978.
3. *G. Birkhoff*. Lattice theory. Third edition, New-York, 1967.

საქართველოს მეცნიერებათა აკადემიის მოამბე, 159, №2, 1999
BULLETIN OF THE GEORGIAN ACADEMY OF SCIENCES, 159, №2, 1999

MATHEMATICS

G. Khimshiashvili

Homotopy Classes of Abstract Elliptic Transmission Problems

Presented by Corr. Member of the Academy N.Berikashvili, March 9, 1998

ABSTRACT. **We have computed homotopy groups of elliptic transmission problems over an arbitrary C*-algebra. The answer is formulated in terms of K-theory of operator algebras. We also present some corrollaries and related results.**

Key words: C*-algebra, Hilbert module, Grassmanian, homotopy groups, K-theory.

Twenty years ago B.Bojarski suggested an interesting geometric interpretation of classical transmission problems for holomorphic functions [1], which appeared useful in various topological aspects of the topic. In particular, the important role of a special Grassmanian and the so-called restricted linear group of a polarized Hilbert space was revealed and they became the object of intensive study [2-4]. The present author used the same ideas for obtaining a homotopy classification of invertible abstract singular operators and showed that similar objects can be naturally introduced in the framework of Hilbert modules over arbitrary C*-algebras [5].

Along these lines, below we compute the homotopy groups of elliptic transmission problems over a C*-algebra and of the restricted linear group of a Hilbert module. It turned out that the answer may be conveniently formulated in terms of K-theory of underlying C*-algebra. The latter theory is understood in the sense of [6] and we will freely refer to that book in the sequel, as well as to the paper of J.Mingo [7] which contains a detailed exposition of Fredholm operators in Hilbert modules over C*-algebras.

Let A be a unital C*-algebra. We denote the standard Hilbert module over A by H_A [6]. As it is well known, there exists a natural A-valued inner product on H, which enables one to introduce direct sum decompositions in H_A, bounded operators and adjoints for operators on H_A [6]. We denote by $B = B(H_A)$ the collection of all bounded linear operators on H_A having bounded adjoints [6]. This is a Banach algebra which plays a crucial role in Hilbert A-module theory. We denote by GB its group of units (operators with bounded inverses) and by UB its subgroup of unitaries. Then an analogon of polar decomposition holds in GB and this implies that GB is retractable on UB [6].

Compact linear operators are defined as A-norm limits of finite rank A-linear operators on H. Their collection will be denoted by $K_A = K(H_A)$.

In order to mimic constructions of [1], let us fix a direct sum decomposition $H_A = H_+ \oplus H_-$ with both summands isomorphic to H_A as A-modules. Following usual convention, any operator on H_A may be written in the form of a (2 x 2)-matrix of operators with respect to this decompostion. We denote by p_+ and p_- the natural orthogonal projections defined by this decomposition.

We introduce now the subgroup GB_r of GB consisting of those invertible operators whose off-diagonal terms belong to K_A. Let U_r denote its subgroup of unitary elements.

Let us recall that there is a wAell defined notion of finite rank submodules of H_A [7].

its kernel and image are finite rank A-modules. It turns out that many important properties of usual Fredholm operators remain valid in this setting. In particular, if one denotes by $F_A = F(H_A)$ the collection of all Fredholm operators on H_A, then there exists a canonical homomorphism $ind = ind_A: F_A \to K_0(A)$, where $K_0(A)$ is the usual topological K-group of the basic algebra A [6].

We introduce now the special Grassmanian $Gr_+ = Gr_+(H_A)$ as the collection of all A-submodules V of H_A such that projection p_+ restricted on V is Fredholm while projection p_- restricted to V is compact.

Theorem 1. *Grassmanian $Gr_+(H_A)$ is a Banach manyfold modelled on Banach space K_A.*

This follows from the existence of natural local coordinate systems on Gr_+ which are obtained as a direct generalizations of coordinate systems constructed in [5] for the special case $A = \boldsymbol{C}$.

According to [1], this Grassmanian may be interpreted as the collection of all elliptic transmission problems over A. Thus our problem reduces to the computation of its homotopy groups. The latter problem may be reduced to consideration of the restricted linear group GB_r whose homotopy type, in turn, may be described in terms of Fredholm operators on H_A. Our main results may be summed up as follows.

Theorem 2. *Group GB_r acts on Gr_+ transitively with contractible isotropy subgroups.*

Theorem 3. *All even-dimensional homotopy groups of $Gr_+(H_A)$ are isomorphic to $K_0(A)$, while its odd-dimensional homotopy groups are isomorphic to $K_1(A)$.*

Of course, the same holds for homotopy groups of $GB_r(H_A)$ because from Theorem 1 it follows that these two spaces are homotopy equivalent. We formulate the result for $Gr_+(H_A)$ because we are mainly interested in the homotopy classification of transmission problems.

Homotopy groups of $GB_r(H_A)$ were first computed by the author in [5] without referring to Grassmanians. Later on, similar results were obtained by S.Zhang [8] in a purely K-theoretical context. Contractibility of isotropy subgroups from Theorem 2 was previously established only in the case $A = \boldsymbol{C}$ [4]. Our generalization becomes possible due to the analogy of Kuiper's theorem in the setting of Hilbert modules obtained independently by E.Troitsky and J.Mingo [7].

Our theorems have several immediate corollaries, of which we mention here only three. The first one recovers the well known answer to the original problem of B.Bojarski [3, 5]. The second and third refer to certain classes of operators over C*-algebras introduced in [5].

Corollary 1. *Even-dimensional homotopy groups of the collection of classical Riemann-Hilbert problems are trivial, while odd-dimensional ones are isomorphic to the additive group of integers $\boldsymbol{Z}$.*

It is worthy of noting that the non-triviality of these groups is closely related to the so-called spectral flow of self-adjoint Fredholm operators [3]. It would be interesting to obtain a similar interpretation for an arbitrary C^*-algebra A.

Corollary 2. *Homotopy groups of invertible singular operators over a C^*-algebra A are given by relations (where n is an arbitrary natural number):*

$$\pi_0 \cong K_0(A), \quad \pi_1 \cong K_1(A) \otimes \boldsymbol{Z} \otimes \boldsymbol{Z}; \quad \pi_{2n} \cong K_0(A), \quad \pi_{2n+1} \cong K_1(A) .$$

As usual, algebra of abstract bisingular operators is defined as the tensor square of the algebra of singular operators. Applying standard rules of computing Fredholm indices in tensor squares [6] one obtains a rudimental Fredholm theory for such operators.

Corollary 3. *Abstract elliptic bisingular operators over a C^*-algebra A are homotopically classified by their indices taking values in $K_0(A)$. The index homomor-*

Corollary 3. *Abstract elliptic bisingular operators over a C*-algebra A are homotopically classified by their indices taking values in $K_0(A)$. The index homomorphism is an epimorphism on $K_0(A)$.*

This suggests that there should exist index formulas for abstract bisingular operators. Such formulas may be really obtained in terms of their symbols but this enterprise involves several ad hoc notions and requires a separate presentation.

In order to give an idea how to prove main results, let us explicate that our strategy for proving Theorems 2 and 3 mimics the approach of [4]. The fact that GB_r acts on Gr_+ is obtained purely algebraically, using simple formulas for action of (2 x 2)-matrices on elements of Gr_+ indicated in ([4], Ch.6). Transitivity is verified by an explicit construction of the element transforming H_+ into a prescribed element of Gr_+, again along the lines of ([4], Ch.6.)

Then one notices that it is sufficient to prove that isotropy subgroups are contractible when the action is restricted to U_r. The transitivity of the action implies that it is sufficient to find the isotropy subgroup of H_+ in U_r. The latter is easily seen to be isomorphic to $U(H_+) \times U(H)$. Now both these groups are contractible according to Kuiper's theorem for Hilbert modules [7].

The homotopy structure of GB_r is determined by presenting this group as a composition of two locally trivial fiber bundles with contractible fibers. The first is defined by taking the first column in the matrix presentation of an $T \in GB_r$. Its base may be described as an open subset, which in turn, may be fibred over $F(H_+)$ by taking the left upper corner element. The base is now the whole space of Fredholm operators and the fiber is again contractible. Thus, we conclude that GB_r is homotopy equivalent to $F(H_+)$. It remains to notice that homotopy groups of the latter space are known to be isomorphic to the K-theory of A [7].

The results above have various modifications and applications. One may define the restricted linear group in a different way by requiring that off-diagonal terms belong to some Shatten-von Neumann classes as it is done in [4] in the case $A = \boldsymbol{C}$. Then it would be possible to construct a central extension of this group and compute some of its characteristic classes.

One also obtains a stratification of Gr_+ indexed by pairs of element of $K_0(A)$, which is similar to Birkhoff stratification from [1] and [4]. An interesting problem is then to describe the homotopy type of a stratum in terms of its indices. Also, following arguments of [9] one easily checks that Gr_+ carries a natural Fredholm structure, which leads to many intriguing problems in the spirit of Fredholm structures theory [9].

This research was carried out with the financial support of Georgian Academy, of sciences, grant 1.8.

Georgian Academy of Siences
A.Razmadze Mathematical Institute

REFERENCES

1. *B. Bojarski*. Differ. integr. uravn. Granichnye zadachi. TGU, Tbilisi, 1979, 45-60 (Russian).
2. *G. Khimshiashvili*. Soobshch. Akad. Nauk GSSR, **108**, 1982, 273-276.
3. *K. Wojciechowsky*. J. Operator Theory. 15, 1985, 201-216.
4. *A. Pressley, G. Segal*. Loop groups. Clarendon Press, Oxford, 1986.
5. *G. Khimshiashvili*. Complex Anal. and Applic.'87. Bulg. Ac. Sci., Sofia, 1989, 231-235.
6. *B. Blackadar*. K-theory for operator algebras. Springer, Berlin, 1986.
7. *J. Mingo*. Trans. Amer. Math. Soc. 299, 1987, 397-411.
8. *S. Zhang*. Bull. Amer. Math. Soc. 28, 1993, 75-83.
9. *G. Khimshiashvili*. Contemporary Mathematics, 131, 1992, 164-178.

საქართველოს მეცნიერებათა აკადემიის მოამბე, 159, №2, 1999
BULLETIN OF THE GEORGIAN ACADEMY OF SCIENCES, 159, №2, 1999

MATHEMATICS

A.Danelia

On the Approximation Property of Abel-Poisson Transformations of Multiple Conjugate Trigonometric Series

Presented by Member of the Academy L. Zhizhiashvili, July 6, 1998

ABSTRACT. **Approximation state of Abel-Poisson transformations of conjugate trigonometric series of a function of the class $H(\omega;C(T^m))$ is considered.**

Key words: conjugate functions of multiple variables, modules of continuity, Abel-Poisson transformation.

1. Let $R^m (m = 1,2,...,R^1 \equiv R)$ be m-dimensional Euclidean space. Let us consider the set $M = \{1,...,m\}$ and assume that B is a nonempty subset of M. We denote the number of elements of the set B by the symbol $|B|$ and by x_B a point in the space R^m, for which all the coordinates of MB are zeros.

If $T^m = [-\pi,\pi]^m$ $(T^1 \equiv T)$, then $C(T^m)$ is the set of continuous functions defined on T^m, with period 2π in each variables and with the norm $\|f\|_{C(T^m)} = \max|f(x)|$, and $L(T^m)$ is the set of Lebesgue integrable functions, defined on T^m, and with period 2π in each variable.

Let $f: R^m \to R$, $m \geq 2$. Let's consider the difference

$$\Delta(h_1,...,h_m) f(x) = f(x_1+h_1,...,x_m+h_m) - f(x_1,...,x_m)$$

and for the functions $f \in C(T^m)$ use its complete modulus of continuity

$$\omega(f;\delta)_{C(T^m)} = \sup_{|h_i|\leq\delta_i} \|\Delta(h_1,...,h_m)\|_{C(T^m)}, \quad (0 < \delta_i \leq \pi, \ i = 1,...,m).$$

Let f and g be nonnegative functions on a set $E \subset R$. If there exists a positive constant D such that $f(x) \leq Dg(x)$ for every $x \in E$, then we write $f(x) << g(x)$, $x \in E$.

Let $H(\omega;C(T^m))$, where ω is a modulus of continuity [1], be a set of the functions such that

$$\omega(f;\delta)_{C(T^m)} << \sum_{i=1}^{m} \omega(\delta_i), \quad (0 < \delta_i \leq \pi, \quad i=1,...,m),$$

and the symbol $\widetilde{f}\,(x, r, B)$ be Abel-Poisson transformation [2, p.187] of multiple conjugate trigonometric series $\overline{\sigma}\,(f, B)$.

If $f \in L(T^m)$, then [2, p.182] the expression

$$\widetilde{f}_B(x) = \lim_{\varepsilon_B \to 0} \widetilde{f}_B(x,\varepsilon_B) = \left(-\frac{1}{2\pi}\right)^{|B|} \lim_{\varepsilon_B \to 0} \int_{\substack{\Pi\{T\setminus[-\varepsilon_j,\varepsilon_j]\} \\ j\in B}} f(x+S_B) \prod_{i\in B} ctg\frac{S_i}{2} dS_B \quad (\varepsilon_j > 0, j \in B)$$

is called the conjugate function with respect to the variables, the indices of which form the set B ($\widetilde{f}_B \equiv \widetilde{f}$, when $m = 1$).

Definition. We say that a modulus of continuity ω satisfies Zygmund's condition if

$$\int_0^{\delta} \frac{\omega(u)}{u}\,du + \delta\int_0^{\delta} \frac{\omega(u)}{u^2}\,du \ll \omega(\delta), \qquad (\delta \to 0+).$$

2. In the theory of functions of real variables there are many works related to the properties of Abel-Poisson transformations of Fourier series of f function and its conjugate series for one as well as for multiple variables.

In 1947 Zygmund [3] proved the following statement: let $\varphi_i : (0, 1] \to (0,1]$ be nondecreasing functions and $\varphi_i \to 0$, when argument $t \to 0$ (i=1,...,m). Let $\lambda \in [1, +\infty)$ be a fixed number and $\lambda^{-1}\varphi_i(t) \le 1 - r_i \le \lambda\varphi_i(t)$ $(i = 1,...,m)$. (1)
If $f \in L(T^m)$ and the coordinates of the point r are satisfying (1), then

$$\lim_{r\to 1-} f(x, r) = f(x) \qquad \text{almost everywhere.}$$

In the case of conjugate functions the following statement is valid.

Theorem (L.Zhizhiashvili [2]). *Let $f \in L(\log^+ L)^{m-1}(T^m)$, then for every $B \subset M$ $(B \neq \varnothing)$*

$$\lim_{r\to 1-} \widetilde{f}\,(x, r, B) = \widetilde{f}_{\,B}\,(x).$$

In the given work we present the following

Theorem. *Let $f \in H(\omega;\ C(T^m))$ $(m \ge 2)$ and ω be a modulus of continuity satisfying Zygmund's condition, then*

a) $$\left\|\widetilde{f}(\cdot, r', B) - \widetilde{f}_B(\cdot, (1-r)')\right\|_{C(T^m)} \ll \omega(1-r)\left|\ln(1-r)\right|^{|B|} \qquad (B \subset M,\ B \neq \varnothing) \quad (r \to 1\text{-}),$$

$$\left\|\widetilde{f}(\cdot, r', M) - \widetilde{f}_M(\cdot, (1-r)')\right\|_{C(T^m)} \ll \omega(1-r)\left|\ln(1-r)\right|^{m-1} \qquad (r \to 1\text{-});$$

where $r' = (r,...,r)$, $(1 - r)' = (1 - r,...,1 - r)$.

b) there exists a function $F \in H(\omega;\ C(T^m))$ such that

$$\left\|\widetilde{F}(\cdot, r', B) - \widetilde{F}_B(\cdot, (1-r)')\right\|_{C(T^m)} \gg \omega(1-r)\left|\ln(1-r)\right|^{|B|} \qquad (B \subset M,\ B \neq \varnothing) \quad (r \to 1\text{-}),$$

$$\left\|\widetilde{F}(\cdot, r', M) - \widetilde{F}_M(\cdot, (1-r)')\right\|_{C(T^m)} \gg \omega(1-r)\left|\ln(1-r)\right|^{m-1} \qquad (r \to 1\text{-}).$$

Tbilisi I. Javakhishvili State University

REFERENCES

1. *S. M. Nikol'skii.* Dokl. Akad. Nauk SSSR, 52, 3, 1946, 191-194 (Russian).
2. *L. V. Zhizhiashvili.* Some Probl. of the Theory of Trigon. Fourier Ser. and their Conjugates. Tbilisi, 1993 (Russian).
3. *A. Zygmund.* Amer. J. Math., 1947, 69, 4, 836-850.

საქართველოს მეცნიერებათა აკადემიის მოამბე, 159, №2, 1999
BULLETIN OF THE GEORGIAN ACADEMY OF SCIENCES, 159, №2, 1999

MATHEMATICS

Ya. Diasamidze, Sh. Makharadze

An Abstract Characteristics of Semigroups of the Class Σ(X;2)

Presented by Corr. Member of the Academy D. Baladze, December 30, 1998

ABSTRACT. **In the present paper we give an abstract characterization of special class of the subsemigroup of the semigroup of binary relation.**

Key words: binary relation, semigroup, lattice.

Let X be an arbitrary set. Under a binary relation on the set X is understood a subset α of the cartesian product $X \times X$ of the set X by itself. If $(x,y) \in \alpha$, where x, y are the elements of the set X, then we shall write $x\alpha y$.

If α and β are the relations on X, then their composition α o β is defined as follows: $x(\alpha$ o $\beta)y$, if there exists an element $z \in Z$, such that $x\alpha z\beta y$. It is obvious that the set B_x of all binary relations on X is a semi-group with respect to the operation (o).

Let $Y \subseteq X$ and $\alpha \in B_x$. Then

$\alpha^{-1} = \{(x,y)/y\alpha x\}$; $Y\alpha = \{x \in X/y\alpha x$ for some $y \in Y\}$; $\alpha Y = Y\alpha^{-1}$.

By $\varnothing$ we denote an empty set or an empty binary relation.

Let now D be a non-empty set of subsets from X, closed with respect to the operations of set-theoretic union of elements from D, i. e., $\bigcup D' \in D$ for any non-empty subset D' from D. In this case the set D will be called a complete X-semilattice of the union.

Further, let f be an arbitrary mapping of the set X into the set D. To every such mapping f we put into correspondence the binary relation α_f on the set X, satisfying the condition

$$\alpha_f = \bigcup_{x \in X} (\{x\} \times f(x)). \tag{1}$$

Denote a set of all such $\alpha_f (f : X \to D)$ by $B_x(D)$. Obviously, $B_x(D)$ is s subset of the semigroup B_x of all binary relations on the set X. Let us prove that $B_x(D)$ is a subsemigroup of the semigroup B_x. Indeed, let α_f, $\alpha_g \in B_x(D)$. Determine the mapping ψ of the set X into the set of all subsets of the set X as follows:

$$\psi(x) = \bigcup_{z \in x\alpha_f} z\alpha_g$$

for all $x \in X$. It is evident that $\psi(x) \in D$ for every $x \in X$, since $z\alpha_g \in D$ for any $z \in Z$, and D is closed with respect to the operations of the set-theoretic union.

Next, by virtue of equation (1) and by definition of multiplication of binary relations the equation

$$x(\alpha_f \text{ o } \alpha_g) = (x\alpha_f)\,\alpha_g = \bigcup_{z \in x\alpha_f} z\alpha_g = x\alpha\psi,$$

is valid for any $x \in X$, i.e. $\alpha_\rho \circ \alpha_\varepsilon = \alpha\psi \in B_X(D)$. Hence $B_X(D)$ is a sub-semigroup of the semigroup B_X. The semigroup $B_X(D)$ will be called a complete semigroup of binary relations defined by the complete X- semilattice of unions D.

Note that if $D = 2^X$, i. e., D is a set of all subsets of the set X, then $B_X(2^X) = B_X$.

Let X be an arbitrary non-empty set and m be an arbitrary cardinal number. Denote by $\Sigma(X; m)$ a set of all complete X- semilattices of unions of power m. If $D \in \Sigma(X; m)$, then we shall say that the semigroup of binary relations $B_X(D)$ is defined by the semi-lattice D from the class $\Sigma(X; m)$.

Obviously, the semi-groups $B_X(D)$ defined by semilattices D from the class $\Sigma(X; 1)$ are one-element, i. e. the semi-groups defined by semilattices of that class are isomorphic.

The semi-lattices D from the class $\Sigma(X; 2)$ are two-element chains of the form $Z_1 \subseteq Z_2$, $Z_1 \neq Z_2$. Note that if $Z_1 = \varnothing$, then the binary relation $\varnothing$ is zero of the semi-group $B_X(D)$, but if $Z_1 \neq \varnothing$, then by Theorem 1 from item 1.3, the binary relations $\delta_1 = X \times Z_1$ and $\delta_2 = X \times Z_2$ are right zeros of the semigroup $B_X(D)$ (see [3]), which are defined by the chains $D = \{\varnothing; Z_2\}$ and $D = \{Z_1, Z_2\}$, where $Z_1 \neq \varnothing$ are not isomorphic. Therefore their separate investigation makes sense.

Let $D = \{\varnothing; Z_2\}$ and

$E_X^{(r)}(D) = \{\alpha \in B_X(D) / \alpha X \cap Z_2 \neq \varnothing\}$,

$O_X(D) = \{\alpha \in B_X(D) / \alpha X \cap Z_2 = \varnothing\}$.

Theorem 1. *Let $D = \{\varnothing; Z_2\}$. Then the following assertions are valid:*

(1) $E_X^{(r)}(D)$ *is a set of all right units of the semigroup $B_X(D)$, i.e., is a semigroup of left zeros;*

(2) *the set $O_X(D)$ is a subsemigroup of the semigroup $B_X(D)$ which is a semigroup with zero multiplication;*

(3) *binary relation $\varnothing$ is zero of the semigroup $B_X(D)$;*

(4) $E_X^{(r)}(D) \circ O_X(D) = \{\varnothing\}$;

(5) $O_X(D) \circ E_X^{(r)}(D) = O_X(D)$;

(6) $E_X^{(r)}(D) \cap O_X(D) = \varnothing$.

Proof. First we note that every element from $B_X(D)$ can be represented as $Y \times Z_2$, where $Y \subseteq X$.

Let now $\alpha = Y_1 \times Z_2$ and $\beta = Y_2 \times Z_2$ ($Y_1, Y_2 \subseteq X$) be arbitrary elements of the semigroup $B_X(D)$. As for α and β, we consider the following cases:

(a) $\alpha \in E_X^{(r)}(D)$ and $\beta \in B_X(D)$. Then $Y_1 \cap Z_2 \neq \varnothing$, and therefore

$$\beta \circ \alpha = (Y_2 \times Z_2) \circ (Y_1 \times Z_2) = Y_2 \times Z_2 = \beta,$$

i.e., the binary relation α is the right unit of the semigroup $B_X(D)$. This, in particular, by virtue of the inclusion $E_X^{(r)}(S) \subseteq B_X(D)$ results in $\beta \circ \alpha = \beta$ for all α and β from $E_X^{(r)}(D)$.

Hence $E_X^{(r)}(D)$ is the semigroup of left zeros.

Thus assertion (1) is proved.

(b) $\alpha, \beta \in O_X(D)$. Then $Y_1, Y_2 \subseteq X \setminus Z_2$, i. e., $Y_2 \cap Z_2 = \varnothing$, and therefore

$$\alpha \circ \beta = (Y_1 \times Z_2) \circ (Y_2 \times Z_2) = \varnothing \in O_X(D).$$

Hence $O_X(D)$ is a subsemigroup of the semigroup $B_X(D)$ which is a semigroup with zero multiplication.

Thus assertion (2) is proved.

Assertion (3) is obvious.

(c) Let $\alpha \in E_X^{(r)}(D)$ and $\beta \in O_X(D)$. Then $Y_2 \cap Z_2 = \varnothing$, and therefore $\alpha \circ \beta = \varnothing$, i. e., the equality

$$E_X^{(r)}(D) \circ O_X(D) = \{\varnothing\}$$

is valid.

Thus assertion (4) is proved.

Assertion (5) follows directly from assertion (1).

If now $\alpha \in E_X^{(r)}(D) \cap O_X(D)$, then $\alpha \in E_X^{(r)}(D)$ and $\alpha \in O_X(D)$. This respectively yields $Y_1 \cap Z_2 \neq \varnothing$ and $Y_1 \cap Z_2 = \varnothing$. But this is impossible. Thus the equality

$$E_X^{(r)}(D) \cap O_X(D) = \varnothing$$

is valid.

Thus assertion (5) is proved and the theorem is complete.

Theorem 2. *Semigroup S is isomorphic to the semigroup $B_X(D)$, where $D=\{\varnothing, Z_2\}$, if and only if S satisfies the following conditions*:

(1) *semi-group S has zero O_S;*

(2) *S is the union of a semigroup of left zeros S_1 with a semiPgroup with zero multiplication S_2;*

(3) $S_2 \cdot S_1 = S_2$;

(4) $S_1 \cdot S_2 = \{O_S\}$;

(5) *the sets S_1 and $E_X^{(r)}(D)$ are equivalent;*

(6) *there exists one-to-one mapping of the set S_2 onto $O_X(D)$ which maps zero of the semigroup S into zero of the semigroup $B_X(D)$.*

Batumi Sh. Rustaveli State University

REFERENCES

1. *K. A. Zaretski.* A semi-group of binary relations. In: Mat. Sborn., **61**, 3, M., 1970 (Russian)
2. *A. Clifford, G. Preston.* Algebraic Theory of semi-groups. M., v. 1, 1972.
3. *Ya. I.Diasamidze, Sh. I. Makharadze.* In: Sbornik of Batumi State University, 1998 (Russian).

საქართველოს მეცნიერებათა აკადემიის მოამბე, 159, №2, 1999
BULLETIN OF THE GEORGIAN ACADEMY OF SCIENCES, 159, №2, 1999

MATHEMATICS

Z. Tediashvili

On the Uniqueness of Inverse Problems of the Potential Theory

Presented by Member of the Academy T.Burchuladze, June 22, 1998

ABSTRACT. **Inverse problems of the potential theory are considered for two- and three-dimensional domains. The uniqueness theorems are proved within specific restrictions for boundaries of the domains and densities of potentials.**

Key words: inverse problems, potential theory.

Investigation of inverse problems of the potential theory has a great practical interest. One of the main moments of the theory of inverse problems is to prove the uniqueness theorems.

Let us introduce the following notations: R^n stands for n-dimensional Euclidean space (with $n = 2$ or $n = 3$); Ω_1 and Ω_2 are bounded domains in R^n; $d\Omega$ denotes the boundary of $\Omega \subset R^n$, $x = (x_1,\dots,x_n)$ and $y = (y_1,\dots,y_n)$ are points of R^n and $r_{xy} = |x - y|$ is the distance between x and y; $K(x, y)$ is the fundamental solution corresponding to the Laplace operator $\Delta = \sum_{k=1}^{n} \frac{\partial^2}{\partial x_k^2}$; $\overline{B(x,\varepsilon)}$ is the closed ball centered at the point x and radius $\varepsilon > 0$;

$V_\Omega(\mu)(x) = \int_\Omega K(x,y)\mu(y)dy$ denotes Newtonian (volume or logarithmic) potential defined by the domain $\Omega \subset R^n$ and the density μ; we assume μ to be a bounded summable function on Ω; for $n = 2$ by $z = x_1 + ix_2$ we denote a complex variable; $\Omega_\infty^{(1,2)}$ represents the connected unbounded component of $R^n \setminus (\overline{\Omega}_1 \cup \overline{\Omega}_2)$ and $\Omega_0 = R^n \setminus \overline{\Omega}_\infty^{(1,2)}$

1.Formulation of problems. Inverse problems are formulated as follows.

Let Ω_1 and Ω_2 be bounded domains of R^n. The density μ is defined on $\Omega = \Omega_1 \cup \Omega_2$. It is known that the potentials $V_{\Omega_1}(\mu)$ and $V_{\Omega_2}(\mu)$ coincide in the domain $R^n \setminus (\overline{\Omega}_1 \cup \overline{\Omega}_2)$, i.e. $\forall x \in R^n \setminus (\overline{\Omega}_1 \cup \overline{\Omega}_2) : V_{\Omega_1}(\mu)(x) = V_{\Omega_2}(\mu)(x)$.

The problem is to define relative positions of the domains Ω_j (j=1,2).

This problem represents a nonlinear illposed problem of mathematical physics. In the above formulation the problem has not a unique solution. It is very important to establish additional conditions that provide the uniqueness of solution.

In the theory of inverse problems the uniqueness questions have been considered by various authors ([1]). The first results in this direction have been obtained by Novikov [1]. He considered star shaped domains with constant densities. In what follows we shall essentially apply the next auxiliary assertion [3].

Lemma 1. *Let $A \subset R^n$ be an open bounded domain and let μ be a bounded locally summable function on R^n such that $V_A(\mu)(x) \equiv 0$ for $x \in R^n \setminus \overline{A}$; then*

$$\int_A \mu(y)U(y)dy = 0 \tag{1}$$

for arbitrary harmonic function U in the domain D where $D \supset \overline{A}$.

2. Uniqueness Theorems. We start with the two-dimensional case and assume that Ω_1 and Ω_2 are bounded domains of R^2.

Theorem 1. *Let there exist a point $z_0 \in \partial\Omega_\infty^{(1,2)}$ and a number $\varepsilon > 0$ such that* 1) $\sigma_0^{\varepsilon} \cap \Omega_2 = \varnothing$ *where $\sigma_0^{\varepsilon} = B(z_0, \varepsilon) \cap \Omega_1$;* 2) *there exist two angles Γ' and Γ'' with the vertex at z_0 and with the expansion less then $\pi/2$ satisfying the conditions $(B(z_0, \varepsilon) \cap \Gamma') \supset \sigma_0^{\varepsilon} \supset (B(z_0, \varepsilon) \cap \Gamma'')$. Moreover, let* 3) *$\mu$ be a bounded summable function on $\Omega_1 \cup \Omega_2$ with the property: $\mu(y) \geq \delta_0 > 0$ or $\mu(y) \leq -\delta_0 < 0$ almost everywhere on σ_0^{ε}, where δ_0 is some positive number.*

Then the potentials $V_{\Omega_1}(\mu)(x)$ and $V_{\Omega_2}(\mu)(x)$ do not coincide on $\Omega_\infty^{(1,2)}$.

Proof. Let us assume the contrary, i.e.

$$V_{\Omega_1}(\mu)(x) = V_{\Omega_2}(\mu)(x), \quad \text{for } x \in \Omega_\infty^{(1,2)}. \tag{2}$$

Without loss of generality the coordinate system can be chosen so that $z_0 = 0$ is the origin and the x_1-axis coincides with the bisector of the angle Γ'.

By virtue of Lemma 1 it can be easily shown that

$$\int_{\Omega_1} U(x)\mu(x)dx = \int_{\Omega_2} U(x)\mu(x)dx \tag{3}$$

for arbitrary harmonic function in D where $D \in \overline{\Omega}$.

It suffices to consider the case $\mu(x) \geq \delta_0 > 0$ almost everywhere on σ_0^{ε} (the case $\mu(x) \leq -\delta_0 < 0$ can be considered similarly).

Taking into account the conditions of the theorem we easily derive

$$I = \int_{\sigma_0^{\varepsilon}} f(x)\mu(x)dx = +\infty, \tag{4}$$

where $f(x) = f(x_1, x_2) = \operatorname{Re}\dfrac{1}{z^2}$ is a harmonic function in the whole plane R^2 except the origin $x = 0$.

Obviously, there exists a natural number $n_0 \in N$ such that $\left(-\dfrac{1}{n}, 0\right) \notin \overline{\Omega_0}$ for $n \geq n_0$.

Let us consider the function

$$f_n(x) = f_n(x_1, x_2) = \operatorname{Re}\left(z + \frac{1}{n}\right)^{-2} \quad \text{with } n \geq n_0 . \tag{5}$$

It is evident that each function f_n is harmonic on $\overline{\Omega}_0$ and $\lim_{n\to\infty} f_n(x) = f(x)$, $x \in \Omega_0$.

Using the equation (3) we derive

$$\int_{\sigma_0^\varepsilon} f_n(x)\mu(x)dx = -\int_{\Omega_1\setminus\sigma_0^\varepsilon} f_n(x)\mu(x)dx + \int_{\Omega_2} f_n(x)\mu(x)dx \tag{6}$$

for $\forall\, n \geq n_0$.

If we apply the Lebesgue theorem [4] in the right-hand side of (6), we conclude the existence of a constant $c(\varepsilon) < +\infty$ such that

$$\lim_{n\to\infty} \int_{\sigma_0^\varepsilon} f_n(x)\mu(x)dx < c(\varepsilon) < +\infty. \tag{7}$$

From (5) it follows that $f_n(x) \geq 0$ for $x \in \sigma_0^\varepsilon$.

Now, Fatou's lemma [4] together with (7) implies

$$\int_{\sigma_0^\varepsilon} f(x)\mu(x)dx \leq c(\varepsilon) < +\infty, \tag{8}$$

which contradicts to the condition (4). This completes the proof.

In the three-dimensional case there holds a similar theorem.

Theorem 2. *Let Ω_1 and W_2 be bounded domains of R^3 and let there exist a point $x_0 \in \partial\Omega_\infty^{(1,2)}$ and a number $\varepsilon > 0$ such that* 1) $\sigma_0^\varepsilon \cap \partial\overline{\Omega}_2 = \varnothing$, *where* $\sigma_0^\varepsilon = B(x_0, \varepsilon) \cap \Omega_1$; 2) *there exist two cones K' and K'' with the vertex at x_0 and the angles less than $\pi/2$ satisfying the conditions $(B(x_0,\varepsilon)\cap K') \supset \sigma_0^\varepsilon \supset (B(x_0,\varepsilon)\cap K'')$. Moreover, let* 3) *$\mu$ be a bounded summable function on $\Omega_1 \cup \Omega_2$ with the property $\mu(x) \geq \delta_0 > 0$ or $\mu(x) \leq -\delta_0 < 0$ almost everywhere on σ_0^ε, where δ_0 is some positive number.*

Then the potentials $V_{\Omega_1}(\mu)$ and $V_{\Omega_2}(\mu)$ do not coincide on $\Omega_\infty^{(1,2)}$.

Proof. Let us assume the contrary, i.e.

$$V_{\Omega_1}(\mu)(x) = V_{\Omega_2}(\mu)(x), \quad \text{for } x \in \Omega_\infty^{(1,2)}. \tag{9}$$

Without loss of generality we assume that x_0 is the origin point of the coordinate system and the x_1-axis coincides with the axis of symmetry of the cone K'. By Lemma 1 we can easily show that

$$\int_{\Omega_1} U(x)\mu(x)dx = \int_{\Omega_2} U(x)\mu(x)dx \tag{10}$$

for arbitrary harmonic function U in D where $D \supset \overline{\Omega}_0$.

It suffices to consider again the case $\mu(x) \geq \delta_0 > 0$ for $x \in \sigma_0^\varepsilon$ (the case $\mu(x) \leq -\delta_0 < 0$ can be treated quite similarly). The conditions of the theorem yield that

$$I = \int_{\sigma_0^\varepsilon} f(x)\mu(x)dx = +\infty, \tag{11}$$

where $f(x) = f(x_1,x_2,x_3) = (x_1^2 - x_2^2)\,|x|^{-5}$. This function is harmonic everywhere in R^3 except the point $x = 0$. Clearly, there exists a natural number $n_0 \in N$ such that $\left(0,0,-\frac{1}{n}\right) \notin \overline{\Omega_0}$ for $n \geq n_0$.

Further, let us consider the sequence of functions

$$f_n(x) = f(x_1,x_2,x_3) = f(x_1,x_2,x_3+1/n) \quad \text{with} \quad n \geq n_0.$$

It is evident that $\lim_{n\to\infty} f_n(x) = f(x)$ for $x \in \Omega_0$.

For arbitrary $n \geq n_0$ the function $f_n(x)$ is harmonic on $\overline{\Omega_0}$ and, therefore, due to (10) we have

$$\int_{\sigma_0^\varepsilon} f_n(x)\mu(x)dx = -\int_{\Omega_1\setminus\sigma_0^\varepsilon} f_n(x)\mu(x)dx + \int_{\Omega_2} f_n(x)\mu(x)dx. \tag{13}$$

If we apply the Lebesgue theorem on majorized convergence [4] in the right-hand side of (13) and use the fact that $f_n(x) \geq 0$ for $x \in \sigma_0^\varepsilon$ and $n \geq n_0$, by Fatou's Lemma we arrive at the inequality

$$\int_{\sigma_0^\varepsilon} f(x)\mu(x)dx \leq C(\varepsilon) < +\infty, \tag{14}$$

where $C(\varepsilon)$ is some positive constant.

This inequality contradicts to (11) which completes the proof.

Tbilisi I. Javakhishvili State University

REFERENCES

1. *A. I. Prilepko.* Matematicheskie zametki, **14**, 5, 1973, 755-767 (Russian).
2. *P. S. Novikov.* DAN SSSR, **18**, 3, 1938, 165-168 (Russian).
3. *A. I. Prilepko.* Differentsialniye uravneniya, **11**,1,1966, 107-123 (Russian).
4. *A. N. Kolmogorov, S. V. Fomin.* Elementy teorii funktsii i funktsionalnogo analiza. M., 1976 (Russian).

საქართველოს მეცნიერებათა აკადემიის მოამბე, 159, №2, 1999
BULLETIN OF THE GEORGIAN ACADEMY OF SCIENCES, 159, №2, 1999

MATHEMATICS

Sh. Makharadze

On the Theory of Binary Relation Semigroup

Presented by Corr. Member of the Academy D. Baladze, December 30, 1998

ABSTRACT. **In the present paper we consider a class of subsemigroups from B_X, whose every semigroup has as its right unit the quasi-order relation on the set X. Each semigroup of that class contains a subsemigroup involving the elements of the semigroup which are contained in the right unit of the given semigroup. The obtained class of semigroups is studied. An abstract characteristics for the subclass of the obtained class, consisting of semigroups, each having as its own right unit the equivalence relations on the set X, is found.**

Key words: binary relation, semigroup, isomorphism.

It is known that any semigroup is isomorphically imbeddable in the semigroup B_X of all binary relations on a non-empty set X [1-3]. Therefore separation and investigation of a class of subsemigroups of that semigroup is of interest.

Let X be an arbitrary non-empty set. Under a binary relation on the set X is understood a subset α of the direct product $X \times X$. If $(x, y) \in \alpha$, where x, y are the elements of the set X, then we shall write $x\alpha y$.

If α and β are relations on X, then their composition $\alpha \circ \beta$ is defined as follows: $x(\alpha \circ \beta)y$, if there exists an element $z \in X$, such that $x\alpha z\beta y$. Obviously, the set B_X of all binary relations on X is the semigroup with respect to the operation (o).

Let $Y \subseteq X$ and $\alpha \in B_X$. Then the relations $\varnothing$, $\Delta_Y = \{(y, y)/y \in Y\}$ and $\alpha^{-1} = \{(x, y)/y\alpha x\}$ denote respectively an empty, a partially identical on the set Y and an inverse to α relations. Further, let $Y\alpha = \{x \in X/y\alpha x$ for some $y \in Y\}$ and $\alpha Y = Y\alpha^{-1}$.

Let α be some fixed element from B_X and let $\Theta_X^{(r)}(\alpha) = \{\beta \in B_X/\beta \circ \alpha \subseteq\}$. It can be easily verified that $\Theta_X^{(r)}(\alpha)$ is a sub-semigroup of the semigroup B_X. Next, let $E_X^{(r)}(\alpha) = \{\beta \in \Theta_X^{(r)}(\alpha)/\gamma \circ \beta = \beta$ for any $\gamma \in \Theta_X^{(r)}(\alpha)\}$. Obviously, $E_X^{(r)}(\alpha)$ is the subsemigroup of all right zeros of the semigroup $\Theta_X^{(r)}(\alpha)$.

Recall that the binary relation $\alpha \in B_X$ is called reflexive if $\Delta_X \subseteq \alpha$, symmetric if $\alpha = \alpha^{-1}$, transitive if $\alpha \circ \alpha \subseteq \alpha$ and idempotent if $\alpha \circ \alpha = \alpha$.

The reflexive and transitive binary relation is called quasi-order relation, and if, moreover, it is symmetric, then this relation is called the equivalence relation.

Let now $V(\alpha) = \{Y\alpha/Y \subseteq X\}$ and $\alpha_* = \{(x, y)/x, y \in X, \alpha x \subseteq \alpha y$.

It is easy to verify that α_* is the quasi-order relation, and $\alpha = \alpha \circ \alpha_*$. Next, we denote respectively by α' and α' the reflexive and transitive closures of the binary relation α i. e.

$\alpha' = \alpha \cup \Delta X$ and $\alpha^* = \bigcup_{n=1}^{\infty} \alpha_n$. In particular, α^{r*} denotes the binary relation $(\alpha \cup \Delta X)^r$.

The theorem below, which will be used in the sequel, has been proved in [6].

Theorem 1. *Let $\beta \in B_X$. Then the following assertions are epuivalent:*

1. $\beta \in \Theta_X^{(r)}(\alpha)$
2. $\beta_* \supseteq \alpha_*$
3. $V(\beta) \subseteq V(\alpha^r)$.

Let $\alpha \in B_X$, $\Theta_X^{(r)}(\alpha) = \{\beta \in \Theta_X^{(r)}(\alpha) \ / \beta \subseteq \alpha^r$. Then it is evident that $\Theta_X^{(r)}(\alpha)$ is a sub-semigroup of the semigroup $\Theta_X^{(r)}(\alpha)$.

Theorem 2. *Let $\alpha \in B_X$, $x \in X$.*

$V_x(\alpha^r) = \{Y \in V(\alpha^r) \setminus \{\varnothing\} / TY \subseteq X^r \alpha^r$ *and* $V = \bigcup_{x \in X} (x \times V_x(\alpha^r))$.

Then the sets $\Theta_X^{(r)}(\alpha)$ and 2^V are equivalent to $2^V = \{T/T \subseteq V\}$.

Proof. Let $\beta \in \Theta_X^{(r)}(\alpha)$, and f be the mapping of the set $O_X^{(r)}(\alpha)$ in the set $X \times V_x(\alpha^r)$, satisfying the condition $f(\beta) \subseteq \bigcup_{x \in \beta X} (x, x\beta)$. Obviously, $x\beta \in V_x(\alpha^r)$, since $\beta \in \alpha^{r*}$. Therefore, for any $x \in \beta X$ the element $(x, x\beta)$ belongs to the set $x \times V_x(\alpha^r)$. This implies that $f(\beta) \subseteq V$, i. e., $f(\beta) \subseteq 2^V$, and f is the mapping of the set $O_X^{(r)}(\alpha)$ in the set 2^V.

If now V' is some element from 2^V, then the binary relation $\delta = \bigcup_{(x,y) \in V'} (x \times Y)$ belongs to the semigroup $O_X^{(r)}(\alpha)$, since $(x, Y) \in V'$ holds for any $\varnothing \neq Y \subseteq x\alpha^r$. Hence f is the mapping of the set $O_X^{(r)}(\alpha)$ in the set 2^V.

Corollary. *Let X be a finite set and $\alpha \in B_X$. Then the following assertions are valid:*

(1) *the order of the semigroup $O_X^{(r)}(\alpha)$ is equal to $2^{|V|}$ (see Theorem 2);*

(2) *if α^r is the equivalence relation on the set X, then the order of the semigroup $O_X^{(r)}(\alpha)$ is equal to $2^{|X|}$.*

Proof. Assertion (1) follows directly from Theorem 2 and assertion (2) is obtained from the fact that $|V_x(\alpha^r)| = 1$ for any $x \in X$, and therefore $|V| = |X|$.

Lemma. *Let $\alpha \in B_X$. Then for the semigroup $O_X^{(r)}(\alpha)$ the following assertions are valid:*

(1) $O_X^{(r)}(\alpha)$ *is the semigroup of transitive binary relations;*

(2) $E_X^{(r)}(\alpha) \subseteq O_X^{(r)}(\alpha)$;

(3) α^r *is the equivalence relation on the set X, then* $\Theta_X^{(r)}(\alpha)$ *is the semigroup of idempotent elements.*

Proof. If $\beta \in O_X^{(r)}(\alpha)$, then $\beta \subseteq \alpha^r$ and $\beta \in \Theta_X^{(r)}(\alpha)$. Therefore $\beta \circ \beta \subseteq \beta \circ \alpha^r = \beta$, i. e., β is transitive.

Let now $\beta \in E_X^{(r)}(\alpha)$. Then $\alpha^r \circ \beta = \alpha^r \supseteq \beta$,since $\alpha^r \supseteq \Delta_x$. Hence $\beta \in O_X^{(r)}(\alpha)$, and therefore $E_X^{(r)}(\alpha) \subseteq O_X^{(r)}(\alpha)$.

Let, further, α^r be the equivalence relation on the set X, and $\beta \in O_X^{(r)}(\alpha)$. Then by assertion (1) we have $\beta \circ \beta \subseteq \beta$. If now $x\beta y$ for some $x, y \in X$, then $y \in x\beta = Y\alpha^r \subseteq x\alpha^r$, where $Y \subseteq X$. But this is possible if and only if $Y \subseteq x\alpha^r$. Hence $y \in x\beta = x\alpha^r$.

In particular, this implies $x\beta y\beta y$, i.e., $\beta \subseteq \beta \circ \beta$. Consequently, $\beta = \beta \circ \beta$ for any $\beta \in O_X^{(r)}(\alpha)$.

Theorem 3. *Let* $\alpha \in B_X$, α^r *be the equivalence relation on the set X and Z be a set of representatives of all* α^r*-classes of the set X. Then the following assertions are valid:*

(1) $\beta \in O_X^{(r)}(\alpha)$;

(2) $\beta = \bigcup_{z \in Z} (\beta(z\alpha^r) \times z\alpha^r)$.

Corollary. *Let* $\alpha \in B_X$, α^r *be the equivalence relation on the set X and Z be a set of representatives of all* α^r*-classes of the set X. Then the following assertions are valid:*

(1) $\beta \in O_X^{(r)}(\alpha)$;

(2) $\beta = \bigcup_{z \in Z} (\beta(z\alpha^r) \times z\alpha^r)$ *and* $\beta(z\alpha^r) \subseteq z\alpha^r$ *for all* $z \in Z$.

Theorem 4. *Let* $\alpha \in B_X$, α^r *be the equivalence relation on the set X and Z be a set of representatives of all* α^r*-classes of the set X,*
$\Delta(z\alpha^r)\{Y \times z\alpha^r | Y \subseteq z\alpha^r\}$,

were $z \in Z$ *and* β, $\beta' \in O_X^{(r)}(\alpha)$. *Then the following assertions are valid:*

(1) $\varnothing \in \Delta(z\alpha^r)$ *for any* $z \in Z$;
(2) $\Delta(z\alpha^r)/\{\varnothing\}$ *is the semigroup of left zeros;*
(3) $\Delta(z\alpha^r) \cap \Delta(z\alpha^r) = \varnothing$ *for any* $z \neq z'$ *and* $z, z' \in Z$;
(4) $\Delta(z\alpha^r) \circ \Delta(z\alpha^r) = \varnothing$ *for any* $z \neq z'$ *and* $z, z' \in Z$;

(5) $\beta = \bigcup_{z \in Z} \beta_z$ *where* $\beta \in \Delta(z\alpha^r)$ *for any* $z \in Z$, *and such a representation of the relation* β *is unique;*

(6) *if* $\beta = \bigcup_{z \in Z} \beta_z$, $\beta' = \bigcup_{z \in Z} \beta'_z$, *where* $\beta_z, \beta'_z \in \Delta(z\alpha^r)$ *for any* $z \in Z$, *then* $\beta \circ \beta' = (\beta_z \circ \beta'_z)$;
$z \in Z$

(7) *if* $|Z| \geq 2$, *then the semigroup* $O_X^{(r)}(\alpha)$ *is the direct product of the semigroups* $\Delta(z\alpha^r)$, *where* $z \in Z$.

Theorem 5. *In order for the semigroup S to be isomorphic to the semigroup* $O_X^{(r)}(\alpha)$ (α^r *is the equivalence relation on the set X), it is necessary and sufficient that for it to be a direct product of the semigroups* $S_i (i \in I)$ *possessing the following properties:*

(1) *a set of all semigroups* $S_i (i \in I)$ *and a set of all* α^r*-classes of the set X are equivalent;*

(2) *for some one-to-one mapping of the* ψ*-set of all semigroups* $S_i (I \in I)$ *on the set of all* α^r*-classes of the set X, the sets* S_i *and* $2^{\psi(S_i)}$ *are equivalent;*

(3) *the semigroup* S_i *has zero* O_{S_i} *for any* $i \in I$;

(4) $S_i \setminus \{O_{S_i}\}$, *where* $i \in I$ *is the semigroup of left zeros.*

Batumi Sh. Rustaveli State University

REFERENCES

1. *G. Birkhoff.* Lattice theory. M.: 1984.
2. *K. A. Zaretskii.* A semigroup of binary relations. In: Matem. sbornik. M., **61**, 3, 1970 (Russian).
3. *A. Clifford, G. Preston.* Alhebraic theory of semigroups. M.: 1, 1972.
4. *K. Kuratovski, A. Mostovski.* The set theory. M.: 1970 (Russian).
5. *E. S. Ljapin.* semigroups. M.: 1960 (Russian).
6. *Ya. I. Diasamidze, Sh. I. Makharadze.* Non-reducible generating sets of some idempotently generated subsemigroups of a semigroup of all binary relations. Batumi, 1996 (Russian).

საქართველოს მეცნიერებათა აკადემიის მოამბე, 159, №2, 1999
BULLETIN OF THE GEORGIAN ACADEMY OF SCIENCES, 159, №2, 1999

MATHEMATICS

K. Bitsadze

On Changes of Variable that Preserve Convergence and Absolute Convergence of Fourier-Haar Series

Presented by Member of the Academy L. Zhizhiashvili, July 27, 1998

ABSTRACT. **It is established that among all differentiable homeomorphic changes of variable only the functions φ_1 and φ_2 defined correspondingly by the equalities $\varphi_1(x) = x$, $\varphi_2(x) = 1 - x$, $x \in [0,1]$ preserve everywhere convergence of Fourier-Haar series. The same is true for everywhere absolute convergence.**

Key words: Fourier-Haar series.

The Fourier-Haar series of an integrable function f has the form

$$f(t) \sim \sum_{n=1}^{\infty} a_n(f)\chi_n(t), \qquad t \in [0,1] \tag{1}$$

where χ_n, $n = 1,2,...$([1], p. 47, or [2], Chapter 3, 1) , are the Haar functions, and

$a_n(f) = \int_0^1 f(t)\chi_n(t)dt$, $p = 1,2,...$ are the Fourier-Haar coefficients of the function f.

A homeomorphism of the interval $[0,1]$ is one-to-one continuous mapping of the interval on itself.

We say that a homeomorphism φ of the interval $[0,1]$ acts in a class A of functions defined in the interval $[0,1]$ if for every function f of the class A the composition $f\circ\varphi$ is in A.

Let A_1 be the class of all functions $f \in [0,1]$ for which $\sum_{n=1}^{\infty} |a_n(f)| < \infty$ |, A_χ - the class of all function $f \in [0,1]$ for which the series (1) absolutely converges everywhere, A^*_χ the class of all functions $f \in [0,1]$ for which the series (1) absolutely converges almost everywhere, S-the class of all functions $f \in [0,1]$ for which the series (1) converges everywhere. It is obvious that $A_\chi \subset S$.

P. L. Ul'yanov [3] has proved that the following relations hold for these classes

$$A_1 \subset A^*_\chi,\ A^*_\chi \setminus A_1 \neq \varnothing,\ A^*_\chi \setminus A_\chi \neq \varnothing,\ A_1 \setminus A_\chi \neq \varnothing,\ A_\chi \setminus A_1 \neq \varnothing.$$

He first began to investigate problems connected with absolute convergence of Fourier-Haar series of composite functions (see [4]).

For historical information and the problems connected with Fourier series of composite functions see [5].

Let φ_1 and φ_2 be homeomorphisms defined respectively by equalities: $\varphi_1(x) = x$, $\varphi_2(x) = 1 - x$, $x \in [0,1]$. It is easy to verify that if $f \in A_\chi$ then the composite function $f\circ\varphi_2$ belongs to A_χ and also that if $f \in S$, then $f\circ\varphi_2 \in S$.

The problems concerning the influence of change of variable on convergence and absolute convergence of Fourier-Haar series were first investigated in the paper [6] by V. Bugadze. In particular, there is obtained the class of all homeomorphisms of the interval $[0,1]$ which act in the class A_1. There is also established that among all the continuously differentiable changes of the variable only φ_1 and φ_2 act in the classes A_χ and S.

We proved that the same is true not only for the class of continuously differentiable homeomorphisms but for the class of all differentiable homeomorphisms. This is confirmed by the first corollary of the theorem stated below.

Theorem. *Let φ be an arbitrary differentiable homeomorphism of the interval $[0,1]$ distinct from φ_1 and φ_2. Then there exists a function f in A_χ such that the composite function $f\circ\varphi$ is not in S.*

Corollary 1. *Among all the differentiable homeomorphisms only φ_1 and φ_2 act in the class A_χ.*

Corollary 2. *Among all the differentiable homeomorphisms only φ_1 and φ_2 act in the class S.*

Tbilisi I. Javakhishvili State University

REFERENCES

1. *G. Alexits*. Konvergenzprobleme der Orthogonalreien. Budapest. 1960.
2. *B. S. Kashin, A. A. Saakyan*. Ortogonalnye ryady. M., 1984 (Russian).
3. *P. L. Ul'yanov*. Matem. Sb., 72 (114), 1967 (Russian).
4. *P. L. Ul'yanov*. Anal. Math. **4**, 3 1978 (Russian).
5. *A. M. Olevskii*. Uspekhi Mat. Nauk, **40**, 3, 1985 (Russian).
6. *V. M. Bugadze*. Matem. Sb. **182**, 2, 1991 (Russian).

საქართველოს მეცნიერებათა აკადემიის მოამბე, 159, №2, 1999
BULLETIN OF THE GEORGIAN ACADEMY OF SCIENCES, 159, №2, 1999

MECHANICS

T. Iamanidze

Investigation of the Dynamics of Rockbreaking Tool as the System with Nonlinear Elastic Characteristics

Presented by Corr. Member of the Academy K. Betaneli, December 30, 1998

ABSTRACT. **Investigating the dynamics of rockbreaking tool the results for defining the resistance of breaking tool with different working end configuration according to dynamic properties have been obtained.**

Key words: rockbreaking tool, dynamics.

To choose necessary interpretation for dynamics investigation of the system "breaking tool-rock" with different mathematical description is quite a difficult task. Though the consideration of a small number of parametres leads to simple mathematical models, the description itself suffers from schematism and does not show all the important characteristics of the investigated process.

The consideration of big number of parametres while giving the object more detailed description makes analysis difficult which leads to bulky computations. The interpretation of the obtained results becomes more complex because of a big number of varied parametres of the determined functional dependences.

Using the results of [1], we'll describe process of bumping interaction of the rock and rockbreaking tool by means of differential equations with initial conditions:

$$\ddot{h}+\frac{K_{sh}}{m}h=\frac{p}{m}\cos\omega t; \tag{1}$$

for cone tool:

$$\ddot{h}+\frac{K_c}{m}h^{1/2}=\frac{p}{m}\cos\omega t; \tag{2}$$

for spherical tool:

$$\ddot{h}+\frac{K_s}{m}h^{3/2}=\frac{p}{m}\cos\omega t; \tag{3}$$

for optimal tool:

$$\ddot{h}+\frac{K_o}{m}e^{\frac{\omega_0}{g}h}=\frac{p}{m}\cos\omega t; \qquad h(0)=\dot{h}(0)=0. \tag{4}$$

Members of dissipation $\Phi(t)h'$ were not taken into account.

General solving of homogeneous linear equation (1) is as follows:

$$h_0=C_1\cos\sqrt{\frac{K_{sh}}{m}}t+C_2\sin\sqrt{\frac{K_{sh}}{m}}t.$$

Solution (1) will be sought in:

$$h_1(t) = A\cos\omega t + B\sin\omega t. \tag{5}$$

Having differentiated (5) twice and put it into (1), we have general equation

$$h(t) = C_1 \cos\sqrt{\frac{K_{sh}}{m}}t + C_2 \sin\sqrt{\frac{K_{sh}}{m}}t + \frac{p/m}{K_{sh}/m - \omega}\cos\omega t. \tag{6}$$

From the given initial conditions we get:

$$C_1 = \frac{p/m}{K_{sh}/m - \omega^2}; \qquad C_2 = 0. \tag{7}$$

Thus, the solution (1) considering (7) will be:

$$h(t) = \frac{p/m}{K_{sh}/m - \omega^2}\left(\cos\omega t - \cos\sqrt{\frac{K_{sh}}{m}}t\right) \tag{8}$$

Solving nonlinear equations (2)-(4) we'll try to reform addends in their left parts in order to make approximated solution easier. For equations (2) and (3) we shall substitute $h = 1 + x$ into the formula

$$(1+x)^2 q = 1 + qx + \frac{q(q-1)x^2}{2!} + \ldots \tag{9}$$

We'll assume that h satisfies the conditions at which series (5) converges.

To solve the equation (4) we'll use the known function expansion Exp into a power series. Then equations (2)-(4) with the same homogeneous initial conditions to the following approximate equation

$$\ddot{h} + \alpha\dot{h} + \beta h^2 + \gamma h^3 = \frac{p}{m}\cos\omega t. \tag{10}$$

Let's note, that here initial conditions are already heterogeneous, as instead of h we have $(1+x)$ and $x(0) = -1$, $x'(0) = 0$. However, as a result it entails the additional constant component which is not interested for us.

Constants α, β, γ have different values for different tools:

$$\left.\begin{array}{lll} \textit{for cone (2)}, \alpha = \dfrac{K}{2m}; & \beta = -\dfrac{K}{8m}; & \gamma = \dfrac{K}{16m}; \\ \textit{for spherical (3)}, \alpha = \dfrac{3K}{2m}; & \beta = \dfrac{3K}{8m}; & \gamma = -\dfrac{K}{16m}; \\ \textit{for optimal (4)}, \alpha = \dfrac{K_0}{m}; & \beta = \dfrac{K_0}{m}\cdot\dfrac{\omega_0^2}{g}; & \gamma = \dfrac{1}{2}\dfrac{\omega_0^4}{g^2}\dfrac{K_0}{m} \end{array}\right\} \tag{11}$$

To solve the equation (10) we use the known method of harmonic linearization [2]. The first convergence of this equation will be found in:

$$h_1 = A\cos\omega t. \tag{12}$$

Substituting (12) into (10) we get:

$$-A\omega^2\cos\omega t + \alpha A\cos\omega t + \beta A\cos^2\omega t + \gamma A^3\cos\omega t = \frac{p}{m}\cos\omega t.$$

Taking into account some trigonometric correlation after some transformations we'll get

$$-A\omega^2+\alpha A+\frac{3\gamma A^3}{4}=\frac{p}{m}. \tag{13}$$

Equation (10) in the first approximation has solution (12) where the value A satisfies cubic equation (13).

To find the second approximation we'll use iteration method. Let's write (10) in:

$$\ddot{h}=\frac{p}{m}\cos\omega t-\alpha\dot{h}-\beta h^2-\gamma h^3$$

and into the right part we shall put first approximation h_1:

$$\ddot{h}=-A\omega^2\cos\omega t-\frac{\beta A^2}{2}\cos 2\omega t-\frac{\gamma A^3}{4}\cos 3\omega t-\frac{\beta A^2}{2}. \tag{14}$$

Integrating equation (14) twice, we'll get final solution:

$$h=A\cos\omega t+\frac{\beta A^2}{8\omega^2}\cos 2\omega t+\frac{\gamma A^3}{36\omega^2}\cos 3\omega t-\frac{\beta A^2}{4}t^2+C_1(t)+C_2, \tag{15}$$

where the constants C_1 and C_2 come out of the initial conditions.

In (13) constant β and γ for every instrument we can express with α: $\beta = B\alpha$ and $\gamma = C\alpha$, where B and C get values, corresponding to different tools.

Thus, (13) can be written:

$$-A\omega^2+\alpha A+\frac{3A^3}{4}C\alpha=\frac{p}{m}ng. \tag{16}$$

Analogous problem with the account of the resistance to friction can be solved:

$$\ddot{h}+K\dot{h}+\frac{K_{sh}}{m}h=\frac{p}{m}\cos\omega t; \tag{17}$$

$$\ddot{h}+K\dot{h}+\frac{K_c}{m}h^{1/2}=\frac{p}{m}\cos\omega t; \tag{18}$$

$$\ddot{h}+K\dot{h}+\frac{K_c}{m}h^{3/2}=\frac{p}{m}\cos\omega t; \tag{19}$$

$$\ddot{h}+K\dot{h}+\frac{K_o}{m}e^{\frac{\omega_0^2}{g}h}\cdot h=\frac{p}{m}\cos\omega t, \tag{20}$$

where $$K=\frac{r}{m}\left(\frac{\pi}{2}+\frac{4}{\pi}\frac{8}{9}\cos 3\omega t\right).$$

As in the previous case these equations can easily be substituted with the following expressions:

$$\ddot{h}+K\dot{h}+\alpha h+\beta h^2+\gamma h^3=\frac{p}{m}\cos\omega t, \tag{21}$$

where α, β and γ are calculated according to the formulae (11) (for chisel instrument $\alpha=\frac{K_g}{m}$; $\beta=\gamma=0$).

Let's look for the first approximation $h_1 = A\cos\omega t + B\sin\omega t$.

Substituting this expression in (21) and comparing coefficients at $\cos\omega t$ and $\sin\omega t$, we get the system of equations:

$$\left.\begin{aligned} -A\omega^2 + \frac{\pi r B\omega}{2m} + \alpha A + \frac{3\gamma A^3}{4} + \frac{3\gamma AB^2}{4} = \frac{p}{m}; \\ -B\omega^2 - \frac{\pi r B\omega}{2m} + \alpha B + \frac{3\gamma B^3}{4} + \frac{3\gamma A^2 B}{4} = 0. \end{aligned}\right\} \tag{22}$$

In these equations we'll ignore the last two summands because of order smallness. The expected simplification corresponds to the substitution of the first approximation not into the equation (21), but into the following:

$$\ddot{h} + \frac{\pi}{2}\frac{r}{m}\dot{h} + \alpha h = \frac{p}{m}\cos\omega t,$$

which does't bring the mistakes while constructing the first approximation.

Formulae to define coefficients A and B:

$$\left.\begin{aligned} A = \frac{4m(\alpha-\omega^2)p}{\pi^2 r^2\omega^2 + 4m^2(\alpha-\omega^2)^2}; \\ B = \frac{2p\pi r\omega}{\pi^2 r^2\omega^2 + 4m^2(\alpha-\omega^2)^2}. \end{aligned}\right\} \tag{23}$$

equation will be written:

$$\ddot{h} = \frac{p}{m}\cos\omega t - \frac{r}{m}\left(\frac{\pi}{2} + \frac{4}{\pi}\frac{8}{9}\cos 3\omega t\right)\dot{h} - \alpha h - \beta h^2 - \gamma h^3$$

and into the right part we shall put the expression for $h_1(t)$.

The final result is:

$$h(t) = A\cos\omega t + B\sin\omega t + \left(\frac{4rA}{9\pi m\omega} + \frac{\beta AB}{4\omega^2}\right)\sin 2\omega t + \left(\frac{4rB}{9\pi m\omega} + \frac{\beta A^2}{8\omega^2} - \frac{\beta B^2}{8\omega^2}\right)\cos 2\omega t +$$

$$+ \left(\frac{\gamma A^3}{36\omega^2} - \frac{3\gamma AB^2}{3\omega^2}\right)\cos 3\omega t + \left(\frac{3\gamma A^2 B}{36\omega^2} - \frac{\gamma B^2}{36\omega^2}\right)\sin 3\omega t + \frac{rB}{9\pi m\omega}\cos 4\omega t - \frac{rA}{9\pi m\omega}\sin 4\omega t. \tag{24}$$

If into (24) we put the values $r = 0$, the solution coincides with the solution without dissipation member.

Thus the obtained results can be used as the basis for defining the resistancde of breaking tool with different working end configuration according to dynamic properties and choice of the tool with definite configuration, taking into account tecnological conditions of its application with the aim of increasing of the effect processes of the breaking of mountain rock.

Georgian Academy of Sciences
G. Tsulukidze Institute of Mining Mechanics

REFERENCES

1. *T. Iamanidze.* K ustanovleniyu optimalnykh kharakteristik porodorazrushayushego instrumenta. IGM AN Gruzii 1991.
2. *V. Bessekerskii, E. Popov.* Teoriya sistem avtomaticheskogo regulirovaniya. M., 1966.

საქართველოს მეცნიერებათა აკადემიის მოამბე, 159, №2, 1999
BULLETIN OF THE GEORGIAN ACADEMY OF SCIENCES, 159, №2, 1999

MECHANICS

O. Kikvidze

Constitutive Equations for Shape Memory Materials when Deforming in the Temperature Intervals of Phase Transformation

Presented by Member of the Academy R. Adamia, March 11, 1998

ABSTRACT. **Constitutive equations of shape memory materials for calculation of increments of nonelastic phase strain components, which describe nongradient flow relatively to loading surface, are given. Additive principle for increment of full strain components is used.**

Key words: strain, martensitic, transformation, increment.

Constitutive equations, which adequately describe the condition of material for the given thermomechanical loading, are of great importance for solving the boundary problems of solid body mechanics.

It is known [1], that the efficient performance of shape memory effect in the solid bodies takes place before plastic strains, and so in calculation it is supposed that plastic strains for given thermomechanical loading don't arise.

According to additive principle, increment of full strain components may be presented as:

$$d\varepsilon_{ij} = d\varepsilon_{ij}^{e} + d\varepsilon_{ij}^{T} + d\varepsilon_{ij}^{Q}, \tag{1}$$

where ε_{ij}^{e}, ε_{ij}^{T} are components of elastic and temperature strains, ε_{ij}^{Q} are the components of nonelastic strains that are bound up with phase (martensitic) transformations and arise at shape memory materials (SMM) thermomechanical loading in the temperature interval of martensitic transformation.

The increments of elastic and temperature strain components are calculated by thermoelasticity theory. The values of ε_{ij}^{Q} are calculated as:

$$d\varepsilon_{ij}^{Q} = d\varepsilon_{ij}^{F} H(M_s - T)H(T - M_f) + d\varepsilon_{ij}^{MF} H(T - A_s)H(A_f - T), \tag{2}$$

where ε_{ij}^{F} are the components of phase strains, that arise by direct martensitic transformation, $d\varepsilon_{ij}^{MF}$ are the components of shape memory strains, that return by reverse martensitic transformation, M_s, M_f are the start and end temperatures of direct martensitic transformation accordingly, A_s, A_f are the start and end temperatures of reverse martensitic transformation of accordingly, H is Heaviside's function.

Arguments of Heaviside's function are chosen so, that the phase strain components are zeros outside the interval $[M_s, M_f]$, while the shape memory strain components are zeros outside the interval $[A_s, A_f]$.

Increments of phase strain components, in the small strains are calculated as [2]:

$$d\varepsilon_{ij}^{F} = a_{kl} d\varepsilon_{kl}^{F} / \partial\sigma_{ij} dT + d\lambda \partial f / \partial\sigma_{ij}, \tag{3}$$

$$d\lambda = \sqrt{3/2} d\varepsilon_{e}^{*F} / \sqrt{\partial f / \partial\sigma_{ij} \partial f / \partial\sigma_{ij}}, \tag{4}$$

$$\overline{d\varepsilon_{e}^{*F}} = \sqrt{2 de_{ij}^{*F} de_{ij}^{*F} / 3}, \tag{5}$$

$$d\varepsilon_{ij}^{*F} = \partial\varepsilon_{kl}^{F} - a_{kl}\partial\varepsilon_{ij}^{F} / \partial\sigma_{ij} dT, \quad (6)$$

where the tensor components a_{kl} located on the main diagonal are equal and the components with different indexes are equal too, σ_{ij} are the stress tensor components, f defines surface of loading and satisfies the condition (z is the hardening parameter)

$$f(\sigma_{ij}, T, z) = 0. \quad (7)$$

Equation (3) geometrically means, that vector de^{*F} with the components $d\varepsilon_{ij}^{*F}$ and the vector gradient of function f with the components $\partial f/\partial\sigma_{ij}$ are collinear, while increment of phase strain vector $d\varepsilon^{F}$ is not perpendicular to surface f, i.e. the flow is nongradient.

Formulae (3)-(6) allow to calculate shear strains, caused by the change of temperature. These shear strains are important for calculating the shape memory bodies, because on the example of torsion thin-walled tubes it is experimentally established, that if we take off torsion moment and continue cooling of the body in the temperature interval of direct martensitic transformation, then phase shear strain is generated [1]. Formula (3) takes into account dilatation by phase transformation. If shear strains do not arise, then in the case of thermoelastic martensitic transformation ($\varepsilon_{ii}^{*F} \approx 0$), $\overline{d\varepsilon_{e}^{*F}} = \overline{d\varepsilon_{e}^{F}}$, and from formulae (3)-(6) we have thermoplasticity theory [3].

Direct and reverse martensitic transformation strain mechanism is similar. Therefore increments of shape memory strain components are calculated by afore mentioned formulae with opposite sign.

If formula (3) and dependencies of thermoelasticity theory of isotropic materials substitute in the expression (1), we have

$$d\varepsilon_{ij} = [d\sigma_{ij} - \delta_{ij} d(3\nu\sigma_0/(1+\nu))]/(2G) + (\alpha\delta_{ij} + a_{kl}\partial\varepsilon_{kl}^{F}/\partial\sigma_{ij})dT + d\lambda\partial f/\partial\sigma_{ij}, \quad (8)$$

where G is the shear module, ν is the - Poisson's coefficient, σ_0 the hydrostatic stress, α the coefficient of line expansion, δ_{ij} -the Kronecker's symbol.

Designate $\alpha_{ij} = \alpha\delta_{ij} + a_{kl} d\varepsilon_{kl}^{F} / d\delta_{ij}$. The values of α_{ij} may be considered as generalised coefficient of temperature expansion. When writing formula (8) it is supposed that $G = const$ and $\alpha = const$, that considerably simplifies model of material. $G(T)$ and $\alpha(T)$ functions may be established when corresponding experimental data of SMM testing are treated. Calculation of non-linear coefficient $d\lambda$ can be done by the iteration method such as the method of additional strains.

Equations (8), $\overline{d\varepsilon_{e}^{F}}$ calculation formula [4], geometrical equation and equilibrium equations with corresponding boundary conditions make the closed system of equations whose solution gives SMM stress-strain situation by thermomechanical loading in the temperature interval of martensitic transformations.

Kutaisi Technical University

REFERENCES

1. *V. A. Likhachov, S. L. Kuzmin, Z. P. Kamentseva.* Shape Memory Effect. Leningrad,1987, 216.
2. *N.A.Machutov, O.G.Kikvidze.* Industrial Laboratory (Diagnostics of Materials). **6**, 1996, 46-48.
3. *I. A. Birger.* Proc. AS USSR. Mechanics and Mechanical Engineering. **1**, 1994, 113-119.
4. *O. G. Kikvidze.* RAS. Problem of Mechanical Engineering and Reliability Machinery, **2**, 1996, 51-56.

საქართველოს მეცნიერებათა აკადემიის მოამბე, 159, №2, 1999
BULLETIN OF THE GEORGIAN ACADEMY OF SCIENCES, 159, №2, 1999

PHYSICS

R. Kokhreidze, S. Odenov, J. Sanikidze

The Josephson Junctions Based on the Composite High Temperature Superconductors

Presented by Corr. Member of the Academy T.Sanadze, February 16, 1998

ABSTRACT. **In this article Josephson junctions in the composite high temperature superconductors (HTSC) are investigated. Between two HTSC regions there was a layer consisting of the composite $Y_1Ba_2Cu_3O_{7-X}$ and $Y_2Ba_1Cu_1O_5$. It is shown that the sample has a clear Josephson effect, when the HTSC concentration in the composite was near the edge of the percolation limit.**

Key words: superconductivity, HTSC composite, Josephson effect.

One of the main superconducting electronic elements is based on the well known Josephson effect[1]. The Josephson junctions have many applications in cryoelectronic devices[2,3]. After the high temperature superconductors (HTSC) were discovered, it became evident that the Josephson effect is one of their important applications[4]. The principal difficulty was to obtain mechanically durable, stable, controllable and reproducible junctions (weak links), made of HTSC.

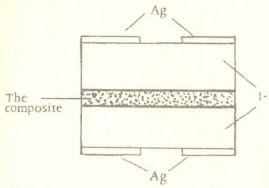

Fig.1

We investigated the percolation processes in HTSC composites[5]. It became evident that such systems may have some Josephson-like properties and for their further improvement it was necessary one of the components of the system to be high enough electrical resistivity. For this purpose the insulator $Y_2Ba_1Cu_1O_5$ was chosen.

The percolation processes in this composite are dependent on many parameters. For the improvement of junction characteristics it was necessary to investigate them and choose an optimal correlation of these parameters in two phase mixtures of HTSC $Y_1Ba_2Cu_3O_{7-X}$ and $Y_2Ba_1Cu_1O_5$.

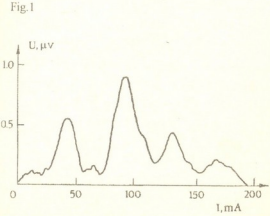

Fig.2

The structure of the samples was the following. Between two HTSC regions there was a layer consisting of the composite (Fig.1). The experiments on these samples showed that the samples had a clear Josephson effect when the HTSC concentration in the composite was near the edge of the percolation

limit. Later the technology of the samples fabrication was modified. In Fig.2 the dependence of the junction voltage on the magnetic flux created by a current in a small coil is shown. The value of the field was of the order of 10^{-3}Gs. The dependence is fully repeating the classical stationary Josephson effect:

$$U \sim \left| \frac{\sin \pi \Phi / \Phi_0}{\pi \Phi / \Phi_0} \right|, \tag{1}$$

where Φ is the magnetic flux in the junction and Φ_0 is one quant of the flux.

The non-stationary effect is given by the relation:

$$2eU = h\nu. \tag{2}$$

Here $2e$ is electron pair charge, h is Plank constant, ν the frequency of the radiation emitted by the junction, when the voltage is equal to U. There also exists an analogical effect.In presence of external radiation on the voltage-current characteristics little jumps of the current are observed, when the voltage corresponds to(2). In Fig.3 the jumps on the characteristics are shown according to relation(2). This demonstrates that in our samples we have seen Josephson effect.

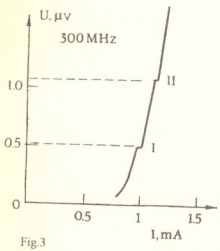

Fig.3

The annealing has an effect on the critical current and resistivity of the junctions. The sample properties may to some extent be controlled by varying annealing time. The samples almost did not change their critical parameters at a number of temperature cycles from 77K to 300K. They proved to be mechanically durable and do not suffer from water vapour influence.

This work was supported by the grant of the Georgian Academy of Sciences.

Georgian Academy of Sciences
Institute of Cybernetics

REFERENCES

1. *B. Josephson.* Phys. Lett. **1**, 1962, 251.
2. *A. Barone, G. Paterno.* Physics and applycations of the Josephson effect. N.Y.,1962.
3. *Van Duser, T.Turner C.* Principles of Superconductivity Devices and Circuits. Elsevier, N.Holland,1981.
4. *J. Bednorz , K.Muller.* Earlier and Recent Aspects of Superconductivity. Springer Verlag, 1990.
5. *J. Sanikidze, S. Odenov, R. Kokhreidze et al.* Superconductivity, **4**, 7, 1991, 1218.

საქართველოს მეცნიერებათა აკადემიის მოამბე, 159, №2, 1999
BULLETIN OF THE GEORGIAN ACADEMY OF SCIENCES, 159, №2, 1999

PHYSICS

N. Dolidze, G.Eristavi, Z.Jibuti, M.Pkhakadze, S.Avsarkisov, M.Merabishvili

Investigation of Photo-stimulated Diffusion Processes in III-V Semiconductors

Presented by Member of the Academy J. Lominadze, March 19, 1998

ABSTRACT. **The paper presents the results of investigation of photo-stimulated diffusion (PSD) processes from continuous source in the GaAs, GaAlAs and GaP during formation of ohmic contacts, p-n junctions, p^+ and n^+ areas and insulation regions. It is shown, that during PSD along with the temperature the role of the ionization factor is very significant. It is suggested, that in the III-V compounds the atoms of the III group might be more mobile during pulse-photon irradiation and probability of vacancy generation in these points might be higher in comparison with the points of the V group atoms.**

Key words: photo-stimulate diffusion, pulse-photon irradiation.

It is well-known that decrease of time and temperature in technological processes of semiconductor device production improves the device characteristics. Limited possibilities of the traditional technology do not permit us to solve these problems. Photo-stimulated processes allow us to eliminate such undesirable factors as creation of special media and a long-term high-temperature heating. This fact is particularly important for III-V compounds.

In the present work the results of the investigation of photo-stimulated diffusion (PSD) processes in the GaAs, GaAlAs and GaP are given. The photo-stimulated diffusion from continuous source was investigated in the process of formation of ohmic contacts, p-n junctions, p^+ and n^+ areas and insulation regions (Table).

Pulse-photon irradiation (PPI) was carried out in the air on a specially designed PPI system by pulses of nonmonochromatic light from tungsten halogen lamps with duration $\tau = 0.1 \div 90$s and radiation power $P=10 \div 300\ W \cdot cm^{-2}$. The structures were irradiated from metal composition side (face side) or the semiconductor side (back side). The wafer temperature was estimated by using a chromel-alumel low-inertial thermocouple (of 0.1 mm thickness).

The optimal regimes for creation of different areas and optimal values of their control parameters after PSD are given in the Table. The last column illustrates the regimes of traditional thermal treatment for comparison. As seen from the Table, formation of one and the same areas, proceeds in easy conditions (without especial medium - in air, small times, relatively less temperatures). It should be noted, that in all the given cases (Table) a number of general regularities are observed:

In one and the same PPI conditions the better results are obtained under irradiation from the back side. For example, in formation of ohmic contacts to GaAs by PPI ($P = 90\ Wcm^{-2}$ and $\tau = 1.9$ s) irradiation from the face side gives $R_c = 0.9\ Ohm.mm^{-1}$ on average, while

Table
Data experiments of photostimulated Diffusion in III-V Compounds. The last column illustrates regimes of Traditional thermal Treatment for comparison.

Formation of	Semicond	Impurity concentr, cm^{-3}	Metal composition	Pulse photon irradiation on the air			measured control parameters	Regimes of traditional thermal treatment
				Pulse power, $w.cm^{-2}$	Pulse duration, sec	Pulse number		
Ohmic contact	epitaxial structure GaAs, i-n-n	$1.5.10^{17}$	Au/Ge/Ni	90	1,9	1	contact resistance R_c =0,7 Ohm.cm^{-2}	vacuum 745K, 1 min
	light emission. structure GaAlAs: -						forward voltage U_{for} =1.6 V,	
Ohmic contact	n-GaAlAs	10^{18}	Pd/Ni/Au/Sn	40	1,8	1	at I_{for} =10 A.	vacuum, 720 K, 10 min
	p-GaAs	$3\div20.10^{18}$	Pd/Ni/Au/Zn	40	1,8	1		720 K 10 min
	light emission. structure GaP:							vacuum, 1000 K, 15 min
p^+ - area	p - GaP	5.10^{17}	Zn	90	1,6	1		
Ohmic	p^+ - GaP	$\sim10^{19}$	Al	80	1,3	1	forward voltage	720 K, 10 min
contact	n - GaP	5.10^{17}	Pd/Ni/Au/Sn	80	1,3	1	U_{for}=2,1 V, at I_{for} =10 mA	720 K, 10 min
n^+ - area	n - GaAs	$1.7.10^{16}$	Ge	70-90	1-3	1-3	surface resistance decreasc 10^3 fold	[10] Si_3N_4 mask >673K, >15 min
p^+ - area	p - GaAs	7.10^{16}	Zn	40-90	1-3	1-7	surface resistance decrease 10^3 fold	[10] Si_3N_4 mask >673K, >15 min
n-p junction	n - GaAs	7.10^{16}	Zn	50-90	1,5-3	1-5	U_{for}=0,4-0,6V and U_{inv}=6-8 V at I =10^{-4} microA	[10] Si_3N_4 mask >973K, >15min
i - area (with SiO_2 mask)	epitaxial structure GaAs, i - n - n	$1.5.10^{17}$	Cr	55-90	2-5	1-20	current between test cells I =35-40 microA, at U =10 V	—

after irradiation from the back side $R_{\square} = 0.7$ Ohm.mm^{-1}. In this case the structure temperature $T \leq 700$K. Thermal burning-in in the furnace gives $R_{\square} = 1.0$ Ohm · mm^{-1}.

The irradiation intensity is very important. If the structures are irradiated with less powerful but longer pulses ($P = 30$W·cm^{-2}, $\tau = 10$s), at which the same temperatures as in the above example are achieved, the contacts remain rectifying.

After thermal burning in all the structures the contact surface is coarse-grained with signs of melting, while after PPT it remains mirror-smooth and the uniform distribution of electrophysical parameters throughout the surface increases (Fig.).

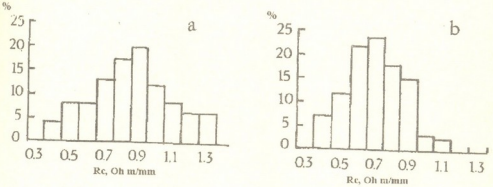

Fig. Histograms of Rc parameter distribution over the wafers:
a) after burning-in in the furnace (T = 745K, t = 1min.),
b) after PPI (P = 90 W.cm^{-2}, t = 1.9 sec.).

It is impossible to account the obtained results, as well as those of [1-4], for the pulse thermal heating only, as it is regarded by majority of researchers [5]. It is necessary that, along with the temperature the role of the ionization factor - the change in the quantum state of the crystal electron subsystem to be taken into account [1-4]. Indeed, as seen from the foregoing experiments, at higher intensity (while the temperature is the same and pulse duration is markedly small) the diffusion proceeds more actively. The mere fact, that diffusion from the metal multilayer is more intensive when irradiation occurs from the back side must be due to the absorption of the photons with lower energy than the band gap, passing through the semiconductor, directly in the defect near-contact semiconductor-metal interface. In this region breaking of the chemical bonds –jump of the electrons from the bonding orbitals to the antibonding orbitals takes place [2,6], which favours solid phase photostimulated diffusion providing the mirror-smooth surface. The very important role of the ionization factor in photo-stimulated processes for the IV group semiconductors is shown in [2]. Unlike the group IV semiconductors, binary semiconductor compounds have the structure with two different atoms in the unit cell and bonding forces are partially covalent and partially ionic. The bonding electron density is nonuniformly distributed between the atoms and the electron density decreases in interstials. Besides, the electron cloud around the element with a lower number of valence electrons is somewhat smaller than it is necessary for total positive charge compensation and on the contrary, around the elements with a higher number of valence electrons it is much bigger than it is necessary for compensation.

It is shown in [7] that the probability of defect formation according to Frenkel depends on the antibonding particle concentration $\sim n^3$, and the diffusion coefficient is pro-

contrary, around the elements with a higher number of valence electrons it is much bigger than it is necessary for compensation.

It is shown in [7] that the probability of defect formation according to Frenkel depends on the antibonding particle concentration $\sim n^3$, and the diffusion coefficient is proportional to $\sim n^5$ [8]. Hence, the probability of defect formation is higher in the crystal points with lower density of bonding electrons. The atoms in such points should also have a higher selfdiffusion coefficient (which is born out by the experiments [9]) . Here, it should be also taken into account that almost in all binary semiconductor compounds the mass of antibonding electrons is lower than that of the holes and antibonding electrons appearing more often in the points, where a positive nuclear charge is not fully compensated by electrons. Thus in III-V compounds the atoms of group III should be more mobile and probability of vacancy generation in this points should be higher in comparison with the point group V atoms.

From these considerations the role of irradiation intensity in PSD processes will be easily understood. During PPI in the III group atoms sublattice vacancies are intensively generated, where the substitution of displaced atoms by diffuser atoms takes place. As a result diffusion actively proceeds in small times and at relatively less temperatures.

Tbilisi I. Javakhishvili State University

REFERENCES

1. *A. G. Italiantsev, V. N. Mordkovich, E. M. Temper*. Fiz. Tekh. Poluprov., **18**, 5, 1984, 928 (Russian).
2. *I. G. Gverdtsiteli, A. B. Gerasimov, Z. V. Jibuti, M. G. Pkhakadze*. Poverkhnost, **11**, 1985, 132 (Russian).
3. *Z. V. Jibuti, N. D. Dolidze*. Pis'ma v Zh.Tekh.Fiz. 5, 1991, 41 (Russian).
4. *A. B. Gerasimov, Z. V. Jibuti, M. A. Kuprava, M. G. Pkhakadze*. Bull. Georg. Acad. Sci., **145**, 1, 1992, 67 (Russian).
5. *A. V. Dvurechenski, G. A. Kachurin, E.V.Nidaev, L.S.Smirnov*. Impulsnyi otdzig v poluprovodnikovykh materialakh, M., 1982, 208 (Russian)
6. *V. V. Kapaev, U. V. Kopaev, S. N. Molotkov*. Mikroelektronika, **12**,6,1983, 499 (Russian).
7. *I. G. Gverdtsiteli, A. B. Gerasimov, Z. G. Gogua et al.* Bull. Georg. Acad. Sci., **127**, 3, 1987, 517 (Russian).
8. *I. G. Gverdtsiteli, A. B. Gerasimov, Z. G. Gogua, Z. V. Jibuti, M. G. Pkhakadze*. Bull. Georg. Acad. Sci., **128**, 2, 1987, 293 (Russian).
9. *B. I. Boltaks*. Diffusiya i tochechnye defekty v p/p-. L-d., 1972, 265 (Russian).
10. *A. V. Cherniyaev*. Metod ionnoi implantatsii v tekhnologii priborov i integralnykh skhem na arsenide galliya. M, 1990, 88 (Russian).

საქართველოს მეცნიერებათა აკადემიის მოამბე, 159, №2, 1999
BULLETIN OF THE GEORGIAN ACADEMY OF SCIENCES, 159, №2, 1999

PHYSICS

A. Bichinashvili, M. Zviadadze, N. Papuashvili, T. Mkhatrishvili, V. Achelashvili

Microtension Regulation within the Martensite - deformative Alloys

Presented by Corr. Member of the Academy N. Tsintsadze, August 31, 1998

ABSTRACT. **The present work outlines the phenomenon of microtension regulation within the martensite-deformative alloys when the correlation within these tensions is observed. We receive the correlation formula by using the quasi-chemical method that represents the function of hyperbolic tangent. Calculations of the parameters of regulating energy and leaping of thermal capacity at critical temperature are given.**

Key words: martensite-deformative alloys, quasi-chemical method.

We have introduced the parameter of microtension regulation in our previous work.

$$L = \frac{N_1 - N_2}{N}, \tag{1}$$

where $N = N_1 + N_2$, N_1 is the quantity of microtensions in the direction of deformation axis, while N_2 – on the contrary. On the other hand L parameter is connected with the deformation of the form restoration in the following way

$$L = \frac{\varepsilon}{\varepsilon_0}, \tag{2}$$

where ε_0 is preliminary plastic deformation. The leaping of the thermal capacity by using the Breg Williams theory was calculated in the above-mentioned work when the correlation is not considered.

The work aims to calculate the same parameter considering correlation within the microtensions and using the quasi-chemical method [1].

The quasi-chemical method is based on admitting the fact that every couple of microtensions may be examined as an independent "molecules" and their free energy corresponds to V_{11}, V_{22}, V_{12}.

Suppose that the martensite-deformative alloys include N microtensions. In case we denote by N_{12} the quantity of the couple microtensions then the free energy could be

$$F = U - TS = U - KT\,LnW, \tag{3}$$

where

$$U = -N_{11}U_{11} - N_{22}U_{22} - U_{12}(N_{12} + N_{22}). \tag{4}$$

According to this system the figure of the various configurations would be proportional to the variant of the figure dividing N_{12} the quantity of the total couples into four N_{11}, N_{22}, N_{12}, N_{21}

$$L = h(L)\frac{(ZN/2)!}{N_{11}!N_{22}!N_{12}!N_{21}!}, \tag{5}$$

Where Z is the coordinate figure. $H(L)$ multiplier depends on L parameter. On the other hand these parameters equal to the variant figure that consists of N_1 and N_2 tensions.

$$W = \frac{(N/2)!}{N_1!\,N_2!}. \tag{6}$$

From (5) and (6) we receive

$$H(L) = \frac{(N/2)!\,N_{11}^0!\,N_{22}^0!\,N_{12}^0!\,N_{21}^0!}{(ZN/2)!\,N_1!\,N_2!}, \tag{7}$$

where $N_{11}{}^0$, $N_{22}{}^0$, $N_{12}{}^0$, $N_{21}{}^0$ correspond to the quantity of the coupled tensions during the discord distribution. Thus

$$W = \frac{(N/2)!\,N_{11}^0!\,N_{22}^0!\,N_{12}^0!\,N_{21}^0!}{N_1!\,N_2!\,N_{11}!\,N_{22}!\,N_{12}!\,N_{21}!} \tag{8}$$

Considering (4) and (8)

$$F = -N_{11}V_{11} - N_{22}V_{22} - V_{12}\,(N_{12}+N_{22}) - KT\,\{N/2(LnN/2-1) + N_{11}{}^0\,(LnN_{11}{}^0 - 1) +$$
$$N_{22}{}^0(LnN_{22}{}^0 - 1) + N_2{}^0(LnN_{12}{}^0 - 1) + N_{21}{}^0(LnN_{21}{}^0 - 1) - N_1(LnN_1 - 1) - N_2{}^0(LnN_2{}^0 - 1) -$$
$$N_{11}(LnN_{11} - 1) - N_{22}(LnN_{22} - 1) - N_{12}(LnN_{12} - 1) - N_{21}{}^0(LnN_{21}{}^0 - 1)\}. \tag{9}$$

N_1, N_2, N_{12}, N_{21} are connecting to one another in the following manner:

$$N_1 + N_2 - N = 0 \qquad 2N_{11} + N_{12} - ZN_1 = 0$$
$$2N_{22} + N_{12} - ZN_2 = 0 \tag{10}$$

In order to calculate F these auxiliary parameters may be considered by the Lagrange multiplier method. Introduce auxiliary function

$$\varphi = F + b_1\,(N_1 + N_2 - N) + b_2\,(N_{11} + N_{12} - ZN_1) + b_3\,(2N_{22} + N_{12} - ZN_2) \tag{11}$$

Considering the condition of minimum we have

$$\frac{\partial\varphi}{N_1} = 0, \quad \frac{\partial\varphi}{N_2} = 0, \quad \frac{\partial\varphi}{N_{12}} = 0, \quad \frac{\partial\varphi}{N_{21}} = 0, \quad \frac{\partial\varphi}{N_{11}} = 0, \quad \frac{\partial\varphi}{N_{22}} = 0, \tag{12}$$

Considering the conditions of (12) we receive the following from (11)

$$KT[LnN_1 - 4Z(N_1/N\,LN_{11}{}^0 + N_2/N\,LN_{12}{}^0)] + b_1 - Zb_2 = 0 \tag{13}$$

$$KT[LnN_2 - 4Z(N_2/N\,LN_{22}{}^0 + N_1/N\,LN_{12}{}^0)] + b_1 - Zb_3 = 0 \tag{14}$$

$$-U_{11} + KTLnN_{11} + 2b_2 = 0 \tag{15}$$

$$-U_{22} + KTLnN_{22} + 2b_3 = 0 \tag{16}$$

$$-U_{12} + KTLnN_{12} + b_2 + b_3 = 0 \tag{17}$$

$$-U_{21} + KTLnN_{21} + b_2 + b_3 = 0 \tag{18}$$

Add (17) to (18) and then deduct the sum of (15) and (16). We receive

where ε is the correlation parameter.

To solve the quadratic equation considering (20) we would have

$$\varepsilon = \frac{1}{4} th \frac{\varpi}{4KT}. \tag{19}$$

The second root is not examined as the correct physical result is not achieved. Take (14) from (13) and we would have

$$(4Z-1)Ln\frac{1+L}{1-L} = \frac{Z}{2} Ln\frac{(1+L)^2+4\varepsilon}{(1-L)^2+4\varepsilon}. \tag{20}$$

Expand the right and the left sides by Tailor range. At critical temperature e.i. when $L \to 0$ we receive

$$(4Z-1)2L = \frac{Z}{2}\frac{4L}{1+4\varepsilon} \tag{21}$$

from (19) and (22) we receive

$$\frac{1}{4} th \frac{\varpi}{4KT} = -\frac{3Z-1}{4(4Z-1)} \tag{22}$$

Expand by the critical temperature considering (23).

$$\frac{\varpi}{4KT} = -\frac{4(3Z-1)}{4Z-1}$$

when $Z = 4$ and $v/KT_0 \approx 3$
from (4) and (3) we receive

$$U = -\frac{NZ}{8}[E_0 + \varpi L^2 - 4\varepsilon\varpi] \tag{23}$$

where $E_0 = V_{11} + V_{22} + 2V_{12}$

The thermal capacity when $T > Tk$, e.i. $L = 0$, according to (19) would be

$$Cv = \frac{\partial U}{\partial T} = \frac{NKZ}{32}\left(\frac{\varpi KT}{Ch\varpi / 4KYT}\right)^2 \tag{24}$$

when $T < Tk$ from (19) and (22) we have

$$\Delta Cv = \frac{3}{8} NK \frac{Z-2}{Z-1}\left(ZLn\frac{Z}{Z-2}\right)^2 \tag{25}$$

Georgian Technical University

REFERENCES

1. *A. A. Smirnov.* Molekulyarno-kineticheskaya teoriya metallov, M., 1966 (Russian).

საქართველოს მეცნიერებათა აკადემიის მოამბე, 159, №2, 1999
BULLETIN OF THE GEORGIAN ACADEMY OF SCIENCES, 159, №2, 1999

PHYSICS

N. Kekelidze, L. Akhvlediani, G. Kekelidze, S. Laitadze, N. Macharadze

Creation of the Highly Doped and Homogeneous InAs, InP Compounds, InAs-InP Solid Solutions and the Determination of some Fundamental Parameters

Presented by Member of the Academy R. Salukvadze, February 2, 1998

ABSTRACT. **The highly doped and homogeneous specimens were created with the help of technology elaborated by us . In case of InAs the creation of highly doped crystals made possible to determine band structure and nonparabolicity of materials.**

Key words: electron effective mass, band structure, nonparabolicity, homogeneity.

The measurement of the electron effective masses makes possible to determine semiconductors' band structure and as the conduction band of InP_xAs_{1-x} solid solutions and their binary components are nonparabolic it is necessary to create the highly doped but homogeneous and perfect materials. It is also necessary to determine doping upper limit and admissible carrier concentration for application of the Kane theory. We had created the specimens on the three-zone device by the method elaborated by us [1].

The created specimens were of high purity and homogeneous. Doping was effected by tellurium (Te). It has sufficiently high dissolution in III-V compounds and relatively low ionization energy therefore it may be applied for doping of crystals in a wide interval. The necessary amount of Te for doping (~12mg) up to the corresponding concentration is weighed with indium (In) placed in the boat. The temperature of synthesis zone slowly increased up to temperature of synthesis zone of corresponding material ($+20^0$C). For dissolution of Te in In the braking occurs at 490^0C. The temperature of cold brims of ampoule is raised step by step up to 450^0C . Braking comprises an hour. Phosphorus is evarorated and is dissolved in In-Te binary solution till 600^0C. Braking comprises an hour. For concervation of equilibrium pressure As is also evaporated and is dissolved in In alloy till $750\ ^0$C. Braking comprises 0.5 hour. By slow decrease of temperature till 700^0C makes the narrowing of synthesis zone with velocity of 8 mm/hr towards the brim of ampoule and reversible passage of synthesis zone with width of 5 mm occurs 3-4 times with velocity of 1mm/hr along the ingot for uniform distribution of impurities. At this time the joining of fine-grained structures takes place as coarse-grained monocrystalline blocks or one monocrystal is formed. The repeated melting forms the concetration gradient with crystallization front inverse to concentration gradient which was formed by first melting. It promotes averaging of alloy composition. Repeated process of band recrystallization increases homogeneity of semiconductive substance.

Te-doped InAs specimens with the electron concentration of 3.8×10^{17}-2.25×10^{19} cm^{-3} and solid solutions with the electron concentration of 8.7×10^{17}- 1.5×10^{19} c.

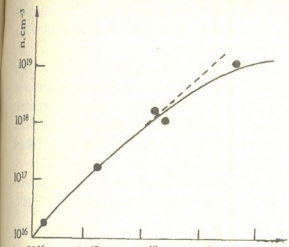

Fig.1. The dependence of electron concentratioon on impurities concentration in Te-doped crystals.

the impuritiy concentration of Te-doped InAS. It is clear , that by the weak doping ($n \sim 10^{18}$ cm^{-3}) the carrier concentration is not distinguished from impurity concentration. The investigations show that by high-doping the impurities behaviour is distinguished from impurities like a hydrogenous. This obviously can be explained by the several positions of Te because of formation of complexes by the interaction of the Te with the structural defects and by formation of neutral complexes of In_2Te type. Inflection points (Fig.1) correspond to the moment when impurities concentration is greater than carrier concentration and maximum dissolution of Te is ($\sim 8\times10^{19}$ at/cm^3).

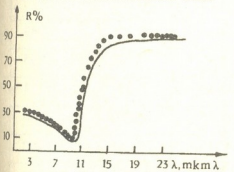

Fig.3. The spectral dependence of reflection coefficient for $InP_{0.3}As_{0.7}$ with $n = 4.5\times10^{19}$ cm^{-3} (points-experiment, full line-theory).

m^{-3} had been grown. InAs was growing from stechiometric alloy of InAs-Te polythermal section. In the case of In_2Te_3, As_2Te_3 and solid solutions formed by doping to low concentration the P_2Te_3 compositions have been dissociated during crystallization and one can suppose that dissolution of Te at azot temperature is atomic. At this time it occupies the place of As and P in lattice points and is donor like hydrogenous. As a matter of fact electrophysical measurements show the appearance of thin donor levels in sublattice of weakly Te-doped As and P (~0,006 ev).

Fig.1 represents the curve of dependence of the electron concentration upon

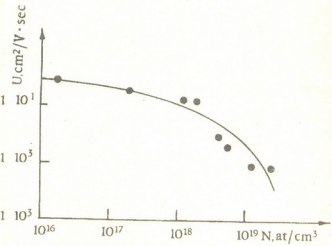

Fig. 2. The dependence of mobility of electrons on impurity concentration.

Fig.2 shows the carrier concentration dependence on the impurities concentration. The strong influence of impurities takes place over the value of mobility in the high concentration area. The optical reflection spectra caused by free carriers provides the determination of the electron effective masses.

Free carrier effective masses had been determined from spectral running of reflection coefficient by means of method [2]. Infrared reflection

spectrum in highly doped crystals had been registered in the area of 2-35 μm using an UR-20, IKC-21 spectrometers. The electrons concetration and mobility had been determined by measuring the Hall effect and electroconductivity.

For the experimental curves of reflection coefficient of InP_xAs_{1-x} (x=0; 0,1; ….0,9; 1) the theoretical curve had been chosen for each specimen separately. Making theoretical curves in compliance with experimental curves were realized with the help of computing technology. Fig.3 shows the spectral running of the reflection coefficient for one of the specimen ($n\text{-}InP_{0,3}As_{0,7}$, $n=4,5\times10^{19}cm^{-3}$). Theoretical curve (full line) obtained, taking into account the scattering mechanism, is in good agreement with the experimental curve (points).

Experimental values of the carrier effective masses were compared with the theoretical values calculated according to the Kane theory. The results are given in the Table. From this theory a formula

$$\frac{m_n^*}{1-m_n^*} = \frac{3/E_y}{\frac{2}{E_g}+\frac{1}{E_g+\Delta}}$$

is obtained for the electron effective masses (m_n^*) at the bottom of the conduction band where E_g is the energy gap (forbidden zone) , D is the value of spinorbital splitting and E_p is the energy parameter. It should be noted that in highly doped solid solutions Fermi level is lifted at 0.1-0.2eV where the nonparabolicity is more considerable and the experimental values of the electron effective masses differs from their values at the bottom of the conduction band. Therefore for the purpose of comparison electron effective masses at

Table

Composition	Electron concetration	Electron effective masses at the bottom of the conduction band		Electron effective mass at the Fermi level m_μ	
		by the Kane theory	by experiment	by theory	by experiment
InAs	$3.5\cdot10^{18}$	0.023	0.022	0.073	0.075
$InP_{0,1}As_{0,9}$	$1.5\cdot10^{19}$	0.026	0.026	0.068	0.070
$InP_{0,1}As_{0,9}$	$8.7\cdot10^{17}$	0.026	0.026	0.036	0.039
$InP_{0,2}As_{0,8}$	$8.4\cdot10^{18}$	0.031	0.030	0.060	0.065
$InP_{0,2}As_{0,8}$	$4.3\cdot10^{18}$	0.031	0.030	0.051	0.053
$InP_{0,3}As_{0,7}$	$4.5\cdot10^{19}$	0.035	0.035	0.097	0.100
$InP_{0,5}As_{0,5}$	$7.2\cdot10^{18}$	0.045	0.046	0.068	0.069
$InP_{0,6}As_{0,4}$	$2.5\cdot10^{18}$	0.051	0.050	0.062	0.065
InP	$6.0\cdot10^{18}$	0.073	0.075	0.092	0.095

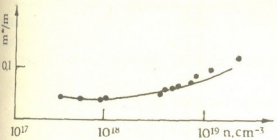

Fig.4. The dependence of electron effective masses on concentration (points-experiment, full line-by Kane theory).

Fermi level were calculated from the formula of Kolodziejczak obtained on the basis of the Kane theory [3]. As the Table shows there is a good agreement with the theory and experiment till the electron concentration of $n = 1.5 \times 10^{19}$ cm^{-3} which indicates the highquality and homogeneity of grown specimens. For the determination of conduction band structure and to determine the concentration limit for application of the Kane theory the electron effective masses in InAs were calculated. Here nonparabolicity is varied essentially. At the same time in case of InAs there are discrepancies between the values of the carrier effective masses in the literature. Fig. 4 represents the dependence of the electron effective masses on concentration. The theoretical curve is constructed according to the Kane theory. Fig. 4 shows that experimental and theoretical values coincid, till concentration of $n = 10^{19}$cm^{-3} (including high zones).

The carried out investigations lead us to conclude that the highly doped specimens created by us are homogeneous. The maximum dissolution of Te $\sim 8 \times 10^{19}$at·cm^{-3}, corresponding electron concentration $n = 2 \times 10^{19}$cm^{-3}. With high level of doping the electron concentration does not rise (Fig. 1) because of formation neutral complexes and clastics. In case of InAs the creation of highly doped crystals made possible to determine band structure and nonparabolicity of materials.

Tbilisi I. Javakhishvili State University

REFERENCES

1. *L. Akhvlediani, N. Kekelidze, G. Kekelidze, S. Laitadze.* N002734, 1997.
2. *A. A. Kukharckii, B. K. Subashiev.* J. Sol. St. Phys. 8, 1966, 753 (Russian).
3. *I. Kolodziejczak, Sosnovski.* Acta Phys., pol, 21, 1962, 399.

საქართველოს მეცნიერებათა აკადემიის მოამბე, 159, №2, 1999
BULLETIN OF THE GEORGIAN ACADEMY OF SCIENCES, 159, №2, 1999

PHYSICS

R. Jobava, P. Shubitidze, R. Beria, D. Karkashadze, R. Zaridze, A. Gheonjian

Aperture Penetration of Fields Radiated by ESD into a Rectangular Cavity

Presented by Corr. Member of the Academy T. Sanadze, March 16, 1998

ABSTRACT. **Numerical study of aperture penetration of transient fields related with indirect electrostatic discharge (ESD) is presented. Computer simulation of ESD from spheroid is performed to model human hand related discharge. Computed ESD fields are in a good agreement with experimental data. Such realistic fields are used as incident fields to investigate electromagnetic compatibility (EMC) problem of aperture penetration into two-dimensional cavities. Time domain analysis of shielding effectiveness of rectangular cavity with aperture is done using FDTD method.**

Key words: electrostatic discharge (ESD), aperture penetration, cavity, electromagnetic fields, computer simulation, FDTD, electromagnetic compatibility (EMC).

This paper presents numerical study of the coupling of transient fields radiated during electrostatic discharge (ESD) into the metallic enclosure with aperture. Computer simulation of ESD is done using an electrodynamic method based on the method of moments in time domain for discharging bodies of revolution, located near the grounded plane [1-4]. For the discharging structure like spheroid, that can be considered as a model of human/hand related ESD, calculated arc currents and fields were compared with experimental data and showed sufficient for EMC applications accuracy of the developed technique [1-4]. Such realistic fields are used in this paper as incident fields to investigate aperture penetration into two-dimensional cavities. Time domain analysis of shielding effectiveness of rectangular cavity with aperture is done using FDTD method.

Let's describe briefly the mathematical model of ESD. In the moment before discharge the static charge distribution $\rho_{stat}(\vec{r})$ is known on all metallic surfaces. During the discharge this distribution will be disturbed. Let us denote this disturbed part of charge by $\rho_{trans}(\vec{r},t)$. The whole charge density in any point on the surface of the body or on the plane is $\rho(\vec{r},t)=\rho_{stat}(\vec{r})+\rho_{trans}(\vec{r},t)$. The current density $\vec{J}(\vec{r},t)$ deals with transient part of charge density. So the transient problem can be stated as the problem of defining the surface current densities $\vec{J}(\vec{r},t)$ and arc-current density $\vec{J}_{arc}(\vec{r},t)$. By these quantities all charges and fields can be calculated. Mathematical model for $\vec{J}(\vec{r},t)$ and $\vec{J}_{arc}(\vec{r},t)$ can be formulated as follows.

1. On the perfectly conducting surfaces $\vec{J}(\vec{r},t)$ satisfies integral equation for magnetic field (IEMF):

$$\vec{J}(\vec{r},t) = 2\hat{n} \times \vec{H}^{arc}(\vec{r},t) + \frac{1}{2\pi}\hat{n} \times \int_S \left\{ \frac{\vec{J}(\vec{r}',\tau)}{R} + \frac{1}{c}\frac{\partial}{\partial \tau}\vec{J}(\vec{r}',\tau) \right\} \times \frac{\vec{R}}{R^2} ds, \quad \vec{r} \in S \tag{1}$$

2. In each point of the arc the current density satisfies Ohm's differential law:

$$\vec{J}_{arc}(\vec{r},t) = \sigma(\vec{r},t) \cdot \left\{ \vec{E}_{stat}(\vec{r}) + \vec{E}^{arc}_{trans}(\vec{r},t) + \vec{E}^{surf}_{trans}(\vec{r},t) \right\}, \ \vec{r} \in V_{arc} \tag{2}$$

3. Initial values are written as follows:

$$\forall \vec{r}, t \le 0 : \begin{cases} \vec{J}(\vec{r},t) = 0; \\ \vec{J}_{arc}(\vec{r},t) = 0; \\ \rho_{trans}(\vec{r},t) = 0. \end{cases} \tag{3}$$

Let us consider terms of these expressions. In the equation (1) $\vec{H}^{arc}(\vec{r},t)$ is magnetic field obtained on the metallic surface. This field is radiated by arc-current. S is the area of surface of the body and of its image. $\vec{r}$ is the point of observation, $\vec{r}'$ is the point of integration, τ is the delay time: $\tau = t - R/c$; $R = |\vec{R}|$, and $\vec{R} = \vec{r} - \vec{r}'$. c is the speed of light, $\hat{n}$ is the outer normal of the surface. In equation (2) $\vec{E}_{stat}(\vec{r})$ is electrostatic field produced by static charge distribution before discharge. This field initiates the spark. $\vec{E}^{arc}_{trans}(\vec{r},t)$ and $\vec{E}^{surf}_{trans}(\vec{r},t)$ are transient electric fields, radiated by the arc and the surface and their mirrors.

Arc conductivity $\sigma(\vec{r},t)$ in equation (2) is the function of electric field in the channel. In this work this conductivity is calculated by empiric model of Rompe and Weizel. According this model arc resistance is function of time [4]:

$$R(t) = \frac{2h}{\sqrt{2a_R \int_0^t I^2_{arc}(t')dt'}}, \tag{4}$$

where $R(t)$ is arc resistance ([Ohm]), 2h is length of arc and its image ([m]), $I_{arc}(t)$ is arc current ([A]), a_R is empiric constant ([m^2/V^2sec]), t is time ([sec]).

The equation (1) coupled with nonlinear equation (2) is solved by time domain Method of Moments. Algorithm allows the calculation of transient fields and simulation of whole electrodynamical process of discharge. The results are compared with measurements and show good agreement [2-4].

The question how the discharging body radiates into the space is of great importance because the answer gives hints about the region where sensitive apparatus might be disturbed.

In all calculations below a metallic spheroid of semi-axes a = 31 cm and b = 5 cm is chosen as a discharging object. Spheroid is charged up to some voltage denoted as V. Discharge occurs at a distance h from the plane. Fig. 1 shows radiated electric fields for two different cases: a) V = 5 kV, h = 0.7 mm; b) V = 10 kV, h = 1.0 mm. Observation point is located on the grounded plane. The distance to the point of observation from the location of arc is 1m.

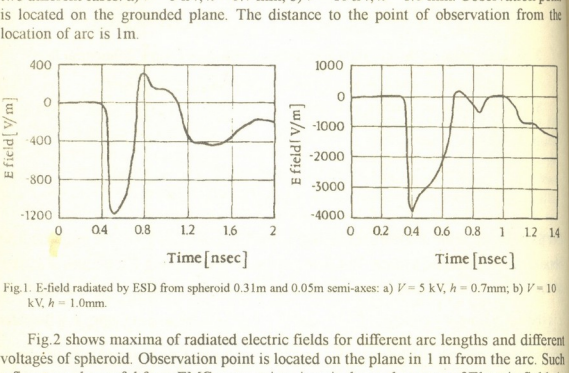

Fig.1. E-field radiated by ESD from spheroid 0.31m and 0.05m semi-axes: a) V = 5 kV, h = 0.7mm; b) V = 10 kV, h = 1.0mm.

Fig.2 shows maxima of radiated electric fields for different arc lengths and different voltages of spheroid. Observation point is located on the plane in 1 m from the arc. Such a figure can be useful from EMC perspective since it shows the range of Electric fields in a close proximity of the discharging body for various ESD events.

In order to estimate how big is the difference between fields, radiated in different directions from the arc, we present Fig.3. Maxima of radiated electric fields are shown on this figure versus angle from the axe perpendicular to the plane. Fields are calculated in 1 m from the arc for ESD with V = 5 kV, h = 0.6 mm.

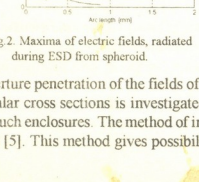

Fig.2. Maxima of electric fields, radiated during ESD from spheroid.

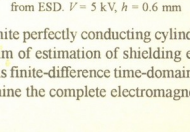

Fig.3. Maxima of electric fields in 1 m from ESD. V = 5 kV, h = 0.6 mm

Aperture penetration of the fields of ESD in infinite perfectly conducting cylinders with rectangular cross sections is investigated with the aim of estimation of shielding effectiveness of such enclosures. The method of investigation is finite-difference time-domain method (FDTD) [5]. This method gives possibility to determine the complete electromagnetic field

in the space surrounding the cylinder for all times of interest.

To estimate shielding effectiveness of the screen we calculate the value

$$S = \frac{\int_{Area} \max\left|\vec{E}^{total}\right| ds}{\int_{Area} \max\left|\vec{E}^{inc}\right| ds} * 100\% \qquad (5)$$

Here "Area" denotes the area of the cavity. Maxima of fields are calculated for each point inside the cavity during all time of observation. In Fig.4 the shielding effectiveness of rectangular cylinder is shown for two cases: a) $V = 5$ kV and b) $V = 10$ kV.

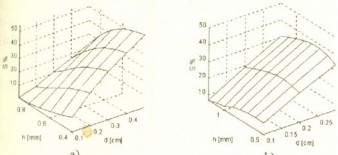

Fig. 4. Shielding effectiveness of rectangular cylinder as function of arc length h and size of aperture d. ESD from a) $V = 5$ kV and b) $V = 10$ kV.

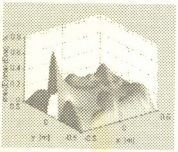

Fig. 5. Normalized maxima of electric field inside rectangular cavity. ESD from spheroid, $V = 5$ kV, $h = 0.6$ mm, $d = 20$ cm.

To demonstrate how maxima of fields are distributed inside the cavity we present Fig.5. One can see that maxima of electric fields that penetrate to the aperture are located near aperture and have smaller values in the inner part of cavity. Shielding effectiveness, calculated by formula (5) gives possibility to estimate average value of fields maxima shown in Fig. 5.

Tbilisi I. Javakhishvili State University

REFERENCES

1. *R. Zaridze, D. Karkashadze, R. Jobava et. al.* EOS/ESD Symposium Proceedings, Phoenix, USA, 1995.
2. *R. Zaridze, D. Karkashadze, R. Jobava et. al.* IEEE Trans. on Components, Packaging and Manuf. Technology Part C: Manufacturing. 19, 3, July 1996 , 178-183.
3. *R. Jobava, D. Karkashadze, R. Zaridze et. al.* EOS/ESD Symposium Proceedings, Orlando, Florida USA, 1996, 203-210.
4. *R. Jobava, D. Karkashadze, P. Shubitidze et.al.* EMC Symposium, Zurich, 1997.
5. K.S. Yee. IEEE Transactions on Antennas and Propagation, vol. AP-14, 1966, 302-307.

საქართველოს მეცნიერებათა აკადემიის მოამბე, 159, №2, 1999
BULLETIN OF THE GEORGIAN ACADEMY OF SCIENCES, 159, №2, 1999

PHYSICS

T. Nadareishvili, Corr. Member of the Academy A. Khelashvili, G. Khelashvili

Unified Formula for Eigenvalues in the Case of Exponential Class Potentials

Presented May 15, 1998

ABSTRACT. **Analytic dependence on inverse magnitude of action radius of regularized linear potential is used to obtain the unified formula for eigenvalues of Schrödinger equation in the case of three various potentials belonging to exponential class. The method of derivation of asymptotic equations for zeros of McDonald's function is described.**

Key words: Schrödinger equation, exponential potentials, Airy and McDonald functions.

In a number of papers [1,2] by investigation of gluon propagator's superconvergent dispersion relation it is proved, that gluon propagator may be of dipole type

$$D(k) \approx C/(k^2 + \mu^2 - i\varepsilon)^2. \tag{1}$$

which in configuration space corresponds to regularized linear potential in infrared region

$$V(R) \approx const + g\,(1-e^{-\mu R})/\mu. \tag{2}$$

In $\mu \to 0$ limit we receive linear potential

$$V(R) \approx const + gR. \tag{3}$$

μ parameter may be understood as an infrared cut off parameter. The finite values of μ correspond to asymptotically free theories, which for arbitrary small but finite μ don't give quark confinement. We notice, that J/ψ quarkonium's radial excitation spectrum was studied in paper [3] by the potential (2) and lately Nakanishi [2] payed attention to this potential.

In this paper we consider more radical example, when μ parameter may change the sign, i.e. we include the case of exponentially increasing potential. In this case Schrödinger equation may be analytically solved for S-wave. It is interesting, that the case of exponentially increasing potential for some reason isn't considered in literature, accessible to us (the reason may be, that appropriate convenient regular formulae for zeros of solutions are not widely known). So we take three potentials

$$V_a(r) = (g/\mu)(1- e^{-\mu r}); \quad V_b(r) = gr; \quad V_c(r) = (g/\mu)(e^{\mu r}-1). \tag{4}$$

Here g, μ are positive parameters. It is clear, that the third case is obtained from the first one, if we continue μ parameter from positive to negative region. When $\mu \to 0$ (more precisely, when $\mu r << 1$), then V_a and V_c potentials smoothly turn into linear V_b potential.

Afterwards we can operate in two ways: solve Schrödinger equation for each potential

separately or continue one of its solutions (V_a or V_c) by μ parameter and obtain solution of other potentials. Now we briefly describe eigenvalues finding procedure. For dipole type potentials radial wave function is [3]

$$\chi(r) = J_q(ce^{-\mu r/2}), \tag{5}$$

where in accordance with boundary condition for bound states(at infinity the solution approaches to zero) J_q is Bessel function of the first kind and the following notations are introduced

$$c = \sqrt{8mg/\mu^3}, \quad q = c\sqrt{1-\mu E/g}. \tag{6}$$

Here E is eigenvalue, which as a consequence of potential behavior is positive. To find discrete levels we demand solution (5) to fulfil the boundary condition in the origin

$$J_q(c) = 0, \tag{7}$$

which shows, that we must find zeros of Bessel function. It is known, that Bessel function has zeroes, when $q < c$. And according to (6) this means that $E < g/\mu$ and we have discrete levels inside a well, what is physically quite clear.

For Bessel function zeros there are tables and numerical programs. But beforehand we don't know q and c and this way is useless. It is more acceptable to use some approximate formulae. For this we consider small values of μ. As we have mentioned above, consideration of this limit has some physical interest. In this case index and argument of Bessel function become very large and therefore we can use the so-called uniform asymptotic (Langer's) formulae for Bessel functions [4].

$$J_p(x) \approx \sqrt{1-arctg(w)/w}[J_{1/3}(z)\cos(\pi/6) - Y_{1/3}(z)\sin(\pi/6)] + O(p^{-4/3}). \tag{8}$$

In this formula $x > p >> 1, w = \sqrt{x^2/p^2 - 1}, z = p(w - arctg(w))$. (9)

For our case

c>q, $w = \sqrt{c^2/q^2 - 1}$, $z = q(w - arctg(w))$, $w = \sqrt{\mu E/g(1-\mu E/g)}$ (10)

Now we perform some transformations, which are necessary for $\mu \to 0$ limit. It's obvious, that $w \to 0$, $z \to pw^3/3$. If we recall, that in [4]

$$Y_\nu(z) = (J_\nu(z)\cos(\nu\pi) - J_{-\nu}(z))/\sin(\pi/3), \tag{11}$$

we obtain $J_p(x) \longrightarrow \sqrt{1-arctg(w)/w}[J_{1/3}(z) + J_{-1/3}(z)]/\sqrt{3}$ (12)

and if we insert $z \to pw^3/3$ in the latter formula and recall the form of w and that $p = q$, we obtain

$$J_p(c) \approx \sqrt{\xi}/3[J_{1/3}\left(\frac{2}{3}\xi^{3/2}\right) + J_{-1/3}\left(\frac{2}{3}\xi^{3/2}\right)] = Ai(-\xi), \tag{13}$$

where Ai(-ξ) is Airy function, and

$$\xi = \sqrt[3]{2m/g^2}(E/(1-\mu E/g)^{2/3}), \tag{14}$$

so in this approximation zeros, which we search coincide with zeros of Airy function: $\xi = \lambda_n$ for which there are tables and approximate formulae. This result was obtained in [3] and used for J/ψ system spectrum. In the $\mu \to 0$ limit the well known results for linear potential were obtained. We now improve this approximation. For this we introduce new variable in asymptotic formula, so

$$z = \frac{2}{3}\xi^{3/2} = q(w - arctg(w)) . \tag{15}$$

In this case we have again Ai(-ξ) function and for eigenvalues we obtain the following formula

$$q(w - arctg(w)) = \frac{2}{3}\lambda_n^{3/2}, \tag{16}$$

which the restores previous result for small μ.

As we have mentioned above, the potentials are regularized so, that they allow analytical extension to negative values of μ, i.e. to exponentially increasing potential. Therefore we can carry out appropriate changes in obtained formulae. It is obvious that we can demonstrate result by solving Schrödinger equation directly.

Now we list final results for potential $V_c(r)$. The solutions are Bessel functions of imaginary argument and imaginary index. Among Bessel functions of imaginary argument only McDonald functions $K_p(x)$ decrease at the infinity. Therefore we must take the follawing as solution

$$\chi(r) \approx K_{2i\alpha/\mu_0}(2\beta e^{\mu r/2}/\mu) \tag{17}$$

where
$$\beta = \sqrt{2mg/\mu}, \qquad \alpha = \beta\sqrt{1+\mu E/g} > \beta . \tag{18}$$

So we get following equation to find eigenvalues
$$K_{ip}(x) = 0 \tag{19}$$

where
$$x = \sqrt{8mg/\mu^3}, \qquad p = 2\alpha/\mu = x\sqrt{1+\mu E/g} > x \tag{20}$$

The problem came to find zeros of McDonald function of imaginary argument. According to the known theorem [5], the McDonald function has positive and non-zero roots only for imaginary index. Besides, for pure imaginary index the least positive root lies in the region, where module of argument is less than module of index. This is just our case, because $x < p$ (or $\alpha > \beta$), i.e., we will get roots and find eigenvalues.

Investigation of asymptotic formulae in [5] shows, that for higher energy levels the equation for $K_{ip}(x)$ function zeros coincides with the equation of Ai(-ξ) function zeros. Therefore we suppose, that in this case we also deal with Airy function zeros and write eigenvalue finding formula so

$$p(Arth(\tilde{w}) - \tilde{w}) = \frac{2}{3}\lambda_n^{3/2} . \tag{21}$$

where λ_n are zeroes of Airy function, and $\tilde{w}$ is obtained from $\tilde{w}$ by $\mu \to -\mu$ analytical extension and it corresponds to

$$c \to ic = ix,\ q \to ip,\ w \to i\widetilde{w} = i\sqrt{1 - x^2 / p^2}, \qquad arctg(w) \to iArth(\widetilde{w}) \tag{22}$$

so

$$q(w - arctg(w)) \to p(Arth(\widetilde{w}) - \widetilde{w}). \tag{23}$$

We see, that we have unified formula for eigenvalues, which for small μ involve all three potentials. To obtain information about spectrum by this formula it is expedient to use standard algebraic programs, which give us possibility to find the whole spectrum by first 2 or 3 levels.

Tbilisi I. Javakhishvili State University
High Energy Physics Institute

REFERENCES

1. *K. Nishijima*. Progr. Theor. Phys. 77, 5, 1987.
2. *N. Nakanishi*. Progr. Theor. Phys. **59**, 1978, 1403.
3. *Sh. Vashakidze, A. Khelashvili*. Proceedings of Tbilisi University. 188, 5, 1977 (Russian).
4. *H. Bateman, A. Erdelyi*. Higer Transcedental functions. v. 2, M., 1966 (Russian).
5. *A. Kratzer, V. Frantz*. Transcedental functions. Leipzig. 1960.

საქართველოს მეცნიერებათა აკადემიის მოამბე, 159, №2, 1999
BULLETIN OF THE GEORGIAN ACADEMY OF SCIENCES, 159, №2, 1999

PHYSICS

K. Kvavadze, M. Nadareishvili, L. Tarkhnishvili, D. Igitkhanishvili, G. Basilia, Sh. Dvali, Z. Khorguashvili

The Influence of OH^- Impurities on Low-temperature Heat Capacity of KCl

Presented by Member of the Academy G.Kharadze, March 16, 1998

ABSTRACT. **The investigation of low-temperature heat capacity of KCl crystals containing hydroxyl impurity in case of high OH concentrations has shown a non-linear increase of impurity part of heat capacity corresponding to unit concentration. The existence of a new effect in the whole measured temperature interval has been revealed in the heat capacity of KCl:OH system after excluding the contributions of resonance beam and light mass effects from the total heat capacity.**

Key words: heat capacity, calorimeter, tunneling, impurity.

It is known that hydroxyl ions are electric dipoles that can exist in KCl crystal in six different equivalent states along <100> crystallographic orientation [1]. OH^- dipoles can make transitions between these states due to quantum tunneling, as a result 6-fold degenerate ground level is splitted up into 3 levels: A_{1g}, T_{1u}, and E_g, the degrees of their degeneracy are 1, 3 and 2, respectively, and the splitting values between T_{1u} and A_{1g} levels is approximately twice more than that between E_g and T_{1u} levels. For theoretical interpretation KCl:OH system is especially convenient, because in a good approximation it can be assumed that we have one atom matrix and the crystal system is simple cubic.

Pure and hydroxyl doped KCl crystals were grown (by us) from the alloy by Kiropulos-Chokhralski method. "HQ" powders of special purity were used. After growing the monocrystals were cooled during 20 hours together with the furnace. Cutting out of samples was carried out from the central parts of massive blocks and then they were polished and finished. The determination of hydroxyl concentration in samples was made by the method of infrared absorption [2]. The analysis has shown that the content of hydroxyl in our crystals was equal to 0.18 and 0.42mol%. The measurements of low-temperature heat capacity in KCl:OH^- crystals were made on the calorimeter of practically new type created by us on pulse differential calorimeter [3]. Fig.1 shows the plots of temperature dependence of ΔC impurity part of heat capacity of KCl crystals containing hydroxyl impurity; curve 1 corresponds to 0.18 mol% and curve 2 - to 0.42 mol% for OH^- concentration.

$\Delta C(T) = C(T)-C_0(T)$, where $C(T)$ is the heat capacity of impurity crystals, and $C_0(T)$ is the heat capacity of the standard (pure crystals). In case of 0.18 mol% hydroxyl concentration on the plot of temperature dependence of heat capacity of impurity part at 6K temperature the pronounced minimum is observed. With the increase of temperature this function increases reaching the maximum in the temperature range of 12-14 K and above

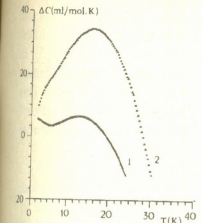

Fig.1 The temperature dependence of impurity part of heat capacity of KCl:OH^-
1- KCl+0.18 mol% OH^-
2- KCl+0.42 mol% OH^-

22 K it becomes negative. In case of 0.42 mol % hydroxyl concentration on $\Delta C(T)$ plot the minimum observed at ~6K disappear, the maximum increases sharply and shifts to the higher temperature (18-19K), while $\Delta C(T)$ function becomes negative above 28K temperature. We tried to explain the minimum observed at ~6K by the effect of Shotky type [4], but without any success. The acceptable agreement of theory with experiment is achieved with due consideration of the contribution of wide spectrum of energy level channel splitting according to Anderson model [5]. The wide spectrum of energy level channel splitting in KCl:OH^- system is obtained as a result of interaction between chaotically distributed OH^- dipoles. With the increase of hydroxyl concentration the maximum splitting of energy levels increases in KCl, which is the reason of disappearance of the minimum at 6K temperature on the curve of $\Delta C(T)$ temperature dependence for large concentrations of this impurity. Above 6K temperature the increase of $\Delta C(T)$ we tried to relate to the existence of resonance level in oscillation spectrum at the frequency of 32 cm^{-1}, the contribution of which in total heat capacity is described by Kagan and Iosilevski formulae [6].

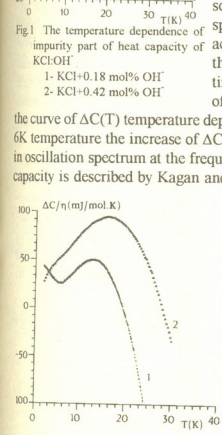

Fig.2 The temperature dependence of impurity part of heat capacity for unit concentration
1- KCl+0.18 mol% OH^-
2- KCl+0.42 mol% OH^-

The analysis shows that it is impossible to explain the formation of $\Delta C(T)$ narrow maximum at 12-14K (0.18 mol%) and 18-19K (0.42 mol %) temperatures only with the consideration of the contributions of energetic splitting and resonance oscillations. The same can be said about the negative magnitudes of $\Delta C(T)$ above 22K (0.18 mol%) and 28K (0.42 mol %). The latter can be explained only by the fact that light OH^- impurity causes the shift of state density from low-frequency area of phonon spectrum to high-frequency area of spectrum (as it was observed at the introduction of light Na ions into KCl crystals [7]) resulting in the decrease of low-temperature heat capacity of impure crystal. Thus, we have simultaneous influence of at least three factors on variation of low-temperature heat capacity of KCl:OH^- system: the contribution of wide spectrum of energy splitting and resonance oscillations (at the frequency of 32cm^{-1}) increasing the low-temperature heat capacity of impure crystal; and the effect of light-mass impurity decreasing low-temperature heat capacity. These effects should be proportional to impurity concentration. Thus, the concentration dependence of impurity part of heat capacity has been studied in detail. Figure 2 shows the plots of temperature dependence of the impurity part of heat capacity for unit concentration; the curve (1) corresponds to 0.18mol% hydroxyl concentration, and -(2)- to 0.42mol%. From the study of concentration dependence it is obvious that for high concentrations a new effect takes place in the

system, superimposing on the contributions of resonance oscillations and light mass and hence, it is difficult to observe clearly. For pronounced isolation of this effect the difference in $\Delta C/\mu$ curves was plotted for 0.42mol% and 0.18mol% concentrations (Fig.3). In case of such treatment of curves, the proportional terms are vanished, i.e. the contribution made by resonance oscillations in low-temperature heat capacity and by light mass. This enables us to isolate without distortion the part of heat capacity related with hydroxyl effect in case of high hydroxyl concentrations, namely the effect that causes nonlinearity of $\Delta C/\mu$ curves above ~ 10 according to concentration.

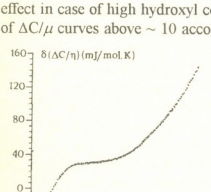

Fig.3 - The difference of $\Delta C/\mu$ curves for 0.42 mol % and 0.18 mol % concentrations.

The peculiarity near 5K temperature shown in Fig.3 can be easily explained by shift of the maximum of wide spectrum of energy splitting to high energies at the increase of concentration, as for the new effect existing above 10K on the basis of present knowledge of solid-state physics we can have two opinions. The first opinion is related to the fact that each OH^- has an electronic dipole moment in KCl, the interaction of which with each other and with a lattice can cause ordering of dipoles at low temperatures, i.e. phase transition of a new type [8].

The second opinion is related to the results obtained recently in investigations of amorphous bodies, in particular to the existence of boson peaks in low-frequently area of phonon spectrum of amorphous bodies, the nature of which is still unclear. But, existing models agree in that, oscillation excitations causing boson peak formation are localised in structure inhomogeneity. They contain indirect information about material structure in the distances of average order [9-11].

Georgian Academy of Sciences
Institute of Physics

REFERENCES

1. *U. Kuhn, F. Luty.* Solid State Commun., **2**, 3, 1964, 281-283.
2. *B. Fritz, F. Luty,* Anger J. Z. Physik, **174**, 2, 1963, 240-256.
3. *K. A. Kvavadze, M. M. Nadareishvili.* Patent N1610415, 1990.
4. *W. D. Seward, V. Narayanamurti.* Phys. Rev., **148**, 1, 1966, 463-481.
5. *P. WAnderson, B. I. Halperin, C. Varma.* Phil. Mag., **25**, 1, 1972, 1-11.
6. *Y. Kagan, Ya. A. Iosilevskii.* JETF. **45**, 3, 9, 1963, 819-821.
7. *K. A. Kvavadze, L.A.Tarkhnishvili et. al.*, J. Low Temp. Phys., **47**, 5/6, 1982, 375-383.
8. *R. V. Saburova.* UFJ, 27, 1982, 1209.
9. *U. Buchenau, Yu. M. Galperin, V. L. Gurevich, M. R. Shober.* Phys.Rev., **B43**, 1991, 5039.
10. *V. K. Malinovskii, V. N. Novikov, A. P. Sokolov.* UFN, **163**, 5, 1993, 119.
11. *F. J.Bermejo, A. Criado, J. L. Martinez.* Phys. Lett. A 195, 1994, 236.

საქართველოს მეცნიერებათა აკადემიის მოამბე, 159, №2, 1999
BULLETIN OF THE GEORGIAN ACADEMY OF SCIENCES, 159, №2, 1999

PHYSICS

S. Gotoshia

Lazer Spectroscopy of Semiconductors

Presented by Member of the Academy T. Sanadze, June 15, 1998

ABSTRACT. **To study semiconductors by laser Raman spectroscopy and photoluminescence we have constructed three laser Raman spectrometers with different parameters and necessary accessories for measurements. Photoluminescence and Raman scattering of various mixed and A^3B^5 semiconductor surfaces modified by ion implantation have been studied by the constructed spectrometers using wide nomenclature of lasers.**

Key words: laser Raman spectroscopy, photoluminescence, semiconductors, mixed crystals ion implantation.

To study semiconductors by laser Raman spectroscopy and photoluminescence (PL) we have constructed three laser Raman spectrometers with different parameters.

The various laser Raman spectrometers constructed by us, on which the works on photoluminescence are fulfilled, give the possibility to carry out widerange fundamental scientific researching and analytic works in physics, microelectronics, chemistry, biology, medicine, geology, ecology, food industry and agriculture.

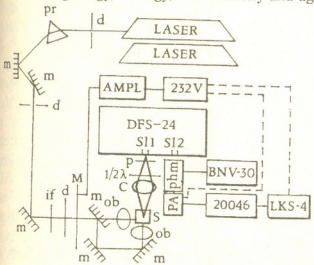

Fig.1. General scheme of home laser Raman spectrometer.

The general scheme of the mentioned home laser Raman spectrometer is shown in Fig.1. The spectrometer has been constructed on the basis of a double monochromator DFS-12 or DFS-24. Different types of lasers have been used as excitation source for photoluminescence or Raman spectra. The parameters are given in the Table.

Laser emission through diaphragm (d), prism (p), interference filter (if), mirrors (m) and objective (ob) is filtered from laser background, plasma lines; highly collimated monochromatic emission in desired direction is formed according to planned scattering configuration and is focused on the semiconductor (s) to be studied. Irradiation scattered in the semiconductor is collected by the condensor (c) and through the polarizator (p) is focused on the monochromator entrance slit (sl.1). Photoluminescence or Raman scattering signal from the exit slit (sl.2) falls on the photomultiplier (phm) and after its ampli-

fying and sorting photoluminescence or Raman scattering spectra are recorded by the recorder LKS-004. Detection and amplification of weak intensity signals of Raman scattering is done by two methods: synchronous detection by the aid of a modulator and a narrow-band amplifier Uniphan 232B or photon counting. In this case we use radiometer 20046. In the visible range of spectrum we work with well selected parameter photomultiplier FEU-79 or FEU-136. If needed the FEU-79 cathod is cooled at about 100°C. For this purpose we have created a low-temperature cryostats of three different types working by different principles. By cooling cathods of FEU-79 in these cryostats we are able to increase noise to signal ratio up to eight which is of great importance when registering Raman spectra. The constructed Raman spectrometer enables us to record spectra at high temperatures (18°C-600°C) as well as at cryogenic ones (with temperature regulation in the temperature interval 300K-80K, or at fixed temperatures of hellium or nitrogen). For this purpose we have created compact optical cryostats especially for Raman spectroscopy taking into account that the direction of exciting laser beam, the semiconductor sample crystallographic axis and scattered light collection angle make a certain configuration.

To study the effect of uniaxial pressure on semiconductor Raman spectra and photoluminescence we have created for the mentioned Raman spectrometer the special cryostat, which operates at liquid nitrogen temperature.

As it is clear from the Table, the nomenclature of lasers employed by us is too large, respectively the spectrometer's spectral range in which the registering of spectra takes place is large too. This requires the corresponding variations of diffraction gratings in the spectrometer which is often inconvenient. That is why we have constructed three Raman spectrometers, in which exciting laser wavelength, diffractional grating spectral range in double monochromator and the wavelength of maximal concentration of light collected by the diffraction grating corresponds each other.

Table

The laser wavelengthes, corresponding quantum energies and types used by us

Lasers	Laser type	Wavelength nm	Energy eV
He-Ne	gas	632.8	1.958
		514.5	2.408
		501.7	2.469
Argon ion	gas	496.5	2.495
		488.0	2.539
		476.5	2.600
		457.9	2.705
		647.1	1.914
Criptonion	gas	568.2	2.180
		520.8	2.379
		476.2	2.601
He-Cd	gas	441.7	2.805
Nd^3:YAG	solid	1064.0	1.17
Copper	metal	510.6	2.428
	vapour	578.2	2.144
Die		540.0-690.0	2.296-1.797

One of these three Raman spectrometers, which we call IR Raman spectrometer is worth mentioning. Infrared garnet laser serves as the exciting source in this spectrometer. Constructed by us this laser has the following parameters: emission wavelength 1.06 μ with one mode, irradiation power 16 wt. Such semiconductors as GaAs, InP, CdTe, S with forbidden gap in the near infrared region, we can study by infrared Raman spectrometer (if their exciting in volume is needed). In infrared Raman spectrometer we have use

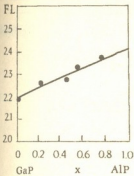

Fig.2. Dependence of green photoluminescence of epitaxial films of mixed Ga_xAl_{1-x} crystals on composition.

infrared photomultiplier FEU-83 as signal detector, the cathod of which is cooled at liquid nitrogen temperature in specially constructed cryostat. By such deep cooling of photomultiplier we have reduced the noise of FEU-83 by three order of magnitude. Besides, for the double monochromator we have selected and installed such diffraction gratings, which concentrate light maximally at 1.5 μ. It is impossible to record GaAs, InP, Si, CdTe Raman spectra on infrared Raman spectrometer without selecting such optimal regime.

With the aid of the above mentioned Raman spectromeeters we have studied photoluminescence of some semiconductors and Raman scattering. Mixed semiconducting crystals of GaAlP are less studied systems. The use of lasers for excitation of the mixed crystal epitaxial film luminescence enables us to record spectra at room temperature what is very profitable for analysis of films in great amount. We have used three types of epitaxial films: undoped, n-type doped and p-type doped. The three types all have green luminescence of high intensity and their wavelengthes varies with mixed crystal concentration (Fig.2). The given dependence is used for determination of an unknown composition. More profound analysis of $Ga_xAl_{1-x}P$ photoluminescence and its possible mechanism will be discussed in the following work.

In the case of GaAs and GaP surfaces modification by ion implantation we have used RS to define amorphization degree to study the dynamics of recrystallization process occuring by annealing and to identify triple mixed semiconductors synthesized by ion implantation.

In Fig.3 there are shown recorded by us RS of crystalline GaP and those of amorphous α-GaP synthesized by ion implantation. According to selection rules in crystalline GaP with (111) surface there are two spectral bands with frequency LO = 402cm^{-1}; with halfwidth of band at maximum intensity $\Delta\nu_{LO}$ = 45cm^{-1} and TO = 365cm with $\Delta\nu$ = 7.5cm^{-1}. When crystal structure transforms into amorphous, the far order is lost and only the nearest order is left at small coherent distance; narrow bands of RS are broadening, the intensity is decreased and finally transforms into wide nonstructural band, which is shown in Fig. 3.

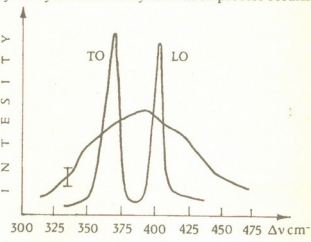

Fig.3. Raman spectra of monocrystaline GaP with (111) orientation and amorphous α-GaP received by ion implantation.

Thus the method of semiconductor investigation by laser spectroscopy (photoluminescence, Raman scattering) has been worked out; three Raman spectrometers with different parameters and accessories have been constructed and briefly given original examples of crystal as well as amorphous semiconductors study by laser spectroscopy.

Georgian Academy of Sciences
R. Agladze Institute of Inorganic Chemistry and Electrochemistry

საქართველოს მეცნიერებათა აკადემიის მოამბე, 159, №2, 1999
BULLETIN OF THE GEORGIAN ACADEMY OF SCIENCES, 159, №2, 1999

PHYSICS

G. Jandieri, I. Jabnidze, N. Gomidze, V. Jandieri

The Radiation Friction of a Charge Moving Oscillator in a Chaotically-Inhomogeneous Medium

Presented by Member of the Academy G. Kharadze, May 7, 1998

ABSTRACT. **Radiation force work connecting with the radiation of anomalous Doppler frequencies generated by moving oscillator in w chaotically inhomogeneous medium are considered in this paper. Using geometrical optic approximation it is shown that small-scale permittivity fluctuations lead to swinging of an oscillator.**

Key words: inhomogeneous medium, oscilator, swinging, transient radiation, permittivity fluctuations.

It is well known that the charge moving in a medium radiates electromagnetic waves. Complicated Doppler effect is connected with stability of a moving oscillator at velocities exceeding the phase velocity of electromagnetic wave in a given medium, while the instability arises in a region of anomalous Doppler effect, i. e., proper vibrations of charged particle are amplified due to interaction between the charge and medium. Radiation reaction force work in isotropic and nonisotropic media was investigated in detail in the papers [1]. The work relating to the generation of normal Doppler frequencies is negative, which leads to the deceleration of oscillator vibrations. Positive work is connected with the excitation of anomalous Doppler frequencies. The selection of Cherenkov's angle in an inhomogeneous medium allows to emit only anomalous Doppler frequencies leading to the oscillator's swinging. Inhomogeneities will reduce to the new effects. The radiation of electromagnetic waves of a moving charged particle in a medium with periodically varying properties has been considered in [2]. Parametrical resonance between the oscillator vibrations and the field of transient radiation takes place. The task of the fixed and moving oscillator radiation reaction in the medium of three-dimensional small-compared to the wavelength with chaotic inhomogeneties of permittivity was solved in [3] by mean field method [4].

Given paper is devoted to the influence of inhomogeneties of nonabsorbing, randomly-inhomogeneous medium on the stability of oscillator vibrations in geometrical optic approach [5].

Initial are equations for the electric field strength [4]

$$\frac{d^2\vec{E}_{x\vec{\omega}\omega}}{dz^2}+\left(\frac{\omega^2}{c^2}\varepsilon(z)-\varpi^2\right)E_{x\vec{\omega}\omega}=-\frac{4\pi i\omega}{c^2}j_{x\vec{\omega}\omega}+\frac{4\pi ik_x}{\varepsilon}\rho_{\vec{\omega}\omega}-ik_xE_{z\vec{\omega}\omega}\frac{d}{dz}\ln\varepsilon(z), \quad (1)$$

$$\frac{d^2\vec{E}_{z\vec{\omega}\omega}}{dz^2}+\frac{d}{dz}\left(E_{z\vec{\omega}\omega}\frac{d}{dz}\ln\varepsilon\right)+\left(\frac{\omega^2}{c^2}\varepsilon(z)-\varpi^2\right)E_{z\vec{\omega}\omega}=-\frac{4\pi i\omega}{c^2}j_{z\vec{\omega}\omega}+4\pi\frac{d}{dz}\left(\frac{\rho_{\vec{\omega}\omega}}{\varepsilon}\right). \quad (2)$$

Equation for $E_{y\vec{\omega}\omega}$ is the same as (1). The permittivity is a function only of coordi-

nate z; $\vec{j}$ and ρ are current and particle densities: $\vec{\varkappa} = \{k_x, k_y, 0\}$

Let's investigate the case when medium properties slightly vary on a distance of wavelength order, i. e. $\lambda \frac{d\varepsilon}{dz} << \varepsilon$. Using geometrical optic approximation for the components of electric field we obtain:

$$E_{\vec{\alpha}\vec{\varkappa}\omega} = \frac{B_\alpha}{2i}\{\exp[i\int_0^z dzq]\int_{-\infty}^{z} dz' I_\alpha(z')\exp[-i\int_0^{z'} q(z'')dz'']] - \exp[-i\int_0^z qdz]\int_{\infty}^{z} dz' I_\alpha(z')\exp[i\int_0^{z'} q(z'')dz'']\} \tag{3}$$

where $\alpha = x, y, z$, $q = \sqrt{\frac{\omega^2}{c^2}\varepsilon - \vec{\varkappa}^2}$, $B_{x,y} = (\varepsilon - \vec{\varkappa}^2)^{-\frac{1}{4}}$, $B_z = \varepsilon^{-\frac{1}{2}}(\varepsilon - \vec{\varkappa}^2)^{-\frac{1}{4}}$, $\vec{\varkappa} = \frac{c}{\omega}\varkappa$,

$$I_{x,y} = \frac{4\pi i}{B_{x,y}q}\left(-\frac{\omega^2}{c^2} j_{x\vec{\varkappa}\omega} - \frac{k_{x,y}}{\varepsilon}\rho_{\vec{\varkappa}\omega}\right), \qquad I_z = \frac{4\pi i}{B_z q}\left(-\frac{\omega^2}{c^2} j_{z\vec{\varkappa}\omega} - \frac{i}{\varepsilon}\frac{d}{dz}\rho_{\vec{\varkappa}\omega}\right).$$

Let's consider the charge e moving along z axis with a constant velocity v_0 and harmonically vibrating with the frequency Ω:

$$j_x = j_y = 0, \qquad j_z = \rho\, v_z(t), \qquad \rho = e\delta(\vec{r} - \vec{R}(t)),$$

$$\vec{R}(t) = \{0,0, v_0 t + R_0 \sin\Omega t\}, \qquad \vec{v}(t) = \{0,0, v_0 + R_0\Omega\cos\Omega t\}.$$

Fourier components for $\rho_{\vec{\varkappa}\omega}$ and $j_{z\vec{\varkappa}\omega}$ are:

$$j_{z\vec{\varkappa}\omega} = \frac{e}{(2\pi)^3}\sum_{n=-\infty}^{\infty} J_n\left(\frac{\omega - n\Omega}{v_0}R_0\right)e^{i\frac{\omega-n\Omega}{v_0}z} + \frac{\Omega R_0 e}{2(2\pi)^3 v_0}\left\{\sum_{n=-\infty}^{\infty} J_n\left(\frac{\omega-(n-1)\Omega}{v_0}R_0\right)e^{i\frac{\omega-(n-1)\Omega}{v_0}z} + \right.$$

$$\left. + \sum_{n=-\infty}^{\infty} J_n\left(\frac{\omega-(n+1)\Omega}{v_0}R_0\right)e^{i\frac{\omega-(n-1)\Omega}{v_0}z}\right\}, \tag{4}$$

$$\rho_{\vec{\varkappa}\omega} = \frac{e}{(2\pi)^3 v_0}\sum_{n=-\infty}^{\infty} J_n\left(\frac{\omega - n\Omega}{v_0}R_0\right)e^{i\frac{\omega-n\Omega}{v_0}z}. \tag{5}$$

We assume that permittivity varies as $\varepsilon(z) = \varepsilon_0 + \delta\varepsilon(z)$; where $\delta\varepsilon(z)$ is a random function.

The expression for $E_{\vec{z}\vec{\varkappa}\omega}$ may be found by neglecting the influence of inhomogoneities on an amplitude of the electric field and taking into account only phase fluctuations. We'll consider the mean field at point z, anuming $z >> l$; where l is a spatial scale of dielectric permittivity fluctuations. Equation (3) is transformed as:

$$E_{z\vec{x}\omega} = \frac{B_{\vec{z}}}{2i} e^{iq_0 z} \int_{-\infty}^{z} dz' J_z(z') e^{-iq_0 z'} e^{i\varphi} - \frac{B_{\vec{z}}}{2i} e^{-iq_0 z} \int_{\infty}^{z} dz' J_z(z') e^{iq_0 z'} e^{i\varphi}, \tag{6}$$

where $\frac{k_0^2}{2q_0} \int_{z'}^{z} \delta\varepsilon(z'')dz'' = \varphi$. We suppose that $\delta\varepsilon(z)$ is normal distributed $< e^{i\varphi} > = e^{-\frac{<\varphi^2>}{2}}$

$$< \varphi^2 > = \frac{k_0^4}{4q_0^2} \int_{z'}^{z} \int dz_1 dz_2 < \delta\varepsilon(z_1)\delta\varepsilon(z_2) > = \frac{k_0^4}{4q_0^2} \int_{z'}^{z} \int dz_1 dz_2 \Gamma_\varepsilon(z_1 - z_2).$$

$\Gamma_\varepsilon(z_1 - z_2)$ is the correlation function of a random function $\varepsilon(z)$. Eq. (6) may be written as:

$$\vec{E}_{z\vec{x}\omega}(z) = \frac{B_{\vec{z}}}{2i} \left\{ \int_{-\infty}^{z} dz' J_z(z') e^{iq_0(z-z') - \frac{k_0^4}{4q_0^2} \int_0^{z-z'} d\varsigma \Gamma_\varepsilon(\varsigma)(z-z'-\varsigma)} - \right.$$

$$\left. \int_{\infty}^{z} dz' J_z(z') e^{iq_0(z-z') - \frac{k_0^4}{4q_0^2} \int_0^{z-z'} d\varsigma \Gamma_\varepsilon(\varsigma)(z-z'-\varsigma)} \right\}. \tag{7}$$

We choose exponential correlation function: $\Gamma_\varepsilon(\varsigma) = <\delta\varepsilon^2> e^{-\frac{|\varsigma|}{l}}$, $z - z' = l_0$. At small distances $l_0 << l$, l_0 give neglecting contribution in the integral. At $l_0 \geq l$, $< \varphi^2 > = \frac{k_0^4 < \delta\varepsilon^2 >}{2q_0} l l_0$. The radiation reaction force work equals to:

$$A = e \int_0^{\tau} d\omega d\vec{x} dt \, \vec{v} \vec{E}_{z\vec{x}\omega}(z = z_e) e^{i(\vec{x}\vec{\rho}_\epsilon - \omega t)} = e v_0 \int_0^{\tau} d\omega d\vec{x} dt \vec{E}_{z\vec{x}\omega}(z_e) e^{i(\vec{x}\vec{\rho}_\epsilon - \omega t)} +$$

$$+ e R_0 \Omega \int_0^{\tau} d\omega d\vec{x} dt \cos\Omega t \vec{E}_{z\vec{x}\omega}(z_e) e^{i(\vec{x}\vec{\rho}_\epsilon - \omega t)} = A_1 + A_2.$$

A_1 and A_2 correspond to the radiation force work on a variation of charge velocity and oscillator amplitude vibrations, respectively. The terms concerning to $n = n'$ and $n = n' \pm 1$ give contribution at great values of τ. Let's consider small oscillator amplitude vibrations: $\frac{\omega - n\Omega}{v_0} R_0 << 1$.

$$A_1 = \frac{e^2 R_0^2 \tau}{4c^3 (2\pi)^2 \beta_0} \int d\vec{x} d\omega \sum_{n=-1}^{1} \omega^2 (\omega - n\Omega) \frac{\omega^2 v_0^2}{\omega - n\Omega} \left[1 - \frac{1}{\beta_0^2} \left(1 - \frac{n\Omega}{\omega} \right)^2 \right] K(\omega, q_0), \tag{8}$$

$$A_2 = \frac{e^2 R_0^2 \tau\Omega}{4c^3(2\pi)^2\beta_0}\int d\vec{\alpha}d\omega \sum_{n=-1}^{1}\omega^2\left[1-\frac{1}{\beta_o^2\varepsilon}\left(1-\frac{n\Omega}{\omega}\right)^2\right]K(\omega,q_0). \qquad (9)$$

Investigate a hypothetical case

$$\varepsilon_0 = \begin{cases} const >> 1, & at\ \ \omega_1 < \omega < \omega_2 \\ < 0, & at\ \ \omega < \omega_1,\ \omega > \omega_2 \end{cases}$$

$\omega_1, \omega_2 >> \Omega$, i. e. excited frequencies exceeding the own frequency of the oscillator are in the domain where the following condition is satisfied $\beta^2\varepsilon >> 1$.

Integrating by $\vec{\alpha}$ and passing to the polar coordinate system, we obtain:

$$A_2 = \frac{e^2\tau R_0^2\Omega}{4c^3\beta_0}\int_{-\infty}^{\infty} d\omega \sum_{n=-1}^{1}\omega^2 n\left[1-\frac{1}{\beta_o^2\varepsilon}\left(1-\frac{n\Omega}{\omega}\right)^2\right]+$$

$$+\frac{e^2\tau R_0^2}{8c^3\beta_0\pi}\int_{-\infty}^{\infty} d\omega \sum_{n=-1}^{1}\omega^2 n\left[1-\frac{1}{\beta_o^2\varepsilon}\left(1-\frac{n\Omega}{\omega}\right)^2\right] arctg\,\frac{2\alpha k_0\sqrt{\varepsilon}}{k_0^2\varepsilon-\beta^2}. \qquad (10)$$

It is easy to show that A_1 is always negative. At $x << 1$, $arctgx \approx x$ and taking into account that the terms $n = \pm 1$ give contribution, we can write

$$A_2^{+1} = -\frac{e^2\tau R_0^2\Omega}{4c^3\beta_0}\int_{\omega_1}^{\omega_2} d\omega\,\omega^2\left[1-\frac{1}{\beta_o^2\varepsilon}\left(1-\frac{\Omega}{\omega}\right)^2\right]+\frac{e^2\tau R_0^2\Omega}{4c\beta_0\pi}\int_{\omega_1}^{\omega_2} d\omega\,\frac{\alpha_1}{\varepsilon(\omega)}, \qquad (11)$$

$$A_2^{-1} = -\frac{e^2\tau R_0^2\Omega}{4c^3\beta_0}\int_{\omega_1}^{\omega_2} d\omega\,\omega^2\left[1-\frac{1}{\beta_o^2\varepsilon}\left(1+\frac{\Omega}{\omega}\right)^2\right]-\frac{e^2\tau R_0^2\Omega}{4c\beta_0}\int_{\omega_1}^{\omega_2} d\omega\,\frac{\alpha_{-1}}{\varepsilon(\omega)}. \qquad (12)$$

The term A_2^{+1} corresponds to the normal Doppler effect, while A_2^{-1} to the anomalous one. First integrals of Eq. (11), (12) are equal in absolute value and have different signs, hence they do not give the contribution. Compare the second integrals:

$$A_2 \approx \frac{e^2\tau R_0^2\Omega v_0^2}{4\pi c\beta_0\varepsilon}\int_{\omega_1}^{\omega_2} d\omega\,\frac{k_0^4 l < \delta e^2 >}{4}\left[\frac{1}{(\omega-\Omega)^2}-\frac{1}{(\omega+\Omega)^2}\right]. \qquad (13)$$

Integrated function is always positive, radiation reaction force work will be also positive, which leads to the swinging of an oscillator.

Georgian Technical University

REFERENCES

1. *V. L. Ginzburg, V. Ya. Eidman.* JETF, 36, 1959, 1823.
2. *V. V. Tamoykin.* Proc. Higher Educ. Inst. Radiophysics, 1964, 432.
3. *G. V. Jandieri, V. V. Tamoykin.* Proce. Intern. Symp. on Transient Radiation of High Energy Particles, Erevan, 1984, 317.
4. *M. L. Ter-Mikaelian.* The Influence of the Medium on Electromagnetic Processes at High Energies. Erevan, 1969 (USSR).

საქართველოს მეცნიერებათა აკადემიის მოამბე, 159, №2, 1999
BULLETIN OF THE GEORGIAN ACADEMY OF SCIENCES, 159, №2, 1999

PHYSICS

T. Berberashvili, E. Vazagashvili, L. Chachkhiani, Member of Academy G. Tsintsadze

The Magnetic Properties of Uranium Ternary Compounds in System PrS-Us

Presented September 25, 1997

ABSTRACT. **The effect of the metamagnetic transition of rare-earth sulphur, uranium ternary compounds (systems PrS-US, TbS-US) is investigated with the use of the regular solutions approximation. The calculated results can be applied to $U_{1-x}Pr_xS$ and $U_{1-y}Tb_yS$, where $x = 0.1, 0.2,...1$; $y = 0.1, 0.2, 0.3$ and 1. The effect is shown to be very important.**

Key words: solid solutions, magnetic phase, ternary, exchange interaction.

The crystal and the magnetic properties of the US, USe, UTe uranium monochalcogenides are widely investigated [1-5] both experimentally and theoretically. They all have NaCl -type cubic structure, which promotes the superexchange. It is necessary to investigate the small-dimension compounds magnetic properties as for the development of technology for preparation of special type alloys. The interpretation of the results up to this day is based on the phenomenological assumption permitting that uranium and easy atom molecule are not sensitive to the interactions with each other (the gas assumption of the regular solutions). The aim of the present work is to study the ternary PrS-Us system properties.

The samples of the $U_{1-x}Pr_xS$ and $U_{1-y}Tb_yS$ solid solutions, where $x = 0.1, 0.2, 0.3, 0.4, 0.5, 0.6, 0.7, 0.8, 0.9$ and 1; $y = 0.1, 0.2, 0.3, 1$ were prepared. These samples were prepared by straight synthesis in vacuum from uranium, praseodymium, terbium and sulphur in quart tubes. After that the samples were annealed for 50-80 hours at 800^0-900^0C, melted in the arc furnace and pressed [2]. The results are obtained from different methods of X-ray diffraction and microstructural analysis. It was shown, that the system of solid solutions is pseudobinary: the uranium and praseodymium monosulphides form NaCl-type solutions. The homogeneous dissolubility is limited by the uranium angle in the phase diagram in the $U_{1-y}Tb_yS$ system. This might be because of different shapes of the impenetrable electron shell of heavy rare-earth element and light actinide.

The magnetic measurements were performed between 4.2^0 and 300^0K temperature range in magnetic fields up to 130kG equipment [2].

The PrS is Van-Fleck's paramagnetic compound and US is the ferromagnetic compound with T_c=180K.

We observed the transition from ferromagnetic to paramagnetic phase in accordance with concentration x in this system. All samples with concentration $x < 0.5$ were paramagnetic, the Curie-Weiss law was executed in the investigated temperature interval. When mixing uranium ions with praseodymium ions, the compounds with $x > 0.5$ are ferromagnetically ordered and the dependence curve of inverse susceptibilities appears.

This hump may be explained as the partially freezing of the orbital moment. The Curie-Weiss law works in the limit temperature interval and we can do the assumptions about the low level structure by deviations from it (the dependence of exchange interaction from distance). Such behavour of the value $\chi^{-1}(T)$ was noted when uranium monochalcogenides were studied. We determined Curie paramagnetic temperature Q_p by the extrapolation of linear ranges $\chi^{-1}(T)$ and the values of effective magnetic per molecula were calculated out of the dependence linear part

$$\mu_{eff} = 2.83\sqrt{\chi(T-\Theta_p)}\cdot\mu_B, \tag{1}$$

where Q_p is the paramagnetic temperature, μ_B is the Bohr's magneton. The correlation $Q_p \cong Q_f$ is carried out in the ferromagnetic range, Fig.1. It means, that this transition is very close to the second order transition and contradicts to imaginations about first order transitions in ferromagnetic alloys. The monotonical, but nonlinear decreasing of paramagnetic temperature Q_p and the Curie-Weiss law realization give us the base to assume that uranium ions are distributed in the dissolvent uniformly in the solid solution matrix. The character of the behavour of Bohr's effective magnetons number helps to conclude that solid solutions are well described by model of regular solutions. In the case, when the composition has $Q_p = 0$ the exchange magnetic field does not make uranium and praseodymium ions magnetic. Such composition is $U_{0.2}\,Pr_{0.8}\,S(Q_p = Q_p(x))$. Comparing the calculation and experimental values of Bohr's effective magnetons we get

$$\mu_{eff}^{cal} - \mu_{eff}^{exp} = 12\mu_B \tag{2}$$

The difference is conditioned by the ligand field's weaking when the parameter of the crystalline lattice increase. The uranium ions orbital moment's freezing is partially taken off. The samples with the concentration $x > 0.5$ experienced ferromagnetic transformations. Curves of the specific magnetization dependence from temperature $\sigma = \sigma(T)$ are shown in Fig. 2. We can not compare the values of magnetic moments determined of paramagnetic and ferromagnetic ranges, if taking into consideration the fact that the saturation on the dependent $\sigma(T)$ at the 4.2 K is not reached in the strong magnetic fields (130kG). This system was studied by experimental investigations like neutron diffraction and temperature measurements of magnetic susceptibilities methods [3-5]. We obtained good agreement between our results and the data [5] aside from compositions x=0.6 and 0.7. The spin-glass groundstate is

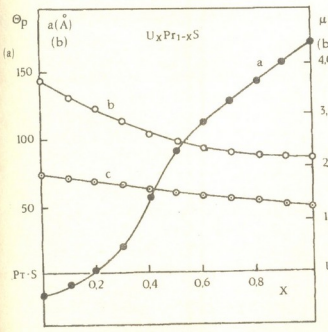

Fig. 1.

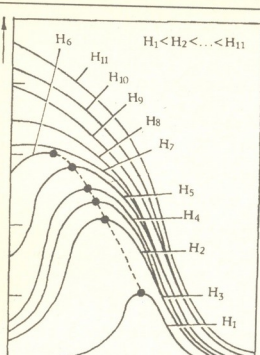

Fig. 2.

realised into compounds $Pr_{0,7}U_{0,3}S$ and $Pr_{0,6}U$ S. It was formulated in the paper [5]. The magnetic magnetization temperature hysteresis phenomenon is observed for these compositions too (at our data). Perhaps, the spinglass groundstate is realized without field and the inducted ferromagnetizm appears in the field. The ferromagnetic transformations points are calculated as T_1= 60K, T_2= 30K for $Pr_{0,6}U_{0,4}S$, $Pr_{0,7}U_{0,3}S$ respectively. Homogeneous compositions for $Tb_{1-y}U_yS$ we investigated only with 10, 20, 30% Tb [2]. The $Tb_{1-y}U_yS$ magnetization dependent curves at temperature above 30K are characterized by properties as in the $Pr_{1-x}U_xS$ solid solution system. The magnetic moment compensation point was observed below 30K on the freezing curve. Such behavior of the curve evidenced the complicated magnetic structure characterized by some sublattices [2].

Georgian Technical University

REFERENCES

1. *L. Chachakhiani, Z. Chachkhiani.* Intermetallicheskie soedineniya Urana, Tbilisi 1990, 176 (Russian).
2. *L. Chachakhiani.* Avtoref. dokt. diss. Kharkov, 1991 (Russian).
3. *L. Chachakhiani, V. Chechernikov, P. Nutzubidze.* Physics, 20, 1984, 678-679 (Russian).
4. *V. Chechernikov, B. Sloviaskix.* Journal teoreticheskoy I experimentalnoy fiziki, 54, 1968, 1715 (Russian).
5. *R. Troc et al.* J. of Magn. and Margn. Mat. 15-18, 1980, 1251-125

საქართველოს მეცნიერებათა აკადემიის მოამბე, 159, №2, 1999
BULLETIN OF THE GEORGIAN ACADEMY OF SCIENCES, 159, №2, 1999

ASTRONOMY

M. Gigolashvili, D. Japaridze, N. Gogoladze

Results of the Spectral Analysis of the Data of Hydrogen Filament Differential Rotation

Presented by Member of the Academy J. Lominadze, March 16, 1998.

ABSTRACT. **We studied the revealing of periodicities in the variations of differential rotation of hydrogen filaments on the basis of observational material obtained at the Abastumani Astrophysical Observatory in 1965-1993.**

By means of spectral analysis the characteristic time fluctuations having discrete nature are selected. The most frequently realized components in the spectrum of oscillation of differential rotation of hydrogen filaments are those of quasi bi-annual with periods of 2.2 at the latitudes (from 25^0 to 45^0) of the northern hemisphere.

Key words: filament, differential rotation, periodisities .

Solar differential rotation, in spite of its thorough study [1-5], is not finally elucidated phenomenon. On the contrary, the obtained results of rotation rate differ from each other not only for different solar formation, which could be explained by the action of various factors in various strata of solar atmosphere, but even for the same objects. It is caused not only by complicated and confusional phenomenon, but in the main, by comparatively low differences in rate (some percent or part of percent) and often they are noised too. In this connection the most important is to use homogeneous data, obtained for a rather long period of time.

Thus, to reveal the temporary change of solar differential rotation we used the prolonged, homogeneous observational material of hydrogen filament, obtained at Abastumani Astrophysical Observatory for 1965-1993 by means of chromospheric telescope AFR-2.

From all observational filaments during the considered period there were chosen relatively stable filaments which didn't significantly change their shape for the period of their existence and their separate fragments could be identified during the whole time of observation. Calm filaments were chosen, not connected directly with active regions. The filaments existing less than for 3 days were considered as instable and were eliminated.

Motion of 578 filaments was measured. In 11707 points the rotation rates of exactly identified fragments of filaments were measured in the range of latitudes 50^0 N-50^0 S and in the limit of $\pm 60^0$ longitude from the central meridian. Beyond these limits measurements were not made, as there were difficulties because of uncertainty arising near the edge of the disk.

For the investigation of periodicities of differential rotation of hydrogen filaments Fourier-analysis of observational data was used for three cycles of solar activity (No. 20-22). Time-distributions of mean annual values of differential rotation of hydrogen filaments were analyzed for 5^0-latitude intervals separately for northern and southern solar hemispheres..

Results of random process investigation can be presented both in time and frequency scales. We prefered spectral analysis of observations, because at statistical processing of the observational material, spectral presentation usually was easier to subject to physical interpretation.

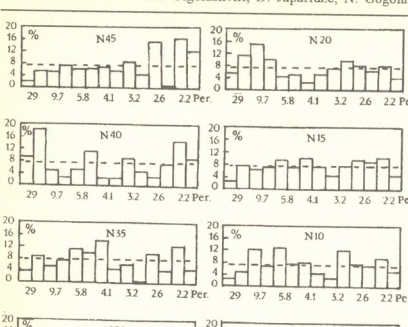

As a result of Fourier-conversion of data a power spectrum for hydrogen filaments was obtained separately for hemispheres and for separate 5^0-latitudinal intervals. The results are presented in Figures 1,2 as histograms. On the abscissa X-axis of each histogram selected periodicities are plotted in years. On Y-axis powers in percents are plotted. Value $Q = P + 3\sigma$ on histograms denoted by dash-lines, where P is the mean value of powers and σ is the standard deviation [6]. If there are some peaks, each of which exists in the power spectrum and is above the noise level (i.e. above the significance level Q), probably, they reflect periods existing in reality.

By means of spectral analysis the characteristic time fluctuations having discrete nature are selected. Amplitudes of selected peaks are changed from one band to another. The most frequently realized components in the spectrum of oscilation of differential rotation of hydrogen filaments are those of quasi bi- annual with periods of 2.2 at the high latitudes (from 25^0 to 45^0) of the northern hemisphere, while in the southern hemisphere 14.5 and 9.7 years periods prevail, probably corresponding to cyclic variation of solar differential rotation.

It should be specially emphasized that in the southern hemisphere there are almost no quasi bi-annual periodicities. If more precizely speaking, they are lower either than the significance level Q, or slightly (1-3%) exceed it and are observed in desorder only at separate latitudinal bands. While in the northern hemisphere quasi bi-annual periodicities exceed the significance level by 2-7% and the highest amplitudes present for latitudinal zones in the range of 25^0-45^0. The maximum amplitude occurs at 45^0 latitude. At lower latitudes they are also observed, but with smaller amplitudes.

On the same observational material in the northern solar hemisphere, near the moment of polarity reversal of the common solar magnetic field [7], was discovered the propagation of quasi bi-annual impulse of residual rates $\Delta\Omega(\theta, i) = \Omega(\theta,c) - \Omega(\theta, i)$, where

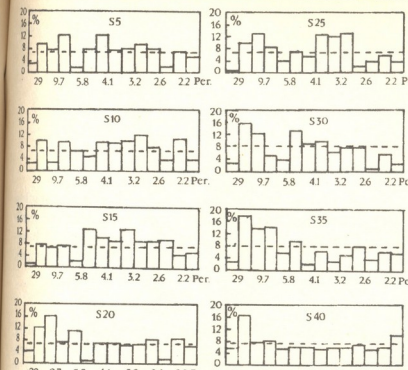

$$\Omega(\theta,c) = \sum_{n=1}^{n} \Omega(\theta_i)/n$$

is the mean cyclic value of rate and $\Omega(\theta, i)$ - is mid-annual for the corresponding i year. Further [8-10] the mentioned phenomenon was theoretically proved with the investigation of MHD equations in the local system of coordinates. Their solution was presented analytically. It was obtained that rate disturbance increased, mainly, at the moment of inversion of magnetic field polarity.There exists the possibility that the presence of significant quasi bi-annual variations in the discrete power spectrum of time series of differential rotation of hydrogen filaments in the nothern solar hemisphere is directly connected with the propagation of quasi bi-annual impulse of residual rates of differential rotation from the high latitudes to the equator of the northern hemisphere near the moment of magnetic polarity reversal of common solar magnetic field.

Georgian Academy of Sciences
Abastumani Astrophysical Observatory

REFERENCES

1. *J. B. Beckers.* The Sun of a Star, (ed.) S. Jordan, CNRS, Paris; NASA, Washington, SP-450, 1981, 11.
2. *H. Howard.* Ann Rev. Astron. Astrophys. 22, 1984, 131.
3. *E. H. Schroter.* Solar Phys. 100, 1985, 141.
4. *H. Zirin.* Astrophysics of the Sun. Cambridge University Press, 115.
5. *M. Stix.* The Sun, Astron. and Astrophys. Springer-Verlag, Berlin, Ch. 7, 1989, 228.
6. *J. R. Taylor.* In: E. D. Comminns (ed.): An introduction to Error Analysis, 1982, 270.
7. *D. R. Japaridze, M. Sh. Gigolashvili.* Solar Phys. 141, 1992, 267.
8. *M. Gigolashvili et al.* Tezis . dokl. 5 nauchn. seminar rab. gruppy, Irkutsk, 1991, 7-8 (Russian).
9. *M. Sh. Gigolashvili, D. R. Japaridze, A. D. Pataraya, T. Zaqarashvili.* Solar Phys., 156, 1995, 221.
10. Idem. Georgian Physical Society, 3, 1996, 46.

საქართველოს მეცნიერებათა აკადემიის მოამბე, 159, №2, 1999
BULLETIN OF THE GEORGIAN ACADEMY OF SCIENCES, 159, №2, 1999

GEOPHYSICS

M. Elizbarashvili

Response of the Temperature Field in Georgia to the Current Global Warming

Presented by Member of the Academy G. Svanidze, March 16, 1998

ABSTRACT. **In this report the temperature field response to the global warming of various landscapes of Georgia has been investigated. It was discovered that semi-humid landscapes have the most response to global warming. As to humid landscapes, they have no response. The possible histories of temperature field of Georgian landscapes have been treated.**

Key words: global warming, landscape, temperature field.

According to the latest generalization of the World Meteorological Organization data, various natural climatic conditions respond quite differently to the current global warming process [1]. Georgia is a country with diverse natural conditions, where more than 70 types of landscapes are being observed [2]. Assessment of the vulnerability of such conditions to global warming will throw light on numerous vague problems of current regional climate change and create a basis for the estimation of expected trends of climate change and possibilities of adaptation on various landscape and climatic conditions.

In this paper results of investigations on vulnerability of temperature field of landscape of Georgia to current global warming are being considered on the basis of observations by 90 meteorological stations during 1906-1995 and scenarios of expected changes of this field are being determined.

The Figure presents dependency of the rate of mean annual air temperature change on the altitude in various landscapes of Georgia.

The Figure shows that temperature change here has a very complicated nature on the background of the global warming of the Earth, though Georgia represents a rather small physical-geographical region. In humid landscapes temperature increase is not considerable. On the contrary, even decrease has been observed. Semi-humid and semiarid landscapes are evidently vulnerable to global warming. As to high mountain meadows there are not sufficient observation points.

More detailed information on the response of various landscapes to global warming is given in Table 1. It results from the Table, that semiarid landscapes are the most vulnerable to global warming. Mean annual temperature increase rate is 0.06°C in every 10 years and that of temperature increase in January makes 0.13°C.

Relatively weak vulnerability is characteristic of semi-humid landscapes and much weaker one of high mountain meadows. Plains and hills of subtropical landscapes practically do not respond to global warming. On the contrary, temperature is slightly decreasing here. The same pattern is observed in the temperately warm humid Colkhic low and middle mountain forest subtype landscapes.

Table 1.

Air temperature change rate in various landscape conditions (°C/10 years)

N	Landscape type	Designation [2]	Number of stations	January	July	Year
1	Plain and hilly subtropical humid	A	15	-0.012	-0.002	-0.085
2	Plain and hilly Mediterranean semi-humid	Б	11	0.10	0.04	0.05
3	Plain and hilly subtropical semiarid	B	9	0.13	0.04	0.06
4	Plain temperate warm semi-humid	D	7	0.10	0.05	0.05
5	Mountain subtropical semiarid	Λ	6	0.13	0.04	0.06
6	Mountain temperate warm humid a) Kolkhic low and middle mountain forest subtype b) low and middle mountain forest subtype transient into semi-humid	H_1-H_4 H_5-H_6	6 5	-0.02 0.07	0.02 0.02	-0.01 0.04
7	Mountain temperate semi-humid and semiarid	П ,P	6	0.10	0.04	0.03
8	High mountain meadows	Y	3	0.02	-0.01	0.01

Low and middle mountain forest landscape subtype has a transient position to global warming among the humid and semi-humid types of landscapes.

On the basis of revealed regularity, scenarios of possible changes of a temperature field of Georgian landscapes may be worked out. The most suitable approach for this purpose is the method of extrapolation. Applying this method implies that both global and regional climate change tendencies will be preserved in the nearest decades, though the scenarios, obtained by this approach need periodical specification.

Table 2 presents temperature data and scenarios for future century in the most vulnerable semi-humid and semiarid landscapes of Georgia.

It is evident that, scenarios, presented here are simplified and need periodical specification with the consideration of natural and anthropogenic factors of global climate change.

Table 2

Expected temperature scenarios (trend constituent) in semi-humid and semiarid landscapes (°C)

Scenario	Month	Landscape type		
		Б	В	П Р
Present	January	-0.3 ---- 0.6	-1.2 ---- 0.6	-4.7 ---- -3.4
	July	22.3 --- 24.0	22.2 --- 25.2	17.9 --- 19.7
	Year	11.0 ---- 12.4	10.9 --- 13.0	7.2 ---- 8.8
2050	January	0.2 --- 2.1	0.5 --- 1.3	-4.2 --- -2.9
	July	22.5 --- 24.2	22.4 --- 25.4	18.1 --- 19.9
	Year	11.2 --- 12.7	11.2 ---13.3	7.4 --- 9.0
2100	January	0.7---1.6	0.1 --- 1.9	-3.7 --- -2.4
	July	22.7---24.4	22.6 --- 25.6	18.3 --- 20.1
	Year	11.5 --- 12.9	11.5 --- 13.6	7.5 --- 9.1

.. Our estimoti ns c incide with D scenori f gl bol climote chonge, prepored by the W rld Mete r l gicol Orgonizoti n, occ rding t which the temperoture chonge rote will be 0.1^0C every 10 yeors in the next century [3].

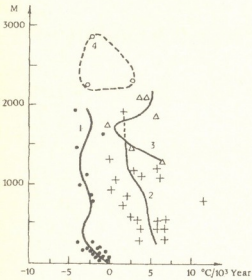

Fig. Vertical distribution of the rate of secular change of air mean temperature: 1- plains and hilly subtropical humid and mountainous temperately warm humid (subtype of Kolkhic low and middle mountain forest) landscapes (A, H_1-H_4); 2-plain and hilly Mediterranean marine semi-humid, plain and hilly subtropical semiarid plain temperately warm semi-humid, mountain subtropical semiarid and mountain temperately warm humid (sub- type of middle mountain-forest transient to semi-humid) landscapes (Б, В, D, L, H_5-H_6); 3- mountain temperate semi-humid (П) and semiarid (P) landscapes; 4- high mountain meadows (Y).

Acc rding t C, B ond A scenori s f gl bol climote chonge, temperoture increose rote will be m re thon 0.1^0C, respectively, 0.2^0C ond 0.3^0C in 10 yeors. In this cose, temperoture volues, presented in the Toble 2 will increose by 1-2^0C by the end f the next century.

Georgian Academy of Sciences
Institute of Hydrometeorology

REFERENCES

1. Climate change 1995; IPCC, Cambridge, UK, 1996.
2. *N. L. Beruchashvili*. Kavkaz: Landshafty, Modeli, Experimenty. Tb, 1995, (Russian).
3. IPCC, 1994; Radiative Forcing of Climate Change, 1994.

საქართველოს მეცნიერებათა აკადემიის მოამბე, 159, №2, 1999
BULLETIN OF THE GEORGIAN ACADEMY OF SCIENCES, 159, №2, 1999

CYBERNETICS

Z. Piranashvili, N. Khutsishvili

Method of Statistical Estimation for Nonlinear Transformation of Gaussian Stochastic Process

Presented by Member of the Academy V. Chavchanidze, July 6, 1998

ABSTRACT: **The problem of finding the statistical estimate for nonlinear transformation of Gaussian stochastic process by piecewise linear function is considered.**

Key words: stochastic process

Simulation methods of the so-called N class stochastic processes are considered in [1,2]. Taking into account, that N class processes are completely characterized by one-dimensional distrubution function $F(x, t)$ and correlation function $\rho(t, s)$, and if $\xi(t)$ is stochastic process of N class, we have:

$$\xi(t) = F_t^{-1}(\Phi(\eta(t))), \tag{1}$$

where $\eta(t)$ is normal stochastic process with parameters (0,1); $\Phi(\cdot)$ is normal distribution with parameters (0,1); $F_t^{-1}(\cdot)$ is inverse function to one-dimensional distribution function $F(x, t)$ of the process $\xi(t)$ with respect to X.

Simulation method of stochastic process $\xi(t)$ of N class is established by (1) representation. In practice one of the main difficulties of realization of this method is a search of $F_t^{-1}(\Phi(X))$ transformation (in stationary case) [3-5].

In order to sufficiently well approximate the function $f(X)$ we may use approximation by lower degree piecewise polynomials instead of construction of high degree polynomials.

In general the segment $[a,b]$ is partitioned on the intervals $(\alpha_i, \alpha_{i+1}]$, $a = \alpha_1 < \alpha_2 < \ldots < \alpha_n = b$ and on each interval $(\alpha_i, \alpha_{i+1}]$ lower degree approximating polynomial is constructed. Polynomials received in this way (in general having the same degree) give approximation of function $f(x)$ on the segment [a,b].

The following problem is considered: to find function $F_t^{-1}(\Phi(x))$, $-\infty < x < \infty$ on the basis of observed values of process $\xi(t)$ by piecewise linear polynomials.

Let $\xi(t)$ be discrete, stationary in the restricted sense ergodic stochastic process and $\xi_1, \xi_2, \ldots, \xi_n$ be the realizations of this process. Since $F_t^{-1}(\Phi(x))$ is increasing function, piecewise linear functions must satisfy this condition.

Optimization criterion of approximation is

$$\int_{-\infty}^{\infty} [F^{-1}(\Phi(x)) - \Psi(x)]^2 d\Phi(x) = \min,$$

where $\Psi(x)$ is a piecewise linear function.

The whole axis is partitioned on the intervals $(\alpha_k, \alpha_{k+1}]$, $-\infty = \alpha_0 < \ldots < \alpha_n = \infty$ so that in each interval the best approximation of increasing function is increasing linear polynomial.

If $\Psi(x) = A_k x + B_k$, $\alpha_k < x \alpha_{k+1}$, $k = 0, 1, \ldots, n\text{-}1$, $\alpha_0 = -\infty$, $\alpha_n = \infty$, then optimization criterion has the following form:

$$\sum_{k=0}^{n-1} \int_{\alpha_k}^{\alpha_{k+1}} [F^{-1}(\Phi(x)) - A_k x - B_k]^2 \, d\Phi(x) = \min_{A_k, B_k}$$

under the conditions

$A_k \alpha_{k+1} + B_k = A_{k+1} \alpha_{k+1} + B_{k+1}$ - continuity conditions,

$A_k > 0$, $k = 0, 1, \ldots, n\text{-}1$ -growth conditions.

When one-dimensional distribution function $F(x)$ is unknown, but realization of $\xi(t)$ process is known, then instead of $F(x)$ function we take its estimate, i. e. empirical distribution function.

In order to find optimal parameters, we must differentiate optimization function with respect to unknown parameters A_k, B_k. We receive system of linear algebraic equations

$$\int_{\alpha_k}^{\alpha_{k+1}} x[F^{-1}(\Phi(x)) - A_k x - B_k]^2 \, d\Phi(x) = 0$$

$$\int_{\alpha_k}^{\alpha_{k+1}} [F^{-1}(\Phi(x)) - A_k x - B_k]^2 \, d\Phi(x) = 0$$

$$A_k \int_{\alpha_k}^{\alpha_{k+1}} x^2 d\Phi(x) + B_k \int_{\alpha_k}^{\alpha_{k+1}} x d\Phi(x) = \int_{\alpha_k}^{\alpha_{k+1}} x F^{-1}(\Phi(x)) d\Phi(x),$$

$$A_k \int_{\alpha_k}^{\alpha_{k+1}} X d\Phi(x) + B_k \int_{\alpha_k}^{\alpha_{k+1}} d\Phi(x) = \int_{\alpha_k}^{\alpha_{k+1}} F^{-1}(\Phi(x)) d\Phi(x).$$

Let $\xi_1, \xi_2, \ldots, \xi_n$ be the observed values of stochastic process $\xi(t)$ and $x_1, x_2, \ldots, x_q$ be different $x_1 < x_2 < \ldots < x_q$ and let in the sequence x_j appear i_j times and $\sum_{j=1}^{q} i_j = N$.

We find ν_1, ν_2 such that the following conditions are satisfied:

$$\frac{1}{N} \sum_{j=1}^{\nu_1} i_j \le \Phi(\alpha_k) < \frac{1}{N} \sum_{j=1}^{\nu_1 + 1} i_j.$$

Then $F^{-1}(\Phi(\alpha_k)) = x_{\nu_1}$ (2)

$$\frac{1}{N} \sum_{j=1}^{\nu_2} i_j \le \Phi(\alpha_{k+1}) < \frac{1}{N} \sum_{j=1}^{\nu_2 + 1} i_j.$$

and $F^{-1}(\Phi(\alpha_{k+1})) = x_{\nu_2}$ (it is evident, that ν_1, ν_2 depends on K).

For definition A_k and B_k we have next system:

$$c_k A_k + b_k B_k = q_k,$$

$$b_k A_k + a_k B_k = p_k,$$

$$\alpha_{k+1} A_k + B_k - \alpha_{k+1} A_{k+1} - B_{k+1} = 0, \quad A_k \geq 0, \; k = 0,1,\ldots,n\text{-}1 \tag{3}$$

where a_k, b_k, c_k, p_k, q_k are defined in such way that:

$$a_k = \frac{1}{\sqrt{2\pi}} \int_{\alpha_k}^{\alpha_{k+1}} \exp\left\{-\frac{x^2}{2}\right\} dx = \Phi(\alpha_{k+1}) - \Phi(\alpha_k), \tag{4}$$

$$b_k = \frac{1}{\sqrt{2\pi}} \int_{\alpha_k}^{\alpha_{k+1}} x \exp\left\{-\frac{x^2}{2}\right\} dx = \frac{1}{\sqrt{2\pi}} \int_{\frac{\alpha_k}{2}}^{\frac{\alpha_{k+1}}{2}} \exp\{-z\} dz =$$

$$= \frac{1}{\sqrt{2\pi}} \exp\left\{-\frac{\alpha_k^2}{2}\right\} - \exp\left\{-\frac{\alpha_{k-1}^2}{2}\right\}, \tag{5}$$

$$c_k = \frac{1}{\sqrt{2\pi}} \int_{\alpha_k}^{\alpha_{k+1}} x^2 \exp\left\{-\frac{x^2}{2}\right\} dx =$$

$$= \frac{1}{\sqrt{2\pi}} \left(\alpha_k \exp\left\{-\frac{\alpha_k^2}{2}\right\} - \alpha_{k+1} \exp\left\{-\frac{\alpha_{k-1}^2}{2}\right\} \right) - \Phi(\alpha_{k+1}) - \Phi(\alpha_k), \tag{6}$$

$$p_k = \int_{\alpha_k}^{\alpha_{k+1}} F^{-1}(\Phi(x)) d\Phi(x) = \int_{F^{-1}(\Phi(\alpha_k))}^{F^{-1}(\Phi(\alpha_{k+1}))} y \frac{1}{N} \sum_{v=1}^{q} i_v \delta(y - x_v) dy =$$

$$= \int_{X_{v_1(k)}}^{X_{v_2(k)}} y \frac{1}{N} \sum_{v=1}^{q} i_v \delta(y - x_v) dy = \frac{1}{N} \sum_{v_1(k)}^{v_2(k)} i_v x_v, \tag{7}$$

where $\delta(\cdot)$ is Dirak function.

$$q_k = \int_{\alpha_k}^{\alpha_{k+1}} x F^{-1}(\Phi(x)) d\Phi(x) = \int_{F^{-1}(\Phi(\alpha_k))}^{F^{-1}(\Phi(\alpha_{k+1}))} y \Phi^{-1}(F(y)) \frac{1}{N} \sum_{v=1}^{q} i_v \delta(y - x_v) dy =$$

$$= \frac{1}{N} \sum_{v_1(k)}^{v_2(k)} i_v x_v \Phi^{-1}\left(\frac{1}{N} \sum_{j=1}^{v} i_j\right). \tag{8}$$

Algorithm.

Problem: Approximation of the function $F^{-1}(\Phi(x))$.

Let observed values of the strochastic process $\xi(t)$, ξ_1, ξ_2,..., ξ_N be given.

1. Order the sequence ξ_1, ξ_2,..., ξ_N by natural ordering $x_1 < x_2 <... < x_q$
2. Count how many times x_j appears in the sequence.
3. Part the axis in the intervals $(\alpha_k, \alpha_{k+1}]$, $-\infty = \alpha_0 < \alpha_1 <...< \alpha_n = \infty$
4. Define ν_1 and ν_2 by (2) formula.
5. Define a_k, b_k, c_k, p_k, q_k by formulae (4)-(8).
6. Compose system (3) for A_k and B_k, $k = 0, 1,..., n-1$.
7. Solve this system.
8. Compose corresponding linear functions $A_k x + B_k$, k= 0,1,...n-1by means of which we approximate the functions $F_t^{-1}(\Phi(x))$.

Finding of statistical estimate for nonlinear transformations has been considered as control examples:

$$F^{-1}(\Phi(x)) = e^x, \qquad F^{-1}(\Phi(x)) = x^3.$$

Let $F_t^{-1}(\Phi(x)) = e^x$. In this case $\xi_2 = e^{\eta_K}$, where $\{\eta_k\}$ is sequence of Gaussian stochastic variables which can be found by simulation method.

Using the algorithm the linear polynomials for function $F^{-1}(\Phi(x)) = e^x$ were constructed. Thereto constructed piecewise linear functions make good approximation of function e^x, that is well seen from the construction of corresponding graph.

The work is supported by grant 1.26 of the Georgian Academy of Sciences.

Georgian Academy of Sciences
Institute of Cybernetics

REFERENCES

1. *Z. Piranashvili*. Sb. Voprosy issledovaniya operatsii, Tbilisi, 1966. (Russian).
2. *Z. Piranashvili*. Works of IPM TGU, 1, Tbilisi, 1969.
3. *Z. Piranashvili, Yu. Burkadze, T. Sulaberidze*. Sb. Methody Monte-Karlo v vychislitelnoi mathematike i mathemat. fizike. Novosibirsk, 1976 (Russian).
4. *Z. Piranashvili, Yu. Burkadze*. Works of GPI, 9, 1977.
5. *N. Khutsishvili, Z. Piranashvili*. Sb. Methody predstavlenii i apparaturnyi analiz polei. Leningrad, 1978 (Russian).

საქართველოს მეცნიერებათა აკადემიის მოამბე, 159, №2, 1999
BULLETIN OF THE GEORGIAN ACADEMY OF SCIENCES, 159, №2, 1999

ANALYTICAL CHEMISTRY

Sh. Shatirishvili, I. Maglakelidze, I. Shatirishvili

Estimation of Efficiency of Liquid Chromatography

Presented by Member of the Academy T. Andronikashvili, April 6, 1998

ABSTRACT. **Efficiency of chromatographic columns used in high performance liquid and ion chromatographies for estimation of the contents of a number of phenol-carboxylic acids and cations in wine products has been determined.**

Key words: liquid-ion-chromatography, high performance, phenol-carboxylic acids, cations, wine products.

As it is known, number of theoretical plates (N) or the height equivalent of theoretical plates (H) is an universally adopted parameter of chromatographic column, used for comparison of different columns. It is also customary to use a reduced number of theoretical plates (N_n) calculated to a meter of a chromatographic column. Columns manufactured by various firms are accompanied with technical certificate and the chromatograms which give the above-mentioned characteristics obtained on model solutions. In practice, N values in relation to the investigated compounds are of special interest. It is considered to be a good result when this value equals to H_n= 2 dp, where dp is a particle diameter of a sorbent. In the most favourable cases the value of H reaches 1.2-1.5 dp [1].

We have investigated brandy "Tbilisi". Chromatographic separation of its heavy fraction was performed by means of A and B systems of solvents, changed according to the gradient-isocratic regime A: H_2O - AcOH (980:20) + 0.02 MNaOAc; B: H_2O - AcOH - iPrOH - MeOH (815:25:20:140) +0.02 MNaOAc.

Analyses were performed on a liquid chromatograph, Altex -344, with double pump block for gradient eluation, equipped with 421 model control system of working regime [2].

In the process of separation treating the data chromatograms for phenol-carboxylic acids were obtained. For the estimation of the effectiveness of 250x4.6 mm column filled with a sorbent 55-ODS particle size -5μm. Chromatogram of separation of phenol-carboxylic acids was deciphered with respect to theoretical plates number (Fig.) according to the known formula:

$$N = 5.54\left(\frac{T_R}{B1/2}\right)^2.$$

Retention time T_R is rather precisely determined by microprocessor, while the other value, peak width by the half-weight is rather indefinite and usually is determined at low precision. It is important that B 1/2 values difference depend on zero line taken for a starting point of the peak. Three possible variants were considered: B1-when a zero line passes along the lower, arched part of the chromatogram; B2 against a general slope of the right side drift; B3 from the moment of sample injection with respect to the straight line. Values of a number of peaks were calculated for these versions; peaks are numbered on the chromatogram. The results are given in Table 1 together with retention and selectivity values of phenol-carboxylic acids. The obtained results are given at the bottom of the chromatogram. It is seen that

number of theoretical plates significantly changes depending on the choice of zero line. According to the first variant N value for some peaks equals to 200000 theoretical plates per meter, which in our case corresponds to H = 1dp, that is, theoretically accessible limit. In two other variants N_n correspondingly was 5 and 10-times less, enabling us to estimate column resolution power at similar efficiency of separation of both, average (B2 variant) and bad quality (B3 variant). At the same time, the view of chromatograms and 60 separated peaks observed there, undoubtedly indicate to column efficiency, irrespective of such a great difference in N_n value in different variants of zero line.

Likewise, the data of column efficiency for ion chromatography are of interest. Eight

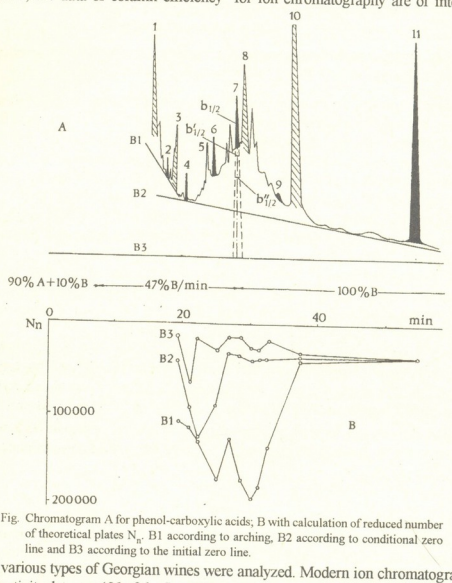

Fig. Chromatogram A for phenol-carboxylic acids; B with calculation of reduced number of theoretical plates N_n. B1 according to arching, B2 according to conditional zero line and B3 according to the initial zero line.

brands of various types of Georgian wines were analyzed. Modern ion chromatograph JLC-1 with conductivity detector 430 of the firm "Waters" was used. Cation separation was performed on a standard column JC-PAC Cation 50 x 4.6 mm, filled with 10μm diameter sorbent. For the separation of univalent cations solution of 1mmol HNO_3 was used as a mobile phase. In case of bivalent cations ethylene diamine solution of 0.5 mmol pH = 6 (HNO_3) was used. Mobile phase charges in both cases equalled to 1.2 ml/min. Selectivity and efficiency of chromatographic columns during separation of different cations are given in Table 2.

Table 1

Estimation of the retention parameters of phenyl-carboxylilic acids and the efficiency of the applied chromatographic columns (t_0 = 0.66 min)

Calculated data / No Compounds	Retention data and selectivity				Reduced number of theoretical plates and height of a theoretical plate					
					Variant B_1		Variant B_2		Variant B_3	
	t_{min}	T_{Rmin}	K'	α	N'_n	h'_n	N''_n	h''_n	N'''_n	h'''_n
1. P-hydroxy-benzoic acid	19.41	18.75	28.41	1.056	104.750	1.91	46.550	4.29	16.750	11.9
2. Vanillic acid	20.47	19.81	30.01	1.078	116.500	1.72	92.050	2.17	67.600	2.96
3. Lilac acid	22.2	21.36	32.36	1.139	135.250	1.47	135.250	1.48	17.900	11.18
4. Coffeic acid	24.99	24.33	36.86	1.048	179.500	1.11	94.950	2.10	23.750	8.43
5.Nonidentifed	26.19	25.50	38.64	1.066	128.000	1.56	24.200	8.27	14.200	14.06
6. Vanilline	27.84	27.18	41.18	1.061	179.500	1.11	36.500	5.48	16.500	12.31
7. P-cumaric acid	29.50	28.84	43.69	1.033	203.350	0.98	40.975	4.88	26.225	7.63
8. M-cumaric acid	30.46	29.80	45.15	1.045	145.000	1.38	39.800	5.02	28.100	7.12
9. Ferulic acid	31.79	31.13	47.17	1.193	191.650	1.04	43.450	4.60	21.300	9.39
10. Sinapic acid	37.79	37.13	56.26	1.475	69.500	2.88	63.050	3.17	57.450	3.48
11. Cinnamylic acid	55.43	54.77	82.98		40.500	4.94	40.500	4.93	39.500	5.06

Table 2

As seen from the data, in this case too, high resolution of the used chromatographic

Cation	Li^+	Na^+	NH_4^+	K^+	Mg^{2+}	Ca^{2+}
Number of theoretical plates of a column	140	515	1085	555	495	585
Reduced theoretical number of plates per 1m	2800	12300	21700	11100	9900	19700
Separation factor	1.93	1.93	1.44	1.20	1.85	1.85

columns has been achieved. At large, the issue of calculation of theoretical plate number and evaluation of column efficiency in gradient regime is a problem to be specifically considered and resolved in a more generalized form, as it is done for gas chromatography in the programmed temperature regime.

Georgian State Agrarian University

REFERENCES

1. *D. Cox.* Abstracts of Pittsburgh Conference., New Orleans 25 February - 1 March, **5**, 1985, 1257.
2. *J. Sh. Shatirishvili.* J. Chromatography, **364**, 1986, 183-188.

საქართველოს მეცნიერებათა აკადემიის მოამბე, 159, №2, 1999
BULLETIN OF THE GEORGIAN ACADEMY OF SCIENCES, 159, №2, 1999

S. Adamia, M. Gverdtsiteli, G. Kvartskhava

Algebraic-Chemical Study of Some Tin-Containing Acetylenic Compounds and the Reaction of their Synthesis

Presented by Corr. Member of the Academy D. Ugrekhelidze, March 9, 1998

ABSTRACT. **Algebraic-chemical investigation of some tin-containing acetylenic compounds and the reaction of their synthesis was carried out within the scope of quasi-ANB-matrices method.**

Key words: tin, acetylenic, quasi-ANB-matrix.

Investigation of the correlation "structure-properties" and algebraic characterization of chemical reactions are two main problems of mathematic chemistry [1-3].

The reaction of synthesis of tin-containing acetylenic compounds was elaborated:

$$R_3SnOH + HOR'C \equiv CH \xrightarrow{-H_2O} R_3SnOR'C \equiv CH \quad (1)$$

where: $R = C_2H_5$; $R = C(CH_3)(C_2H_5)$;

$$H_2\overline{C}-CH_2 \succ C \qquad\qquad H_2C \prec \begin{matrix} CH_2-CH_2 \\ CH_2-CH_2 \end{matrix} \succ C$$

Algebraic characterization of this process was carried out within the scope of quasi-ANB-matrices method [4]. ANB-matrices are modificated contiguity matrices of molecular graphs; the diagonal elements of ANB-matrices represent the atomic number of chemical elements, nondiagonal ones - multiplicities of chemical bonds. For large molecules and their transformations the calculations on the base of ANB-matrices are very labour-consuming. Thus we have elaborated simple model, where the fragments of molecules, which unchangeably transfers from initial to final state, are considered as "quasi-atoms".

Correspoding modernized ANB-matrix is called quasi-ANB-matrix ($\widetilde{ANB}$).

The simple model of (1) process has the form:

$$A - OH + H - B \rightarrow A - B + HOH \quad (2)$$

where A designates R_3Sn fragment; B-OR'C-CH fragment.

The register of (2) process in ($\widetilde{ANB}$) matrices form is brought below:

$$\begin{Vmatrix} Z_A & 1 & 0 & 0 & 0 \\ 1 & 8 & 1 & 0 & 0 \\ 0 & 1 & 1 & 0 & 0 \\ 0 & 0 & 0 & 1 & 1 \\ 0 & 0 & 0 & 1 & Z_B \end{Vmatrix} \rightarrow \begin{Vmatrix} Z_A & 1 & 0 & 0 & 0 \\ 1 & Z_B & 0 & 0 & 0 \\ 0 & 0 & 1 & 1 & 0 \\ 0 & 0 & 1 & 8 & 1 \\ 0 & 0 & 0 & 1 & 1 \end{Vmatrix} \quad (3)$$

where Z_A and Z_B are the sums of the atomic numbers of chemical elements, A and B fragments of which consist:

$$Z_A = \Sigma Z_a \quad (4)$$

$$Z_B = \Sigma Z_b \quad (5)$$

Consider the expression:

$$\Delta_r = \Delta_f - \Delta_i \quad (6)$$

where Δ_i is the value of determinant of $(\widetilde{ANB})$ matrix for initial system; Δ_f is the value of determinant of $(\widetilde{ANB})$ matrix for final system; Δ_r - is the change of value of determinant. Calculations show that the value of Δ_r for (2) process is negative. Thus the algebraic criterion on this process is determinant of $(\widetilde{ANB})$ matrix (in terms of this approach).

Three A-B compounds and their $T_{boil.}$ are brought below:

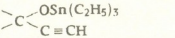
$T_{boil.}=70^0C$

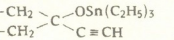
$T_{boil.}+99^0C$ (7)

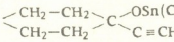
$T_{boil.}=110^0C$

The correlation equation $T_{boil.} \sim \lg(\Delta_{(\widetilde{ANB})})$ was constructed on computer and it has a form:

$$T_{boil}=499,9 \lg(\Delta_{(\widetilde{ANB})}) - 1774,8 \quad (8)$$

Correlation coefficient r = 0.99961, so correlation is "satisfactory"(according to Jaffe's criterion).

Tbilisi I. Javakhishvili State University

REFERENCES

1. *P. R. Rourvay*. Chemical Application of Topology and Graph Theory. (Ed. A. T. Balaban). Amsterdam, 1983.
2. *G. Gamziani*. Mathematic Chemistry. Tbilisi, 1990 (Georgian).
3. *G. Gamziani, M. Gverdtsiteli*. Phenomenon of Isomery from Point of View of Mathematic Chemistry. Tbilisi, 1992 (Georgian).
4. *N. B. Kobakhidze, M. G. Gverdtsiteli, D. S. Tugushi, M. I. Gverdtsiteli*. Correlation "Structure - properties" in Algebraic Chemistry. Tbilisi, 1997 (Russian).

საქართველოს მეცნიერებათა აკადემიის მოამბე, 159, №2, 1999
BULLETIN OF THE GEORGIAN ACADEMY OF SCIENCES, 159, №2, 1999

ORGANIC CHEMISTRY

D.Tsakadze, M.Sturua, T.Vepkhvadze, Sh.Samsoniya

Phenolic Compounds of *Magnolia obovata* D.C.

Presented by Corr. Member of the Academy D.Ugrekhelidze, June 1, 1998

ABSTRACT. ***Magnolia obovata* was investigated on content of phenolic compounds. Sum preparation was obtained. After separation by chromatographic methods individual phenolic compound was obtained. On the basis of spectral analysis it was identified as isoferulic acid.**

Key words: phenolic compounds, *Magnolia obovata*.

Phenolic compounds were completely extracted from leaves of magnolia by 75% ethanol. After ethanol distillation the aqueous extract was extracted by ethylacetate. After solvent isolation the aqueous and ethylacetate sum preparations were obtained (2.1%), which were studied by paper chromatography in various systems.

Fractionation of aqueous sum preparation was carried out on the column with polyamide sorbent. Eluation was carried out by water and ethanol (with augmenting concentration). Eluate from 85% ethanol was purified and separated on silica gel column. From ether - ethanol (7:3) eluate crystalline compound was isolated; T_{melt}: 224-226°C; R_f 0.16 (benzene-ethanol, 4:1); R_f 0.65 (n.buthanol, pyridine, water 6:4:3) $C_{10}H_{10}O_4$, M^+ 194 (mass-spectrum).

In UV-spectrum of the compounds the maxima of adsorbtion were obtained: 217, 242, 294, 323 nm (lgε 4.33; 4.29; 4.24; 4.26), which are characteristic for phenol derivatives.

In IR-spectrum the bands of absorption were obtained 3420 cm^{-1} (hydroxyl group), 1630, 1615 (conjugated double bonds); 1585, 1515 cm^{-1} (benzene ring); 2855, 1280-1270 (methoxy group); 1700 (carboxyl group).

On mass-spectrum following peaks were obtained: m/z 194, (M^+), 179 $(M-15)^+$, 177 $(M-17)^+$ (100%), 164 $(M-30)^+$, 151 $(M-43)^+$, 149 $(M-45)^+$, 133, 123, 105, 89, 78 and 77. Such fragmentation is typical for aromatic unsaturated acids [1].

On the basis of our results and its comparison with literature data [2], we suppose that isoferulic acid was isolated from *Magnolia obovata* and it has the structure:

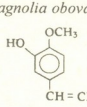

As sorbents for column and thin-layer chromatography polyamide sorbent and silica gel were used. As system for thin-layer chromatography benzene-methanol (4:1), buthanol-acetic acid - water (4:1:5), 15% acetic acid were used.

IR-spectrum was taken on UR-20 (KBr); UV-spectrum - on Specord (ethanol); mass-spectrum - on MX-1310.

Isolation of phenolic compounds. 0.5 kg of dry leaves of magnolia were reduced to fragments and extracted with 75% ethanol. Ethanol was distilled off on water-vacuum, residuum was washed by chloroform and extracted with ethylacetate; ethylacetate was fully distilled off. Brown viscous liquid-phase with ethylacetate was obtained. From water-extract water was evaporated on water-bath and water-phase was obtained. By paper and thin-layer chromatography it established that water-phase contains 6 components and ethylacetate phase contains 8 components. By means of qualitative analysis the content of flavonoids and phenol-carbon acids were established.

The fractionation of water-phase was carried out on column with polyamid sorbent. As eluents distilled water, 50%, 75% and 85% ethanol, methanol and methanol-chloroform (1:1) were used.

Each eluate was examined by thin-layer and paper chromatography. The content of phenol-carbon acids were established in eluates. 75% and 85% ethanol eluates were identical - their R_f is equal: 0.23; 0.49; 0.92 (buthanol-acetic acid- water 4:1:5); R_f 0.17; 0.45 (benzene-methanol 4:1). United eluates were separated on silica gel column.

From ether-ethanol (7:3) eluate crystals were isolated $T_{melt.}$ 225-226°C; R_f 0.16 (benzene-ethanol, 4:1); R_f 0.65 (benzene-pyridine-water, 6:4:3). $C_{10}H_{10}O_4$, M^+194 (mass-spectrum).

The full coincidence of spectral and chromatographic data for isoferulic acid isolated from *Cicerbita pontica* (Boiss) permits us to conclude, that the compound isolated from *Magnolia obovata* is isopherul acid.

Ethylacetate-phase was separated on column with polyamide sorbent. Eluation was carried out with water, 45%, 75% ethanol. On the basis of paper and thin-layer chromatographic analysis, water and 45% ethanol eluates were united. Thus, 3 types of eluates were obtained: water, 75% and 85% ethanol. Presence of flavonoids were established on the basis of qualitative reactions. The volume of each fraction was decreased to 10 ml. By chromatographic examination with some markers in different systems, it was established, that plant contains aglicon quercetin R_f 0.10 (methanol-water, 8:2), 0.04 (methanol-water, 6:4) 0.20 (methanol).

Tbilisi I.Javakhishvili State University
Adjara Cooperation Institute

REFERENCES

1. *G. G. Buzikevich et al.* Interpretatsiya mass spectrov organicheskikh soyedinenii. M., 1966, 237-245.
2. *D. M. Tsakadze, T. N. Kiparenko et al.* Bull. Acad. GSSR, 84, 1, 1976.

საქართველოს მეცნიერებათა აკადემიის მოამბე, 159, №2, 1999
BULLETIN OF THE GEORGIAN ACADEMY OF SCIENCES, 159, №2, 1999

ORGANIC CHEMISTRY

Corr. Member of the Academy L. Khananashvili, Ts. Vardosanidze, E. Markarashvili, D. Girgvliani, M. Gverdtsiteli, J. Kubaneishvili

Investigation of the Relation Between the Physico-Chemical Properties of Organocyclosiloxanes and their Structure within the Scope of Quasi-ANB-matrices Method

Presented March 30, 1998

Abstract. **The relation between physicochemical properties of organocyclosiloxanes and their structure was investigated within the scope of quasi-ANB-matrices method.**

Key words: organocyclosiloxanes, quasi-ANB-matrix.

Contiguity matrices of molecular graphs and their various modifications are widely used in algebraic chemistry [1-3] and ANB-matrixes fall into their type; their diagonal elements represent atomic numbers of chemical elements whereas nondiagonal ones–the multiplicities of chemical bonds. For an arbitrary ABC molecule ANB-matrix has the form:

$$\begin{matrix} 1 & 2 & 3 \\ A & B & C \end{matrix} \quad \begin{Vmatrix} Z_A & \Delta_{AB} & \Delta_{AC} \\ \Delta_{AB} & Z_B & \Delta_{BC} \\ \Delta_{AC} & \Delta_{BC} & Z_C \end{Vmatrix} \qquad (1)$$

where: Z_A, Z_B, Z_C are atomic numbers of chemical elements A, B, C; Δ_{AB}, Δ_{BC}, Δ_{AC} - represent the multiplicities of chemical bonds between A and B, B and C, A and C.

It should be admitted that for large molecules calculation on the base of ANB-matrices are rather labour-consuming. We have elaborated a simple model, which reproduces a specific character of the system (molecules or their transformations) and at the same time is less labour consuming [4]. The modified ANB-matrix is called a quasi-ANB-matrix ($A\tilde{N}B$).

The properties of organocyclosiloxanes and their transformations are intensively investigated [5]. In present work we have studied the correlation "structure-properties" for some organocyclosiloxanes within the scope of $A\tilde{N}B$ matrices method. The simplest model was elaborated for organocyclosiloxanes and it has a form: A-B,

where A corresponds to $[(CH_3)_2SiO]_3-\underset{CH_3}{\overset{|}{Si}}-O^{\uparrow}$, B–to CH_3, CH_2 = CH or C_6H_5. (2)

The record of organocyclosiloxanes in the $A\tilde{N}B$ matrix form is presented below:

$$\begin{Vmatrix} Z_A & 1 \\ 1 & Z_B \end{Vmatrix} \qquad (3)$$

where: Z_A and Z_B are the sums of atomic numbers of chemical elements, which A and B fragments contain:

$$Z_A = \Sigma Z_a \quad (4)$$

$$Z_B = \Sigma Z_b \quad (5)$$

The values of d_4^{20}, n_D^{20}, E(energy of activation of the polymerization reaction) and $\lg(\Delta_{A\tilde{N}B})$ for corresponding organocyclosiloxanes are listed in the Table.

Table

d^{20}_4, n_D^2 and $\lg(\Delta_{A\tilde{N}B})$

Compound	d_4^{20}	n_D^{20}	E(ccal/mol)	$\lg(\Delta_{(A\tilde{N}B)})$
$[(CH_3)_2SiO]_4$	0.9558	1.3975	19.5	2.204
$[(CH_3)_2SiO]_3-\underset{\underset{CH_3}{|}}{\overset{\overset{CH=CH_2}{|}}{Si}}-O$	0.9706	1.4095	-	2.220
$[(CH_3)_2SiO]_3-\underset{\underset{CH_3}{|}}{\overset{\overset{C_6H_5}{|}}{Si}}-O$	1.0166	1.4488	17.83	2.283

Correlation equations were constructed on computer:

$$d_4^{20} = 0.7558 \lg(\Delta_{A\tilde{N}B}) - 0.7088 \quad (6)$$

$$n_D^{20} = 0.6395 \lg(\Delta_{A\tilde{N}B}) - 0.1121 \quad (7)$$

$$E = -21.6593 \lg(\Delta_{A\tilde{N}B}) + 65.9146 \quad (8)$$

Correlation coefficient, r for these equations are equal: r = 0.999; r = 0.999; r = 0.998. So, according Japhe's criterion, correlations are excellent.

Thus we can consider $\lg(\Delta_{A\tilde{N}B})$ as topologic index for considered systems.

Tbilisi I. Javakhishvili State University

REFERENCES

1. *P. R. Rouvray*. Chemical Application of Topology and Graph Theory. (Ed. A. T. Balaban). Amsterdam, 1983.
2. *M. Gverdtsiteli, G. Gamziani, I. Gverdtsiteli*. The Contiguity Matrices of Molecular Graphs and their Modifications. Tbilisi, 1996.
3. *G. Gamziani*. Mathematic Chemistry. Tbilisi, 1990 (Georgian).
4. *N.B. Kobakhidze, M. G. Gverdtsiteli, D. S. Tugushi, M. I. Gverdtsiteli*. Correlation "Structure-properties"in Algebraic Chemistry. Tbilisi, 1997.
5. *L. M. Khananashvili, E. G. Markarashvili, Ts. Vardosanidze et al.* J. Gen. Chem., **53**, 1983, 1575-1578.

Dependence of reaction processing on polymer yield and viscosity was studied by polycondensation of dichloranhydride di-(p-carboxyphenyl)propylarsinoxide with dichlordiane (concentration 0.2 mole/l), in dichlorethane at 30°C in the presence of triethylamine. It was found that polymere yield and molecular mass which is determined by reduced viscosity reaches maximum during an hour. On the basis of this result all other polymers synthesis was carried out for an hour.

It should be noted that in the mentioned conditions the polymer doesn't fall out from dichlorethane solution i.e. the reaction takes place in homophasic conditions.

The action of organic area on polycondensation course i.e. polymer yield and molecular mass was studied. For this, polycondensation between dichlordian and dichloranhydride di-(p-carboxyphenyl)propyl-arsinoxide in different organic solvents with 0.2 mol/l concentration and with triethylamine presence at 30°C was studied. Benzene, dichlorethane and acetone were used as solvents. It appeared that in dichlorethane and benzene polycondensation proceeds in homophasic system i.e. polymer is fallen out from reaction solution from the very beginning (Table 1).

Table 1

Organic area action on yield and molecular mass of arsenic-containing complex polyether

Organic area	Polymer yield g, %	*$\eta_{red.}$ dl/g	$T_{decomp.}$ °C (in capilar)	Content of As found, % / calculated $C_{32}H_{27}Cl_2O_5As$, %
dichlorethane	0.8 50	0.25	199	11.57; 11.56 / 11.76
acetone	0.4 50	0.26	192	11.49; 11.40 / 11.76
benzene	0.7 90	0.14	183	11.44; 11.52 / 11.76

*The reduced viscosities of polymer given in Table 1 are determined in phenole and tetrachlorethane mixture at 25°C.

In order to increase polymer molecular mass, a succession of monomers input on yield and viscosity characteristics in reaction area was studied. This research was carried out by polycondensation of dichlordiane and di-(p-carboxyphenyl)propyl-arsinoxide dichloranhydride concentration 0.2 mol/l in dichlorethane at 30°C in the presence of triethylamine. The obtained data are given in Table 2. It is demonstrated that the succession of reagents input in reaction area has an effect on both polymer yield and $\eta_{red.}$ Polyarilate with high reduced viscosity was obtained by B-method due to which further, each synthesis was performed by this method, i.e. the third of amine was input in reaction area.

The action of bisphenols structure on polymer yield and molecular mass was studied by polycondensation of di-(p-carboxiphenyl)propil-arsinoxide dichloranhydride with diane, dichlordian, dimethyldiane, bis-(4-oxiphenyl) phenylmethane, bis-(4-oxyphenyl) phenylmethylmethane, phenylphtalein and 1.1-dimethyl-1.3-bis-(4-oxyphenyl)propane in dichlorethane at 30°C in the presence of triethylamine.

Table 2

Succession effect of monomers input in reaction area on yield and molecular mass of arsenic-containing polymers on the example of dichloranhydride di-(p-carboxypheyil)propylarsinoxide and dichlordiane polycondensation in the presence of triethylamine at 30°C

Method of synthesis	Polymer yield g, %	*$\eta_{red.}$ dl/g	$T_{decomp.}$ °C (in capillar)	Content of As found, % calculated $C_{32}H_{27}Cl_2O_5As$, %
a	0.45 65	0.10	199	11.42; 11.56 11.76
b	0.80 50	0.25	199	11.57; 11.66 11.76
g	0.59 87	0.10	199	11.52; 11.59 11.76

*At the end in the reaction area we introduced: method A – dichloranhydride; method B – triethylamine; method G – bisphenol.

The results of carried out works show that with comparatively high reduced viscosity dichlordiane and phenylphtalein polymers are obtained, i.e. electroacceptor substitutes (Table 3, NN2,6) (CH_3) having electrodonor substitutes or without substitutes in case of using bisphenols polymers are obtained with higher yield (about 99%), but with less viscosity.

Table 3

The action of bisphenols structure on arsenic-containing polyarylates yield and molecular mass, di-(p-carboxyphenil)propil-arsinoxide dichloranhydride and bisphenols condensation in dichlorethane (concentration 0.2 mol/l) at 30°C

N	Bisphenol	Polymer yield g, %	*$\eta_{red.}$ dl/g	$T_{decomp.}$ °C (in cappillar)	Content of As found, % calculated
1	dian	0.70 99	0.15	165	12.49; 12.60 13.20($C_{33}H_{29}O_5As$)
2	dichlordiane	0.80 50	0.25	199	11.57; 11.66 11.76($C_{33}H_{27}Cl_2O_5As$)
3	dimethyldiane	0.60 94	0.17	151	11.85; 12.07 12.58($C_{34}H_{33}O_5As$)
4	bis-(4-oxyphenyl)-phenylmethane	0.76 99	0.16	195	11.96; 12.00 12.21($C_{33}H_{29}O_5As$)
5	bis-(4-oxyphenyl)-phenylmethylmethane	0.70 91	0.13	180	12.00; 11.61 11.92($C_{36}H_{31}O_5As$)
6	phenylphtalein	0.5 63	0.22	219	11.62; 11.57 11.40($C_{41}H_{31}O_5As$)
7	1,1-dimethyl-1,3-bis-(4oxyphenyl)propane	0.70 94	0.17	142	12.35; 12.52 12.58($C_{34}H_{33}O_5As$)

To check these results polycondensation was performed in the same dichloranhydride and diane and on the other hand with dichlordiane in the other solvent-acetone, but in the same conditions as it is in case of dichlorethane (Table 3).

Despite the fact, that in acetone the reaction proceeds in heterophasic conditions, in dichlorethane —in homophasic, polycondensation results are in good agreement with found regularity, i.e. in both cases with diane the polymer was obtained with larger yield and lower viscosity than it is with dichlordiane (Table 4).

Table 4

Results of polycondensation of bisphenole and di-(p-carboxyphenyl)propil-arsinoxide dichloranhydride in organic solution with 0.2 mol/l concentration and 30°C

Bisphenole	Solution	Polymer yield g, %	$*\eta_{red.}$ dl/g	$T_{decomp.}$ °C (in cappillar)	As content found, % / calculated
diane	acetone	0.4 67	0.15	165	13.19; 13.08 / 13.20($C_{32}H_{29}O_5As$)
dichlordiane	acetone	0.4 50	0.26	168	11.49; 11.40 / 11.76($C_{32}H_{27}Cl_2O_5As$)
diane	dichlorethane	0.7 99	0.15	165	12.49; 12.60 / 13.20
dichlordiane	dichlorethane	0.8 50	0.25	199	11.37; 11.66 / 11.76

Synthesis of As -containing polyarilates.

In three-necked flask we put 0.7425 g (0.0025 mole) dichlordiane and 1.1237 g (0.0025 mole) di-(p-carboxyphenyl)propilarsinoxide dichloranhydride 12.5 ml (0.2 mol/l) in dichlorethane at 30° during 1 or 2 sec. Add 1.04 ml (0.6 mol/l) triethylamine. The reaction was passing in CO_2 area. In an hour the polymer was precipitated in spirit, filtrated, washed with vacuum. We obtained polyarylate with 0.8 g (50%) yield and $\eta_{red.}$ = 0.25 dl/g. Arsenic was determined by Evince method [4].

Tbilisi I.Javakhishvili State University

REFERENCES

1. *T. Gogiashvili, T.Alavidze et al.* Bull. Georg. Acad. Sci., **127**, 2, 1987, 289.
2. *Idem, Ibidem*, **129**, 2, 1988, 325.
3. *Idem, Ibidem*, **158**, 3, 1998.
4. *R. Kh. Freidlina.* Sinteticheskie metody v oblasti metaloorganicheskikh soedinenii myshyaka. M.-L., 1945, 100, 164.

PHYSICAL CHEMISTRY

N. Kakhidze, T. Kordzakhia, L. Eprikashvili,
Member of the Academy T. Andronikashvili

Study of Desiccation of Ethylacetate over Clinoptilolite Containing Tuffs Modified by Alkali and Alkaliearth Metal Cations

Presented March 23, 1998

ABSTRACT. **It has been shown that the nature of cations introduced into the zeolite framework significantly affects the character of desiccation process of ethylacetate. Desiccation process of ethylacetate was studied in dynamic conditions over modified clinoptilolite.**

Key words: clinoptilolite-containing tuff, adsorption, dynamic characteristics.

Ethylacetate is the most widely used solvent applied in high performance liquid chromatography. Efficiency of the above mentioned solvent is predominantly conditioned by its purity and namely by its moisture content. Therefore thorough desiccation of a solvent is of special importance, because the noncontrolled moisture leads to deterioration of reproduction of results. Even a slight change of the moisture of a solvent can markedly change the capacity factor (K^1) and the degree of component separation [1]. At present, for complete removal of moisture from organic solutions, method of adsorption desiccation over synthetic zeolites is most widely applied [2].

The present study deals with the possibility of application of natural zeolites of Georgia, and namely the clinoptilolite-containing tuffs of Khekordzula origin, enriched by cations of alkali and alkaliearth metals in processes of deep desiccation of ethylacetate.

Enrichment of clinoptilolites by the cations of alkali and alkaliearth metals, as well as preparation of the so-called "hydrogen form" was made according to the method elaborated earlier [3]. Introduction of the most hydrophilic cations, such as of magnesium, and especially of lithium, into the zeolite framework is rather difficult [4], and therefore, in our case, we could not manage to achieve high substitution.

Detailed process of the experiment and calculation formulae for the estimation of dynamic (a_d) and equilibrium (a_e) adsorption activity, as well as times of loss protective action of an adsorption layer (τ) are given in the papers [3, 5]. Initial water concentration in ethylacetate equalled to 3.1%, breakthrough concentration - 0.02%, solvent flow speed in the adsorption column - 1.3 ml/cm.sec. Moisture content of the product was determined chromatographically [5]; adsorbent - Porapak Q.

The Table presents the values of dynamic and equilibrium adsorption activities and times of protective activity of an adsorption layer, in dependence on the nature of cations of the zeolite framework. As it is seen from the Table data, among the clinoptilolites containing cations of alkali metals, the higher adsorption activity was inherent to potassium enriched and hydrogen forms, the fact conforming with the results obtained during desiccation of solvents such as dioxane and dymethylphormamide [5]. Low values of these indices in case of lithium forms, which seems rather illogical, most probably would

be connected with low degree of substitution of this cation in the zeolite framework as well as with the high values of their heats of hydration.

Table

Dynamic and equilibrium adsorption activity of clinoptilolite-containing tuff layer with respect to water, depending on the zeolite framework cation nature

Heat of hydration of cations Kj/mol	Ionic radius of cations Å	Sorbent	Dynamic activity of sorbent layer in relation to water (a_d) g/100g at 25°C	Equilibrium activity of sorbent in relation to water (a_{eq}) g/100g at 25°C	Time of loss protective action of a sorbent (τ) min
K^+-343.25	K^+-1.33	Kcl	11.8	14.3	70
Sr^{2+} - 1356.26	Sr^{2+} - 1.27	Srcl	10.9	12.8	65
Mg^{2+} 1829.28	Mg^{2+} -0.78	Mgcl	10.5	13.8	62
Ba^{2+}-1243.24	Ba^{2+} - 1.43	Bacl	10.1	11.7	60
Ca^{2+} -1511.15	Ca^{2+} -1.06	Cacl	10.0	11.0	59
H^+ - 1109.29	H^+ -0.2	Hcl	9.9	11.5	59
Rb^+-322.32	Rb^+-1.49	Rbcl	9.7	10.9	58
Na^+-414.41	Na^+ -0.98	Nacl	9.6	10.9	57
Cs^+ -297.21	Cs^+ -1.65	Cscl	9.2	10.1	54
-	-	cl (init.)	8.5	11.2	50
Li^+ -468.83	Li^+ -0.78	Licl	6.2	7.8	37

A series of selectivity of desiccation is given below which is constructed according to the dependence of dynamic adsorption activity values and time of loss protective activity of adsorption layer with respect to water from the cation nature of alkali metals in the zeolite: Kcl > Hcl > Rbcl ≥ NaCl > Cscl > cl init. > Licl.

Among the zeolites enriched by alkali-earth metal cations the highest adsorption values are inherent to strontium and magnesium containing tuffs. Apparently, it can be explained by the fact that strontium can more fully substitute initial cations of a zeolite [4], while magnesium, by the selectivity of ion exchange in clinoptilolite exceeds lithium and is characterized by vividly expressed hydrophilic capacity.

At large, clinoptilolite with alkali-earth metal cations are characterized by higher indices of dynamic adsorption activity than the initial clinoptilolites. For these forms of zeolites the following order of selectivity is inherent: Srcl ≥ Mgcl > Bacl ≥ Cacl > cl init.

For all clinoptilolite-containing tuffs studied by us, the following order of selectivity is established with respect to cation nature, determining their desiccation capacity towards ethylacetate: Kcl > Srcl ≥ Mgcl > Bacl > Cacl ≥ Hcl > Rbcl ≥ Nacl > Cscl > cl init. > Licl.

Georgian Academy of Sciences
P. Melikishvili Institute of Physical and Organic Chemistry

REFERENCES

1. *E. L. Styskin, L. B. Itsikson, E. V. Braude.* Prakti. vysokoeffekti. khromatografiya. M., 1986, 287 (Russian).
2. *N. B. Keltsev.* Osnovy adsorbtsiyonnoi tekhniki. M., 1984, 591 (Russian).
3. *T. Kordzakhia, L. Gamkrelidze, L. Eprikashvili, T. Andronikashvili.* Zh. fiz. khim., 1996, 70 1999 (Russian).
4. *G. Tsitsishvili, T. Andronikashvili, G. Kirov et al.* Natural Zeolites, 1992, 295.
5. *T. Andronikashvili, T. Kordzakhia, L. Eprikashvili et al.* Chem. Anal. Warsaw, **42**, 1997, 555 (Polish).

საქართველოს მეცნიერებათა აკადემიის მოამბე, 159, №2, 1999
BULLETIN OF THE GEORGIAN ACADEMY OF SCIENCES, 159, №2, 1999

PHYSICAL CHEMISTRY

I. Sarukhanishvili, N. Kurshubadze, V. Makhviladze, A. Sarukhanishvili

Physical and Chemical Processes Conducted by Heating Trachyte Containing Binary Systems

Presented by Member of the Academy G. Tsintsadze, June 1, 1998

ABSTRACT. **Experimental results which confirm the possibility of predicting some physical and chemical processes proceeding in the mixtures based on feldspar - containing raw materials are presented. It is shown that in the mentioned mixtures the processes proceed more rapidly and are completed at lower temperature than it is known from literature data.**

Key words: trachyte, sanidine, thermodynamic, derivatographic, roentgenogram.

Trachyte, kainotypical small grainy volcanit attracts attention as one of the basic raw materials in hard melting silicate materials production. As is known, trachyte is used in glass technology [1-3]. It positively impacts different articles of production, but in various cases the reasons of such influence are not clear. This is caused by the fact that physical and chemical processes conducted by thermal processing of trachyte-containing systems have not been studied yet.

The present work is a part of the research of the above-mentioned systems. It is dedicated to the study of ternary, conditionally binary systems, in which the content of trachyte change is as follows: trachyte- 70-100 wt.%, quartz sand 0-30 wt.%, limestone 0-30 wt.%, soda ash 0-15 wt.%. The results presented in the work were obtained by using complex physical and chemical analysis, in particular, by thermodynamic and petrochemical calculations, as well as derivatographical, roentgenophase, mineralogical and chemical analysis.

Trachyte and bentonite loam (ascanite) extracted from open rock in Ozurgeti region, quartzs sand with "O" mark from Novoselov, soda ash with "p.f.a", limestone of Dedoplistskaro were used as initial raw materials. To determine average oxide content of trachyte, literary data and the results of our analysis were used (25 samples).

According to petrochemical calculations, roentgenophase and mineralogical analyses the basic components of trachyte are high temperature potassium aluminosilicate-sanidine (77%), plagioclases (≈6%), as well as minerals of mica and loam groups (≈7%). The correlation between the last two components was not determined. Slurry obtained by trachyte washing contains mainly the minerals of montmorillonite group, pyrite and organic substances, complying with the data presented in [2].

By complex studying of physical and chemical processes while trachyte thermal processing it was detemined that at 500^0C the feldspars and first of all sanidine, existed in trachyte, trasform by "order-disorder" mechanism. This fact is supported by reflexes differentiation chracterised for feldspars on diphractogram, as well as the exothermal effect at 480^0C on derivatogram.

The reaction of mica and loam minerals while trachyte thermal procession at 950-1000^{0}C is shown by loss of weight on TG curve. Trachyte, processed at high temperature, reveals d α/n lines of minerals of enstatite group on diphractogram. Trachyte processed at 950^{0}C does not undegro considerable changes. Leucite, a new component of trachyte, is only formed by thermal processing at 1150^{0}C. This is due to incongruent melting of sanidine (orthoclase):

$$8KAlSi_3O_8 \rightarrow 5KAlSi_2O_6 + 3\ KAlSi_3O_8 + 5SiO_2$$

orthoclase leucite melt

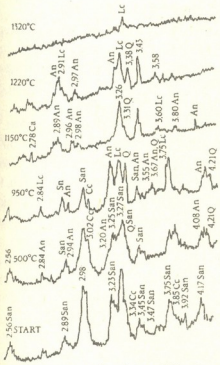

Fig. 1 Diphractograms of trachyte and limestone system relative denotations. (San) - sanidine (orthoclase); (An) - anorthite containing minerals; (Cc) - calcite; (Q) - quartz; (Lc) - leucite; (Ab) - albite containing minerals; (Ks)-calsilite; (S) - socla.

The product obtained after procession at 1220^{0}C consists of leucite and silicates formed by decomposition of admixture minerals. At 1350^{0}C these minerals partly and at 1450^{0}C entirely dissolve in primarily formed melt. The quantity of liquid phase of the system also increases by melting plagioclases. This is the reason of trachyte transfering into viscosity condition at much lower temperature as compared with leucite melting temperature.

The derivatogram of the trachyte (70-90wt.%) and limestone (30-10wt%) system shows the endoeffects of limestone decomposition. With an increase in the limestone content its maximum as that of the incongruent melting temperature of sanidine reduces from 920^{0}C to 850^0 C and from 1150^{0}C to 980^{0}C respectively. These are connected with interaction of feldspar and limestone (calcite).

As a result of thermal processing at 500^{0}C anorthite was revealed in the obtained products (Fig. 1). By 950^{0}C calcite completely disappears, while on its diphractogram the reflexes of anortite and quartz are clearly shown. This enables the processes going on in the intervals of 500-960^{0}C to be imagined in the following way:

$$2(K,Na)AlSi_3O_8 + CaCO_3 \rightarrow (K,Na)_2CO_3 + CaAl_2Si_2O_8 + 4SiO_2$$
$$2(K,Na)AlSi_3O_8 + CaCO_3 \rightarrow (K,Na)_2O + CaAl_2Si_2O_8 + 4SiO_2 + CO_2$$
$$2(K,Na)AlSi_3O_8 + CaO \rightarrow (K,Na)_2O + CaAl_2Si_2O_8 + 4SiO_2$$
$$(K,Na)_2CO_3 + 4SiO_2 \rightarrow (K,Na)_2Si_4O_9 + CO_2$$

Putting into brackets of K and Na does not correspond to isomorphism. It is a summary presentation of aluminosilicates of Na and K.

The obtained products interact with each other actively, since Na and K silicates on the one hand create easy-melting eutectics with fieldspar and on the other hand have low melting temperature. This causes a decrease in $CaCO_3$ dissolution as well as in melting temperature of $KAlSi_3O_8$ during an increase in limestone content. In thermally processed products leucite appeares at 1100^{0}C, while the system completely passes into amorphous

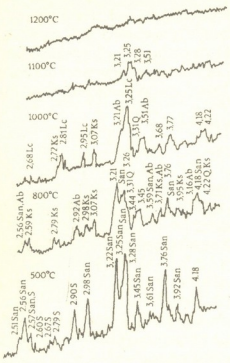

Fig. 2. Diphractogram of trachyte and soda system's mixtures. Same denotations as in Fig. 1.

condition at lower temperatures by 100°C-150°C as compared with trachyte.

The thermally processed system of trachyte (70-90) and quartz sand (30-10wt.%) at 500°C-1350°C does not change considerably. First parts of the liquid phase appears at 1000-1100°C when the content of quartz sand is average. Then sanidine melts, causing an increase in the amount of the liquid phase. This influences the interaction of the components noticeably.

It is worthwhile to note that in the mentioned system quartz does not pass into tridymite, indicating that alkali atoms existence is not enough to get tridymite [4]. Their ability to take part in this transformation is of decisive importance.

In trachyte (95-85) and soda (5-15wt.%) system first parts of soda cause activation of intercomponent processes (Fig. 2). At 500°C soda still maintains its individuality, although the intensity of reflexes characterised for it reduces considerably. After processing at 800°C quartz and formations like albite and calsilite appear in the system.

Thermally processed product has rather complex mineralogical compound, that could be logically explained by the following literary data: $KAlSiO_4$ is formed by the presence of Na_2O [5], while myrmekites formation in feldspar is a result of interaction of Na_2O and potassium feldspars [6].

By using these data and the results of researches, obtained by thermal processing at 300-400°C the interaction of components may be expressed by the reactions as follows:

$$2KAlSi_3O_8 + Na_2CO_3 \rightarrow 2NaAlSi_3O_8 + K_2O + CO_2$$

$$KAlSi_3O_8 \xrightarrow{Na_2O} KAlSi_2O_6 + SiO_2$$

In this system leucite is formed at lower temperature due to the fact that at 500-1000°C a lot of easy melting eutectics appear. Eutectic of leucite is added to the liquid phase obtained by melting of sanidine and plagioclase, that considerably decreases system's passing into amorphous condition.

Georgian Technical University

REFERENCES

1. *I. I. Kitaigorodski.* Steklo i steklovarenie. M., 1950, 136-137 (Russian).
2. *K. S. Kutateladze, V. L. Denchenko.* Trudy GPI 5(40) 1985, 102-113 (Russian).
3. *I. Sarukhanishvili.* Candidate thesis. 1997 (Georgian).
4. *U. A.Dir, P. A. Khaudi, G. Zusman.* Porodoobrazuyushchie mineraly 4., M., 1996, 225, (Russian).
5. *N. A.Toropor.* Diagramy sostoyaniya silikatnykh sistem. Spravochnik 3., L., 1979, 151-169, 184-190 (Russian).
6. *A. V Vinchel, G. Vinchel.* Opticheskie svoistva iskusstvenykh mineralov. M., 1967, 372-373 (Russian).

საქართველოს მეცნიერებათა აკადემიის მოამბე, 159, №2, 1999
BULLETIN OF THE GEORGIAN ACADEMY OF SCIENCES, 159, №2, 1999

ELECTROCHEMISTRY

R. Kvaratskhelia, E. Kvaratskhelia

Voltammetry of Formic and Acetic Acids at the Solid Electrodes Aqueous Solutions and Mixed Media

Presented by Corr. Member of the Academy J. Japaridze, March 30, 1998

ABSTRACT. **Voltammetry of two first representatives of the homologous series of carboxylic acid-formic acid and acetic acid at the Cu, Pt, Ni and Cu-Hg rotating disk electrodes in aqueous solutions and mixtures of water with acetone, acetonitrile, ethanol, dimethylformamide and pyridine has been studied. The kinetic parameters of the hydrogen ions discharge process proceeding in the solutions of above-mentioned acids and the dissociation constants of these acids in aqueous and mixed solutions have been determined.**

Key words: formic acid, acetic acid, voltammetry, electrode, dissociation constant, organic solvent.

Carboxylic acids in aqueous solution and some anhydrous media form the polarografic waves which correspond to a hydrogen ions discharge process [1]. Information of electrochemical behaviour of carboxylic acids at the solid electrodes and in mixed media is hardly available. The measurements were carried out by the methods of voltammetry at the rotating disk electrodes and chronovoltammetry at the stationary electrodes from high-purity Cu, Pt, Ni and Cu-Hg in the sealed cell with a pure helium atmosphere. Technique of a preparation of the electrodes for the measurements has been described in [2]. The background electrolyte-$NaClO_4$ has been twice recrystallized from a bidistillate and then has been dried for several days at 190°C distilled H_2SO_4 has been also used in the work. Formic and acetic acids were used as pure reagents. Technique of purification and drying of used organic solvents–acetone, acetonitrile, ethanol, dimethylformamide and pyridine has been described in [3,4]. The saturated calomel electrode has been used as a reference electrode. The measurements have been carried out at 20°C and 25°C.

At the voltammograms of HCOOH and CH_3COOH in 0.1 $NaClO_4$ the well-defined waves are observed. The $E_{1/2}$ values of these waves in the case of formic acid are equal to -0.93V(Cu), -1.47V(Cu-Hg), -0.72V(Ni) and -0.47V(Pt) and in the case of acetic acid -0.98V(Cu), -0.78V(Ni) and -0.51V(Pt) (wave for Cu-Hg electrode is ill-defined). These values are close to the $E_{1/2}$ values for a hydrogen ions discharge process in 0.1M $NaClO_4$ with 10^{-3} N H_2SO_4; this fact together with above-mentioned literature data gives us a possibility to attribute these waves to this process. In Fig. 1 the voltammograms of HCOOH and CH_3COOH for various electrodes are presented. For all the used electrodes the i_{lim}-$\sqrt{w}$ linear relationship is observed; this fact testifies to proceeding of a process in diffusion regime. Addition of the small quantities of H_2SO_4 to the solution causes a sharp increase of a wave height; the $E_{1/2}$ values in this case do not practically change (HCOOH) or shift slightly in the negative direction (CH_3COOH). In the case of copper electrode the

chronovoltammograms with well-defined current peaks have been registered; with the aid of the parameters of these peaks the k_0 rate constants have been calculated. The values of these constants are equal to 2.38×10^{-9} cm/s (HCOOH) and 6.62×10^{-9} cm/s (CH_3COOH).

Electrochemical behaviour of HCOOH and CH_3COOH has been also studied in the mixtures of water with acetone, acetonitrile, ethanol, dimethylformamide and pyridine. Addition of organic component causes the gradual decrease of the wave height which is more pronounced in the water-ethanol and water-dimethylformamide mixtures, less pronounced in the water-acetone system and least of all-in the water - actetonitrile mixture. This fact testifies to an important role of the increase of viscosity of the mixtures with the rise of organic component content. The small additions of high-basic pyridine (0.0005-0.01 M) cause the sharp decrease of the i_{lim} values and shift of $E_{1/2}$ values in the negative direction. These phenomena are more pronounced in case of formic acid.

The results of the study of voltammetry of the HCOOH and CH_3COOH solutions in water and water-organic mixtures give us a possibility to determine the concentration of hydrogen ions and the dissociation constants of carboxylic acids in above-mentioned solutions. We have used for this purpose the experimental values of i_d of H_3O^+ ions in 0.1 M $NaClO_4$ with 10^{-3} N H_2SO_4. The average value of i_d in aqueous solution (taking into account the values for all the used electrodes) is equal to 2.3×10^{-3} A/cm^2 (20°). For a verification of validity of this value we have calculated (with the aid of Gregory-Riddiford equation which is more precise than Levich equation) the diffusion coefficient of hydrogen ion in the above-mentioned conditions. The latter is equal to 7.71×10^{-5} cm^2/s. This value is close to the values obtained by Stackelberg, Vielstich and Jahn in 1M KCl by the rotating disk and Cotrell methods (correspondingly 7.5×10^{-5} cm^2/s at 23°C and 7.3×10^{-5} cm^2/s at 25°C) [5]. The i_d value in 0.1M $NaClO_4$ with 10^{-3}M HCOOH is equal to 1.393×10^{-3} A/cm^2; in the case of 10^{-3} M CH_3COOH this value is equal to 0.604×10^{-3} A/cm^2 (25°). Taking into consideration that i_d value in 0.1 M $NaClO_4$ with 10^{-3} N H_2SO_4 ($2.5 \times$

Table 1

C_{org}, %(vol.)	pK_a of HCOOH			
	acetone	acetonitrile	ethanol	dimethylformamide
10	3.21	3.20	3.07	3.18
20	3.37	3.40	3.16	3.16
30	3.64	3.44	3.16	3.17
40	3.67	3.40	3.24	3.15
50	3.82	3.36	3.13	3.09
60	3.75	3.31	3.13	2.88

Table 2

C_{org}, %(vol.)	pK_a of CH_3COOH			
	acetone	acetonitrile	ethanol	dimethylformamide
10	4.12	4.06	4.11	4.18
20	4.22	4.08	3.98	3.99
30	4.29	3.98	4.05	3.98
40	4.19	3.98	4.05	3.98
50	4.06	-	3.93	3.83
60	3.79	-	3.77	3.54

10^{-3} A/cm^2) corresponds to 10^{-3} M H_3O^+ we obtain that hydrogen ions concentration in the case of HCOOH is equal to 5.57 x 10^{-4}M and in the case of CH_3COOH - 2.34 x 10^{-4} M. Correspondingly the K_a value for HCOOH is equal to 7 x 10^{-4} and for CH_3COOH - 7.15 x 10^{-5} (the corresponding pK_a values are equal to 3.16 and 4.15). We have also calculated the values of the dissociation constants of formic and acetic acids in the used water-organic mixtures; these values are hardly available in literature. In Table 1 the pKa values of HCOOH are presented; in Table 2 - the same values for CH_3COOH (25°).

The data presented in Tables 1 and 2 show that in the broad interval of the binary mixtures contents (where the main state of solvated proton is H_3O^+ ion) the K_a values of HCOOH and CH_3COOH do not undergo sharp changes. This fact is connected with a comparatively small difference between a basicity of water and used organic solvents; it is also connected with the fact that dielectric permeability of mixtures in the used interval of their contents is sufficiently high. The K_a values in the concentrated organic media (50-60% of organic component) increase in the

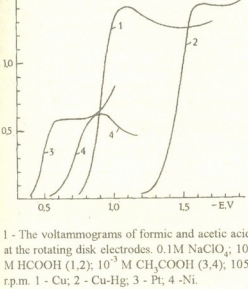

Fig. 1 - The voltammograms of formic and acetic acids at the rotating disk electrodes. 0.1M $NaClO_4$; 10^{-3} M HCOOH (1,2); 10^{-3} M CH_3COOH (3,4); 1050 r.p.m. 1 - Cu; 2 - Cu-Hg; 3 - Pt; 4 -Ni.

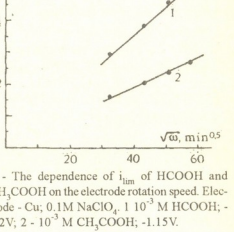

Fig. 2 - The dependence of i_{lim} of HCOOH and CH_3COOH on the electrode rotation speed. Electrode - Cu; 0.1M $NaClO_4$. 1 10^{-3} M HCOOH; - 1.2V; 2 - 10^{-3} M CH_3COOH; -1.15V.

series: acetone < acetonitrile < ethanol < dimethylformamide. This fact is connected with a more high basicity of ethanol and especially dimethylformamide in comparison with acetone and acetonitrile. Dielectric permeability of the above-mentioned concentrated mixtures in the case of water-acetonitrile and water-dimethylformamide systems is practically the same but acetonitrile has the lowest basicity among used solvents. These experimental facts prove the principal role of medium basicity in the processes of acide dissociation.

Georgian Academy of Sciences
R. Agladze Institute of Inorganic Chemistry and Electochmistry

REFERENCES

1. *L. Eberson*. In: Electrochemistry of organic compounds. Moscow, 1976.
2. *R. K. Kvaratskhelia, T. Sh. Machavariani*. Electrokhimiya, **20**, 3, 1984, 303.
3. *R. K. Kvaratskhelia, M. G. Zhamierashvili, G. R. Kvaratskhelia*. Elektrokhimiya, **27**, 5, 1991, 582.
4. *R. K. Kvaratskhelia, M. G. Zhamierashvili, H. R. Kvaratskhelia*. Electrokhimiya, **28**, 12, 1992, 1869.
5. *J. V. Pleskov, V. J. Philonovski*. Rotating disk electrode. Moscow, 1972.

საქართველოს მეცნიერებათა აკადემიის მოამბე, 159, №2, 1999
BULLETIN OF THE GEORGIAN ACADEMY OF SCIENCES, 159, №2, 1999

CHEMICAL TECHNOLOGY

G. Agladze, N. Demuria, N. Gogishvili

Investigation of the Suspension Process in the Manganese Dioxide Electrosynthesis

Presented by Corr. Member of the Academy L. Japaridze, March 30, 1998

ABSTRACT. **The influence of suspension of the fine-suspended particles into the acidic manganese sulphate electrolyte solution during electrosynthesis of the manganese dioxide, on the quality of the product and current efficiency, on the values of anodic potential and bath voltage, was investigated. It was shown that suspension of manganese-containing particles, as well as of graphite and inert materials - glass and corundum, results in considerable increase of titanium electrode resistance towards passivation: at 2 A/dm^2 current density the anodic potential and the bath voltage retained stable values. The overal picture of incorporation of the supspended particles into the electrode deposite and their total expenditure are evaluated. It was found that EMD specimens obtained in such conditions contain mainly γ-MnO_2, which could be utilized in a current sources as a cathode material, unlike ε-MnO_2 obtained in the same conditions but in the non-suspension bath.**

Key words: electrolytic manganese dioxide (EMD); suspension, particle, passivation, anodic potential polarization.

One of the crucial problems in production of the electrolytic manganese dioxide (EMD) is selection of the anode material. The corrosion-resistant titanium and its alloys, which in the last decades were used as an anode material, have a passivation trend because at the high current densities (>1 A/dm^2), during anodic polarization, their surface is covered by the phase oxides' film. This causes sharp increase of the voltage and limits the output [1-3].

The ten-year utilization of the anodes manufactured of the titanium-manganese alloys [4,5], partially solved the problem of intensifying the process, but the very process of manufacturing of these anodes is highly labour-consuming.

When using titanium-containing anodes at the current densities, along with passivation, there occurs production of ε-MnO_2, which is characterized by the one order lesser electronic conductance in comparison with γ-MnO_2 obtained at lower current densities. This restricts utilization of the former in the chemical electric batteries [6].

In some published patents [7,8] the authors point to the possibility of addition of various particles into the manganese sulphate solution in a course of the EMD synthesis. Unfortunately, these publications do not allow to assess specific technological characteristics of the process.

The aim of present study was establishment to the main processes in the manganese dioxide electrical synthesis in conditions of addition of various particles - MnO_2, graphite, corundum, glass, - into the electrolyte for the EMD.

The galvanostatic curves of the BTI-0 brand titanium cylindrical electrodes were recorded. The sulphate electrode of $[Hg/Hg_2SO_4\text{-}1NH_2SO_4]$ system was used as a reference electrode. Platinum plate served as an auxiliary electrode.

The preparational electrolysis was performed in the 1.5 l volume thermostabilized fireresistant glass vessel, placed on the magnetic stirrer. The BTI-0 brand titanium plate and titanium foil were used as an anode. Graphite rod served as a cathode.

The electrolyte was prepared of acid solution of the $MnSO_4 \cdot 5H_2O$ salt with addition of the fine particles of MnO_2, graphite, glass, and corundum (αAl_2O_3).

As was shown by the polarization measurements (Fig. 1), in conditions of addition of the fine-disperse particles of the MnO_2 into the acid manganese sulphate solution, during constant stirring, the anode potential values of the BTI-0 brand titanium anode, in the range of 0.01-0.02 A/cm^2 current density, are very stable and along the 2-hour polarization change insignificantly (Curves 1-4). Only at the 0.025 A/cm^2 current density there occurred constant rise of potential, which is due to the passivation of the electrode surface (Curve 5), while during precipitation of the EMD from the non-suspension bath this phenomenon already occurs at 0.0125 A/cm^2 current density (Curve 7).

Above results of the polarizational measurements were verified in the preparational electrolysis experiments.

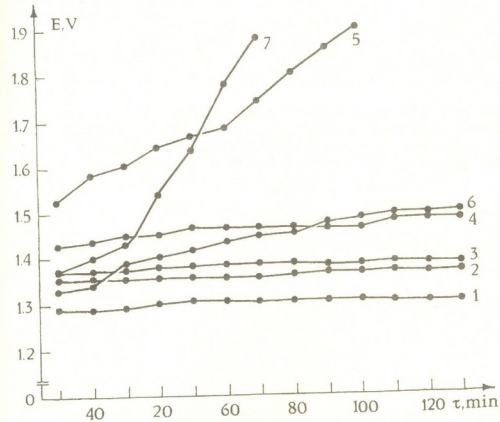

Fig. Potential changes of Ti anode during various current densities in a stationary conditions and in the suspension bath (The potential values are calculated against the hydrogen electrode). Suspension electrolyte solution: $MnSO_4$ - 130 g/l; H_2SO_4- 20 g/l, dispers. MnO_2 particle - 1 g/l. t = 92°C, anode current density (A/cm2): 1 - 0.01; 2 - 0.015; 3 - 0.0175; 4 - 0.02; 5 - 0.025. Stationary conditions: $MnSO_4$ - 130 g/l; H_2SO_4- 20 g/l, t = 92°C. Anode current density (A/cm2): 6 - 0.01; 7 - 0.0125.

Table 1

Influence of the anode current density (i_a) of the EMD electrosynthesis from the suspension electrolyte. Electrolysis conditions: C_{MnSO_4} -125 - 135 g/l, $C_{H_2SO_4}$ - 18 - 20 g/l, t=93-95^{0}C. Anode-titanium plate or titanium foil, S_{an}- 0.6 dm^2, S_{cat} - 0.3 dm^2. Experiment duration -6-9 hours.

Anode current density, A/dm^2	Voltage on the bath, V	Suspended particles, g/l, addition				EMD current, efficiency, %	Content of anode product (EMD) %		
		MnO_2	Glass	Graphite	Corundum		Mn	MnO_2	Ti
1.15	2.3-2.2	1.0	-	-	-	99.26	61.33	92.24	-
1.80	2.3-2.2	1.0	-	-	-	97.44	61.00	90.72	0.008
2.00	2.5-2.4	1.0	-	-	-	95.06	60.27	90.17	0.009
2.50	2.7-4.0	1.0	-	-	-	82.58	59.18	86.17	0.013
1.50	2.4-2.3	-	1.0	-	-	99.04	60.70	93.67	0.006
1.80	2.5-2.4	-	1.0	-	-	97.14	61.36	92.34	0.007
2.00	2.6-2.5	-	1.0	-	-	96.00	61.52	92.26	0.004
1.50	2.0-2.1	-	-	1.0	-	98.89	61.50	92.60	0.004
1.80	2.0-2.1	-	-	1.0	-	98.63	61.18	92.97	0.001
2.00	2.4-2.3	-	-	1.0	-	98.22	61.06	94.16	0.007
2.20	3.2-3.0	-	-	1.0	-	97.00	60.71	93.06	-
2.50	2.4-3.2	-	-	1.0	-	91.46	60.84	92.48	0.003
1.50	2.2-2.1	-	-	-	0.20	99.59	58.86	92.88	-
1.80	2.3-2.1	-	-	-	0.20	98.44	60.10	91.20	-
2.00	2.3-2.2	-	-	-	0.20	98.20	60.15	91.00	-

Table 2

Influence of the suspended, in the electrolyte, particle concentration on the electrosynthesis of the EMD. Experimental conditions: C_{MnSO_4} -125 -135 g/l, $C_{H_2SO_4}$ - 18-20g/l, t = 93-95^{0}C. Anode - titanium foil, S_{an} = 0.6dm^2, current (I)-0.9 A, current density (i_a) - 1.5 A/dm^2, cathode - graphite, S_{cat} - 0.3 dm^2, time of electrolysis (τ)- 6 hours

N N	Voltage V	Suspended particles, g/L		EMD current efficiency, %	Content of anode product (EMD), %				
		MnO_2	Graphite		Mn	MnO_2	SO_4^{2-}	Ti	Hygroscopic
1	2.3-2.2	0.01	-	95.60	61.45	93.30	1.40	0.009	3.12
2	2.5-2.4	0.10	-	95.60	61.92	91.30	1.48	0.021	4.03
3	2.5-2.4	0.25	-	100.00	61.70	91.20	1.43	0.013	3.97
4	2.4-2.3	0.50	-	96.20	61.59	91.20	1.39	0.008	3.97
5	2.5-2.4	1.00	-	99.20	61.33	92.20	1.30	-	3.80
6	2.2-2.4	-	0.010	100.00	61.47	93.90	1.12	0.008	3.64
7	2.3-2.0	-	0.0.25	98.80	60.57	94.00	1.12	0.003	4.13
8	2.4-2.4	-	0.200	100.00	60.99	92.60	1.02	0.003	4.31
9	2.5-2.3	-	0.350	99.60	60.71	92.20	1.40	0.003	4.15
10	2.0	-	1.000	98.80	61.50	92.60	0.34	0.004	4.30

Investigation of the influence of current density changes on the process of the EMD production during suspension of 1g/l fine-disperse MnO_2, graphite, glass, and of 0.2 g/l corundum, has shown (Table 1) that increase of current density from 1 A/dm^2 to 2.2 A/dm^2 results in passivation-free performance of the titanium anode. The voltage values in the bath are stable and do not exceed the established ones. The EMD current efficiency retains high, 95.1-99.6%, values. The content of MnO_2 in the EMD precipitate is high as well –

92-94%. The same Table shows that increase of the anode current density up to 2.5 A/dm^2 is not expedient because of decrease of the EMD current efficiency output and increase of the voltage in the bath. The content of MnO_2 in the anode product decreases in such a case.

It should be noticed that consumption of the added particles, during electrosynthesis of the EMD from the suspension electrolyte, is variable. Namely: in case of MnO_2 it was 43-52%, graphite – 9.8-11.7%, pirex glass – 9-15%, corundum – 8.8-12%.

All the obtained specimens represent an amorphous γ — MnO_2. The additional phase is represented by Mn_2O_3, the content of which complies with the Government Standards [9]. The same is true for the content of hygroscopic water in the precipitate. This points out on the suitableness of the precipitates for their use in the batteries.

The work has established the marginal concentrations of suspended, in the solution, particles of MnO_2 and graphite -0.01-0.25 g/l (Table 2), which correspond to the maximal values of the EMD current efficiency and content of MnO_2 in the latter.

Georgian Academy of Sciences
R. Agladze Institute of Inorganic Chemistry
and Electrochemistry

REFERENCES

1. *L. N. Japaridze*. Electrolytic Manganese Dioxide. Tbilisi, 1987 (Russian).
2. *A. Makahashi, J. Kozawa*. J. Electrochem. Soc., 37, 1969, 57.
3. *R. I. Agladze, T. A. Berezovskaya*. The Authorship Certificate 233918, 1967 (Russian).
4. *R. I. Agladze, L. A. Zauatashvili, K. Sh. Vanidze*. Electrokhimiya, 16, 1980, 1779 (Russian).
5. *K. Vanidze, L. Zautashvili, T. Aglodze*. Proc. First R. Agladze Int. Symp. on Electrochemistry of Manganese. Tbilisi, 1991, 67.
6. *E. Preisler*. J. Appl. Electrochem, 19, 1989, 540.
7. *M. Misava, K. Matsura, T. Okuda*. Jap. Pat. 57-42711, 1982.
8. Application No 47-7587, 1972.. Publication VP No 2573, 1976.
9. State Standard 25823-83. Manganese Dioxide for Chemical Sources of Current, Moscow, 1983 (Russian).

საქართველოს მეცნიერებათა აკადემიის მოამბე, 159, №2, 1999
BULLETIN OF THE GEORGIAN ACADEMY OF SCIENCES, 159, №2, 1999

PHARMACEUTICAL CHEMISTRY

M. Sikharulidze, M. Davitishvili, L. Kintsurashvili

The Improved Method of 3β - Acetoxy -5α-pregn-16-en-20-one Preparation

Presented by Member of the Academy E. Kemertelidze, June 8, 1998

ABSTRACT. **Applicability of NH_4Cl/ pyridine complex in the process of oxidative degradation of tigogenine spiroketal moiety was studied. Industrial importance of this method is conditioned by availability of a catalyst, which simplifies the process and by the high yield of final product.**

Key words: tigogenine, steroid, catalyst, oxidative degradation.

To carry out degradation of spiroketal moiety by simple technique and to provide the high yield of intermediate product 3β - acetoxy -5α-pregn-16-en-20-one is very important for synthesis of 5α-steroid hormonal preparations based on steroid sapogenine - tigogenine.

Some years ago at the Institute of Pharmacochemistry of the Georgian Academy of Sciences the original scheme of synthesis of the said intermediate was developed permitting to carry out the process without autoclave and to combine all the chemical reactions of this process in one technological stage. It simplifies the process and provides the high yield of final product. In this process titanium tetrachloride ($TiCl_4$) was used as a catalyst [1].

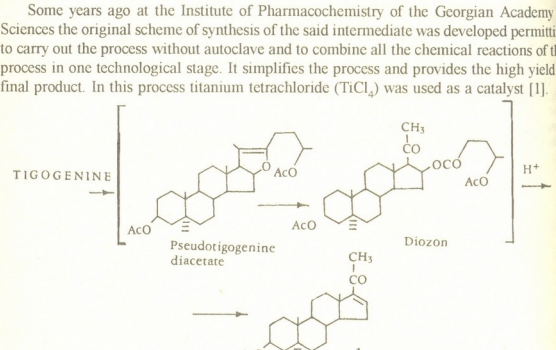

In order to improve the process of oxidative degradation of the spiroketal moiety of tigogenine we have studied applicability of more available NH_4Cl/ pyridine complex [2] as a catalyst instead of titanium tetrachloride.

We have established that maximum of transformation is reached in case of equimolar ratio of tigogenine and the catalyst.

When a catalyst was titanium tetrachloride oxidation of $\Delta^{20\text{-}22}$ double bond of

pseudotigogenine was carried out by using of chromic anhydride - acetone mixture. We also conducted the mentioned reaction in the way of oxidation with sodium bichromate in acetic acid. The best results were obtained in the latter case, particularly, the final technical product was filtered and purified better. The cleavage of 16β-ester group from the intermediate diozon was also carried out rather simply and hydrolysis in acidic conditions gave the compound of formula 1.

Thus, application of NH_4Cl/ pyridine complex as a catalyst in the process of tigogenine cleavage without autoclave by the use of sodium bichromate in acetic acid as an oxidazing agent provides the high yield of final product and greatly simplifies the known method of 3β - acetoxy -5α-pregn-16-en-20-one synthesis. All above permits to apply this method in industry.

Synthesis of 3β - acetoxy -5α-pregn-16-en-20-one. The solution of 20g tigogenine in 200 ml acetic anhydride was added by 4 ml of pyridine and 2.6g of NH_4Cl. The mixture was stirred at 132-135^{0}C for 5-6 hr. The reaction was controlled by TLC. The reaction mixture was then cooled to room temperature and 20ml of acetic acid and a solution of 9g of sodium bichromate in 30ml of acetic acid were added. The mixture was heated to 60-70^{0}C for 1 hr, treated with 1.3g of sodium bisulphite and then heated to reflux for 3 hr. The cooled mixture was diluted with water, the obtained precipitate was filtered, washed with 45% acetic acid and water and dried to give 15g of crude product (1) which was resolved in hexane. Filtration of the hot solution through an aluminium oxide pad gives 12g (71% yield) of chromatographically pure product 5 α pregnenolone; m. p. 157-160^{0}C, UV spectrum λ_{max} (lgε): 241 4.2) 319 (2.1) nm.

Georgian Academy of Sciences
I. Kutateladze Institute of Pharmacochemistry

REFERENCES

1. *L. Kavtaradze, R. Dabrundashvili, N. Menshova et al.* Bull. Georg. Acad. Sci. **132**, 3, 1988, 537-539.
2. *I. V. Micović, M. D. Ivanović, D. M. Piatak.* Synthesis, 7, 1990, 591-592.

საქართველოს მეცნიერებათა აკადემიის მოამბე, 159, №2, 1999
BULLETIN OF THE GEORGIAN ACADEMY OF SCIENCES, 159, №2, 1999

G. Guniya, L. Kartvelishvili

Monitoring of Changes in Chemical Composition of the Atmosphere Precipitation

Presented by Member of the Academy G. Svanidze, June 22, 1998

ABSTRACT. **The amount of mineral substances precipitated during a driving rain per km^2 has been defined in Georgia. The obtained results will be used for designing the buildings.**

Key words: mineralization, driving rain, corrosion

For the last several decades atmosphere chemistry has become a separate branch of meteorology, which studies the physical and chemical properties of aerosols and different gas mixtures in the atmosphere, and the chemical processes taking place below 50 km.

Monitoring of chemical composition of the atmosphere is very important to study the changes in chemical composition of the earth's surface in the process of precipitation of partitioned substances in the atmosphere. Estimation of the amount of the precipitated substances is very important.

One of the authors of this work has derived a formula, by means of which the amount of precipitated substances and the concentration of mineral materials in them can be defined according to the amount of atmospheric precipitations:

$$M = q\ H\ 10^{-3}\ t/km^2 p.a., \qquad (1)$$

where M is the amount of precipitated materials t/km^2 per year, q is the concentration of mineral materials in the precipitation (mg/l) and H is the amount of precipitation in a given period (mm). Using formula 1 the amount of precipitation on horizontal surface was calculated. The results are given in Table 1.

Table 1 shows that in the selected region a lot of substances are washed down during the atmospheric precipitation. It strongly affects on the ecosystem of the region and causes significant damages of buildings and objects of cultural heritage.

It is well known, that atmospheric precipitation is the main factor in rectification of the atmosphere from aerosols [1-3]. Therefore, the concetration of the mineral substances in the atmosphere is inversly proportional to the amount of precipitation. It is important to find the correlation between the amount of atmospheric precipitation and the amount of precipitated substances on the surface of the earth. Therefore the statistical characteristics of the relations among the variables given in Table 2 were calculated using the data given in Table 1. Here n is the number of analyzing pairs; M is the mean value of the amount of precipitated minerals on the surface of the earth; H_V is the amount of the precipitation over the years; σ_M and σ_H are the standard deviations of M and H, respectively; Γ_r is the corellation coefficient. F is the corellation coefficient estimating parameter and σ_{MH} is the estimation of the agreement among the regression line and observed variables

Table 1

The amount of precipitated substances in different regions of the Caucasus (t/km^{2}p.a.)

Region	Years	H, mm	Substances				
			SO^{2-}	Cl^-	HCO_3	Na^+	Σ_i
Tbilisi	1972-1978	650.0	7.6	1.6	5.2	1.2	21.8
" ----- "	1982-1987	542.2	5.6	1.4	8.2	0.9	22.1
Sukhumi	1972-1978	1556.3	7.5	3.0	7.0	1.8	26.1
" ----- "	1982-1987	1658.4	11.8	3.0	9.5	2.5	35.2
Chakva	1972-1978	2545.2	13.3	7.8	13.3	3.0	49.0
" ----- "	1982-1987	2564.9	14.9	6.5	13.0	4.4	50.2
Gudauri	1972-1978	1396.5	6.9	2.2	11.1	1.2	29.7
Abastumani	1982-1987	683.0	4.8	1.4	6.1	1.2	18.2
Krasnoselsk	1982-1987	647.0	5.1	1.3	5.6	1.0	17.0
Tsimliansk	1982-1987	429.3	5.6	1.5	3.7	1.1	15.5

Table 2

Statistical characteristics of the correlation among the amount of precipitation and the precipitated substances

Substance	Statistical characteristics							
	n	M	H	σ_M	σ_H	r	F_r	σ_{MH}
SO^{2-}	10	8.3	1270	3.67	810.0	0.70	7.69	2.61
Cl^-	10	3.0	"---"	2.38	"---"	0.82	16.30	1.36
HCO_3	10	8.3	"---"	3.35	"---"	0.80	14.22	2.01
Na^+	10	1.8	"---"	1.15	"---"	0.81	15.53	0.67
Σ_i	10	28.5	"---"	12.63	"---"	0.87	25.25	6.19
Σ_i mg/l	10	26.1	"---"	8.12	"---"	0.71	8.07	5.57

The positive sign of the correlation coefficients in Table 2 indicates that the relation among the amount of precipitation and the precipitated substancies is linear.

On the other hand, the concentration of the ion sum, which is given in the bottom line of Table 2 indicates the relation between the ion sum concentration and the amount of precipitation.

Thus, we can conclude that the increase of the precipitation causes the inerease of the amount of precipitated substances, but their relative concentrations are decreased.

The above results need to be adjusted on estimation of the environment damage in different regions. This is mainly due to the change in chemical composition of the surface of the earth. The above results are obtained for the precipitation on the horizontal surface, but to solve a number of problems in industry and agriculture requires to take into account the amount of the precipitation on every kind of surface.

According to the formula [5] we have calculated the number of precipitation on the surface of any kind of inclination in Georgia for the first time.

The surface is defined to be vertical when the angle between the surface and the vertical β is zero. Then the amount of precipitation on the vertical surface can be calculated by the following formula:

$$H_v = H_g tg\alpha cos(\theta - \theta_0), \qquad (2)$$

where H_V is the amount of driving rains, H_g is the rainfall on the horizontal surface; α the angle of the rain inclination against the vertical; θ is the orientation of the rainfall and θ_0 is the orientation of the inclined surface.

Using this formula the amount of the vertical rainfall was calculated for several different regions of Georgia. We tried to define the amount of precipitated materials in the driving rains per km^2 in different regions of Georgia.

The results are shown in Table 3.

Table 3

Place	Warm period				Annual			
	M_2	M_1	M	discrepancy	M_2	M_1	M	discrepancy
Tbilisi	4.3	12.7	17.0	25	5.6	16.9	22.5	25
Sukhumi	5.8	12.7	18.5	31	11.2	22.8	34.0	33
Gudauri	14.2	20.6	34.8	44	17.8	30.8	48.5	37
Batumi	12.4	27.5	33.9	31	16.3	50.2	66.5	24

M_2 is the amount of precipitated materials on a vertical surface (t/Km^2);
M_1 is the amount of precipitated material on a horizontal surface (t/Km^2);
M_2/M_1 is the discrepancy ratio (%).

From Table 4 we can see that the amount of materials precipitated on vertical surfaces oscillates in a wide range, up to 25-41% annually. This must be taken into account to prevent the corrosion and study the moisturing of the buildings.

Georgian Academy of Sciences
Institute of Hydrometeorology

REFERENCES

1. *G. S. Guniya.* Voprosi monitoringa zagriaznenia atmosf. vozducha na territorii Gruzinskoi SSR. L, 1985. (Russian).
2. *G. S. Guniya.* Bull. Georg. Acad. Sci., **157**, 1, 1998 (Georgian).
3. *G. S. Guniya.* e.a. Problems of the transfer of industrial waste over distances. - Proceedings of the WMO Conference on Air Pollution Modelling and its application (v.III, Leningrad, USSR, 19-24 May 1986) - Technical Document, WMO/TD, N187. March 1988, 165-170.
4. *L. G. Kartvelishvili.* Trudi molodikh rabotnikov TGU. Seria fiziko-matematicheskich I estestvennikh nauk. Tbilisi, izd. TGU, 1982 (Russian).

საქართველოს მეცნიერებათა აკადემიის მოამბე, 159, №2, 1999
BULLETIN OF THE GEORGIAN ACADEMY OF SCIENCES, 159, №2, 1999

HYDROGEOLOGY

M. Shaorshadze

On the Subject of the Formation of Georgian Block's Lower Cretaceous Horizon's Nitric Poorly Salinated Thermal Waters in Terms of Factor and Component Analyses

Presented by Corr. Member of the Academy I. Buachidze, March 30, 1998

ABSTRACT. **The paper substantiates the application of the factor analysis, Varimax rotation is accomplished. Four factors of the thermal waters formation have been distinguished: factor I (42%) is called a relic one, factor II (16%) is treated as that of carbonate balance, factor III (12%) is considered a negative depth's factor and factor IV (11%) is termed a surface-related one.**

Key words: factor, component, weight, score, eigenvalue, communality.

The poorly salinated (nitric) thermal waters of Georgian Block's Lower Cretaceous horizon are characterized with high discharges, a wide range of water temperature (from 20°C to 110°C) and a great variety of chemical composition. This results in the diversity of the chemical components content, and their distribution is mostly different from the normal one, being frequently polymodal.

Twelve components have been investigated (see Figures and the Table). The non-uniformity of the data forced us to make a complex use of the component (PCM) and factor analyses (FA), peculiar for their advantages and shortcomings. The weak point of the FA is its requirement for the normal distribution of the data, that is true for the majority of our components, whereas the PCM requests no hypothesis concerning the distribution pattern. However, Lawley has proved that the factor weights, obtained through the maximum likelihood method, are rather stable even under considerable deviation from the normal distribution [1]. Aivazian showed that when the principal components are estimated on the basis of correlation matrix and the first two factors are rather explicitly pronounced, the PCM and FA produce nearly the same results [2]. As an attractive point of the FA should be considered the fact that, though the correlation matrix is sensitive to the data non-uniformity, the FA results undergo insingificant variability, because the non-uniformity factor is determined separately and can be easily excluded [3].

From the above considerations the scheme of our research is the following. First, we found the solution to the PCM. Then we proceeded to the FA with onés on the correlation matrix's principal diagonal. After that the communality estimates were inserted along the principal of the correlation matrix. The results of the solution to this matrix in terms of the FA are not the only possible or privileged. There are several methods of rotation, meeting variuos Thurstone's requirements. These are: Varimax, Quartimax and Equimax methods. As all the four solutions are equivalent, we interpret the simplest sructure [4].

There are several methods available for distinguishing a number of factors. The most suitable for our objective was considered Kaiser's and Dickman's criterion [5], according

to which we have to proserve the factors with their eigenvalues exceeding 1. Table 1 shows that there are four such factors, accounting for 81% of the correlation matrix. We shall note that the results produced by PCM and FA (with the communalities on the principal diagonal) are identical to an accuracy of a constant multiplier. Through this procedure we extended the advantage of the PCM to the FA. Besides, we made sure that the results, obtained through the component and factor analyses, are not contrary to each other, and the departure of the variables distribution from the normal one proved to be rather smooth. The nonunformity of the chemical composition also happened to run smoothly (Fig. 2).

Table

Varimax Rotated Factor Matrix

Variable	Factor				Communality
	1	2	3	4	5
PH	-0.073	0.457	0.109	-0.132	0.243
Na^+	0.904	0.183	-0.088	0.293	0.944
Mg^{2+}	0.857	-0.181	0.138	0.338	0.901
Ca^{2+}	0.774	-0.128	0.545	0.177	0.886
Cl^-	0.968	0.147	0.191	-0.040	0.996
Br^-	0.792	0.279	0.353	-0.121	0.843
I^-	0.419	0.710	-0.146	0.192	0.738
SO_4^{2-}	0.401	-0.167	0.200	0.867	0.980
HCO^-_3	-0.194	-0.268	-0.773	-0.224	0.756
CO_3^{2-}	0.000	0.824	0.172	-0.030	0.710
SiO_2	0.243	0.515	0.471	-0.286	0.629
S (salination)	0.939	0.054	0.126	0.312	0.997
Eigenvalues	5.034	1.942	1.416	1.283	9.676
Communality percent	52.06	20.06	14.62	13.26	
Cumulative percent	52.06	72.13	86.76	100.0	
Dispersion percent	41.95	16.18	11.80	10.69	
Cumulative percent	41.95	58.13	69.83	80.62	

The varimax rotated factor matrix proved to be simpler to interpret (Fig. 1, Table). First of all calls attention the high value of the macrocomponents communalities, indicating that our factor-weight matrix corresponds to the common hydrogeochemical concept. The first factor (42% of the cumulative dispersion and 52% has of the communalities) has high weights on Na^+, Mg^{2+}, Ca^{2+}, Cl^-, Br^- and salination, i. e., the components, that are peculiar for ocean water. Thus, this factor can be considered as relic one. This factor is correlated with the minor part of I and SO_4^{2-} as well.

The second factor (16% of the cumulative dispersion, 20% of the communality) has significant weight on CO_3^{2-}, I^- and moderate one on pH, HCO^-_3 and SiO_2. Such a strange association is somewhat difficult to explain, therefore let us apply to Fig. 1. The figure clearly illustrates that along the second factor CO_3^{2-} and HCO^-_3 occupy the polar positions with pH inbetween them. So it would be quite natural to call this factor that of carbonate balance. The figure shows that the carbonate balance and the related alkali-acid index

also affect I- and SiO_2 accumulation in the solution, though their main sources are other factors. To a minor scope the same is true for Br^- as well.

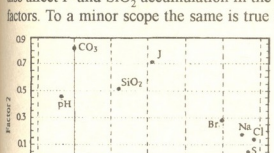

Fig. 1. Plot of first two factor weights

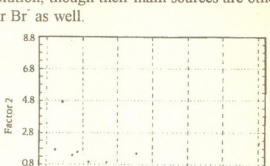

Fig. 2. Plot of first two factor scores

The third factor (12% of the dispersion, 15% of the communality) is rather difficult to explain. It has a considerable negative weight on HCO^-_3, and as it is a common idea that the source of HCO^-_3 are not deep processes, we can term it a negative depth factor. Such an awkward expression can be considered quite justifiable, because according to Belonin [2] the mark of the factor weight should only be regarded conventional. Factor III well complies with this definition as it features positive moderate weight on Ca^{2+}, Br^- and SiO_2, and the latter can never be deemed superficial variables. It is especially true for SiO_2, which is in positive considerable correlation with the temperature and, thus, the depth as well.

The fourth factor (11% of cumulative dispersion, 13% of the communality) has high positive weight on SO_4^{2-} and moderate positive one on Mg^{2+}, Ca^{2+} and salination, and again negative moderate weight on HCO^-. If we consider it a SO_4^{2-}-factor, then a question arises concerning its positive moderate weight on Mg^{2+} and Ca_{2+}. We might also attribute this factor to gypsum and anhydride effect the more so that it has negative, though quite insignificant weight on pH. As SO_4^{2-} is believed to be a surface or, at any rate, an active water-exchange indicator, we should call this factor a surface-related one, otherwise we will have to seek the source of SO_4^{2-} somewhere in the mantle.

Thus, the sedimentogenic component is the primary factor in the formation of the thermal waters under study, though the latter is much more desalted than the ocean water. Next comes the factor of carbonate balance, but it may also be regarded a depth's function if we consider its great weight on SiO_2. The two factors are characteristic of the other regions and other types of water as well. The rest factors are only peculiar for the specified waters.

Institute of Hydrology and Engineering Geology

REFERENCES

1. *D. N. Lawley, A. E. Maxwell.* Factor Analysis as a Statistical Method. 2nd. ed., London, 1971, 153 p.
2. *S. A. Aivazian, Z. N. Bezhaeva* at al. Klassifikatsiya mnogomernykh nabludenii. M., 1974, (Russian).
3. *K. Iberla.* Faktornii analiz. M., 1980, 400 (German).
4. *M. D. Belonin, V. A. Golubeva, G. T. Skublov.* Faktornii analiz v geologii. M., 1982, 269 (Russian).
5. *H. F. Kaiser, K. Dickman.* Amer. Psychol. 14, 1959, 425.

საქართველოს მეცნიერებათა აკადემიის მოამბე, 159, №2, 1999
BULLETIN OF THE GEORGIAN ACADEMY OF SCIENCES, 159, №2, 1999

HEAT ENGINEERING

T. Megrelidze

Effect of Active Basic Factors of Tea Drying Process on Machine Productivity

Presented by Corr. Member of the Academy A.Prangishvili, October 12, 1998

ABSTRACT. **Constituent regressive equations and heat calculation method are given for determination of tea drying machine productivity.**

Key words: tea drying, regressive equation.

The study of twisted tea drying process is aimed at adjustment of those parameters which provide optimization efficiency and maximal value of machine specific duty (q, kg/sec, m).

According to the analysis of literature data [1,2] the following makes significant action on drying process: air temperature, humidity of drying tea, speed and humidity of air flow, vibration amplitude and frequency, etc. The area of these changes and characteristics are given in the Table.

Table

Characteristics of basic parameters action on tea drying process

Factors	Actual denotation and determination	Area of actual changes	Factors level	Interval of factual variation	Pitch
Air temperature	T_1,K	263-268	265.5	2.5	0.5
Absolute air humidity	d, kg/kg	0.014-0.016	0.015	0.001	0.0001
Air speed	v, m/sec	0.5-0.9	0.7	0.2	0.03
Specific load of lattices	σ, pa	20-160	90	70	10
Vibration amplitude	A, mm	0-8	4	4	0.5
Vibration frequency	f, nm^{-1}	4-16	10	6	0.9
Initial humidity of drying tea	W_1, %	60-62	32	28	4

According to the Table data and method of drying process optimization given in [1] a regressive equation composed for twisted tea fractions in case of harmonic oscillation of the working organ is expressed as:

for the first fraction

$$q = 0.0114+0.00336(T-265.5)+0.00976(v-0.7)-1.63(d-0.015)-0.0000132(\sigma -90) - - 0.00029(A-4)+0.000168(f-10)-0.0001743(W_1-32) \quad (1)$$

for the second fraction:

$$q=0.0109+0.00328(T-265.5)+0.0097(v-0.7)-1.654(d-0.015)-0.0000139(\sigma-90)+ +0.000283(A-4)+0.000161(f-10)-0.000175(W_1-32) \quad (2)$$

for the third fraction:

$$q=0.0099+0.00321(T-265.5)+0.0093(v-0.7)-1.667(d-0.015)-0.0000143(\sigma-90)+ +0.000277(A-4)+0.000152(f-10)-0.000178(W_1-32) \quad (3)$$

But in case of biharmonic oscillation it will be:

for the first fraction

$$q=0.01425+0.00417(T-265.5)+0.01222(v-0.7)-1.6112(d-0.015)- -0.000011(\sigma-90)+ +0.00032(A-4)+0.00018(f-10)-0.0001735(W_1-32) \quad (4)$$

for the second fraction

$$q=0.01285+0.003753(T-265.5)+0.01102(v-0.7)-1.6182(d-0.015)- -0.000012(\sigma-90)+0.000305(A-4)+0.000176(f-10)-0.0001785(W_1-32) \quad (5)$$

for the third fraction

$$q=0.01225+0.003633(T-265.5)+0.01042(v-0.7)-1.6201(d-0.015)- -0.0000128(\sigma-90)+0.000297(A-4)+0.000170(f-10)-0.0001825(W_1-32) \quad (6)$$

The equations (1), (2), (3), (4), (5), (6) express experimental data in the area of factor varieties (see the Table), which were examined on adequacy according to Fisher criterion by 5% level.

It was established that the mentioned regressive equations are adequate to physical process. They can be used for optimization of tea drying process, for determination of drying machine production and for estimation action of factors both in case of harmonic as well as biharmonic oscillations of working organ.

If the effect of all the factors acting on drying process will be conditionally estimated by 100 points then in concrete case during harmonic and biharmonic oscillations of working organ, the action of basic factors on machine productivity in case of the first fraction of tea drying can be expressed in points as follows:

Air temperature – 44.3; 47.6; air speed – 9; 11; air humidity – 8; 7.4; specific load of lattices - 4; 3.5; oscillation amplitude – 6; 5.8; oscillation frequency – 4.5; 5; relative humidity of tea mass – 28.7; 22.8.

Proceeding from the analysis of numerical value estimated from the regressive equations changing the factors acting on drying process, machine productivity changes also. During the similar values of the factors in case of biharmonic oscillation of working organ the productivity of drying machine is 22% more than during harmonic oscillation.

Determination of the value of drying machine productivity is necessary for its construction, estimation and operation.

Georgian Technical University

REFERENCES

1. *I. Drenei*. Proizvodstvo bystrorastvorimykh productov. M., 1983, 184 (Russian).
2. *G. Jomarjidze*. Chais sashrobi mankanebis modernizeba da garemos ekologiuri mdgomareobis gaumjobeseba. Tbilisi, 1990, 62 (Georgian).

საქართველოს მეცნიერებათა აკადემიის მოამბე, 159, №2, 1999
BULLETIN OF THE GEORGIAN ACADEMY OF SCIENCES, 159, №2, 1999

AUTOMATIC CONTROL AND COMPUTER ENGINEERING

V. Mdzinarishvili

New Orthonormal Systems Based on Odd Numbers

Presented by Member of the Academy V. Chichinadze, July 27, 1998

ABSTRACT. **The new orthonormal systems based on odd numbers are received. The fractal structure is noted. The illustrative example is given.**

Key words: orthonormal, fractal, approximation.

Let's consider a sequence of functions $f_1(t)$, $f_3(t)$, $f_9(t)$ and $f_{27}(t)$ shown in Figs. 1-4. Laplace transform of these functions is:

$$F_1(s)=\frac{1-e^{-\tau s}}{\tau s},\quad F_3(s)=\left(1-e^{-2\tau s}\right)F_1(s),\quad F_9(s)=\frac{1-e^{-9\tau s}}{1-e^{-3\tau s}}F_3(s),$$

$$F_{27}(s)=\frac{1-e^{-27\tau s}}{1-e^{-9\tau s}}F_9(s).\ \text{where } s=\sigma+j\omega,\ \text{and}\ \ j=\sqrt{-1}.$$

Using the orthonormalized process [1] to these functions we have the following system of orthonormal functions.

$$M_1 = 1(t)\ t\in[0,1];\qquad M_3=\sqrt{\frac{3}{2}}\begin{cases}1 & t\in\left[0,\frac{1}{3}\right)\\ 0 & t\in\left(\frac{1}{3},\frac{2}{3}\right)\\ -1 & t\in\left(\frac{2}{3},1\right]\end{cases};\qquad M_9=\frac{3}{\sqrt{2}}\begin{cases}1 & t\in\left[0,\frac{1}{9}\right)\\ 0 & t\in\left(\frac{1}{9},\frac{2}{9}\right)\\ -1 & t\in\left(\frac{2}{9},\frac{3}{9}\right)\\ 1 & t\in\left(\frac{3}{9},\frac{4}{9}\right)\\ 0 & t\in\left(\frac{4}{9},\frac{5}{9}\right)\\ -1 & t\in\left(\frac{5}{9},\frac{6}{9}\right)\\ 1 & t\in\left(\frac{6}{9},\frac{7}{9}\right)\\ 0 & t\in\left(\frac{7}{9},\frac{8}{9}\right)\\ -1 & t\in\left(\frac{8}{9},1\right]\end{cases}\qquad (1)$$

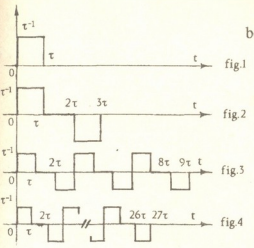

For each m system the m function M_m may be written down:

In general case we have:

$$M_1 = 1(t) \qquad t \in [0,1];$$

$$M_m = \left(\frac{m}{2}\right)^{\frac{1}{2}} \begin{cases} 1 & t \in [0,1/m) \\ 0 & t \in (1/m, 2/m) \\ -1 & t \in (2/m, 3/m) \\ \vdots & \\ 1 & t \in (m-3/m, m-2/m) \\ 0 & t \in (m-2/m, m-1/m) \\ -1 & t \in (m-1/m, 1] \end{cases} \quad (2)$$

$m = 3^n, \quad n = 0,1,2,\ldots$

Starting with $m = 9$ expression (2) of function M_m is not unique. So M_3 and M_9 except (1) may be written in following two functions M_{59} and $M_{9'}$

$$M_1 = 1(t)\ t \in [0,1]; \quad M_{59} = \frac{3}{2} \begin{cases} 1 & t \in [0, \frac{2}{9}) \\ \frac{1}{2} & t \in (\frac{2}{9}, \frac{4}{9}) \\ 0 & t \in (\frac{4}{9}, \frac{5}{9}) \\ -\frac{1}{2} & t \in (\frac{5}{9}, \frac{7}{9}) \\ -1 & t \in (\frac{7}{9}, 1] \end{cases} \quad M_{9'} = \frac{3}{\sqrt{2}} \begin{cases} 1 & t \in [0, \frac{1}{9}) \\ -1 & t \in (\frac{1}{9}, \frac{2}{9}) \\ 1 & t \in (\frac{2}{9}, \frac{1}{3}) \\ -1 & t \in (\frac{1}{3}, \frac{4}{9}) \\ 0 & t \in (\frac{4}{9}, \frac{5}{9}) \\ 1 & t \in (\frac{5}{9}, \frac{2}{3}) \\ -1 & t \in (\frac{2}{3}, \frac{7}{9}) \\ 1 & t \in (\frac{7}{9}, \frac{8}{9}) \\ -1 & t \in (\frac{8}{9}, 1] \end{cases} \quad (3)$$

Orthonormalized functions M_{59} and $M_{9'}$ are shown in Figs. 5, 6.

Let's generalize system (3) in case when number of intervals m is equal to arbitrary odd numbers $m = 2k+1$ $k = 0,1,2,3,\ldots$

Thus, the generalization of system (3) for m intervals may be written down by the following expression:

$$M_1 = 1(t) \qquad t \in [0,1];$$

$$M_{lm} = \frac{m^{\frac{1}{2}}}{2} \begin{cases} 1 & t \in [0, \frac{2}{m}) \\ (\alpha_k - 1)\alpha_k^{-1} & t \in (\frac{2}{m}, \frac{4}{m}) \\ (\alpha_k - 2)\alpha_k^{-1} & t \in (\frac{4}{m}, \frac{6}{m}) \\ \vdots & \\ \alpha_k^{-1} & t \in (\frac{k-2}{m}, \frac{k}{m}) \\ 0 & t \in (\frac{k}{m}, \frac{k+1}{m}) \\ -\alpha_k^{-1} & t \in (\frac{k+1}{m}, \frac{k+3}{m}) \\ \vdots & \vdots \\ -(\alpha_k - 2)\alpha_k^{-1} & t \in (\frac{m-6}{m}, \frac{m-4}{m}) \\ -(\alpha_k - 1)\alpha_k^{-1} & t \in (\frac{m-4}{m}, \frac{m-2}{m}) \\ -1 & t \in (\frac{m-2}{m}, 1] \end{cases}$$

$$M_m = \left(\frac{m}{2}\right)^{\frac{1}{2}} \begin{cases} 1 & t \in [0, \frac{2}{m}) \\ -1 & t \in (\frac{2}{m}, \frac{4}{m}) \\ 1 & t \in (\frac{2}{m}, \frac{4}{m}) \\ \vdots & \vdots \\ -1 & t \in (\frac{k-1}{m}, \frac{k}{m}) \\ 0 & t \in (\frac{k}{m}, \frac{k+1}{m}) \\ 1 & t \in (\frac{k+1}{m}, \frac{k+2}{m}) \\ \vdots & \vdots \\ -1 & t \in (\frac{m-3}{m}, \frac{m-2}{m}) \\ 1 & t \in (\frac{m-2}{m}, \frac{m-1}{m}) \\ -1 & t \in (\frac{m-1}{m}, 1] \end{cases} \qquad (4)$$

where $l = k+1$, $k = 0{,}5(m-1) > 1$, $\alpha_k = [0{,}5k+1] - 1$, $m = 5,7,9,\ldots$, $[\alpha]$ - the whole part of number α.

If we create orthonormal system by module P which is equal to arbitrary odd numbers

3,5,7,..., we shall get the following theorem.

Theorem. Let P be odd number for which the orthonormal system (4) is created, then limited relation

$$\lim_{m_n\to\infty}\int_0^1\left|\varphi(x)-\sum_{i=1}^{m_n}(\varphi M_i)M_i(x)\right|^p d\mu\to 0 \qquad (5)$$

$m_n = P^0, P^1, P^2, P^3, \ldots, P^n$, $P = const$, $n\to\infty$, executed by Lebesgue measure $d\mu$ is just for each function $\varphi(x)$ belonging to L^p class, that is $\varphi(x)\in L^p$, $p = 2k_1+1$, $k_1 = 0,1,2,\ldots$

Example. The function $\varphi(t) = t$, $t\in[0,1]$ is given. It is necessary according to (5) to find the approximating function $\varphi_M = \sum_{i=0}^{n}(\varphi M_i)M_i$ p

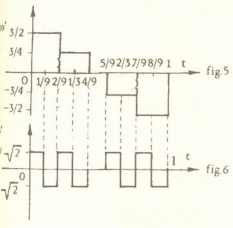

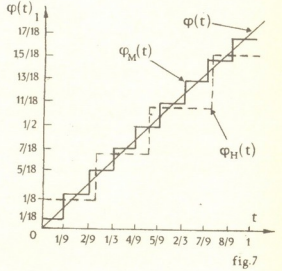

In Fig.7 we show the approximation curve φ_M for $p = 3$, $n = 2$.

From Fig.7 we see that the convergence of function φ_M is uniform as Haar's function φ_H.

But for function φ_M approximation error is smaller than φ_H $\sum_{i=0}^{n}(\varphi H_i)H_i$ $p = 2$, $n = 2$.

Gori State Economic-Humanitarian Institute

REFERENCES

1. *V. Mdzinarishvili*. Bull. Georg. Acad. Sci., **159**, 1, 1999, 121-125.

საქართველოს მეცნიერებათა აკადემიის მოამბე, 159, №2, 1999
BULLETIN OF THE GEORGIAN ACADEMY OF SCIENCES, 159, №2, 1999

SOIL SCIENCE

Corr. Member of the Academy T. Urushadze, G. Gogichaishvili,
O. Gordjomeladze, V. Shelia

Soil Erodibility Variation during a Year in Georgia

Presented May 8, 1998

ABSTRACT. **Nine year data from erosion plots at Keda (Zendidy), 3 years data from plots at Kelasury and 1 year data from Khevy were used to study variation in soil erodibility through the year. It was suggested that erodibility could be predicted using a variability function based on normal air temperature data described by a cosine function and average annual K factor values.**

Key words: erodibility variation, soil erosion, USLE, K factor, erosion predicting.

Soil detachability is inversely related to soil strength; strength is generally low at high water contents and high at low water contents. Erosion processes start after soil saturation with rain water [1-4]. Generally, variation of water content from high to low during the cool winter and early spring seasons and during the hot summer and early fall is similar to measured soil erodibility. The purpose of this research was to record this variation of erodibility during the year using erosion plot data and to suggest future studies to modify the universal soil loss equation for variable soil erodibility.

The universal soil loss equation (USLE) [5] is

$$A = R K L S C P, \quad (1)$$

where A is soil loss t/ha, R is the rainfall factor MJ×mm/ha×h, K is the soil erodibility factor t×ha×h/ha×MJ×mm, L and S are the dimensionless slope length and steepness factors, C is the dimensionless cover and management factor and P is the dimensionless support practice factor. Units for the variables of the USLE are those recommended by Foster. The factors are fully defined and described in agricultural handbook 537 [5].

By definition, the K factor is the average amount of soil A, eroded annualy from a standard fallow plot per unit of erosion index (EI), from average rainfall. The rainfall factor R is the average annual sum of EI for a given locality; EI is defined later. The standard plot is of 22.1 m (72.6 f) leng on a uniform slope of 9%, in continuous fallow and tilled up and down the slope. When these plot conditions are met,

$$K = \Sigma A / \Sigma E I \quad (2)$$

for a part of a year and

$$K = A / R \quad (3)$$

for average annual use, and the other factors of the USLE are equal to one.

Values of K determined from erosion plots operated since 1930 s are given in Agricultural Handbook 282 [6]. They include values from seven soils under continuous fallow and 16 other values computed from row crop data. These direct measurements were

expensive and time-consuming.Therefore rainfall simulation studies were used to colled quickly additional data of soil erodibility [2,7,8]. Research using erosion data from simulated rainfall resulted in soil erodibility nomograph [9] that has been widely used to assign K factors to most of the soil in the U.S.In all these rainfall simulation studies, some methods of grouping storms was used to approximate antecendent soil moisture conditions and storm characteristics found throughout the year. Thus, variability was averaged out in the single-value determination of soil erodibility.

The use of a single valued K-factor has resulted in a soil erodibility component in the C-factor(or soil loss ratio) used for cropstages. When an attempt was made to divide the cover and management factor, C, into subfactors, it was necessary to represent the hidden erodibility component using a coefficient Kc, to be applied to the conventional K factor [10]. Thus, the USLE was changed to

$$A = R\,K\,K_c\,L\,S\,C_s\,P, \tag{4}$$

where K_c is a dimensionless number that varies around unity, and C is a set of dimensionless subfactors. A major reason for determining the K-factor coefficient is to be able to study and use the cover and management subfactors more effectively.The reaserch was carried out on the experimental plots in vil.Zendidy, Kelasury(Institute of Tea and Subtropical Plants) and Khevy (Institute of Soil Science and Agricultural Chemistry).

Length of plot in v.Zendidy was 15m(49,21 ft), inclination 25 (46%); with mountain brown forest soil; in v.Khevy, length of plot was 20m(65,62ft),inclination -12-14 (21-24%), with mountain-brown forest soil ; in Kelasury length of plot was 30m(98,43ft), inclination 22 (40%), with mountain brown forest soil. All the soil was eroded. Surface of soils were bere fallow around the year. For registration of rain the rain recording instrument - Pluviograpf-P-2 was used. Precipitation more than 10mm (3,94in) was recorded. Erosion index of storms was computed as defined in Agricultural Handbook 537 [5].

In v.Zendidy average annual K- factor is 0.00041 t×ha×h/ha×MJ×mm (Table 1), in v. Khevy, K- factor is 0.00604 and in v. Kelasury - 0.00149 t×ha×h/ha×MJ×mm.K of the USLE is suitable for average annual soil loss prediction. However, K must be adjusted for a monthly estimation of erodibility. This correction or variability coefficient is

$$K_c = K_m / K \tag{5}$$

as given in the Table. To smooth the data, Kc was plotted as shown in Fig.1, as a function of time. The periodic cosine function,

$$K_c = A + a\cos\theta \tag{6}$$

was chosen to describe the data because of its good fit.

For v.Zendidy,

$$K_c = 1{,}13 + 0{,}34\cos[(t - 2.86)\,2\pi/12] \tag{7}$$

Time *t* is expressed in months where January 15 is 1.5; February 1 is 2.0 and so forth.Thus, using equation (5) and (7), soil erodibility (K_m) for our Zendidy plots can be computed for anytime of the year.

Data from v. Khevy and v. Kelasury resulted in

$$K_c = 1.31 + 0.45\cos[(t - 1.4)\,2\pi/12] \tag{8}$$

$$K_c = 1.23 + 0.72 \cos [(t + 2.27)\ 2\pi /12] \quad (9)$$

Equations (7), (8) and (9) with data points are shown in Fig.1. There is little difference between the amplitudes of the functions, except data from v.Khevy.However, the K_c for v.Zendidy lags that for v.Khevy and v.Kelasury by about 1 month.

Table 1

Monthly soil erodibility values at vil. Zendidy, Kelasury, Khevy

Month	EI average MJ.mm/ha.h	A average t/ha	K_m	K_c
vil. Zendidy				
April	70	0.590	0.00067	1.47
May	417	1.563	0.00030	0.67
June	74	0.566	0.00061	1.35
July	267	0.780	0.00023	0.51
August	357	1.520	0.00033	0.75
September	631	4.243	0.00053	1.18
October	938	5.242	0.00044	0.98
November	328	1.241	0.00030	0.67
December	260	1.725	0.00052	1.16
Annual	3342	17.47	0.00041	
vil. Kelasury				
April	20	1.333	0.00494	3.31
May	222	4.600	0.00153	1.03
June	400	10.533	0.00195	1.31
July	580	11.533	0.00147	0.99
August	48	0.167	0.00026	0.17
September	729	12.500	0.00127	0.86
October	245	4.633	0.00140	0.95
November	26	0.467	0.00133	0.93
December	32	0.400	0.00093	0.62
Annual	2289	46.166	0.00149	
vil. Khevy				
June	243	2.92	0.01202	1.99
July	106	0.28	0.00264	0.44
August	1513	3.53	0.00233	0.39
September	1596	14.15	0.00887	1.47
Annual	3458	20.88	0.00604	

Monthly temperature variations were examined hoping to predict the variation of soil erodibility for other locations without taking direct measurements using erosion plots. This turned out to be en excellent choice since temperature seems to be well described by the periodic cosine function also. For v.Zendidy

$$T' = 1 - 0{,}78 \cos [(t - 4.54)\ 2\pi /12] \quad (10)$$

for v.Khevy

$$T' = 1 - 1{,}05 \cos [(t + 4.5)\, 2\pi / 12] \quad (11)$$

for v.Kelasury

$$T' = 1 - 0{,}66 \cos [(t + 4.39)\, 2\pi / 12] \quad (12)$$

T' is equal to average monthly temperature divided by average annual temperature

$$T' = T_m / T_{ann} \quad (13)$$

and t is time as described earlier for equation (7). The fact was established that K_c identically describes variation of the soil erodibility during the year. T' function coincide with K_c function. Therefore, we can use T' for determination K_c function, which gives us the chance to define K factor without direct measurements of erosion.

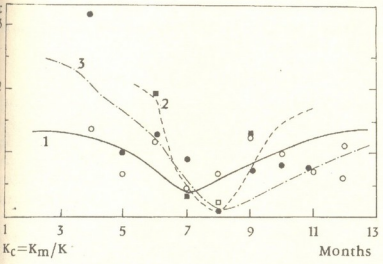

Fig. 1. Variability of soil erodibility on the erosion plots at v.Zendidy, Khevy and Kelasury.

Function of K_c was defined for more than of hundred meteorlogical stations of Georgia and was found possibility to compute K factors (K and K_c) for any time of year and locality of Georgia. Same work was carriedg out in the U.S.A., and received the results same [11]. That show, that compute of K_c any time of year can be used everywhere in moderate climate zone of the earth.

Agroecological Research Centre.

REFERENCES

1. *M. Al - Durrah. and J.M. Bradford*, -Soil Science Society of America, J. 45, 1981, 945-953.
2. *A. P. Barnett*, In.: Soil Erosion: Prediction and control (Proceedings of a National Conference on Soil Erosion, May 24-26 1976, Purdue Univ.,IN), 1977 , 97-104, Soil Conservation Society of America, Ankeny,IA.
3. *G. R. Foster, D. K. McCool, K. G. Kenard, W. C. Moldenhauer*, J.Soil and Water Conservation,36(6), 1981, 355-359.
4. *Ts. Mirtskhoulava*. Engieering methods of calculation and prognosis of water erosion. M., 1970.
5. *W. H. Wischmeier, D. D. Smith*. Agricultural Handbook 537, U.S.D.A., 1978, 58.
6. *W. H. Wischmeier, D. D. Smith*. Agricultural Handbook 282. U.S.D.A., 1965, 47.
7. *W. H. Wischmeier, J. V. Mannering*. Soil Science Society of America Proceedings, 33, 1969,131-137.
8. *R. A. Young, C. K. Mutchler*. J. Soil and Water Conservation. 32(4), 1977, 180-182.
9. *W. H. Wischmeier, C. B. Johnson, B. V.Kross*, -J.Soil and Water Conservation, 26(5), 1971, 189-193.
10. *C. K. Mutchler, C. E. Murphiee and K. C. McGregor*. TRANSACTION of the ASAE,St. Joseph, Mich.,25(2), 1982, 327-332.
11. *C. K. Mutchler , C.E.Karter*. TRANSACTION of the ASAE. St.Joseph.Mich., 26(4), 1983, 1102-1104.

საქართველოს მეცნიერებათა აკადემიის მოამბე, 159, №2, 1999
BULLETIN OF THE GEORGIAN ACADEMY OF SCIENCES, 159, №2, 1999

BOTANY

M. Akhalkatsi, G. Gvaladze, N. Taralashvili

Ultrastructural Study of Mature Pollen Grain in *Peperomia caperata* (*Piperaceae*)

Presented by Corr. Member of the Academy G. Nakhutsrishvili, March 23, 1998

ABSTRACT. **The submicroscopic peculiarities of cells of mature pollen grain in *Peperomia caperata* Yunker, were revealed.**

KEY WORDS: pollen grain, cell wall, vegetative cell, generative cell.

The previous light-microscopical studies of male gametophyte of *Peperomia* [1-4] have shown that the anther is two-lobed. The formation of the cell walls in the microsporangium is centripetal. Hypodermal archesporial cells divide periclinally cutting off the primary parietal and primary sporogenous layers. The parietal layer divides to form endothecium, middle layer and glandular tapetum. The endothecium and epidermis persists when the anther is mature. The meiosis I and II in the microspore mother cells are normal without deviations. The tetrad formation follows simultaneous type.

The present paper describes the ultrastructure of the mature pollen grain of *Peperomia caperata* Yunker (*Piperaceae*) for the first time. These data may contribute to define ultrastructural peculiarities of male gametophyte of genus *Peperomia.*

The material was collected from plants growing in the Greenhouse of Tbilisi Botanical Gardens in 1988-1989 years. For electron microscopical study the inflorescences of *P. caperata* at different developmental stages were pre-fixed in 3% glutaraldehyde at room temperature for 2h in 0.1 M phospate buffer at pH 7.2. The samples after buffer wash were post-fixed in 2% osmium tetroxide overnight. The fixed materials were dehydrated through acetone series and embedded in epon. Ultrathin sections were cut with glass knives on LKB-V ultramicrotome and stained with lead citrate. Sections were examined with a Tesla BS-500 transmission electron microscope.

The mature pollen grain is bicellular (Fig.I). The vegetative cell contains large nucleus showing more or less ellipsoidal outlines (Fig. 1-4). It is located on the periphery and possesses uniformly distributed heterochromatin and single nucleolus. In the ground cytoplasm occur free ribosomes and large lipid bodies. Plastids are represented by amyloplasts containing 3-5 starch grains. Mitochondria of different shape are abundant (Fig. 3, 4). They are scattered in the cytoplasm and have well developed interior organization. Endoplasmic reticulum (ER) is scarce. Some rough ER cisternae are observed in the spaces between other organelles. Golgi apparatus shows moderate activity. Dictyosomes are surrounded by a few small vesicles. Small discrete vacuoles arise at the later stages of maturation of the pollen grain. They are randomly distributed in the cytoplasm and possess electron transparent content. The vegetative cell is separated by plasma membranes both from the pollen wall and generative cell.

The generative cell (Fig. 1,2) is located on the periphery, opposite to the nucleus of

the vegetative cell. The two irregular plasma membranes defining the boundary between the generative and vegetative cells form the pericellular space containing globular substances. Plasmodesmata are absent between the two cells. The generative cell is more or less spherical in all sections. The nucleus adjoins to the plasma membrane and occupies one half of the cell. It shows uniform density. The nucleolus is absent. The ground cytoplasm is electron transparent, a few free ribosomes, however, can be observed. Mitochondria, proplastids and ER cisternae are distinguishable among membranous structures distributed in the cytoplasm. The separate microtubules are generally disposed along the plasma membrane.

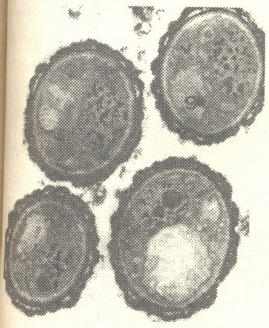

Fig.1 Pollen grains of *Pepperomia caperata*. x4000

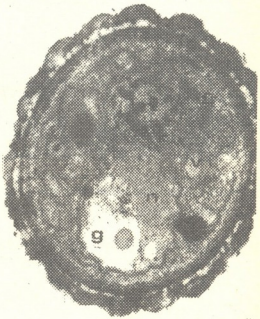

Fig. 2 Vegetative and generative cells in mature pollen grain of *Peperomia caperata*. x9000

The pollen wall (Fig. 2, 4) is stratified into an outer unevenly thickened tectum, granular bacula stratum, thin dark stained nexine and intine containing cellulose microfibrills.

The formation of the pollen grain considerably outstrips the development of the female gametophyte. There are already two-celled mature pollen grains in the anther when archesporial cell or megaspore mother cell arise in the ovule.

According to the obtained data vegetative cell of *P. caperata* may be regarded as a storage cell containing the nutritional material necessary for pollen tube growth in form of starch grains and lipid bodies. The starch was observed in vegetative cell of *Spinacia* [5]. In other plants there are found lipid aggregates [6] or both substances simultaneously [7]. These storage substances are degradated during the germination of pollen. The presence of RER, ribosomes and Golgi apparatus showing activity may be indicative of ability of pollen grain to produce wall material necessary for pollen tube elongation.

The generative cell surrounded by a well complex typical for other dicotyledons [5-7]

Fig. 3 Nucleus and mitochondria in vegetative cell of *Peperomia caperata*. x9000.

Fig. 4 . Pollen wall. x9000
g-generative cell; v-vegetative cell; b-bacula space; d-dictiosome; I-intine; m-mitochondrion; n-nucleus; t-tectum.

contains a few organelles with poor developed interior membrane systems, indicative that they are metabolic inactive. The microtubules found near the plasma membrane of generative cell are considered as structures which can maintain the shape of the generative cell in movement during the growth of pollen tube [7].

Georgian Academy of Sciences
N. Ketskhoveli Institute of Botany

REFERENCES

1. *Z. Y. Nikitcheva.* Sravnitelnaya embryologiya tsvetkovykh rastenii -*Winteraceae-Juglandaceae.* Ed. M. S. Yakovlev, Leningrad, 1981, 84-90 (Russian).
2. *G. Tockholm, E. Söderberg.* Sven. bot. tidskr. **12**, 2, 1918, 189-201.
3. *K. S. Semple.* Ann. Missouri Bot. Gard. **61**, 3, 1974, 868-871.
4. *B. M. Johri, K. B. Ambegaokar, P. S. Srivastava.* Comparative Embryology of Angiosperms. Berlin, 1992, 309-312.
5. *H. J. Wilms, A. C. van Aelst.* Fertilization and embryogenesis in ovulated plants. Bratislava, 1983, 105-112.
6. *M. Charzynska, M. Murgia, M. Cresti.* Protoplasma,, **152**, 1989, 22-28.
7. *M. Cresti, C. Milanesi, P. Salvatici, A. C. van Aelst.* Bot. Acta, 103, 1990, 349-354.

საქართველოს მეცნიერებათა აკადემიის მოამბე, 159, №2, 1999
BULLETIN OF THE GEORGIAN ACADEMY OF SCIENCES, 159, №2, 1999

BOTANY

J. Kereselidze, M. Loria

Some Questions of Plant Introduction and Reintroduction

Presented by Member of the Academy G. Gigauri, September 2, 1998

ABSTRACT. **Some theoretical and practical questions of plant introduction and reintroduction are considered in the article.**

Key words: plant, introduction, reintroduction, indigenous, invasion, conservation.

Two main points exist on the problem of plant introduction. Some authors consider, that introduced plants are those which are brought into one country from another and identify them with the so-called exotics [1, 2]. In most countries of the world wider sense is given to the plant introduction [3-5]. All the species are considered to be introduced which are gathered as a collection in botanic gardens and arboretums or cultivated in agriculture. According to the geographical origin Shneider [6] singles out two groups in plants: authochthonous and allochthonous.

Authochthonous are all the species of local origin that grow naturally in a certain region. Allochthonous are plants introduced from other countries, propagation of which is connected with some economic purposes.

Cultivation of introduced plants on the widest scale is connected with distinct problems even nowadays. Some of the introduced species propagate naturally. They may invade into ecosystems (invasion) which consequently provokes degradation of local plants and sometimes it gives rise to disastrous effects for a country.

Among the invasive woody plants in Georgia *Robinia pseudoacacia*, *Amorpha fruticosa*, *Acer negundo* and others are distinguished to be more aggressive. The former two species are spread in lowlands and lower forest zone of west Georgia and the third one in Kvemo Kartli. Their populations are considerable rivals of such rare and relict species of Georgian flora as *Quercus imeretina*, *Q. hartwisiana*, *Q. pedunculiflora*. Flower nectar of some introduced plants is toxic for insects, including bees. *Tilia tomentosa*, *Aesculus hippocastanum* belong to this kind of species. Sometimes introduced plants cross with local species and consequently give birth to hybridogenic populations. Hence it follows, that cultivation of the exotic plants on the widest scale must be carried out with great care. First of all, they must be cultivated in the urbanized environment, forest, for economic purposes, specialized plantations and so on. As for renewal of degraded plants, in case of planting trees and shrubs on wide scale around towns, great advantage must be given to local species and first of all to the main local phytocenosis.

Recently preservation of plants' bio-diversity, conservation of rare and endangered plants, protection of natural ecosystems and renewal of degraded plants has become a global problem. Study and development of practical recommendation for the above-mentioned problems is one of the essential directions for botanic gardens. In the sixties of the twentieth century with the introduction of rare and endangered plants and conservation of

their genofond an idea has been born about propagation of endangered plants on the widest scale and spreading them later in their natural places. In literature it is called plant reintroduction. Such work supported by scientific basis was carried out at the end of the seventies in Spain [7]. Later the same kind of work was realized in Israel, France, the USA, India and other countries [8]. At present, the reintroduction of plants is considered to be one of the main directions of botanic gardens.

For its part, plant reintroduction serves to three main problems.

1. Propagation of endemic, rare and endangered plants and their reintroduction to their natural places.

2. Propagation of useful plants among local flora (fruitful, medical, dyeing, forage) and their reintroduction in natural conditions.

3. Propagation of main species of local phytocenosis and their reintroduction among degraded plants.

The work in this direction has been also carried out at the Tbilisi Central Botanical Gardens. Some endemic, rare and endangered plants of Georgian flora have been studied: *Amygdalus georgica*, *Berberis iberica* and *Hedera pastuchowii*. These species are introduced to the Tbilisi Botanical Gardens.

At present the programme is being worked out for their propagation and reintroduction in the outskirts of Tbilisi to renew their populations.

Reintroduction means to protect rare and endangered plants or to renew degraded and impoverished populations and spread them in natural areas.

In renewal process of degraded ecosystems the priority to reintroduction of local phytocenosis and main economic plants is given.

Georgian Academy of Sciences
Tbilisi Central Botanical Gardens

REFERENCES

1. *M. L. Loria*. Bot. Journ. **54**, 3, 1969 (Russian).
2. *V. I. Nekrasov*. Important questions of development of plant acclimatization theory. M., 1980, 102. (Russian).
3. *N. A. Bazilevskaia*. Theory and methods of plant introduction. M; 1964, 131. (Russian).
4. *J. Akeroyd*, Wyse Jackson P. A. Handbook for Botanic Gardens on the reintroduction of plants in wild. 1995, 97.
5. *S. Wallace*. Bot. Gard. Conserv. News. **1**, 1992, 34-39.
6. *E. Y. Shneider*. Zur Klassificierung der Antropolochren. Vegetatio, **16**, 1969, 225-238.
7. *H. Sainz-Ollero, I. E. Hurandez-Bermejo*. Experimental reintroductions of endangered plant species in their natural habitats in Spain. Boil. Cons. **19**, 1979, 195-226.
8. *I. Y. Lesouef*. From rescue to reintroduction: the example of *Ruisia cordata*. In Heywood, V. H. and Wyse Jackson, P. S. eds. Tropical Botanical gardens., 217-222.

საქართველოს მეცნიერებათა აკადემიის მოამბე, 159, №2, 1999
BULLETIN OF THE GEORGIAN ACADEMY OF SCIENCES, 159, №2, 1999

PLANT PHYSIOLOGY

G. Alexidze

The Study of *Triticale* Leaves Lectins Subcellular Localization

Presented by Corr. Member of the Academy N. Aleksidze, March 30, 1998

ABSTRACT. **The lectins distribution in the subcellular fractions of Triticale leaves was established (plasmalemma, microsomes, mitochondria, chloroplasts, nuclei). Only membrane proteins have been characterized by lectin activity in all analyzed subcellular fractions. The high lectin content was revealed in chloroplasts and low lectin content - in mitochondrial fraction. The plasmalemmma and microsomes lectins carbohydrate-binding specificity displayed highest sensitivity to N-acetyl-D-galactosamine, D-glucose, D-dezoxi-D-glucose and lactose, but chloroplast lectins - to lactose and D-galacturonic acid and mitochondrial and nuclei lectins had no specificity to any tested sugars (16 analyzed sugars).**

Key Words: *Triticale,* lectins, subcellular location

The study of the lectins subcellular distribution in plant tissues revealed the presence of lectins not only on the cell surface, in cytosole, endoplasmatic reticulum, lyzosomes, Golgi apparatus and vesicles [1-3], but also in such autonomic organelles, as mitochondria, leucoplasts, chloroplasts and nuclei [4-6].

In spite of sparse information about this problem, according to the already existing data lectins take part not only in cell surface processes, but also in functional activity of subcellular organelles. So the study of subcellular localization of lectins in the photosynthetic leaves tissue cells is of particular interest, since this problem has not been investigated so far.

The aim of this report is the study of lectins distribution in subcellular fractions of *Triticale* leaves.

The objects of our investigation were the fortnight sprouts of *Triticale* leaves (a wheat and rye hybrid, *Triticale* species, "Boce-1"). The plants grew in factor-static conditions: light intensity - 5000LX, temperature 20°C, the 12 h of light/night cycle. The 7-8 cm long young leaves of plant were used in our experiments.

Subcellular fractions were obtained by differential ultracentrifugation in saccharose density gradient. Plasmalemma and microsomes fractions were obtained by Hodges method [7].

Fractions purity was analyzed by electron-microscopy [8]. The nucleus and chloroplast fractions obtained with method modified by Jokhadze [9,10], their purity was controlled by the light microscopy and determination of activities of the marker-enzymes: NAD H-cytochrom C-reductase [11], alcoholdehydrogenase [12], cytochrom-C-reductase [13] and DNA-dependent RNA-polymerase [9]. Mitochondrial fraction was isolated [5,14] and its purity checked.

Lectins were isolated from subcellular fractions using method [6]. Lectin activity was assayed as minimum protein concentration with agglutination reaction on tripsin-treated

rabbit erythrocytes 2% suspension.

Hemagglutination assays were carried out in microtiter-U-plates by Tacachi and light scattering (determined with KFK-3-photocolorimeter) methods. Control and experimental cuvettes contained 400 μkl of trypsin-treated rabbit erythrocytes suspension and a protein fraction with lectin activity. Light scattering was measured at 670 nm. The protein concentration was determined by Lowry method.

The nucleus and chloroplast fractions purity was controlled by light microscopy and assay of marker-enzymes activities: NAD H-cytochrom C-reductase [11], alcohol-dehydrogenase [12], cytochrom-C reductase [13] and DNA-dependent RNA-polymerase activities [9].

Table 1

Subcellular Fractions	Water soluble proteins			Membrane proteins		
	proteins mg	lectin.act. mkg/ml	lectin** content	proteins mg	lectin.act.* mkg/ml	lectin** content
plasmalemma	0.05	_	_	1.2	0.15	8000
microsomes	0.4	_	_	2.1	0.2	10500
chloroplasts	2.6	_	_	7.4	0.6	12333
mitochondrion	3.1	_	_	5.4	2.1	2571
nuclei	4.0	_	_	3.5	0.3	11.666
cytosole	230	_	_	_	_	_

Lectin content and hemagglutination activity of lectins from *Triticalale* subcellular fractions

*Lectin activity units minimum protein concentration (mg/ml) giving visible agglutination.

**Lectin content in hemagglutinative units.

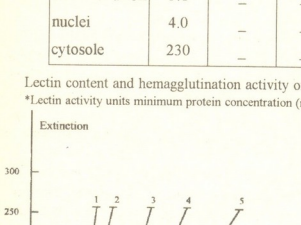

Fig.1. Triticale leaves subcellular lectins hemagglutination kinetic analysis. 1 - plasmalemma, 2 - microsomes, 3 - nuclei, 4 - chloroplasts, 5 - mitochondria, 6 - cytosole

We analyzed the water-soluble and membrane lectins contents in subcellular fractions of *Triticale* leaves. Table 1 shows that only membrane lectins were revealed. According to the lectin activity the subcellular fractions were distributed in the following way: plasmalemma (0.15) > microsomes (0.2) > nuclei (0.3) > chloroplasts (0.6) > mitochondria (2.1), but this distribution varies with lectin content. The chloroplasts are characterized by higher content of lectins - 12.3, then come nuclei - 11.7, mi-

crosomes - 10.5 and plasmalemma - 8. Mitochondrial fraction is characterized by low level of lectin content - 2.6. The lectin contents are expressed in hemagglutination units.

The kinetic analysis of subcellular fractions membrane proteins agglutination activity revealed the differences between them (Fig1). According to the velocity of erythrocytes sedimentation the subcellular fractions consequence is as follows: plasmalemma > microsomes > nuclei > chloroplasts > mitochondria. The erythrocyte sedimentation characteristics correlate with lectin activities of the subcellular fractions membrane proteins and differ in lectin contents.

Table 2.

Carbohydrate-binding specificity of the lectins from triticale leaves subcellular fractions

Carbohydrates (3-200 mM)	Hemagglutination activity of the lectins from triticale leaves subcellular fractions				
	plasma-lemma	micro-somes	chloro-plasts	mito-chondria	nuclei
N-acetyl-D-galactosamin	100	75	+	+	+
N-acetyl-D-glucosamin	+	+	+	+	+
D-manopiyranoside	+	+	+	+	+
D-galacturonic acid	+	+	2	+	+
L-fucosa	+	+	+	+	+
D-glucosamine	+	+	+	+	+
D-glucoso-6-phosphate	+	+	+	+	+
melibiose	+	+	+	+	+
lactose	25	50	25	+	+
D-celibiose	+	+	+	+	+
D-galactose	+	+	+	+	+
L-ribose	+	+	+	+	+
saccharose	+	+	+	+	+
D-glucose	33	62	+	+	+
2-dezoxi-D-glucose	40	50	+	+	+
D-monopyranoside	+	+	+	+	+

Carbohydrate-binding specificity of the subcellular fractions lectins was determined by hapten-inhibitory assays using hemagglutination area. A series of simple sugars (16) were tested (Table 2). It was shown that the lectins from plasmalema and microsomes have different specificity to lactose, N-acetyl-D-glucosamine, D-glucoside and 2-dezoxi-D-glucose. Obviously, lactose is a major hapten-inhibitor and the others are its derivatives.

The lectins from chloroplasts showed specificity to lactose and D-galacturonic acid. There was not revealed carbohydrate-specificity for the lectins from nuclei and mitochondria; these findings indicate the polysaccharide nature of their hapten.

So, there were revealed the membrane proteins from *Triticale* leaves subcellular fractions. The obtained results indicate that the lectin-like (sugar-binding) receptor-proteins are distributed at different levels of the cell structural-functional organization.

The biological properties of subcellular fractions lectins will be studied in future.

Tbilisi I. Javakhishvili State University

REFERENCES

1. *J. F. Manen, A. Pusztai.* Planta.**155**,1982,328-334.
2. *D. J. Bowles, H. Lis, N. Sharon.* Planta. **145**,1979, 193-201.
3. *R. F. Pont-Lezica, R. Taylor, JE.Vazner.* In J.Plant Phys.**137**,1991,453-458.
4. *C. E. Jefree, M. M. Yeoman.* New Phytology. **87**, 1981, 463-466.
5. *G. A. Alexidze, E. I. Viskrebentseva.* Fiziol. Rast. **33**, 1986, 213-220 (Russian).
6. *G. A. Alexidze, G. A. Sanadze.* Bull. Georg. Acad. Sci., 137, 1990.
7. *R. T. Leonard, P. Hansen, T. K. Hodges.* Plant Phys. **51**, 1973, 749.
8. *I. L. Semionov, E. I. Viskrebentseva, G. A. Alexidze.* Structura i funktsii biol.membran rast. Novosibirsk, 1985, 47-50. (Russian)
9. *D. I. Jokhadze, M. I. Balashvili.* Biokhimia. **41**, 1976, 161-172. (Russian)
10. *W. Bottomley, D. Sencer, A. Wheller.*Arch.Biochem.Biophys. **143**, 1971, 269-276.
11. *E. Mohler.* Methods in Enzymology. **2**, 1955, 688-693.
12. *E. Racher.* Methods in Enzymology. **1**, 1955, 500-503.
13. *E. Racher.* Biochem.Biophys.Acta. **4**, 1956, 211-214.
14. *A. G. Shugaev, E. I. Viskrebentseva.* Fiziol. Rast. **29**, 1982, 799. (Russian)

საქართველოს მეცნიერებათა აკადემიის მოამბე, 159, №2, 1999
BULLETIN OF THE GEORGIAN ACADEMY OF SCIENCES, 159, №2, 1999

FORESTRY

T. Bakhsoliani

Natural Regeneration of Beech Stands of East Georgia in Connection with Forest Types

Presented by Member of the Academy G. Gigauri, February 10, 1998

ABSTRACT. **Indexes of natural regeneration of beech forest formation of East Georgia have been presented in connection with forest types. It has been observed that *Fageta nuda, Fageta asperulosa, Fageta mixtoherbosa* forest types are characterized by very good natural regeneration. *Fageta poosa* and *Fageta festucosa* forest types are characterized by good regeneration, while *Fageta caricosa* forest type by satisfactory regeneration and beech stands by *Fageta rubo-driopterosa, Fageta driopterosa* and *Fageta altherbosa* by weak regeneration.**

Key words: regeneration of beech stands.

Natural regeneration of beech stand forest in separate regions of the Transcaucasus has been studied [1-9]. Natural regeneration of beech stand forest of East Georgia according to the groups of forest types in connection with close order of alley canopy and degree of grass covering have been studied by the author in all regions through natural zones.

As the data of investigation show, regeneration of dry beech stand with *Caricosum* of IV and V bonitet mostly takes place with root shoots. In case of 0.5-0.6 close order of forest canopy amount of shoots under 5 years is defined as 6.8 thousand units, and amount of shoots above 5 years reaches 1.1 thousand. In case of 0.3-0.4 close order of stands canopy forest regeneration becomes considerably worse. Total amount of shoots on 1 ha. area is defined as 4.3 thousands, where beech occupies 56%.

In spite of weak development of herbage (degree of herbage is 0.4) small amount of shoots (6.8 thousands) is mostly stipulated by unfavourable edaphic conditions, namely by thin, washed off brown forest soils.

Unlike the above mentioned group, beech stand forest type group with *Caricosum* of IV(III-V) bon., with 0.5-0.6 close order of alley canopy is characterized by better conditions of regeneration. Its total amount on 1 ha is defined as 16 thousands, among which beech is 72.6%. As for the low plenitude stage forest types of this group, for increasing degree of grass coverage up to 0.7, total amount of regeneration decreases to 6.7 thousand units where amount of shoots of more than 5-year age is only 18% and beech takes 40% of the total amount. Here process of regeneration takes place with alternation of species (with hornbeam and other species). In beech stand with *Festucosum* forest types, in case of 0.8-0.7 close order of stock, beech shoots of more than 5-year age are insignificant (0.4 thousand) and total amount of regeneration is defined as 5.1 thousand, where beech stand takes 72.5%. Low indexes of regeneration are conditioned by the lack of illumination and maximum amount of regeneration (22.5 thousands) is observed in the stands of average density, 87% of which is presented with beech. The reasons of good regeneration are

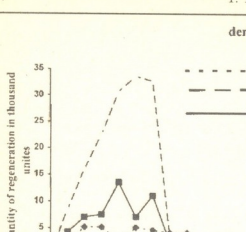

Fig. Natural regeneration of beech stands of East Georgia according to the forest types
1. *Fageta caricosa* IV (V) bon;
2. *Fageta poosa* IV (III-V) bon
3. *Fageta festucosa* III (II-IV) bon;
4. *Fageta nuda* I-II (III) bon;
5. *Fageta asperulosa* II-III bon;
6. *Fageta mixtoherbosa* I-III bon;
7. *Fageta rubo-driopterosa* I-III (I) bon;
8. *Fageta driopterosa* I-II (III) bon;
9. *Fageta altherbosa* III-(IV) bon.

optimum illumination and thin herbage, as well as good conditions of soil characteristic of this group.

In the stands of low density amount the of regeneration is almost satisfactory (7.4 thousand units), though it occurs by other species.

The fact that natural regeneration of the forest in the stands with average density takes place more or less well (30.3 thousand units) and leading species is beech (91.4%), has been stated with the study of old beech stands. Regeneration takes place in groups, mostly in the small and middle sized windows. 1-2 year old shoots are met here in small quantities (5.9 thousand), as for the shoots of more than 5 year age, their amount exceeds 16 thousand units: this should be explained by weak seed germination due to condensed, greatly developed dead herbage. Seeds on the surface like this, undergo lack of humudity, because of quick drying up of dead, feltlike covering.

In spite of well-development of herbage in the stands with 0.3-0.4 close order of canopy, regeneration is still satisfactory (13.5 thousand units), though with small advantage of hornbeam over the beech.

Together with growing the depth of dead herbage and decreasing of illumination of the soil surface, conditions of the forest regeneration with 0.7-0.8 close order of canopy little by little becomes worse (up to 2.4 thousand units) and in case of 0.9-1.0 close order conditions decreases up to 0.4 thousand units. In real virgin stands with dead herbage intensive regeneration process of the forest is connected with the natural thinning of these stocks (with falling out of overaged trees). In the presented stocks process of natural thinning is still weak in spite of their age. As we see, the stocks of the presented forest type are distinguished by longer life, than other forest types for the conditions of favourable location.

Apart from the above-mentioned forest types, the best indices of regeneration has *Fagetum asperulosum* of II-III bonitet, in case of 0.5-0.6 close order of canopy total amount of regeneration is 33.5 thousand units, where beech takes 89.8%. In thick stocks (0.7-0.8) herbage is developed weakly (0.1-0.2 degree of coverage), though, the process of natural regeneration of the forest takes place here weakly too, for the lack of illumination as 92% of its total amount is up to 5 year age and while growing older, most of them die. Regeneration of the forest is also weak in case of 0.3-0.4 close order of the forest canopy, where highly developed herbage interferes with the development of shoots.

Abundance of regeneration (32.5 thousand units) has also been noticed in the

Mixtoherbosum beech stands of II-III bonitet with 0.5-0.6 close order of canopy, and satisfactory amount in the stands with low density. The above-mentioned fact, should be conditioned by the considerable amount of preliminary existed shoots in the period of gradual thinning of stocks.

In all stages of density of *Fagetum rubodriopterosum* of II-III (1) bonitet and *Fageta Driopteroza* beech stands of II-IV bonitet, natural regeneration of the forest takes place weakly. Maximum amount of regeneration is in the close-order places of the stock canopy with 0.1-0.3 degree of grass covering. In case of 0.5-0.6 close order of canopy degree of grass covering increases up to 0.6-0.7 and in case of lowing of close order of canopy (up to 0.3-0.4) degree of grass covering increases up to 0.8-1.0. Together with the above-mentioned, the quantity of natural regeneration of the forest consequently decreases.

The Figure distinctly indicates the dynamics of natural regeneration of beech formation of East Georgia in connection with the groups of forest types. The following conclusions have been made:

1. Forest is characterized by very good natural regeneration in case of beech stands with *Fagetum nudum, Fagetum asperulosum* and *Fagetum mixto-herbosum;* by good regeneration – beech stands with *Poosum* and *Festucosum;* by satisfactory regeneration – beech stands with *Caricosum* and by weak regeneration – beech stands with *Rubo-driopterosum, Driopterosum* and *Aletherbosum.*

2. In case of 0.5-0.6 close order of forest canopy maximal amount of regeneration has been observed in the beech stands with *Asperulosum, mixto herbosum* and *Nudum* and in case of 0.7-0.8 close order of canopy in beech stands with *rubo driopterosum, Fageta Driopterosum* and *Fagetum altherbosum.*

Georgian Academy of Sciences
V. Gulisashvili Institute of Mountain Forestry

REFERENCES

1. *G.D.Yaroshenko.* Dok. AN Arm. SSR, 1926 (Russian).
2. *G.D.Yaroshenko.* Bukovye lesa. Armenia, tipy lesa, vozobnovlenie, sistemy rubok, Yerevan, 1962, 178 (Russian).
3. *V.Z.Gulisashvili.* Gornoe lesovodstvo. M., 1956 (Russian).
4. *A.G. Dolukhanov.* Trudy Tbil. bot. instituta AN Gruz. SSR, Tbilisi, **18**, 1956, 46 (Russian).
5. *I.A.Abashidze.* Lesnoe khozyaistvo, N11, 1953 (Russian).
6. *G.V. Tsimamdzgvrishvili.* Trudy Tbil. inst. lesa AN GSSR, VII, 1957, 171-197.
7. *B.I.Sudjashvili.* Trudy Tbil. inst. lesa AN GSSR, X, 1961, 161-171 (Russian).
8. *T.G.Bakhsoliani.* Trudy Tbil. inst. lesa. XVII, M., 1969.
9. *T.G.Bakhsoliani.* Vestn. Gruz. bot. obshch, IV, Tbilisi, 1969 (Russian).

საქართველოს მეცნიერებათა აკადემიის მოამბე, 159, №2, 1999
BULLETIN OF THE GEORGIAN ACADEMY OF SCIENCES, 159, №2, 1999

BOTANY

L. Jinjolia

Palynomorphology of Subgenus *Hyalinella* species *Centaurea* (Compositae)

Presented by Corr.Member of the Academy G.Nakhutsrishvili, July 6, 1998

ABSTRACT. **Based on critical revision of subgenus *Hyalinella* (Tzvel.) Tzvel., palynomorphological features have been studied in detail.**

Key words: pollen grain, *Centaurea* L., morphology, scanning electron microscopy.

Herbarium specimens of the Institute of Botany, (TBI) and the author's field collections from various regions of the Greater and Minor Caucasus were studied. The acetolysis method [1] was used for pollen grain treatment. Preparations were examined under the light microscope (4 M). To obtain scan micrographs pollen grains were slightly soaked in ethanol, dried, attached on sticky tape and cool-spattered with gold. Splites from pollen coats were obtained during the preparation of material randomly without special treatment methods. Pollen grains were studied under a scanning-electron microscope JSM-35.

All the examined pollen grains belong to the palynomorphological type *Dealbata*, established by Wagenitz [2]. According to general palynomorphological description [3] species of subgenus *Hyalinella* are of *Psephellus* type. The following palynomorphological features were revealed. Pollen grains prolonged pole-axed, oblonged elliptic, triangular from pole, widely elliptic from equator, sculpture smoothly-spined, appertures complex tricolporate colpate shallow margin irregular, indistinct, usually fused with general surface. Membrane irregular small - tuberculated. Pores well expressed, differ in shape. Mexine rather thicker than nexine. Cexine with well-developed columnar layer, columnar vigorous, branched (Fig.II). Shape of pollen grains vary from elliptic (*C.simplicicaulis*) (Fig.I,a) to almost spheric (*C.bella*) (Fig.I,b,c,d).

Palynomorphological features [4] are also used for comparative infraspecific determination of some *Centaurea* species.

Thus, palynological data obtained are well correlated with classical macro-morphological features [5] and are considered as one of the important diagnostic characteristics for establishing of taxonomy and nomenclature of this Caucasian -Minor Asian subgenus. Its formation center covers the areas situated mostly in Eastern and partly in Western Transcaucasus and in North-Eastern Anatolia.

Specimens investigated:

Centaurea simplicicaulis Boiss. Prov.Kars Distr Olty Prope p.Alos 5.VII.1911 Sosnowsky (TBI). *C.bella* Trautv. Georgia. Borjomi region. Chobiskhevi "Tsikheebi" 10.VIII.1986, Jinjolia (TBI). *C.bella* Trautv, var, *nathadzeae* (sosn.) Jinjolia. Georgia, Imereti, Kutaisi region r. Tskaltsiteli gorge, near the Motsameta cloister 3.IV.1928. Sos-

Table 1

Species	Pollen grain size		Exine sculpture				Notes
	Polar	Equatorial diameter	Colpus length	Colpus width	Mesocolpium width	Exine width	
Sect.Hyalinella (Tzvel.) Tzvel *C.simplicicaulis* Boiss	44.2-50μm	40.5μm	34.5μm	3.3μm	21.1μm	3.8μm	Tubercules more acuted
C.betta Trautv.	42.2-44.1μm	38μm	30.1μm	3.8μm	21.1μm	3.8μm	Smallcolpated, tips acuted
C.bagadensis Woronow	38.4-42.2μm	34.0μm	28.2μm	3.0μm	15.3μm	4.8-5.1	Irregular exine
C.adjarica Albov	36.4-40.3μm	32.5μm	32.6μm	1.34μm	21.1μm	3.8μm	Small pollen grains, extremely narrow-sulcated, deep, expressed
Sect.Albovia Tzvel. *C.pecho* Albov	36.4-38.4μm	32μm	23.0μm	1.6μm	21.1μm	1.7μm	Small pollen grains, narrow-sulcated with almost tuberculose projections

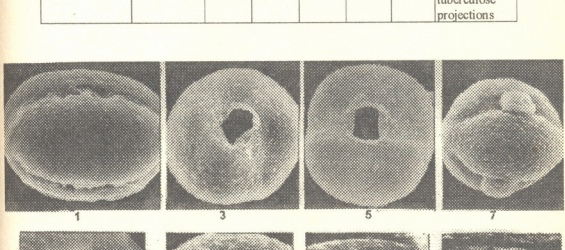

1-2 *C.simplicicaulis* x 2000;
3-4 *C.bella* x 2000;
5-6 *C.bella var.nathadzeae* x 2000;
7-8 *C.*"-" var. svanetica x 2000;

nowsky (TBI). *C.bella* Trautv.var.svanetica (Mardaleishvili) Jinjolia. Western Georgia, Lower Svaneti right bank of r.Tskenistskali Upper reaches of r.Mananauristskali, 1820 m "Skimeri". 24.VII.1979 Mardaleishvili (TBI). *C.bagadensis* Woronow. Western Geor-

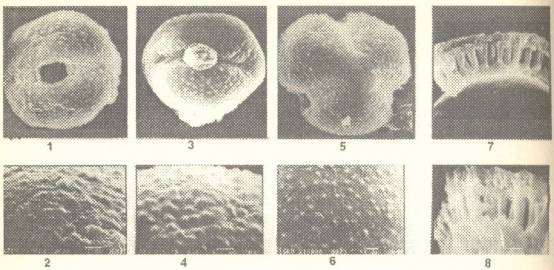

1-2 *C.bagadensis* x 1.800
3-4 *C.adjarica* x 2000
5-6 *C.pecho* x 2000
7-8 *C.adjarica* - exine structure x 10.000; x 20 000.

gia, Abkhazeti, Kodori gorge. Bagati calcareus cligls. 700 m. 16.VI.1986, Jinjolia (TBI). *C.adjarica* Albov Georgia.r.Adcharistskali gorge, rocks near Khulo, Elelidzeebi (TBI). *C.pecho* Albov Lomashen, Batumi region, Arthvin, 24.VII.1907 Andropova (TBI).

Georgian Academy of Sciences
N.Ketskhoveli Institute of Botany

REFERENCES

1. *G. Erdtman.* Svensk.Bot.Tidskr., **54**,1960, 561-564.
2. *G. Wagenitz.* Pollen Morphologie und Systematik in Der Gattung Centaurea L. Flora **142**, 2, 1955, 213-279.
3. *E. Avetissian.* Materials Bot. Inst. Akad. Nauk, Arm., **14**, 1964, 31-47.
4. *N. Pinars, Ö. Inceoglu.* Turkis Jor. of Bot. **20**, 5, 1996, 395-398.
5. *L. Jinjolia.* Materials of the III Conference of botanists, Leningrad, 1990, I, 25-35.

საქართველოს მეცნიერებათა აკადემიის მოამბე, 159, №2, 1999
BULLETIN OF THE GEORGIAN ACADEMY OF SCIENCES, 159, №2, 1999

ECOLOGY

G. Agladze, N. Khozrevanidze

Economic and Ecological Aspects of Natural Greenlands Fertilization

Presented by Corr.Member of the Academy P.Naskidashvili, August 31, 1998

ABSTRACT. **We present the results of six year study of fertilizers utilization in mountain natural greenlands of Adjara. Economic and ecological advantages of fertilization by optimal quantities are shown.**

Key words: fertilization, greenland.

The natural mountain pastures and meadows are the main sources in nutrition balance and necessary food base for livestock [1,2]. According to the data of 1980-1990 in Georgia 38-43% of fodder was obtained from mountain natural greenlands. It should be marked that the low net cost and high quality of the fodder were produced on these pastures (hay, green mass, pasturage)[3-6]. The economic aspect and ecological significance of mountain greenlands and hayfields should be also noted [7,8]. It is on high mountain slopes that erosion processes took their beginning and often developed lawer to the settled territory hard consequences of which were registered more than once [4]. Such phenomena are extremely noteworthy in mountainous Adjara, where the results of erosion are especially grave. It is necessary to conduct special antierosion measures and protection of soils. The productivity of greenlands is of primary importance. Particularly increase of aerial and underground biomass as well as herbage thickness by increase ecologically secure technologies such as fertilization [4,5,9]. Our observations show that by fertilization of low sledge meadow festuca cenosis the quality of grass coverage increased from 25 to 60%, soil erosion decreased from 600 to 113 m^3/ha and the increase of coverage up to 80-90% completely stopped this process.

The necessity of using fertilizers in Georgian mountaineous nutritive pastures is conditioned first of all by their present poor state and at the same time by their high potential possibilities. Statistic data and the results of study make it evident that due to the long time unsystematic exploitation, unsufficiency of care and improvement measures the productivity of natural greenlands and feed quality is rather low. In average from the greenlands 4-8 c/ha green mass, and from the meadows – 10-14 c/ha hay are obtained. The most serious problem is overload of mountain greenlands by the excess number of cattle which causes hard spreading of weeds, thin vegetation, development of erosion processes and other negative phenomena. Our studies prove that the raise of greenlands productivity in three times and more will be quite real if necessary measures are taken.

In 1981-1997 we examined natural nutrient greenlands fertilization in Adjara subalpine and alpine mountaineous belts and worked out the measures for its improvement.

The efficiency of mineral and organic fertilizers application in natural greenlands of subalpine zone was studied in Khulo region.

The tested plot was chosen on 1950 m ASL, near the Goderdzi pass, on the north-eastern exposition, 6-8^0 inclination slope . The soil is swardy, of average depth, in the upper layer of which humus reaches 10.8%, total nitrogen 0.69%, phosphorus 0.32%. In vegetation covering among fodder cereals *Agrostis capillaris* L., *A.planifolia Poa pratensis* L., *Dactylis glomerata* L., from fabaceous plants - *Trifolium montanum* L. and *Trifolium repens* L., from herbs: *Ranunculus caucasicus, Euphrasia stricta, Veronica gentionoi, Plantago lanceolata* L., *Taraxacum officinale, Alectrolophus*, etc. previal. There was tested the action of yearly placement of ammonium nitrate, granular superphosphate, potassium salt and in the first year of experiment the effect of one-time placement of cattle dung on green mass productivity, on botanical and chemical composition as well as on nitrates content. Besides fertilizers action on density of greenmass and degree of soil coverage by vegetation was calculated. Phosphorus and kalium were introduced in autumn in every variant, nitrogen by norm 60 kg/ha in autumn, in the sixth variant 60 kg/ha in autumn and 60 kg/ha in spring, and in the seventh variant 120-120 kg/ha in autumn and early spring. The data of six year trial are demonstrated in the Table.

The apply of mineral fertilizers increase the productivity of dry greenmass as compared with the control test in average on 6.3-33.4 c/ha within the six year period and by the action of manure in 21.7 c/ha. The effect of fertilization varies due to climatic conditions.

Among the examined combinations of mineral fertilizers the most increase of dry greenmass as compared with the control was marked during application of complete mineral fertilizers, and among nitrogen norms the highest yield was obtained while placing 240 kg/ha. The effect of one-time apply of 40 t manure on hectar (by 6 year data) equals to action of 60-60 kg/ha of complete minerals (variant 5) and it is rather high in the sixth year. The use of single phosphorus increases the productivity by 6.3 c/ha and this positive effect increase from the second and third year of experiment and at the end of the experiment reaches 10.1 c/ha. It is evident that kalium has more positive effect than nitrogen and phosphorus. The calculations show that from the economic point of view it is advisable to use $N_{60}P_{60}$ because the compensation of 1 kg NP gives the increase of hay in 16.0 kg whereas in case of the P_{60}; $P_{60}K_{60}$; $N_{60}P_{60}K_{60}$; $N_{120}P_{60}K_{60}$ and $N_{240}P_{60}K_{60}$ introduction this number makes correspondingly 10.5; 8.4; 11.6; 12.1 and 9.2 kg of hay. It means that there can't be used more than 120 kg/ha nitrogen.

The apply of fertilizers significantly changes the botanical composition of greenmass. First of all the herbage sharply decreases. Their amount diminished from 44.3% (control variant) to 18.6 (the seventh variant, $N_{240}P_{60}K_{60}$). The positive effect of phosphorous and phosphorous-kalium fertilizers is evident on the development of leguminous crops percentage of which in the greenmass increases as compared to control (6.7%) correspondingly up to 10.4 and 13.7%. Nitrogen has positive effect on fodder cereals which percentage in the greenmass on the background of $N_{240}P_{60}K_{60}$ reaches 76.5% and the apply of 60 kg/ha nitrogen on the background of PK almost has no action on leguminous crops. At the same time the introduction of 120-240 kg/ha nitrogen by norm effects the amount of leguminous crops and their percentage in greenmass decreases as compared to control.

Table

The effect of fertilization of sub-alpine meadow lands of Adjara on quantitative and qualitative indices of grass stand (1990-1995)

Test variants	Average productivity of hay during 6 years (c/ha)	Botanical composition of green-mass (%)			Quantity of nutrient elements in 100 kg hay			Productivity of 1 ha meadow lands			Per kilogram dry mass contains	
		Cereals	Leguminous-crops	Mixed fodder grass	Feed unit	Digestive protein (kg)	Exchange energy (MJ)	Feed unit	Digestive protein (kg)	Exchange energy (GJ)	Carotene (mg/kg)	Nitrates (mg/kg)
1.without fertilizers	12.7	49.0	6.7	44.3	46.2	7.9	598.2	586.7	100.3	7.62	45	176
2.P_{60}	19.0	49.6	10.4	40.0	48.1	8.2	622.8	913.9	155.8	11.84	43	186
3.$P_{60}K_{60}$	28.8	48.2	13.7	38.1	48.8	8.4	640.0	1112.6	191.5	14.6	48	194
4.$N_{60}P_{60}$	31.9	59.1	8.5	32.4	49.3	8.7	638.9	1572	277.5	20.38	57	260
5.$N_{60}P_{60}$	33.6	63.7	8.1	28.8	49.9	8.9	651.3	1676.6	299	21.9	61	248
6.$N_{120}P_{60}K_{60}$	41.8	69.3	6.2	24.5	50.0	9.2	663.7	2090	384.6	27.7	63	291
7.$N_{240}P_{60}K_{60}$	46.1	76.5	4.9	18.6	50.6	9.4	659.9	2327.6	433.3	30.43	68	357
8.manure 40t/ha	33.9	63.9	11.5	23.6	49.7	8.8	647.4	1684.4	298.3	22.04	59	252

The effect of fertilizers on productivity of greenmass is positive: in 100 kg of dry feed the content of nutrient units increases by 5.6-9.5%, of digestive proteins by 3.8-11.9% and of megajoules by 4.1-10.3%. Productivity of greenmass is increased within the increasing of crop-capacity. Using optimal and recommended norms ($N_{60}P_{60}K_{60}$ and $N_{120}P_{60}K_{60}$)

10. "მოამბე", ტ. 159, №2, 1999

from each fertilized hectare correspondingly on (1089.9-1503.3) extra feed unit, 198.7-284.3 kg of digestive protein and 14.25-26.14 gigajoule exchange energy is obtained. Fertilizers (especially with K and N) considerably increase the content of carotene in greenmass. The productivity of greenmass also increases by the use of manure and it reaches 60-60 kg/ha.

Ecological aspects, when fertilizers are used, is of special interest. It should be noted that mountain pastures and meadow-lands are characterized by high sensitivity and erosional danger. That's why much attention has to be paid to the environment and especially to protection the soil from the erosion. Our observations testify that fertilization increases the quantity of herbage. If the number of sprouts didn't excess 1042 per unit area by the first year of experiment then, after six years it reaches 1115-1187; and after fertilizing the soil by P_{60}; $P_{60}K_{60}$; $N_{60}P_{60}$; $N_{60}P_{60}K_{60}$; $N_{120}P_{60}K_{60}$; $N_{240}P_{60}K_{60}$ and 40t/ha manure it reached respectively 1476; 1553; 1707; 1794; 1849 and 1798. The coverage of soil by vegetation on the sixth year of experiment increased in control variant from 81% to 91-97%. It is evident that the danger of erosion decreases when the soil is completely covered by vegetation.

As to the nitrates content, from the data in Table it is seen that tested norms of nitrogen don't increase nitrates content in the dry mass of herbage up to the acceptable rate 1500 mg/kg). After fertilization by the maximum tested quantity of nitrogen 240 kg/ha content of nitrates increases only up to 357 mg/ha and this index varies within 248-291 mg/kg by recommended optimal norms (60-120 kg/ha).

Thus our study shows economic and ecological advantages of fertilization of mountain natural greenlands by optimal quantities.

Georgian State Zooveterinary Institute

REFERENCES

1. *G. Agladze*. Sakartvelos mtis satib – sadzovrebis ganokiereba. Tbilisi, 1980. 1.152 (Georgian).
2. *A. Kutuzova et al.* J.Kormoproizvodstvo, N5, 1997.
3. *G. Agladze, N. Khozrevanidze*. J. Sakartvelos soplis meurneoba. 4, 1985.
4. *G. Agladze, N. Khozrevanidze*. In: Sakartvelos metskhoveleobis sakvebi bazis ganmtkitseba, sakvebis tsarmoebis teknologiisa da tskhovelta kvebis srulkopa. Tbilisi, 1990, 6-11 (Georgian).
5. *A. Zotov, K. A. Erishev.* J.Kormoproizvodstvo, 3, 1998 (Russian).
6. *S. Smelov*. Teoreticheskie osnovy lugovodstva. Moskwa, 1966 (Russian).
7. *G. Agladze, A. Zotov*. Gornye pastbishcha i senokosy Kavkaza, Tbilisi, 1987, 1-462 (Russian).
8. *A. Zhuchenko*. Strategia addaptivnoi intensifikatsii selskogo khoziaistva. Puschino, 1994, 1-147.
9. *J. Frame*. Grass. Forage Sc. 44, 3, 1989, 267-276.
10. *P. Kuchler*. Angepasste Dungung der Schafweiden. Kleinvihzuchter, 37, 16, 1989, 945-949.
11. *F. Jansen-Minssen*. Grundlanderneuerung verlagt sorfattige Planung. Landw. BL-Weser-Ems, 1989, 136, 35, 34-36.
12. *R. Thomet, R. Elmer, F. Zwefel*. Einfluss der Stickstoff-dungung und des Schnittregimes aus Pflanzenbestand und Entrag von Natur weisen hoheren Lagen. Landwirtsch. Schweiz. 2, 1/2, 1989, 67-75.

საქართველოს მეცნიერებათა აკადემიის მოამბე, 159, №2, 1999
BULLETIN OF THE GEORGIAN ACADEMY OF SCIENCES, 159, №2, 1999

BIOPHYSICS

T. Zaalishvili, N. Gachechiladze, M. Giuashvili, G. Gogoladze,
G. Getashvili, M. Makharadze, A. Gvritishvili, L. Lomidze,
Member of the Academy M. Zaalishvili

Study of Temperature Action on Structural Properties of Titin Molecule Using Intrinsic Fluorescence and Calorimetry Methods

Presented March 23, 1998

ABSTRACT. **Native titin preparation has been obtained by the Trinick method. The action of temperature on structural properties of titin has been studied using the intrinsic fluorescence method. It is shown that amino acid residues of tryptophane and tyrosine play a key role in spectra intensity of the intrinsic fluorescence of titin. It is shown that a rise in temperature from 40°C to 60°C results in a sharp change of fluorescence intensity and a shift of spectra to the long wave range. The calorimetry method was used to study thermal denaturation of titin. The protein under question is not found to have a thermodynamically stable state.**

Key words: titin, elastic protein, fluorescence intensity, quantum yield.

Recently it has become known that apart from main contractile proteins the muscle also contains giant proteins with high molecular weights. Worthy of notice among these is an elastic protein - titin, with a molecular weight of 3000 kDa. Titin molecule stretches from the Z line to the M line, it runs through the I band and binds the myosin filament. It positions the myosin filament at the centre of a sarcomere and is responsible for passive (resting) tension transfer. In vitro the mother molecule of titin - α-titin (titin 1, molecular weight 3000 kDa) always coexists with its proteolytic fragment - β-titin (titin 2, molecular weight 2000 kDa). In contrast to β-titin, isolation of α-titin in its native form is attended with certain difficulties, due to which the data available in the literature of the subject are often discrepant and require further refinement.

The available data indicate that titin molecule constitutes an extremely long molecule (1.3 μm) consisting of 300 globular domains of two different types. These domain alternate with different frequency along the entire length of a molecule. Domains of the both types basically consist of β-sheets and β-turns that are parallel to the main axis of the molecule. Elasticity of the titin molecule that is responsible for elastic properties of the sarcomere is definitely related to the folding and unfolding of β-sheets and β-turns. However, this problem, similarly to the many others concerned with the structure of the protein under question and its interaction with other proteins remains obscure [1,2]. Electron microscopy showed that the actin-free I band of a sarcomere from where actin was removed through treatment with gelsolin, is a location of a titin filamentous structure that connects the tip of a myosin filament with the Z line. It is presumed that these filaments consist of several titin molecules that are laterally associated to one another and at the tip of the myosin filament they unite into one filament (the so-called "end fila-

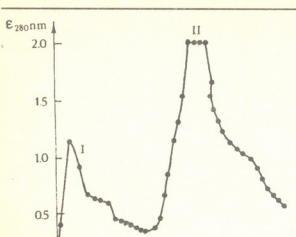

Fig.1 Gel chromatography of myofibril-derived titin on a SERVACELL CL 2B column (1.6 x 90 cm). Washing solution: 0.6 M KCl, 30 mM potassium phosphate buffer, pH 7.2. Passage rate 8 ml/hour. I - titin, II - myosin and other fractions.

ment") [3]. There are certain data, though still open to discussion, which indicate that due to its position in a sarcomere, one end of titin is bound to α-actinin present in the Z line and with the other end - to other proteins present in the M line (M-protein and others) [4,5].

Thus, it is clear that isolation of this giant protein in its native form and further investigation and elucidation of its structure, size, as well as physical and chemical properties are of paramount importance for complete characterization of the sarcomere structure. In this context it is of interest to study the melting process of native titin, using the intrinsic fluorescence and calorimetry methods. The intrinsic fluorescence method is particularly sensitive to structural changes occurring in the molecule, enabling their registration. It is well known that changes in any of luminescence parameters are recorded on the basis of registering the fluorescent radiation intensity. Especially sensitive are the relative quantum yield and maximum fluorescence intensity. The quantum yield value is determined by fluorescence intensity measured at a spectrum maximum. It should be mentioned that changes in the quantum yield and spectrum position provide fairly reliable information on conformational changes going on in the molecule. Namely, spectrum shifts only occur with a change in protein conformation, whereas quantum yield undergoes change with a disruption in the protein secondary and tertiary structure [6].

Titin native preparation was obtained using the Trinick method [7] with a certain modification. Namely, the titin preparation passed through SERVACELL CL 2B (Fig.1), for further purification, passed through a hydroxylapatite column (1.6 x 5 cm) in the KCl gradient (0.1-0.6 M KCl, 30 Mm potassium phosphate buffer, pH 7.2). Titin preparation was concentrated with polyethylene glycol.

Titin concentration was determined by the burette method. Purity of the preparation was examined by the electrophoresis method in the polyacrylamide gel gradient, in the presence of Na dodecyl sulfate (Fig.2).

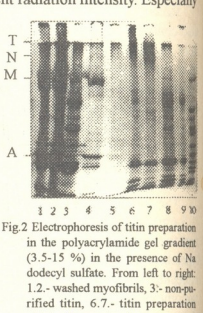

Fig.2 Electrophoresis of titin preparation in the polyacrylamide gel gradient (3.5-15 %) in the presence of Na dodecyl sulfate. From left to right: 1.2.- washed myofibrils, 3:- non-purified titin, 6.7.- titin preparation obtained by passing through sefarose CL 2B (1 peak, Fig.1), 4.-II peak (Fig.1), 5.- purification of titin obtained on sefarose CL 2B on a hydroxylapatite column, 9.-markers (molecular weights: 205000 - 6500 Da). T - titin, N - nebulin, M - myosin heavy chain, A - actin.

The fluorescence spectra were measured with the RF-500 "Shimadsu" spectrofluorimeter. Spectra position and maximum intensity were determined automatically. During the experiment the rate of cuvette heating was of the order of 1-2°K/min.

Calorimetric measurements were taken using a DASM-4 type microcalorimeter , with a heating rate of 1°K/min. The use of similar calorimeters rules out such effects of heat capacity that are related to changes in viscosity of titin giant molecule occurring in the process of denaturation.

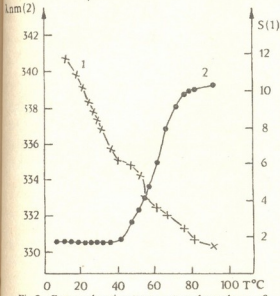

Fig.3 Curves showing temperature dependence of titin fluorescence spectrum position (1) and relative quantum yield (2). Excitation wave length 280.4 nm. (titin - 0.05 mg/ml, 0.6 M KCl, 30 mM K^+ phosphate buffer, pH 7.2)

The action of temperature on titin structural properties was studied by the intrinsic fluorescence method. The presence of fluorescent amino acids in the titin molecule (tryptophane, tyrosine) allowed to study the action of temperature on the quantum yield and spectrum position at 0.1-0.05 mg/ml concentrations. Comparison between spectra at $\lambda = 280$ nm and $\lambda = 296$ nm showed that tryptophane and tyrosine residues both contribute to the intensity of titin intrinsic fluorescence spectra (Fig.3). A rise in temperature is attended with a sharp change of quantum yield at 40-60°C and a 6 nm shift of the spectrum to the long wave band, which is due to relocation of fluorescent amino acids from internal position to the surface, i.e. a partial unfolding of the titin molecule takes place. This finding is in good agreement with elasticity of the titin molecule which, in its turn, is conditioned by the β-sheet structure.

Calorimetric studies show that thermal denaturation of titin starts at 40°C and ends at 80°C (Fig.4). Transition temperature is $T = 59.4$°C, melting temperature interval is $T = 40$°C. Calorimetric enthalpy is $\Delta H + 10.9$ J/g. Vant-Hoph's enthalpy is less than calorimetric enthalpy, which is indicative of the fact that the protein is not found to have a thermodynamically stable transient state.

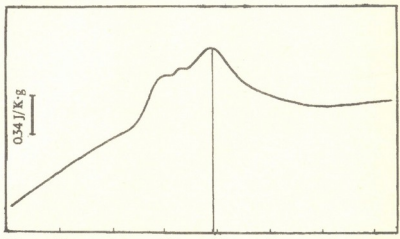

Fig.4 Thermogram of titin heat absorption during thermal denaturation. Protein concentration 3.5 mg/ml, 0.6 M KCl, 30 mM K^+ phosphate buffer, pH 7.2. Heating rate 0.5 k/min.

Thus, data obtained by the calorimetry and intrinsic fluorescence methods agree well and demonstrate that titin thermal denaturation takes place within a 40-80°C temperature range. In addition, according to calorimetric measurements, melting process of the titin molecule showed a low enthalpy value, which is in good agreement with the fact that the molecule contains almost no α-helices and consists of domains made up of β-sheets and β-turns.

Georgian Academy of Sciences
Institute of Molecular Biology

REFERENCES

1. *Koscak Maruyama*, Biophys. Chem. 50, 1994, 73-85.
2. *J. Trinick, P. Knight, A. Whiting*. J.Mol.Biol. 180, 1984, 331-356.
3. *T. Funatsu, H. Higuchi, S. Ishiwata*. J.Cell.Biol. 110, 1990, 53-60.
4. *S.M.Wang, C. J. Jeng*. Biomed.Res. 13,1992, 197-203.
5. *R. Tanabe, R. Tatsumi, K. Takahashi*. J.Biochem. 115, 1994, 351-359.
6. *E.A.Chernitsky*. Luminestsensiya i structurnaya labilnost belkov v rastvore i kletke, Minsk, 1972 (Russian).
7. *A. Soteriou, M. Ganage, J. Trinick*. J.of Cell. Science, 104, 1993, 119-123.

საქართველოს მეცნიერებათა აკადემიის მოამბე, 159, №2, 1999
BULLETIN OF THE GEORGIAN ACADEMY OF SCIENCES, 159, №2, 1999

BIOPHYSICS

M. Chelidze, T. Sanikidze, T. Chigogidze, D. Kiviladze, L. Managadze, B. Lomsadze, M. Tsartsidze, N. Kotrikadze

Investigation of Blood Metabolic Paramagnetic Centers in Patients with Prostatic Tumors

Presented by Member of the Academy T. Oniani, December 28, 1998

ABSTRACT. **Blood metabolic paramagnetic centers and peroxide oxidation of blood lipids were studied in healthy donors, patients with benign hyperplasia, and patients with prostatic adenocarcinoma. It was found that development of prostatic malignant tumor is associated with significant activation of peroxide oxidation of blood lipids, inactivation of adrenoreceptors, production of methemoglobin complex, etc.**

Key words: oxidation of lipids, methemoglobin, fatty acids, radicals.

The aim of present investigation was to study the changes of the physicochemical properties of blood in the patients with benign prostatic hyperplasia (BPH) and prostatic adenocarcinoma (PAC). The specific goal of investigation was to study the state of blood metabolic paramagnetic centers and peroxide oxidation of lipids (POL) in the blood. It was found that in the blood of patients with PAC an increased activity of POL is evident as compared to the blood of the donors, while the blood of the patients with BPH showed an intermediate rate of POL (Table 1). The rise of POL intensity in the blood of patients with PAC and accumulation of peroxides as compared with the blood of healthy donors may be due to increased concentration of the principal substrates of peroxide oxidation - arachidonic and linolenic acids (Table 1). The presence of POL initiators in the blood is noteworthy as well as the state of those enzyme systems, which participate in initiation and inhibition of peroxide oxidation [1]. Investigation of metabolic paramagnetic centers of blood has shown that the blood EPR-spectrum is characterized by diversity of paramagnetic centers (Fig. 1). The EPR-signal intensity rise of the Mn^{2+}-containing complexes ($g = 2.14$) was identified in the blood of patients with PAC, as compared with the blood of donors and the patients with BHP (Table 2). It was shown earlier that in such cases membrane structures' destruction and superoxide dismutase inactivation do occur [2]. The EPR-

Table 1

The percentage changes of the blood POL (mol/ml) and some fatty acids in the blood plasma

Substance	Disease		
	Healthy donor blood	PBH	PAC
Peroxide oxidation of lipids	$0.0435 \cdot 10^{-5} \pm 0.02$	$0.077 \cdot 10^{-5} \pm 0.02$	$0.117 \cdot 10^{-5} \pm 0.04$
Unsaturated fatty acids:			
Linolenic acid C(18:3)	516.6 ± 3.4	632.0 ± 4.8	683.0 ± 4.4
Arachidonic acid C(20:4)	351.2 ± 1.2	383.2 ± 1.6	386.8 ± 0.9

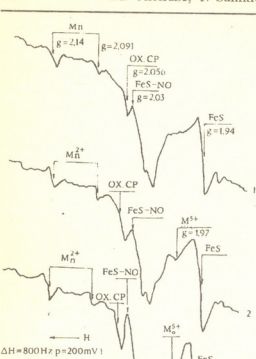

Fig. 1. The EPR-spectrum of the human blood. DH = 800 Gs; p = 200 mvT.

1 - The healthy donor blood; 2 - The blood of the patients with BPH; 3 - The blood of the patients with PAC.

signal intensity of the nitrosil complexes of the iron-sulfuric centers (g = 2.03) in the blood of patients with PAC was almost 3-times as high than in the blood of healthy donors (Fig. 1, Table 2). The FeS-NO EPR-signal intensity in the blood of patients with BPH was negligibly changed as compared the blood of healthy donors. It is known from the literature [2] that the nitrosil complexes of the iron-sulfuric centers are characteristic of the pathologies. Insignificant revealing of the FeS-NO complexes' EPR-signals in the blood of healthy donors could be attributed to the hypoxic conditions. Insignificant increase of the FeS-NO complexes' EPR-signals in a case of BPH and almost 3-fold increase in the PAC indicate that in the malignant tumors increase of the hypoxic state as well as increase of interaction between iron-sulfuric centers and nitric oxidedo occur. It is believed that NO is produced as a result of NO-synthetase activation, when an excess quantity of Ca^{2+} accumulates in the cell [3]. The resulting NO, in a condition of superoxid-dismutase inactivation, interacts with superoxide radicals and produces the hydroxyl radical, which activates POL. The above complexes were found in animal tissues during various pathologies [2].

Ceruloplasmin is known as a polyfunctional coppercontaining protein of the blood serum, which is characterized by superoxide-dismutase, peroxidase, and amine-oxidase activity. Oxidizing ceruloplasmin-Cu^{2+} the iron (Fe^{2+} —> Fe^{3+}) promotes its inclusion into the apo-transferrin, due to which the Fe^{2+} content in the blood serum decreases [4]. All the above-mentioned permit to suggest that insofar in our experiments the oxidized ceruloplasmin (g = 2.056) EPR-signal intensity was increased in patients with PAC, content of Fe^{3+} should be increased respectively, which causes activation of POL (Table 1). It is known that Fe^{3+} is unable to transport molecular oxygen [5]. Insofar we suggest that Fe^{3+} content in the blood of patients with PAC is elevated, than, on the background of increased Fe^{3+}, molecular oxygen transport should be either ceased or hampered, inducing thus the methemoglobin (MetHb) production, which was the case in our experiments (Table 2, Fig. 2). It should be noted that the EPR-signals characteristic of MetHb (g = 6.0) were not present in healthy donors' blood, while in the blood of patients with BPH these signals just appear and in the blood of patients with PAC they increase about threefold. The rise of the EPR-signals, characteristic MetHb, is directly correlated with increase of POL intensity [2]. The rise of the above signal intensity must induce increase of the oxidized ceruloplasmin EPR-signals (g = 2.056) and *vice versa.* In our experiments the MetHb EPR-signals in the blood of patients with PAC were increased and, respectively was increased an intensity of oxidized ceruloplasmin EPR-signals. We cannot exclude any other

Table 2

Changes of the EPR-signals' intensity in the blood - I(mm/mg)

Substance	Diseases		
	Healthy donor blood	Prostatic benign hyperplasia	Prostatic adenocarcinoma
Inactivated adrenoreceptors (g=2.01)	8.0±1.0	12.8±1.0	13.8±1.3
Mn^{2+}-containing complexes (g=2.14)	1.0±0.1	1.1±0.03	1.4±0.06
Nitrosilic complex of nonhemic iron FeS-NO; g=2.03	5.3±0.8	9.0±0.3	14.0±0.9
Oxidized ceruloplasmin g=2.056	20.0±1.0	19.6±0.3	27.8±0.4
Fe^{3+}-transferrin g=4.3	20.0±1.8	18.7±0.4	15.0±1.0
Mo^{5+}-containing complexes g=1.97	–	7.9±0.4	12.0±1.4
Methemoglobin MetHb; g=6.0	–	10.1±1.1	26.3±2.7

parallel mechanism of the MetHb EPR-signal induction, e.g. its appearance may be due to the various factors inducing the blood hemolysis [2]. Transferrin is an active co-participant of erythro- and hemopoiesis [6]. In our experiments increase of the oxidized ceruloplasmin (g = 2.056) EPR-signal intensity (Fig. 1, Table 2) and decrease of the Fe^{3+}-transferrin (g = 4.3) EPR-signal intensity (Fig. 2, Table 2) were recorded in the blood of patients with PAC. This fact points at blood antioxidant property reduction [1], activation of POL, and reduction of hemopoiesis. The latter is in accordance with the volume of Hb in the blood of patients with PAC. In such a case the volume of Hb is reduced as compared with the norm (Table 3). In the blood of patients with BPH and the patients with PAC, the molybdenum-containing complex (g = 1.97) EPR-signal was detected as well (Fig. 1, Table 2). It is noteworthy that Mo^{5+}-containing complex EPR-signal intensity in patients with PAC was twice as much as in the BPH. Presumably, occurrence and increase of Mo^{5+}-containing complex EPR-signals may be determined by production of Mo^{5+}-containing xanthine oxidase, which is a generator of superoxide radicals [2]. The signal, characteristic of inactivated adrenoreceptors (g =

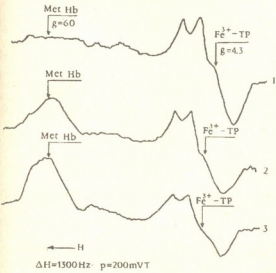

Fig. 2. The EPR-spectrum of the human blood.
DH = 1300 Gs; p = 200 mvT.
1 - The healthy donor blood; 2 - The blood of the patients with BPH. hyperplasia; 3 - The blood of the patients with PAC.

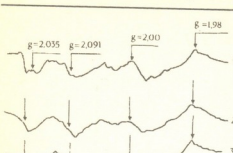

Fig. 3. The EPR-spectrum of human blood. DH = 200 Gs; p = 0.5 mvT.
1 - The healthy donor blood; 2 - The blood of patients with BPH; 3 - The blood of patients with PAC.

2.01), has been revealed in the pathologies (Fig. 3, Table 2). According to the literary data g = 2.01 signal was found after the repeated administration of adrenaline [4]. Particularly in a case of staphylococcal sepsis [7], stresses, and radiational injury [4]. It is known that increase of Mn^{2+} concentration induces inactivation of certain receptors to the adenylate cyclase system [8]. The adenylate cyclase system plays an important role in the process of adrenoreceptors activation. It could be suggested that in the conditions of activation of POL, intensification of free oxygen forms' induction, inactivation of seperoxide-dismutase, and damage to the membrane structures an inactivation of the adrenoreceptors take place. The latter interferes with development of the organism's compensatory reparative reactions, which promotes establishment of irreversible processes. It should be mentioned as well that hypersecretion of catecholamines also determines increase of POL [4]. It could be concluded that development of human PAC elicits significant activation of POL, which presumably is a certain index of pathological

Table 3

Changes of hemoglobin and erythrocyte quantity in the blood of the patients with BPH and PAC. G - the tumor differentiation degree; PIN - the benign hyperplasia differentiation degree.

Item	Diseases				
		PBH		PAC	
	Donor blood	-	$PING_{(1-3)}$	$G_{(1-5}$	$G_{(5-10)}$
Hemoglobin Hb	130.0-160.0	134.4±7.8	123.8±7.0	120.6±3.4	115.1±5.1
Erythrocytes	4.0-5.0	4.36±0.8	4.36±0.9	4.35±0.5	3.9±0.5

reactions and is displayed in decreased antioxidant properties of the blood [2]. Such manifestations are inactivation of adrenoreceptors and production of MetHb complexes (g = 6.0). These certifies for the possibility of weakening of the compensatory-reparative reactions in the organism [9], which promotes development of irreversible processes.

Tbilisi I. Javakhishvili State University
A. Tsulukidze Scientific-Research
Institute of Urology, Tbilisi

REFERENCES

1. *E. B. Burlakova et al.* Biofizika, 25, 1980, 859, (Russian).
2. *T. Sanikidze.* Ph.D.Thesis, Tbilisi, 1997, (Georgian).
3. *G. N. Mozhayeva et al.* Biologicheskyie Membrany, 8, 1991, 431, (Russian).
4. *M. K. Pulatova et al.* In: Electron-Paramagnetic Resonance in Molecular Biology. Moscow, 1989, (Russian).
5. *E. D. Goldberg* In: Handbook of Hematology. Tomsk, 1989, 32, (Russian).
6. *T. T. Zhumbayeva et al.* Radiobiologiya, 27, 1987, 384, (Russian).
7. *T. Gogoladze et al.* Pathfiziologiis aktualuri sakitkhebi, 8, 1995, 4, (Georgian).
8. Advances in Cyclic Nucleotide Research. P.Greengard, A.A.Robinson (Eds.), Raven Press, 1981.
9. *B. M. Lotter, H. Runze.* Biochem. Int., 28, 1992, 961.
10. *V. L. Trudean et al.* Gen. Comp. Endocrinol., 89, 1993,

საქართველოს მეცნიერებათა აკადემიის მოამბე, 159, №2, 1999
BULLETIN OF THE GEORGIAN ACADEMY OF SCIENCES, 159, №2, 1999

BIOCHEMISTRY

I. Lomouri, Corr. Member of the Academy N. Aleksidze

Choline Kinase Activity in Subcellular Fractions of Brain

Presented December 30, 1998

ABSTRACT. **Choline kinase is represented in the cytosol of cerebral subcellular fractions of *Gallus Domesticus*. Molecular mass of this enzyme has been defined (66000±1000 kDa). It has been established that practically choline kinase has not undergone any evolutional changes.**

Key words: ATP-adenosinetriphosphate, ADP-adenosine 5'-diphosphate, AMP-adenosinemonophosphate, CTP-cytidine 5'-triphosphate, CDP-cytidine 5'-diphosphate, CMP-cytidine monophosphate.

First choline kinase (E.C.2.7.1.32; ATP: choline phosphotransferase) was found in yeast and acetone preparations of some animal tissues [1]. Since then this enzyme has been studied in a number of organs, tissues, cells and subcellular fractions. Choline phosphorylation with ATP participation is the first stage in biosynthesis of phosphatidylcholines. It is considered to be universal and its mechanism is known [2,3]. Nowadays, universality of choline kinase reactions are considered to be solved but it can't be said about subcellular distribution of this enzyme. Data on this subject are heterogeneous and require further assertion. A part of works [4-9] prove that choline kinase is a soluble enzyme and it is mainly found in the cytosol of the cell. According to some data 70-80% of choline kinase in filaments of the angiospermic parasite is associated with the fraction of mitochondria [10]. In goat brain 75% of choline kinase is in cytosol, 20% in microsome fraction and in the liver it is totally in cytosol [6]. According to the same data in the brain and liver of rats and mice choline kinase as well as ethanolamine kinase are found only in microsome fraction. It makes an impression that apart from the phylogenetic hierarchy of organism the origin of each organ and tissue are also important.

The present work introduces the data on choline kinase distribution in subcellular fractions of *Gallus Domesticus* brain.

Subcellular fractions of *Gallus Domesticus* brain were obtained by differential centrifugation [6]. Purity of subcellular fractions was tested by protein markers. Protein was defined by the method of Lowry and others [11]. Choline kinase activity and the compounds of phospholipids were defined according to Kates [12]. Experiments were carried out on the icy water bath (2-5°C). 0.4 ml of incubation medium contained: 1.25 mM of $MgCl_2$; 40 μM of tris-HCl; pH-9.5; 1.25 μM of choline chloride; 1.25 μM of ATP; 0.1 ml of enzyme preparation (20-100 mg of protein) obtained from subcellular fractions. Incubation was carried out for an hour at 38°C. At the end of incubation the samples were placed over the boiling water for 5 min. The enzyme was preliminarily inactivated for the control tests. The samples were centrifugated for 10 min at 700 g. In transparent supernatant the choline, phosphorylcholine (Pch) and in some cases acetylcholine (Ach),

cytidinediphosphorylcholine (CDPch), CTP, CDP, CMP, ATP, ADP, AMP and phosphor amount were defined. On this purpose the incubated mixture was evaporated in microcrucibles under the warm air pressure. After concentration the substances were chromatographied on Wathman paper or Filtrak N11 in rising chromatography (solvents: isopropanol-frozen acetic acid - water 8:1:1 or ethanol - isopropanol - ammonium 6.8:2.0:3.5). At the beginning together with the samples the standard substances were carried to chromatography paper in micropipette. Along the standards we cut stripes of dried chromatography, developing them under iodine steam and ultraviolet light. Contours of stains were fixed with a pencil. After defining the R_f we cut the corresponding loci of the samples of choline, Pch, Ach, CDPch, ATP, ADP, AMP, CTP, CDP, CMP extracting, identifying and defining them.

In some cases the marked choline (^{3}H-choline 'Amercham' England, in the sample 0.5-0.7 μ Ci) was used. After chromatography the Pch radioactivity was determined in scintillation mixture of toluol.

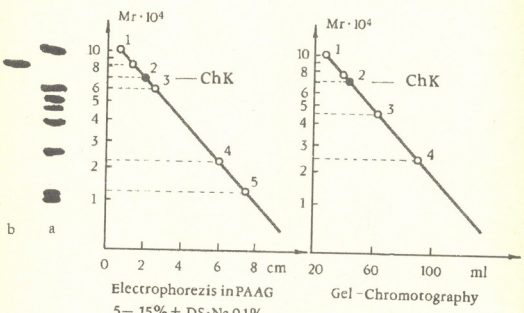

Fig. Determination of molecular mass of choline kinase
a) Protein markers 1.phosphorylase Mr-94000,
2. Albumin Mr-68000
3. Ovalbumin Mr-44000,
4. Prechymotrypsin Mr-25000
5. Cytochrome Mr-12500
b) Choline kinase.

Quantitative data of choline kinase activity in the subcellular fractions of *Gallus Domesticus* brain are given in the Table, assertaining that really, choline kinase is mainly presented in the cellular cytosol of brain [4-9].

The mass of extracted choline kinase was defined by chromatography on Sephadex G-100 [13]. Molecular mass was computed by the equation $lgMr = 5.941-0.847\ (Ve/Vo)$. On the column (60x1.6) Vo with blue dextran ("Ferak" m.m 2000000, Berlin) was 59 ml

and Ve of the protein of study 78 ml. Here, lgMr = 5.941-0.847 (78/59) or lgMr = 4.82, where the molecular mass was 66069 kDa. On the polyacrylamide gel it was also established by disk-electrophoresis (Fig. 1) that molecular mass and specific activity of choline

Table

Fractions	Cholinekinase activity	
	nM Pch/mg Protein/min	% 20 40 60 80 100
homogeneous	1.108±0.041	
nucleoli	0.011±0.001	
mitochondria	0.014±0.002	
microsoms: light	0.023±0.004	
heavy	0.019±0.003	
cytosol	0.997±0.029	

kinase of *Gallus Domesticus* brain (66000 ± 1000kDa, 3.41 unit/mg) equals the preparation [14] obtained from brewer's yeast (67000kDa, 3.3 unit/mg). It shows their biological similarity. Thus, it can be concluded that choline kinase hasn't undergone any evolutional changes.

Tbilisi I. Javakhishvili State University

REFERENCES

1. *J. Wittenberg, A. Kornberg.* J. Biol. Chem., **202**, 1, 1953, 431-444.
2. *E. P. Kennedy, S. P. Weiss.* J. Biol. Cchem., **222**,1, 1956, 193-214.
3. *E. P. Kenedy.* Trudy V mezhdunarodnogo biokhimicheskogo kongressa, simpozium, VII, 115-127. Moskva, 1962 (Russian).
4. *P. A. Weinhold, V. B. Rethy.* Biochemistry, **13**, 25, 1974, 5135-5141.
5. *H. Fukuyama, S. Yamashita.* FEBS Lett., **71**, 1, 1976, 33-36.
6. *R. K. Upreti, G. G. Sanval, P. S. Krishnan.* Archives of Biochemistry and Biophysica, **174**, 1976, 658-665.
7. *R. E. Ulane, L. L. Stephenson, P. M. Farrell.* Anal. Biochem., **79**, 2, 1977, 526-524.
8. *P. A. Latishev.* Ukrainskii biokhimicheskii zhurnal. **52**, 6, 1980, 778-782.
9. *I. Lomouri.* II vsesojuznaia mezhuniversitetskaya konferentsya molodykh uchienykh. 244-245, Tbilisi, 1980.
10. *P. N. Setty, P. S. Krishnan.* Biochem. A Bioph. Research Communication. **40**, **4**, 1970, 320-824.
11. *O. H. Lowry, N. L. Rosebrouch, A. K. Farr, L. Randall.* J.Biol. Chem., **193**, 1951, 265-270.
12. *M. Kates.* Tekhnika lipidologii. Moskva, 1975.
13. *G. Tkemaladze, G. Kvesitadze.* Praktikuli enzimologia. Tbilisi, 1975.
14. *M. A. Brustrom, E. T. Browing.* J. Biol. Chem., **218**, 7, 1973, 2364-2371.

საქართველოს მეცნიერებათა აკადემიის მოამბე, 159, №2, 1999
BULLETIN OF THE GEORGIAN ACADEMY OF SCIENCES, 159, №2, 1999

BIOCHEMISTRY

J. Lagidze, L. Talakvadze, E. Tskrialashvili

Synthesis and Biological Activity of Aralkyl Nitrogen-, Sulphur- and Phosphororganic Compounds

Presented by Member of the Academy T. Beridze, June 15, 1998

ABSTRACT. **The growth requlating and fungicide activities of aralkyl nitrogen-, sulphur- and phosphororganic compounds have been studied at the Russian Scientific Institute of Plant Protection by Chemical Agents. It has been shown that these compounds stimulate the growth of alga *Chlorella vulgaris* cells. Some of them have high fungicide activity.**

Key words: plant stimulator, fungicide.

We have recently synthesized a number of structural analogues of biogenic amines, vitamins and other physiologically active compounds. It has been shown that some of these compounds have high antiblastomatic activity, radioprotective, spasmolytic and hypotensic properties [1-3].

On the basis of 3-aryl-1-bromobutanes we have synthesized a number of nitrogen-, sulphur- and phosphororganic compounds in order to study their biological activity.

(I-IV)

(V_VI)

(I) Ar = p - $CH_3C_6H_4$, R = H, n = 2. (II) Ar = p - C_6H_4 - SO_2NH_2, R = C_2H_5, n = 2.

(III) Ar = p - C_6H_4 - SO_2N - , R = C_2H_5, n = 2. (IV) Ar = C_6H_5, R = H, n = 4.

(V) Ar = p - C_6H_4 - $SO_2N(C_2H_5)_2$. (VI) Ar = p - CH_3 - C_6H_3 - $SO_2N(C_2H_5)_2$

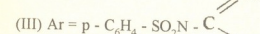

(VII - VIII)

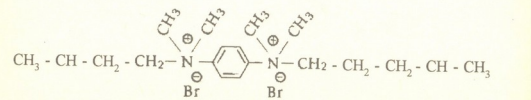

Ar (IX - X)

Ar

(VII) R = H. (VIII) R = NO. (IX) Ar = C_6H_5. (X) Ar = m - $C_6H_3(CH_3)_2$

3-(p-tolyl)butylphosponic acid (1) m. p. 86-87^{0}C.

0.0-diethyl-3-(p-sulphonamidophenyl)butyl-phosphonate (II), m. p. 116^{0}C

0.0-diethyl-3-(p-N-guanidylsulphonamido-phenyl) butylphosphonate (III), m. p. 192^{0}C

5-phenylhexylphosphonic acid (IV), m. p. - 67-68^{0}C.

4-(p-N, N-diethylsulphonamido-phenyl) pentanic acid (V), oil, n_D^{20} 1.5240 d_4^{20} 1.1358.

4-(3-N, N-diethylsulphonamido-p-methylphenyl) pantanic acid (VI), oil, n_D^{20} 1.5200, d_4^{20} 1.1580.

3-phenylbutylurea (VII), m. p. 80-81^0 C.

1-(3-p-phenylbutyl) - 1- nitrozourea (VIII), m. p. 45-47^{0}C.

Dibromide (IX), m.p. 57-60^{0}C.

Dibromoide (X), m. p. 73-75^{0}C.

The activity of the synthesized compounds was studied on different microorganisms at the concentration of 0.003%. Tetramethyl thiuramidsulphid was used as a controller. The Table shows that the compounds have different fungicide activity. The highest activity they exhibit against the mycelium of *Verticillium dahliae*. In particular, fungicide activity (90%) of sulphonamidoacid (V) approaches the control, while its equal to the control (100%) for salt (X). Fungicide activity of urea and nitrozourea derivatives (VII) and (VIII) as well as ammonium salt (IX) make up 70%. It has been shown that fungicide activity of acids (I) and (IV) against tomato phytophtorosis make up 85.3 and 84.8%, accordingly.

Table

Compounds	Suppression of microorganisms, %				
	Botrytis cinerea	Fusarium onolif	Verticillum	Aspergillums niger	Verticillium dahliae
1	0	15	0	5	50
II	0	15	0	5	50
III	0	15	0	5	0
IV	0	15	0	5	30
V	0	15	0	0	90
VI	15	15	0	0	50
VII	0	5	0	0	70
VIII	0	0	0	0	70
IX	15	15	0	0	70
X	20	15	20	0	100
control	100	100	100	100	100

The growth regulation activity of aforesaid compounds on alga *Chlorella vulgaris* cells has also been studied.

Sulphonamidoacids (V) and (VI) have the highest biostimulating activity 233% and

187%, accordingly. Other compounds also exhibit high growth stimulating activity in comparison with control. Aforesaid salts and their structural analogues exhibit high antibacterial activity and at the same time in certain cases they prohibit the growth of the intestinal bacillus. They also exhibit pronounced cardiotonic effect increasing the intensity of heart muscle. Some of these compounds also have high hypotensic and spasmolytic activity [4-5].

The investigations of biological activity of the synthesized compounds are in progress.

Oncological Scientific Centre, Tbilisi.

REFERENCES

1. *J. Lagidze, V. Machradze, T. Revazishvili, V. Chernov.* Farmackokinetika protivoopukholevykh preparatov. Material III Vsesoyuznogo Soveshchaniya. Tomsk, 1987 (Russian).
2. *J. Lagidze, L. Talakvadze, R. Lagidze.* Khimea geterotsiklicheskikh soedinenii. 12, 1976 (Russian).
3. *G. Gvishiani, D. Kvachadze, et al.* Farmacologiya fisiologicheski aktivnykh veshchestv. Frunze, 1973 (Russian).
4. *J. Lagidze, E. Rudzit, R. Lagidze.* A. S. SSSR. N514460, 1974 (Russian).
5. *G. Gvishiani, M. Mchedlishvili, J. Lagidze.* A. S. SSSR. N6772768, 1977 (Russian).

საქართველოს მეცნიერებათა აკადემიის მოამბე, 159, №2, 1999
BULLETIN OF THE GEORGIAN ACADEMY OF SCIENCES, 159, №2, 1999

BIOCHEMISTRY

T. Lekishvili, N. Koshoridze, G. Alexidze, Corr. Member of the Academy
N. Aleksidze

Biological Characterization of Chick Brain Glial Cells Lectin

Presented March 2, 1998

ABSTRACT. **D-galactose and inositol sensitive lectin was separated from chick brain glial cells. The pH optimum of lectin activity was from 7.0 to 7.5. The lectin hemagglutination activity was inhibited at 0.5 mM Ca^{2+} and 1.5 mM Mg^{2+} concentration. Some of the amino acids, such as L-glutamine, L-serine and L-arginine, like sugars inhibited chick brain glial cells lectin hemagglutination activity.**

Key words: lectin, glia, amino acid, carbohydrate.

The vertebrate lectins attract a great attention as they may play an important role in many physiological and biochemical processes of cells, in particular, in brain plasticity, synaptogenesis, transmission of metabolic signals, cells adhesion and etc. [1]. Therefore, the glial cells are of interest as they have a fundamental role in trophic function of brain [2]. Considering the fact, that lectins intensify uptake of some metabolites by liver cells, we supposed that analogical mechanisms might function in glial cells too. That's why we made an attempt to study the lectins from glial cells.

The white leghorn chickens brain was used in all experiments. The chick brain glial cells enriched fractions were obtained according to the method, as described previously [3]. The lectin was separated by the 0.3% Triton X-100 solution (1:5). The suspension was centrifuged at 20000g for 20 min. The supernatant was decanted and was dialyzed against 40 mm potassium buffer (pH 7.4) during 24 h. The lectin hemagglutination activity was assayed by the trypsinized rabbit erythrocytes in microtiter U-plates [4]. The protein concentration was determined according to Lowry *et al.* [5]. The extent of hemagglutination was evaluated by the specific activity of protein extract (SA = $titer^{-1} \cdot mg\ protein/ml^{-1}$)[6]. The carbohydrate-binding specificity was studied by the hapten-inhibitor technique [7].

Table 1.

Hemagglutination activity of chick glial cells lectin like protein fractions extracted by EDTA and Triton X-00 buffers

Extragent	Specific activity $titer^{-1} \cdot mgprotein/ml^{-1}$
2mM EDTA	-
5mM EDTA	-
0.3% Triton X-100	35.4

In the first series of experiments, we attempted to testify the extraction solutions, where the lectin activity reaches maximum. The results are listed in Table 1.

One can see, that the highest lectin activity was discovered in chick brain glial cells protein fractions extracted by the 0.3% Triton X-100 solution. Therefore, in future experiments lectins were separated by the above-mentioned technique. After extractions, the lectin like protein fraction from chick brain glial cells, were

Table 2.

The influence of carbohydrates on chick brain glial cells lectin hemagglutination activity

Carbohydrate	Minimum concentration of carbohydrates for inhibition of lectin activity (mM)
D(+)-galactose	0.6
D(+)-lactose	>100
D(+)-mannose	>100
D(+)-glucose	>100
D(+)- arabinose	>100
D(+)-maltose	>100
L(+)-rhamnose	>100
D(-)-fructose	>100
D-galacturonic acid	>100
N-acetyl-D-glucosamine	>100
D(+)-xylose	>100
D(+)-trehalose	>100
inositol	3.12
D(+)- melibiose	>100

On the other hand, the influence of different amino acids on chick brain glial cells lectin like proteins hemagglutination activity was studied. The results are presented in Table 3, which shows, that the amino acids, like sugars, can inhibit lectin hemagglutination activity as hapten-inhibitors. In our case the glutamine serine and arginine were the most potent inhibitors from all selected amino acids.

It seems, that glial cells lectin may play an important role in brain trophic function.

fractionated by ammonium sulfate at different saturation (20%, 40%, 60%, 80%, 90%, and 100%). The suspension was stayed during 15-20 min and was centrifuged at 16000g for 20 min. The lectin activity in pellets was discovered in fractions, which was precipitated at 80% saturation by ammonium sulfate.

In order, to purify the proteins with the lectin activity from chick brain glial cells by absorption chromatography, we held special experiments for detecting their specificity to carbohydrates (Table 2).

Table 2 clearly shows, that the lectin activity is inhibited by D-galactose and inositol. On the basis of these results in further experiments lectins were isolated by affinity chromatography on tris-acryl immobilized galactose column. It should be noted that the specific activity was detected and it was from 7.0 to 7.5. As the other experimental results show, the lectin hemagglutination activity was inhibited at 0.5 mMCa^{2+} and 1.5 mM Mg^{2+} concentration.

Table 3.

The influence of amino acids on hemagglutination activity of chick brain glial cells lectin

Amino acids	Minimum concentration of amino acids for inhibition of lectin activity (mM)
L-cysteine	>100
L-cystine	>100
L-arginine	4.5
L-lisine	>100
L-alanine	>100
L-serine	4.5
L-aspartate	>100
L-asparagine	>100
L-glutamate	>100
L-glutamine	9.0

Tbilisi Iv. Javakhishvili State University

REFERENCES

1. *N. Aleksidze*. Neirokimiis sapudzvlebi. Tbilisi, 1992 (Georgian).
2. *S. Nemechek et al.* Vvedenie v neirobiologiu, Praga, 1978 (Russian).
3. *Y. Nagata, Y. Tsukada*. Rev. Neurosci. **3**, 193, 1978.
4. *S. H. Barondes*. Science **223**, 1984, 1259-1264.
5. *O. Lowry* et al. J. Biol. Chem. **193**, 1, 265-75, 1961.
6. *M. D. Lutsick* et al. The Lectins, Visha Skola, Lvov, 1981.
7. *I. E. Liener*. The Lectins. Acad. Press. Inc.,1986.

საქართველოს მეცნიერებათა აკადემიის მოამბე, 159, №2, 1999
BULLETIN OF THE GEORGIAN ACADEMY OF SCIENCES, 159, №2, 1999

R. Zosidze

Hydrofauna of the Chvanistskali River

Presented by Corr. Member of the Academy B. Kurashvili, September 2, 1998

ABSTRACT. **Species diversity and quantitative indices of the benthos and fishes in the Adjarian (South-West Georgia) river Chvanistskali were investigated. Living conditions of the animals were evaluated. The habitat of some species as well as biological-environmental aspects of the fishes were determined. Investigation provides some hints and recommendations on the fish farming and reproduction in the river.**

Key words: mountain river, benthos, invertebrates, fishes, environment, fish farming.

A systematic utilization and protection of the water basins' natural resources attains ever-increasing interest today and implies their over-all investigation. The main goal of the present study was evaluation of the natural resources of the tributaries of the two largest Adjarian rivers - Chorokhi and Acharistskali. This is a continuation of the earlier studies, which were carried out for several years.

The Chvanistskali river is one of the principal tributaries of the Acharistskali river. However, from the hydrobiological standpoint the river is poorly studied so far. The main target of our investigation was the species diversity and quantitative indices of the hydrofauna in the above-mentioned river. The other goals were: the faunistic-ecological investigation of the hydrofauna, determination of the habitat of the species, *etc*. The hydrofaunistic material was collected at the whole length of the river. The specimens were collected at the upper-, middle-, and lower streams. The Chvanistskali river, a right tributary of the Acharistskali river, is a typical mountain river, which flows in a narrow and deep ravine. The river bed is rich with boulders and stones, which make a number of the waterfalls and whirlpools. Almost the whole year the water is clear and transparent. The water temperature varies between 2-16°C. It could be claimed that the river provides good conditions for the normal development of the hydrobionts.

Investigations have shown that the majority of the river benthofauna is comprised of invertebrates, which dwell on the plants' roots. Total of 50 species have been recorded, the species and quantitative indices of which are presented in Table 1. As could be seen in the Table the benthofauna consists of the following groups of the invertebrates: *Oligochaeta, Mollusca*, *Crustacea*, and *Insecta* (larvae). About 80 % of the river benthofauna species is comprised of insects. The insects build up the most part according to their quantitative volume as well. A brief account of the separate species is presented bellow:

Oligochaeta. These animals in the waters of Georgia most exhaustingly were investigated by A.Pataridze [1, 2]. In the rivers of Adjaria 21 species of these animals were recorded by us [3-6]. Six species were found in the Chvanistskali river - *Dero obtusa* Ud., *Aulophorus fuscatus* Mull., *Pristina rosea* Pig., *Wais barbata* Mull., *Dulodrilus limnobius*

Bret., *Tubifex tubifex* Mull. (Table 1).

Mollusca - Total of two species were found in the Chvanistskali river - *Ancylus fluviatilis* Mull., and *Radix ovata* D.

Table 1

The species and quantity (per m^2) content, and biomass (mg/m^2) of the benthofauna

Group	Upper stream		Middle stream		Lower stream	
	Number	Biomass	Number	Biomass	Number	Biomass
Oligochaeta	14	33	86	215	143	330
Mollusca	20	110	14	97	26	190
Insecta (larvae)						
Ephemeridae	660	2495	1477	5095	790	2610
Plecoptera	63	545	118	1876	59	422
Diptera	371	935	485	1069	460	629
Trichoptera	165	965	534	4315	820	4963
The total quantity and biomass(g)	1230	5.0	2714	11.6	2298	9.1

Insecta - These (larvae forms) presented the majority of the benthofauna. About 10 species of *Ephemeroptera* were found: *Baetis pumilus* Burm., *Baetis alpinus* Pict., *Epeorus torrentium* Eot., *Ecdyonurus fluminum* Pict., *Heptagenia perflava* Brod., *Heptagenia sulphurla* Mull., *Rhythrogena auriantеace* Barm., *Poligenia longicaude* Ol., *Ephemera vulgata* L., *Ephemerella ingata* Pod. Total of 9 species of *Plecoptera* were recorded: *Perla caucasica* Guer., *Perla marginata* Panz., *Perla pallida* Guer., *Perlodes microcephala* Pict., *Isoperla caucasica* Bolin., *Chloroperla fausca L., Amphinemura mirabilis* Mart., *Capnia nigra* Pict. Out of *Trichoptera* about 10 species were found: *Rhyacophila nubila* Zett., *Rhyacophila cuprecorum* Mart., *Glossosoma unguiculatum* H., *Hydropsyche ornatula* Mull., *Hydropsyche instabilis* Curt., *Silo poximus* Mart., *Drusus caucasicus* Vlm., *Cheumatopsyche lepida* Pict., *Psychomyia pusilla* Fabr. Out of *Diptera* total of 10 species were identified, including 2 species of *Simulidae* (*Eusimulus ex gr. aureum Fri., Vilhelmia mediterranea* Puri.), 7 species of Chironomidae were found as well (*Tanitarsus ex gr. exigus* Joh., *T. ex gr. labatifrons* Kieff, *Polypedilum ex gr. pedesta* Mg., *Limnochironomus nervosus* Steag., *Euciefferiella cyanea* Th., *Orthocladius rivicda* Kieff, *Diamesa ex gr. tienemanni* Kieff.) but their number was negligible.

As to the vertical distribution of the benthofauna it should be noted that the middle stream of the river is the richest, which is due to the best hydrological conditions. The benthofauna strongly depends on the seasonal changes as well. The highest biomass was recorded in the spring-summer periods.

In the Chvanistskali river the four fish species were found: *Salmotrutta lablax Pall.m.faria* L., *Barbus tauricus escherichi* Stend., *Chindiostoma colchicus* Kessler., *Gobius melanostomus* Poll. All these species are the aboriginal forms. In the upper and middle

streams of the Chvanistskali river the most frequent are *Salmotrutta* and *Barbus*. Description of these fishes is presented in our earlier paper [7]. In the present paper their feeding properties and interrelations are evaluated. An analysis of the feeding spectrum has shown that the above fishes feed entirely on the benthos animals (Table 2). Although, there is certain difference in their feeding habits. As could be seen from the Table 2 *Salmotrutta* prefers *Ephemeroptera*, *Barbus* - mostly feeds on *Trichoptera*, *Chondiostoma* - on *Oligochaeta*, but mostly on the algae. As one can notice there is almost no competition between the fishes. Besides, in the river, generally, there are few fishes and the large amount of the benthos food remains unclaimed. This fact permits to state that in the Chvanistskali river the fish protection means should be carried out with an aim to promote their reproduction for the fisheries purposes. In the middle stream of the river there are enough resources to reproduce the fishes by means of artificial introduction of the fry.

Table 2

The fish feeding spectrum (The components' weight in %, and filling index in %)

The food components	*Salmotrutta labiax*	*Barbus tauricus*	*Chondiostom colchicus*
Oligochaeta	-	10.5	25.0
Mollusca	-	16.5	4.5
Trichoptera	10.5	25.5	4.0
Ephemeroptera	73.4	14.2	10.0
Plecoptera	3.5	16.2	1.5
Chironomidae	4.0	-	5.6
Adult insects	12.0	10.5	-
Algae	-	-	50.1
Filling index	280	50.5	75.5

In conclusion it could be noted that in the Chvanistskali river there were recorded about 50 species of the benthos animals, the most frequent of which are insects (larvae). The bioecological evaluation of the above organisms did show that the majority of them are widely distributed species and only few are the endemic ones.

Analysis of the feeding spectrum of the fishes in the river under study has shown that all the species feed on the benthos organisms and there is no competition. This fact allows to recommend an artificial reproduction of the valuable species (e.g. the river trout) in this water basin. An artificial water-ponds could be recommended for this end.

Batumi Sh. Rustaveli State University

REFERENCES

1. *A. I. Pataridze*. Oligochaetofauna of the Tbilisi reservoir. Funds of the Institute of Zoology, Georg. Acad. Sci., Tbilisi, 1956 (Russian).
2. *A. I. Pataridze*. Bull. Acad. Sci. Georgian SSR, 22, 1959 (Russian).
3. *R. Sh. Zosidze*. Thesis of Ph.D. Diss., 1971 (Georgian).
4. *R. Sh. Zosidze*. In: 17th Conf. Young Scientists, Tbilisi, 1972 (Georgian).
5. *R. Sh. Zosidze*. In: Proc. Batumi Pedagogical Institute, 10, 1973 (Georgian).
6. *J. S. Meskhidze, R. Sh. Zosidze*. In: Proc. of the Georgian Pedagogical Institute, Natural Sciences Series, Tbilisi, 5, 1978 (Georgian).
7. *J. S. Meskhidze*. In: Proc. Batumi Pedagogical Institute, 9, 1952 (Georgian).

საქართველოს მეცნიერებათა აკადემიის მოამბე, 159, №2, 1999
BULLETIN OF THE GEORGIAN ACADEMY OF SCIENCES, 159, №2, 1999

EXPERIMENTAL MORPHOLOGY

E. Nikabadze-Orjonikidze

Prolapse of Heart Valves Concomitant to Marfan's Syndrome, Complicated with Mitral Insufficiency in Children

Presented by Corr. Member of the Academy T. Dekanosidze, March 25, 1998

ABSTRACT. **The medical history of 7 year old patient suffering from Marfan's syndrome concomitant to small (3-4 mm) prolapse of mitral valve is presented. During next years the prolapse was increased up to 7 mm. Also the prolapse of tricuspid valve was observed. Patient's general condition in the age of 14 became worse; insufficiency of mitral valve was developed (++). The patient is being under the cardiosurgeon's supervision.**

Key words: Marfan's syndrome, mitral valve, tricuspid valve.

Marfan's syndrome belongs to the systemic hereditary pathology of connective tissue. It is characterized with disorders of locomotor and cardiovascular system and sight disturbances. Its characteristic clinical signs are: excessive height, rather little body weight, severe structural changes of skeleton (scoliosis, kyphosis, funnel-shaped or pigeon breast, dolichocephally, high gothic hard palate, flat-foot, arachnodactylia, syndactylia, etc.). As for sight: crystal displacement, spheropakia, cataract, glaukoma, blue sclera, etc. Cardiovascular system is characterized by following disorders: aortic pathology ((65.6%) dilatation of its root, aneurism, coarctation, etc.). Prolapse of mitral valves is often concomitant to Marfan's syndrome (16,0%). Many scientists indicate cases of several heart valves (mitral, tricuspidal, aortic) prolapse simultaneous concomitance to Marfan's syndrome [1-4, 10].

Some authors [1, 6, 7, 9] explain concomitance of these two pathologies in pathogenetic aspect by similar biochemical and pathomorphologic changes. The main factor of cardiac valves prolapse is myxomatic degeneration of valves. It causes curving inward of atrioventricular valves in auricle in systolic phase and semilunar valves in ventricle tract in diastolic phase.

Complications generally associated with heart valves prolapse are chord loss, valve acute and chronic insufficiency, bacterial endocarditis, thromboembolism (mainly in vertebrobasular vessels), heart rhythm disorders dangerous for the life, sudden cardiac arrest [8, 9, 11, 12].

Our aim was to present to our colleagues an interesting case of prolapse of heart valves concomitant to Marfan's syndrome, complicated with mitral insufficiency, tactics of its treatment and mechanisms of acting of some medications.

There were six patients with Marfan's syndrome treated at the Center of Children's Rehabilitation. All children had concomitant valves prolapse (100%). In three of these cases prolapse was complicated with mitral insufficiency. Medical record of one of them is presented: patient 7 years old, was admitted at the Orthopedic Department of the Center of Children's Rehabilitation with diagnosis of Marfan's syndrome. Complaints were: weak-

ness, fatigue, chest pain. It was worth of taking into consideration medical history of mother's complicated pregnancy and delivery. Birth was in time, development was normal, exceptions were the cases of syncope in the age of 2-4. In the age of 5-6 years mother noticed deviation of vertebral column.

Boy had asthenic constitution, kyphoscoliosis, pigeon breast, arachnodactylia, high gothic hard palate, flat-foot, myopia. Physical signs: by percussion - heart left border was normal, determination or right border was impossible due to the deviation of vertebral column.

On the basis of auscultation (systolic click), phonocardiography (late systolic murmur and extratones) and echocardiography (slight 3-4 mm prolabation of mitral valve) the diagnosis of mitral valves prolapse was determined. Syndrome of prolonged QT interval, disorders of the process of ventrical miocardium repolarisation (depressive and deformed T-waves in I, II, III, V5 and V6 leads), signs of left atrium overtension were defined by ECG (Fig. 1,2). Cardiointervalography revealed sympathetic direction of the tonus of vegetative neural system and centralized regulation of heart rhythm. Sympathetic direction of the reaction was revealed by clinoorthostatic test. Among psychoemotional disorders the state of subdepression must be mentioned (slight hypothimia, passiveness during speaking, simple answers).

Complex treatment based on general sanitation and vegetotrophic principles was prescribed and had two directions: nonmedicamental and medicamental. Nonmedicamental treatment included psychotherapy, physiotherapy, reflexsotherapy, balneotherapy, physical exercises. Medicamental therapy was directed on the improvement of miocardium metabolism, regulation of vegetative homeostatis, prevention of neurodistrophya and bacterial endocarditis (riboksin, panangin, obsidan, complex of vitamins, antibiotics, the latter is necessary in case of surgical intervention, medical herbs). Great attention was paid to the sanation of chronic deceases.

After discharging from the hospital the patient's parents were given necessary consultation concerning the life regime of the child. He was treated in an out-patient clinics and was prescribed to perform ECG, phonocardiography and echocardiography once every six months.

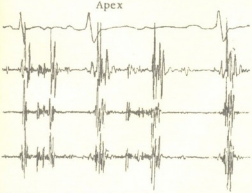

Fig. 1. Diagnosis _ Marfan's syndrome, moderate prolapse of mitral valve. ECG in 12 leads - syndrome of prolonged QT - interval, disturbance of ventrical miocardium repolarization process.

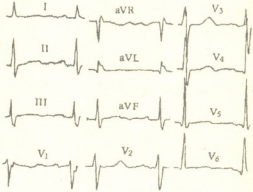

Fig 2. The same patient in the age of 7, high frequency and low amplitude telesystolic murmur while two extratones (indicated by arrows), paper speed in first cycle is 50 mm/sec, in the second 100 mm/sec.

The second examination of a patient showed that the condition became worse. The complains were: weakness, pain in heart area palpitation, fatigue, shortage of breath, there was no peripherial swelling. Liver enlarged while palpation for 1.5 cm, pulse with normal tension, pulse rate 100, increasing to 125 in orthostatic state, breath rate 24 per

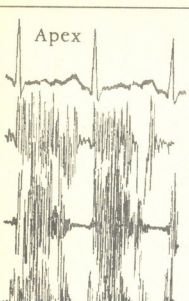

Fig. 3. The same patient in the age of 14. Diagnosis - Marfan's syndrome concomitant to heart valves (mitral, tricuspid) prolapse, complicated by mitral insufficiency. Holosystolic of high frequency and amplitude in orthostatic state.

min, blood pressure 113/65 mm/Hg, while auscultation - ping systolic murmur was heard, phonocardiography revealed holosystolic murmur of high frequency and high amplitude increasing in orthostatic state; echocardiography revealed dilatation and hypertrophy of left ventricle, enlargement of aortic bulb, exfoliation of aortic walls, prolabbation of tricuspid (3-4 mm) and mitral (>7 mm) valves, doplerechocardiography revealed systolic turbulent blood flow from left auricle (++) Fig. 3.

Cardiosurgeon examined the patient and made the decision that surgical intervention wasn't necessary on the given stage. Parents were advised to hospitalize the child.

For the treatment of mitral insufficiency associated with lung functional hypertension and miocardium instability, for avoiding blood failure and secondary lung hypertension, doses for maintaining heart glycosides were prescribed (digoxin - 1/5 of saturation dose, – 0.03 mg/kg twice a day and for systemic blood circulation non-hypotensive dose captoprile - 0.5 mg/kg twice a day long-term administration (according to the general state of patient)). Improving the function of left ventricle captoprile reduces number of cases of such complications as secondary hypertension of lungs. The given mechanism includes local angiotensive influence of captopril on lungs vessels. As an inhibitor of convertive enzymes this preparation reduces lungs vessels sensitivity to angiotensin, thus decreases their vasoconstructive response to hypoxia and sympathetic-adrenal mechanisms [1]. The treatment in general was similar to the tactics presented in this work, rendered to the patient when he was 7 years old. ECG and PCG of patient are shown in dynamics in Figures.

Tbilisi Center of Children's Rehabilitation

REFERENCES

1. *I. M. Belozerov, S. F. Gmusaev.* Mitral valve prolapse in children. M., 1995, 120 (Russian).
2. *N. A. Belokon, M. B. Guberger.* Heart and vessels diseases in children, M. , 2, 1987, 480 (Russian).
3. *D. N. Bochkova, N. T. Artamonova, N. N. Cuzmina et. al.* Mitral valve prolapse as a symptom of an Inherited diseases" Issues of Safety Motherhood and Childhood", N10, 1979, 12-18.
4. *E. Nikabadze-Orjonikidze.* Ist. Georgian Scientific-Practical Conference "Rea-96", Tbilisi, 1996, 65-67 (Georgian).
5. *N. A. Osina, E. A. Efimova.* Marfan's syndrome clinico-echocardiographic chracteristics in children. Ultrasound Diagnosting in Pediatrics. Gorky, 1968, 5-9 (Russian).
6. *D. R. Duren, A. E. Becer, A. L. Dunning.* J. Amer. Coll. Cardiol., 11, 1988, 42-49.
7. *M. Godfrley, V. Menashe, R. G. Weleber et al.* Am. J. Hum. Genet., 1990, 653-660.
8. *J. P. Petitalot, A. FChaix,* R. Barraine. J. Clin. Ultrasound, 14, 9, 1986, 707-711.
9. *R. E. Pyerits, M. A. Wappel.* Am. J. Med., 74, 1983, 797-807.
10. *J. W. Simpson, J. J. Nora, D. G. McNamara.* Am. Heart J. 77, 1969, 96-99.

საქართველოს მეცნიერებათა აკადემიის მოამბე, 159, №2, 1999
BULLETIN OF THE GEORGIAN ACADEMY OF SCIENCES, 159, №2, 1999

EXPERIMENTAL MEDICINE

N. Vanishvili, D. Tsiskarishvili

Dynamics of Left Ventricle Functional Indices in Conditions of Essential Hypertension Irregular Treatment

Presented by Member of the Academy N.Kipshidze, May 4, 1998

ABSTRACT. **We have examined heart functional indices of 21 patients with soft and moderate forms of essential hypertension (EH) undergone irregular hypertension treatment. Examinations were carried out by EKG and Dopler echocardiographic methods. It appeared, that on the background of irregular (actually unsystematic) treatment even in case of hypertension effect the final diastole volume of LV doesn't change essentially. Mean indices of left auricle area and right ventricle final diastole diameter increase which is a result of overtension of lesser circle blood vessels.**

Key words: left ventricle, hypertension.

The treatment of essential hypertension (EH) is one of the serious problems of contemporary medicine. It is conditioned not only by wide-spread of the mentioned pathology but also by its specific weight in the general structure of mortality and invalidism.

It is known that well-timed and etiopathogenically justified, differentiated treatment considerably reduces fatal result and improves patients "life rate" [1-3].

The treatment of EH doesn't imply only regulation of arterial pressure. The effect of hypertension treatment should be also taken into account on those structural and hemodynamical disorders which develop on the background of high arterial pressure. Therefore the treatment should take long term, regular character (often throughout the whole life). It should be also noted that today the most "popular" is the so-called irregular symptomatic treatment of arterial hypertension. The patients failed to receive adequate hypertension treatment even in the well developed countries of the world e.g. in the USA (36%), Great Britain (39%), Germany (42%), Russia (72%). No better situation is in Georgia [4-6].

The data of the majority of scientists testify that on the background of irregular hypertension treatment there is not observed any considerable correction of structural and hemmodynamical disorders as a result of arterial hypertension and profilaxis of the so-called target organ disorders. [4] However some scientists consider that during the above treatment the complications caused by arterial hypertension are more frequent as compared to the untreated patients. The main reason of it is a wide fluctuation of day/night arterial pressure. We studied the above indices of a group of patients with EH. The results of examination of those patients who undergone the so-called irregular hypertension treatment are of interest. It should be marked that this group was not specially formed by us. It was formed by itself from those patients, who failed (or cannot) realize the treatment suggested by us and took various hypertension means for a long time, but mainly without any system.

Materials and Methods. Generally there were examined 21 patients with EH treated irregularly, two of them with soft form of disease and 19 patients with moderate form. The

average age was 45.8+3.9. In order to obtain the data of pure forms of EH we didn't examine the patients with: cardiac rythm and conduction disorder, symptoms of coronary pathology, diabetes mellitus and those with II-III stage fatness.

The existence of myocardial hypertrophy of central and intracardiac hemodynamics as well as left ventricle (LV) and quantitative evaluation were carried out on one or two-dimensional echocardiography by standard method using the echoscanner (Aloka S-SD 280, Japan).

A diastole function of LV was evaluated by the Doppler echocardiographic examination in impulse regime. Using Doppler echocardiographic block (UGR-23 Aloka, Japan) we determined the maximum rate of transmital blood flow, rapid filling of LV and left verticle systole phases. By coefficient of these two values ratio E/A we considered LV diastole. On the one hand by h.i.d. exclusion, and on the other hand with the aim to set tolerance in relation to physical tension the patients underwent veloergometric test, stepwise, in sitting position, according to the generally adopted criteria using apparatus Mingograf-34 (Sweden). The group was consisted of patients systematically using adelphane, cloffeline and raunatine as monotherapy or in combination with each other. Therefore the patients of this group don't have the status of nontreated patients because they underwent treatment but nonadequately and insufficiently. The group was formed from the patients examined at least twice (in the first and six month).

Results and Discussion. The Table shows the dynamics of some indices of central and intracardiac hemodynamics on the background of irregular treatment. Despite hypotensive effect in the group in general an increasing tendency of LV miocardiac mass is statistically insignificant.

As a result of irregular treatment LV final diastole volume doesn't change essentially. Mean indices of left auricle area and right ventricle final diastole diameter increase is statistically insignificant. As to the right auricle area its mean value after 6 month increases statistically significantly which might be the result of blood circulation lesser circle overtension. In favoure of the above mentioned is the fact that on the background of irregular treatment both systole and diastole function characteristics statistically significant aggravation was marked which once more proves that all hypertension preparations and different kinds of treatment don't provide the target organ i.e. heart protection on the background of arterial hypertension.

As a result of treatment an increase of minute volume indices which were mainly conditioned by the increase of palpitation frequency because mean indices of beat volume don't change essentially. Despite this as a result of irregular treatment common resistance of peripheric blood vessels increases ($P>0.05$).

Worsening of LV systole and diastole function is associated with the tolerant decrease of patients in relation to physical load. It should be noted that the power of veloergometric load decreases statistically insignificantly but the decrease of mean indices of test duration is statistically significant ($P<0.05$).

During repeated examination on the background of irregular treatment the patients complaint on frequent headache, dizziness, mouth dryness, general weakness and so on. If we also take into account reduction of their working ability we can say that as a result of mentioned way of treatment patients "life quality" didn't improve.

Thus this study demonstrates that long-term irregular but unadequate hypertension

Table

M ± m

Parameters	Before treatment	After treatment
Systematic arterial tension (mm Hg)	179.4±6.2	155.2±4.1*
Diastolic arterial tension (mm Hg)	107.6±5.8	97.5±3.9
Miocardic mass of LV(g)	199.1±10.1	213.8±14.3
Final diastolic volume of LV (ml)	142.1±29.8	137.8±24.6
Minute volume l\min	5.2±0.4	6.1±0.6
Peripheric BV common resistance (dn\cm)	1777±80	1992±76**
Ejection fraction(a\a)	63.9±1.7	58.4±1.6
vcf (c^{-1})	1.4±0.05	1.19±0.03*
E\A (unit)	0.92±0.05	0.84±0.04
Power of veloergometric load (wt)	106.5±12.3	103.1±9.9*
Test duration (sec)	5.11±0.57	3.61±0.39*
Left auricle area (cm^2)	15.8±1.2	17.2±2.6
Right auricle area (cm^2)	14.7±0.6	16.3±0.5*

*- $P < 0.05$
** - $P < 0.01$

treatment of patients with EH soft and moderate forms even if there is a hypertension effect doesn't cause correlation and reserve development of structural and hemodynamic disorders developed due to arterial hypertension and can't provide protection of the target organ heart and perfection of patients "life quality". Therefore it can't satisfy contemporary demands of hypertension treatment.

Scientific-Research Institute of Experimental and
Clinical Therapy, Tbilisi

REFERENCES

1. *N. Burkadze*. Candidate thesis, Tbilisi, 1998 (Georgian)
2. *D.Tsiskarishvili*. Hipertonuli daavadebis mkurnalobis zogierti tanamedrove aspekti. Tbilisi, 1989 (Georgian)
3. *W. Nayler*. J. Cardiovasc. Pharmacol. **26**, Supp.A, 1995, 318-324.
4. *Yu. B. Belousov*. Ter. Arch. **69**, 8, 1997, 73-75
5. *M. Fifer*. J.Heart Failure, **4**, 1, 1997, 143.
6. *H. Feigenbaum*. Echocardiography, 5-th edit. 1994.

საქართველოს მეცნიერებათა აკადემიის მოამბე, 159, №2, 1999
BULLETIN OF THE GEORGIAN ACADEMY OF SCIENCES, 159, №2, 1999

EXPERIMENTAL MEDICINE

A. Abdusamatov

Lipid Peroxidation in Rat Liver Tissue with Heliotrin Poisoning and its Correction with Cobalt Coordinate Compound

Presented by Member of the Academy T.Oniani, December 14, 1998

ABSTRACT. **The process of peroxide oxidant lipids (POL) in rats with heliotrin poisoning was studied. Cobavit, silibor and essentiale were introduced to correct the process of lipid peroxidation disturbances.**

Key words: heliotrin, liver, poisoning, cobavit.

Acute and especially chronic liver diseases of elementary toxic origin can be caused by grain used in food littered with seeds of weeds such as heliotrop fetusfallen which contains hepatotoxic compound called heliotrin [1]. Therefore we think it is important to study the condition of peroxide oxidation of lipids (POL) in rats poisoned with heliotrin and lipids correction with new coordinate cobalt compound: cobavit preparation.

The investigations showed that toxic liver damage hepatotrope poison, heliotrin, in rats of control series tests on the 45^{th} day in the first stage and 75th day in the second stage of experiments provoked the activity of the processes POL and accumulation of toxic products: dien conjugates, malon dialdehyde in liver tissue. Conjugated dien and dienketone content was increasing correspondingly by 107, 170% and 65.2, 38%. Analogous changes were observed in malon dialdehyde, which was increasing by 112.1 and 64.2% against the results of intact series tests (Table).

Increasing of POL processes activities and accumulation of reactive metabolites are straight evidences of heliotrin toxic activity on hepatocytes function and metabolic processes in liver. It is proved by decreasing the activity of two basic enzymes of antioxidative systems: superoxide dismutase and catalase during chronic heliotrin hepatitis [2], as the depression of the activity of these enzymes leads to the formation of singlet oxygen and hydroxile radical with high chemical activity, provoking POL activity intensity and biomembrane damage.

Introduction of the investigated preparations simultaneously with hepatotoxine stopped the increasing POL process activity and accumulation of initial and final POL products in liver tissue. Cobavit had inhibited action on the process of peroxide lipids of biomembrane hepatocytes, decreased the concentration of diene conjugates correspondingly by 58.7 and 66.7%, and malone dialdehyde by 51.2%. While silibor and essentiale decreased the accumulation of initial POL products in liver tissue by 38.2, 37.2 and 26.7, 32.4%, also they decreased malone dialdlehyde level by 34.9 and 40.05% compared with the data from control series tests on animals.

Analogous changes were observed in the treatment series of investigation. Under cobavit influence diene conjugates and malone aldehyde content decreased by 55.8, 41.7 and 27.3%. While treating chronic heliotrin hepatitis with hepatoprotectors silibor and

essentiale POL product level decreased correspondingly by 48.6, 27, 17.4 and 39.3, 20.8, 11.0% against the results of control series tests in animals

Table

Cobavit, silibor and essentiale influence on POL product content in rats' liver tissue during chronic heliotrin poisoning (M±)

Tests Series	N	Conjugated		Malone Dialdehyde nmol/lg tissue
		Diene D on 1 mg lipid	Dienketone D on 1 mg lipid	
Treatment and Profilaxis				
1.Intact (phys.)	6	0.746±0.049	0.209±0.016	33.91±2.1
2.Control, heliotrin in 45 days	6	1.549±0.09	0.565±0.056	71.9±1.5
3.Cobavit	7	0.624±0.039	0.188±0.009	35.1±1.7
4.Silibor	6	1.121±0.053	0.355±0.03	46.8±2.2
5.Essentiale	6	1.135±0.049	0.382±0.027	43.1±1.1
Treatment				
1.Intact (phys.)	6	0.564±0.054	0.231±0.028	51.3±2.1
2.Control heliotrin in 45 days	6	0.932±0.056	0.374±0.026	84.6±3.0
3.Cobavit	6	0.412±0.026	0.218±0.017	61.5±0.45
4.Silibor	6	0.479±0.02	0.273±0.017	69.9±2.4
5.Essentiale	6	0.566±0.03	0.296±0.002	75.3±1.9

The obtained results testify that new cobalt coordinate compound cobavit, used to correct POL processes disorder, has evident antioxidant activity and thus prevails over such known hepatoprotectors as silibor and essentiale.

The effect of preparation probably is connected with potentiality of bioactive ligand activity, glutamine acid and methylmethioninsulphonic chloride with cobalt, as these ligands are antioxidants of not direct activity and they are glutathion precursors. Most possibly these compounds increase glutathion system activity, which is important for protection of the cell from peroxide.

From the above said we can prove an extraordinary important role of functional POL processes and system of antioxidant hepatocytes control in the genesis of pathobiochemical changes during chemical liver damage. The problem of correction of hepatocyte metabolic function disturbance must be considered taking into account the above mentioned investigations.

Tashkent Pediatric Medical Institute
Republic of Uzbekistan

REFERENCES

1. *N. Abdulaev, R. Azimov, T. Makhamedov et al.*, Elementarno-toksicheskie porazhenia pecheni. Tashkent, Meditsina, 1978.

2. *Z. Khakimov, E. Zueva, A. Rakhmanov.* Reports AN Ruz. 10, 1990, 56-57.

საქართველოს მეცნიერებათა აკადემიის მოამბე, 159, №2, 1999
BULLETIN OF THE GEORGIAN ACADEMY OF SCIENCES, 159, №2, 1999

PALAEOBIOLOGY

Member of the Academy L. Gabunia, E. Gabashvili, A. Vekua, D. Lordkipanidze

The Taxonomic Position of *Udabnopithecus garedziensis* Burtsh. *et* Gabash. (Udabno Georgia) and its Geological Age

Presented February 22, 1998

ABSTRACT. **A new view on Late Miocene Hominoid *Udabnopithecus garedziensis* Burtsh. et Gabash. from Udabno(East Georgia) as discussed. The maxilla fragment of *Udabnopithecus* in size and general morphological features closely resembles the hominoid genus *Dryopithecus*. The particular morphological traits of the *Udabnopithecus* with relatively late stratigraphic and isolated geographic position in the Trans-Caucasus region may afford a separate taxonomic classification of *Dryopithecus garedziensis*.If our estimate of age (8-8,5 million years) is correct *Dryopithecus garedziensis* appears to be one of the youngest known *Dryopithecines* in Eurasia.**

Key words: Late Miocene, Udabno, hominoid, *Dryopithecus.*

In 1939 N.O. Burtshak-Abramovitch and E.G. Gabashvili in Garedja desert (Udabno, Gare-Kakheti, East Georgia) in Late Miocene sediments discovered remains of a hominoid-like ape, considered as a new taxon: *Udabnopithecus garedziensis* [1,2].

The *Udabnopithecus* is represented by the right P4 and M1 imbedded in a maxilla fragment (Figs a, b).During the extraction of the maxilla fragment the P4 has been detached.

The P4 is oval shaped, rather squeezed in on its medial and distal sides. Its labial facet is shorter than the lingual one, while the dorsal surface is less convex than the ventral one. The paracone is slightly higher and sharper than the protocone. These two coni are separated by a central groove, which joins the fovea *posterior* and they are connected by a transversal medial crest, coming down from the top of the paracone. The

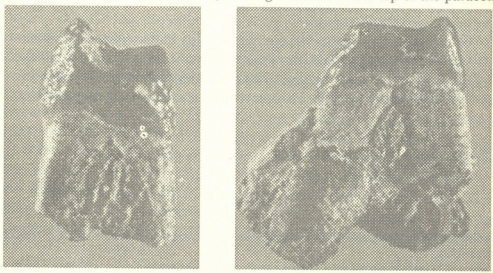

a. b.

Fig. 1. *Dropithecus garedziensis* Burtsh. et Gabashv. (Udabno, Georgia). a. P^4(dex.); b. M^1(dex.).

protocone comprises the larger part of the occlusal surface of the tooth and is more eroded than the paracone. The *fovea* anterior is located at the medial edge of the tooth, bordering with the medial crest coming down from the top of the paracone in the lingual direction. The *fovea posterior* is quite deep, situated at the distal edge of the crown and continues, transversely up to the middle of the occlusal surface. There is a small ridge coming down from the top of the paracone, in the distal-lingual direction, which joins the *fovea posterior*. On the labial surface of the crown, though it is quite eroded, a slight convexity of its middle part could be observed, flattening out and widening down towards the base of the crown. Slight side grooves can be observed, the distal one deeper than the medial one. Both of them blur out towards the base of the crown. The protocone has three occlusal surfaces: a frontal one inclined towards the medial edge, a central and a dorsal one, inclined slightly towards the distal side. The layer rather thin which is evidenced by the clearly observed dentine patch in the central facet of the protocone of this only slightly eroded tooth. At the base of the convex lingual surface of the tooth, there is a barely observed "neck" or swelling of a kind. On the distal side of the tooth there is a large, clearly outlined facet of attrition with M1, while on the medial side there is a smaller and less observed one of the contact with P3. The dimensions (in mm) of the tooth are: maximum length of the crown – 6.5, maximum width – 10.1, and the height of the slightly eroded crown – 7.3.

The M1 has a squarish appearance (its occlusal surface is of a rhomboid shape). The paracone and metacone are located at the very edge of the crown, while the labial crest connecting them is quite deeply cut in the middle, its deepest point being still quite high above the central fossa of the trigonide. The labial coni are nearly of the same height (the paracone is only slightly larger than the metacone and slightly smaller than the protocone). Well discernable crests bind the tops of this coni with the protocone, which, though only lightly eroded, shows a clear dentine exposure. A similar dentine exposure, though of smaller dimensions is seen on the surface of the hypocone. The latter, though of the same height as the protocone, is smaller. It is almost isolated from any occlusal contacts though a very thin line of attrition connects it with the distal-lingual edge of the protocone. The *trigone fossa* is divided by quite a deep transversal line, continuing along the labial wall of the crown, where it touches upon the longitudinal notch which delineate the attrition facets along the external edges. In the central part of the trigonide is a weakly developed longitudinal notch, separating the labial convexities from the protocone. The *fossa anterior*, which can be traced in the labial part of the tooth, is narrow and is situated between the medial part of the crown and the transversal crest which connects the paracone with the protocone. The fovea posterior is quite deep, delineated in the front by the lingual crest of the metacone and at the back by the distal edge of the crown. An obliquely located notch, in the fovea posterior, constitutes the lingual border of the hypocone, approached, from the medial-labial side, by a slightly observed transversal swelling (apparently a remnant of the eroded labial crest of the hypocone). Relatively narrow transversal facets of attrition are clearly noticeable on the distal and medial edges of the occlusal surface, as well as along the crest connecting the metacone with the protocone. The attrition surfaces of the protocone and the hypocone are quite horizontal. The labial surface of the crown bears two weak vertical convexities, matching the paracone and metacone. At the base of the lingual side of the crown a very weak cingulum could be observed.

The dimensions of the tooth (in mm) are: maximum length of the crown – 9, maximum width – 10.7 and the height of the slightly eroded crown – 6.

The Hipparion dominated fauna of Udabno was found ca. 70 km north-east Tbilisi in a dry valley between the mountains of Dodo (to the north-east) and Udabno (to the south-east). Here, not far from the old monastery of David Garedji of the VI century A.D. solid fossilized sand formations are gradually replaced by clayey-sandy sediments containing Middle Sarmatian mollusk fauna, followed by very thick (more than 400 m) sediments of continental origin, interspersed by colorful clay layers with inclusions of sand dunes and conglomerates. All along the section of the colorful continental layers (containing the Shiraq fauna) in various stratigraphic locations one can find vertebrae bones, but the richest deposits are to be found mainly in two horizons ca. 110 m below the basis of the Shiraq complex (Udabno I) and ca. 40-50 m beneath the contact of this complex with the continental layers below (Udabno II).

The Udabno I faunal assemblage comprises *Deinotherium giganteum, Tetralophodon cf. longirostris, Miohyaenotherium bessarabicum (=Ictiterium hipparionum var. garedziensis), Plesiogulo cf. brachygnathus, Adrocuta eximia, Hipparion garedzicum, Aceratherium cf. incisivum, Chalicotheriidae cf. Ancylotherium, Microstonyx erimanthius, Giraffidae cf. Samotherium, Cervidae gen., Tragocerus sp., Gazella sp.* and other [1,3-6] The maxillary fragment of the *Udabnopithecus garedziensis* [6] was recovered ca. 40 m above this first bone-bearing horizon. Close-by to the maxillary fragment a skull fragment of *Deinotherium giganteum* was recovered.

The fauna of Udabno II differs little in its context from its preceeding complex of Udabno I. Besides the species mentioned earlier this complex comprises also *Hyaenotherium magnum, Udabnocerus georgicus,. Hipparion cf.garedzicum* and a very small variety of a bovine.

The *H. cf.garedzicum* from this upper level of Udabno seems to be more advanced than the typical species, as judging by its metapodial proportions it is very close to the group of *H. moldavicum-mediterraneum*.

It seems that the faunal complexes of Udabno I and Udabno II, even though quite similar, reflect two consecutive stages of the evolutionary sequence of the Hipparion fauna in Georgia. In general they portray more or less analogous natural surroundings, characterized by moderately lush forest biotopes interlaced with relatively more open settings.

According to the faunal composition of the two assemblages: Udabno I and Udabno II, both of them could be assigned, especially the latter, to the Lower Turolian) or MN 11, which is also supported by their differences from the more archaic faunal complex of Eldari [3, 7-9]. This faunal complex is found in the Upper Sarmatian marine sediments of eastern Georgia correlated with the Upper Valesian (MN 10). This observation is not contradictory to the finds from the paleomagnetism studies [7], according to which Udabno I dates to an intermediate period which binds a normal to reversed polarity chrons. Udabno II is attributed to a reversed chron, identified with stage 8 in the paleomagnetic stratigraphic sequence of the Eastern Paratetic or the lower part of stage C4 of the European paleomagnetic stratigraphic sequence [10]Eventhough the lower part of the reversed magnetic stage 8 is correlated with the Upper Sarmatian [7], it is impossible at present to pinpoint the exact paleomagnetic boundary between the Sarmatian and the Meotic era. Thus we are obliged to rely on the Hipparion fauna which relates the Udabno I fauna to the most Upper Sarmatian or Lower Meotic, while the fauna of Udabno II is identified as Lower Meotic.

Thus the *Udabnopithecus garedziensis* should be dated to the Upper Sarmatian or Lower

Meotic, which correlates with the Lower Turolyan (MN 11) of the continental Neogene sequence.

First we have to exclude the possibility of associating *Udabnopithecus* with the earlier sub-family of the *Kenyapithecini* [8] from whom it differs, especially if compared with their Middle Miocene representatives, the Pashalarian *Dryopithecinae* [11] in its smaller dimensions, the small cingulum and the thinner enamel. It is quite obvious that the *Udabnopithecus* is closer to another sub-family of the *Dryopithecinae*, namely to the *Dryopithecini*, which comprises *D. fontani, D. laietanus, D. carinthiacus* and *D. crusafonti* [8]. Unfortunately, since there are only the two teeth to compare to, it is difficult to determine which of the above is closest to the *Udabnopithecus*. As said before, some authors indeed identify the latter with *D. fontani* [12,13] but there is not enough evidence to bear this out. The *Udabnopithecus* is as similar to *D. fontani* as to *D. laiteanus* or *D. carinthiacus* while at the same time showing some particularities which are not present in all three of them.

The *Udabnopithecus* differs from *D. fontani* [8,12,13] in the significant reduction of the cingulum, a somewhat different shape of the teeth crowns, the total absence of anamel hypoplasia and some minor differences in the location and developments of the P4 and M1 coni.

It differs from *D. carianthiacus* from Rudabani [8,14,15] in the relatively reduced length of the lingual part of the P4, the rhomboid shape of the M1 crown, the more labial position of the para- and metacone of M1, the traces of a 'neck' , the somewhat smaller dimensions and possibly higher crowns of the cheek teeth. The difference between the *Udabnopithecus* and *D. laiteanus* from Can Lobaterus [16,17] is that in the latter, the hypocone is nearly the larger of the molar cones, the protocone is well defined and there is no cingulum to speak of. Besides, the teeth of this Spanish Dryopithecus show high anamel hypoplasia, they are larger and most probably relatively longer than those of the Ubadno *Dryopithecus* M1 are. It is difficult to compare between the Udabnopithecus and the Valesian *D. crusafonti* from Can Ponsic [17] since only mandibular molars represent the latter. Yet judging by the relatively long and narrow P4 [16,18] and the relatively large dimensions of the mandibular molars, it seems that the *Udabnopithecus* differs also from this hominoid.

The particular morphological traits of the *Udabnopithecus* compiled with its relatively late stratigraphic context and isolated geographic position in the Trans-Caucasus region may indeed afford it a separate taxonomic classification. Thus it is prudent, till more data accumulates, to reserve judgment and classify it as before, namely *Dryopithecus garedziensis* Burtshak & Gabashvili It is not just one of the latest Dryopithecinae but also one of the smallest variants of this family, characterized by a remarkable reduction of the cingulum in the cheek teeth (slight traces of a neck on the lingual surface of P4 and M1) as well as the smaller differences which were detailed above .

We would like to thank Prof. Anna Belfer-Cohen for her help in editing the manuscript.

Georgian Academy of Sciences
L. Davitashvili Institute of Palaeobiology

REFERENCES

1.*N. O. Burtschak-Abramovitsch, E. G. Gabashvili*, - Soobshenia . AN. Gruzii, **6** , 1945, 458-464 (Russian).
2.*N. O. Burtschak-Abramovitsch, E. G. Gabashvili*. Priroda, **9**, 1950, 70-72 (Russia).

3. *L. K. Gabunia.* K istorii Gipparionov.Moskva, 1959, 570 (Russia).
4. *E. G. Gabashvili.* Vestnik Geologicheskogo obshchestva, 1970, **1**, I-2,88-99 (Russia).
5. *G. K. Meladze.* Obzor gipparionovoi fauni Kavkaza.Tbilisi, 1985, 1-168 (Russia).
6. *G. Tsiskarishvili.* Pozdnetretichnie nosorogi Kavkaza. Tbilisi, 1987, 1- 142 (Russia).
7. *E. L. Vangengeim, L. Gabunia, et al.* Izv. AN SSSR, Ser. Geolog. **8**, 1989, 70-77 (Russia).
8. *P. Andrews, T. Harrison, et al.* In (Bernor R.L.Fahlbusch V. Mittman H-V.Ed) The Evolution of Western Eurasian Neogene Mammal Faunas. 1996, 169-207.
9. *L. K. Gabunia.* Traits essentiels de l'evolution des faunes de Mammiferes de la region mer Noire-Caspienne. XXVI Congress geol. Paris. 1980, 195-204.
10. S. *Sen.* Paleogeography. Paleoeclimatology. Paleoecology. **133,** 1997, 181-204.
11. *B. Alpagut, P. Andrews, L. Martin.* J. Hum. Evol., **19** , 1990, 399-422.
12. *E. L. Simons, D. R. Pilbeam.* Folia Primatologia. **3**, 1965, 81-152.
13. *F. Szalay, E. Delson.* Evolutionary History of the Primates. Acad.Press.London. 1979, 580.
14. *M. Kretzoi.* Nature. **257**, 1975, 578-581.
15. *D. Begun.* Amer.J.Phys.Anthropology, **87**, 1992, 291-309.
16. *D. Begun, S. Moya-Sola, M. Kohler.* J. Hum. Evol., **19**, 1990, 255-268.
17. *S. Moya-Sola, M. Kohler.* J. Hum. Evol., **29**, 1995, 101-139.

საქართველოს მეცნიერებათა აკადემიის მოამბე, 159, №2, 1999
BULLETIN OF THE GEORGIAN ACADEMY OF SCIENCES, 159, №2, 1999

M. Rusieshvili

Is a Proverb Performative?

Presented by Corr. Member of the Academy M. Andronikashvili, April 27, 1998

ABSTRACT. **The author proposes that the main pragmatic function of a proverb is constative. Other functions such as performative are derived, and actualized in a context.**

Key words: constative, performative, proverb, pragmatics, function.

Having got acquainted with the scientific studies on the subject we agree with the existing viewpoint that while studying the pragmatic effect of an utterance on the interlocutor great attention is paid to the general types of utterances. Their concrete realizations in concrete communicative situations remain beyond the focus of the scientists' attention [1, 2].

By the term "pragmatic effect" we mean the classification of concrete perlocutionary functions of a proverb, the study of its illocutionary force and pragmatic purpose, dependence of the perlocution on linguistic and extralinguistic factors, etc.

A proverb states some wisdom, general truth, consequently, its illocutionary force. Its function is the statement and therefore a proverb will be constative, e. g., "one scabby sheep will mar a whole flock".

A proverb is an utterance characterised by general reference. Thus its meaning is independent of a context. But during its actualization in a situation / context all the levels of its semantic structure are realized. [3]

The study of a problem has revealed that besides the main function of a proverb - being constative, in the context it may obtain other perlocutionary functions. One and the same proverb "Tkuils mokle pexebi akvs" meaning in Georgian a lie has short legs maybe directive, menacive, it may have the function of warning against smth or *post factum* advice, summing up, conclusion, etc. Consequently, besides being constative a proverb may become performative e.g., "make hay while the sun shines".

We propose that neither of the above-mentioned functions, except that of constative, may go into a general pragmasemantic model of a proverb. This statement also refers to the function of performative as one of its distinctive features, consequently, all the functions except that of constative are derived and can be gained by a proverb in a concrete situation/ context. The performative function as well as any other derived, contextual function, comes from the semantics of a proverb and depends on what a speaker really implies. In a context a proverb "make hay while the sun shines" may be constative, a constative-performative, *post factum* advice, conclusion or summing up if "the sun has been set and the hay hasn't been made yet".

A proverb used in the performative function is different from other performatives. A proverb used as performative has *post factum* whereas other performatives have not;

"come here" or "go away" are direct performatives, but one can't use them, or, in other words, one can't address a person in this way if he has already come or gone away. But in the case of the proverb used as performative this is possible.

Besides the above-mentioned, any constative fact may become an implicit performative. "It's hot here" may become performative if someone opens the window, and on the contrary, such "rude" imperative as "get out" may not become performative if the interlocutor doesn't obey this command.

We can conclude that in spite of the fact that a proverb may become performative in the context, being generally, not performative.

Tbilisi I. Javakhishvili State University

REFERENCES

1. *E. B. Paducheva.* Vyskazyvanie I ego sootnesennost s deistvitelnostyu. M., 1980 (Russian).
2. *M. S. Vegenkova.* Progmatika i tipologya kommunikativnykh edinits yazika. Dnepropetrovsk, 1989 (Russian).
3. *M. Rusieshvili.* IV sci. conf. of B. Jorbenadze society. Tb., 1997 (Georgian).

საქართველოს მეცნიერებათა აკადემიის მოამბე, 159, №2, 1999
BULLETIN OF THE GEORGIAN ACADEMY OF SCIENCES, 159, №2, 1999

LINGUISTICS

T. Sikharulidze

Levels of Bilingualism

Presented by Member of the Academy K. Lomtatidze, December 30, 1998

ABSTRACT. **The dynamics of interrelations of full and partial forms of bilingualism, (in connection with language communities) depending on linguistic and extralinguistic character is considered in the article.**

Key words: bilingualism

Two forms of bilingualism are usually distinguished: 1) full form, when the knowledge of two languages is practically the same and 2) partial form, when the knowledge of the nondominated language prevails over the dominated one. It should be noted, however, that absolutely full form is meant only in that case, when two idioms, composing bilingual pair can be equally used in all the spheres of communication (e.g., Georgian - Russian, etc.). In the other cases when one of the languages is not used in any of the spheres (e. g., when one of the languages has no writing), the "fullness" of the bilingualism will bear relative character.

The relations between lingual societies can be changed depending 1) on the linguistic factors, such as developing writing and therminosystems for the language, and 2) extralinguistic factors, connected with the status of the language (official or factual) and the position of the people speaking that language.

However knowledge of one of the languages, composing the linguistic pair, may be constantly decreasing, if there is a tendency to the language shift. This tendency is clearly revealed on Udin language, which might disappear in furture if the situation doesn't change. Due to historical conditions partially Vartashen Udins moved from Azerbaijan to Georgian religion, which seriously weakened the position of the Udin language. The compactness of the settlement in the historic country land was broken while muslims following endogamous marriages favoured the development of the language in Azerbaijan. Georgians and Udins are diophysites. They both profess orthodox and their marriages are not exceptions moreover it's the norm. This circumstance solved the fortune of the Udin language, as these families are oriented on more perspective and prestige Georgian language. In 1934 Jeirany Fedor and Jeirany Michail Udins by origin, published Udin ABC Book in Georgia. The eight-year Udin language school was opened. But there was not any opportunity to get further education in the Udin language, which made Udin school to be changed into Georgian.

In 1998 the socio-linguistic test was carried out at the philological departament of the Tbilisi I. Javakhishvili State University.

It revealed the direct and regular connection between the language of education in school and its identification as the native language.

It was shown that the connection between the nationality and native language may

be considered insignificant (relative).

The education languages for Udins both in Azerbaijan and in Georgia are not native. In Azerbaijan it is Russian and in Georgia - it is Georgian. In both cases the second component of the bilingual pair (for written Russian and Georgian languages) is nonwritten Udin language. So the sphere of its application as limited within the family and the knowledge of it depends on the age: older generation knows Udin well, middle - aged know their native language quite well, school children don't know the language.

Many little ethnic groups have the same problem. Due to their minority and dispersion settlement they have no opportunity to study on their own language and accepted the languages of big nations.

Analogous situation exists in Georgia, where Udin people left their writing designed for them on the basis of Latin graphic in 1934, in favour of the perspective Georgian language.

Tbilisi I. Javakhishvili State University

საქართველოს მეცნიერებათა აკადემიის მოამბე, 159, №2, 1999
BULLETIN OF THE GEORGIAN ACADEMY OF SCIENCES, 159, №2, 1999

E. Abuladze

Some Cases of Sound Appearance and Reduction in Anton Purtseladze's Prose

Presented by Corr. Member of the Academy G.Topuria, July 27, 1998

ABSTRACT. **The paper discusses phonetic peculiarities of Anton Purtseladze's literary works. Appearance and reduction of vowels as well as consonants are studied.**

Key words. Anton Purtseladze, Georgian dialects.

Anton Purtseladze together with the other progressive writers of the epoch stood for critical realism. The source of his language is Kartlian dialect. We have studied the cases of sound appearance and reduction in A. Purtseladze's literary works.

Consonant reduction. In the speech of A. Purtseladze's personages reduction of some consonants takes place. The consonants *g* and *m, v, n, r, s, sh* are reduced in different cases.

The ending *m* is reduced together with *g* in the conjunction *magram*. This phenomenon is characteristic of Imeretian and Gurian dialects. A.Purtseladze puts the words into the Megrelian personages' mouth, which are peculiar to the dialects of West Georgia [1, p.55]: "*ki, ma(g)ram(m), tu magre satanǯvelad kristian ḳacs geimetebdi, ar megona*" [2, p.74].

d as the marker of the instrumental case is reduced: "*tanabrad cdiloben magra(d) eċirot boyċis naskvebi* [3, p.26].

v is reduced:

1) when it is the prefix of the first subjective person and the verb begins with *v* or *u*. It is peculiar to Kartlian and Kakhetian as well as to all the dialects of East Georgia. In A.Purtseladze's works this phenomenon is noticed in personage's speech and in the author's words as well.

"*sixarulisagan kinaγam orives* ***miv(v)ardi*** *saḳocnelada*" [4, p.57];

"*bolo* ***mo(v)uγot*** *bnelsao*" [5, p.129];

2) in front of *o* (in personage's speech):

"*isa da totoγa ertad unda* ***iċ(v)odnen*** [6, p.63];

3) between the vowels:

"*mtrisa xelita sikvdils* ***rče(v)oben***" [7, p.30];

4) in the vicinity of *d* (in the author's speech):

"*imat ǯarebsa emateboda Kartveli ǯari, mtris šeḳ(v)domas danatrebuli*" [8, p.8];

5) in the interjection *neṭa*(*v*) (in personages' speech):

"***neṭa***(*v*) *kveqnistvis rasa hpikroben*" [6, p.21].

6) in the pronoun *tviton* (himself/herself):

"*daekorcinos mas, vinc* ***t(v)iton*** *miaẖnia tavis γirsad*" [9, p.13].

m is reduced:

1) when it is followed by another consonant:

"*ertad gvixilavt ʒmurebr* ***(m)ḳvdrebada***" [6, p.16];

2) at the end of the particles and conjunctions. Generally at the end of the word it becomes voiceless.

"***ro(m)*** *ɕamosuliqav, imistana alagebši šegiqvandi, sadaca ɣirs šesvlata*" [4, p.29];

"*me xo(m) unda imas ert tumanši txutmeṭi maneti mivce*" [2, p.384]

Similar examples cannot be found in the author's words.

n is reduced within the stem of the noun (in the personages' speech):

"*pašasagan* ***pirma(n)s*** *miiɣeb*" [2, p.514].

r is reduced in *brʒ, grʒ, zrd, prt* complexes:

1) between *b* and *ʒ* consonants. We suppose that just these consonants make favourable conditions for its reduction.

"*gicnob, ra švili* ***b(r)ʒandebi***" [3, p.13];

2) when *grʒ* appear together (in the personages' speech):

"*naxe, rogor ena* ***ɕaig(r)ʒela***" [2, p.317];

3) in *zrd* complex:

"*šenma* ***gaz(r)dam****, didi bednierebа geɕia*" [3, p.33];

4) in the word *ḳargi* together with the consonant *g*:

"*titko ʒaan* ***ḳa(rg)i*** *gulis ḳacia*" [4, p.56].

s is reduced:

1) in the dative case if noun with the consonant at the end of the stem is the object preceding the predicate: (Analogous examples cannot be found in the author's words);

"*mis xorcsa sɕamda,* ***sisxl(s)*** *hsvamda*" [10, p.39]

2) at the end of the determinant in the accusative case standing before the determining word (in personages' speech):

"*ra mṭeri gaumagrdebis, ʒesa* ***ṗiṭali(s)*** *klḍisasa*" [10, p.48];

3) in composites and words formed by suffixes:

"*vamɣerebinebt* ***ḳai(s)*** ***ʒilisirebs***" [2, p.86];

"*ortav šveneba kartlisa da imeretisa* ***ma(s)ši*** *saocrad ertad iqo šexamebuli*" [7, p.31];

4) when it is the marker of the 3rd subjective person:

"*bedi kalsa* ***hgav(s)*** *ḳapassa*" [11, p.39];

5) in demonstrative pronouns *es* and *is,* used as attributes. After reduction we have *e* and *i* (in personages' speech):

"*šemʒagda* ***e(s)*** *chveni sicocxhle*" [6, p.50].

"*ager hmɣeris ḳidev* ***i(s)*** *zemota mezobeli*" [6, p.81].

š(sh) is reduced in the affirmative particle *maš* (in the personages' speech):

"***ma(š)*** *ras izam rom ar irazboiniḳeb*" [6, p.22].

As it is noted in scientific literature, reduction of *s* is characteristic of Kartlian and Kakhetian as well as of all the Georgian dialects.

Vowel reduction. When the ending vowel meets the initial vowel of another word the vowel elision takes place. It is characteristic of personage's speech. In *ai* demonstrative particle *i* vowel is reduced and *a* joins demonstrative pronouns *im, is* and take the form *aim* and *ais.*

"*ho! Ager* ***aisa****! – tkven ras icnobt*?" [4, p.111].

Analogous cases can be found in the author's words:

"*šehxede aba* ***a(i)im*** *virs, ...* " [5, p.130].

Sound appearance is peculiar to Kartlian and Kakhetian as well as to other dialects. Sonorous sounds such as *v, m, n, r* appear in various cases.

v appears:

1) in Kartvelian languages and their dialects because of soft rise before the vowels in anlaut [12, p.168].

"*mtla* ***voxeri*** *qopilxart*" [6, p.22];

"*akamdis mas marǯve dro ar elevoda*" [7, p.16];

2) in front of *u*. It is peculiar to Megrelian and Imeretian personages:

"***vubeduri*** *maci kai iqo, mara...*" [2, p.63];

3) between the vowels. Supposedly it appears to part the vowels [13, p.64]

"*dγes gamxdarxar čemni* ***uaxlovesni*** *pirni*" [14, p.3];

4) in front of sonorous *n* (in the author's words):

"*didis codvnit daarγvies mat ertoba*" [5, p.90].

m appears:

1) in front of a voiceless consonant *č* (in personages' speech):

"*sacodavi viγac ǯalian* ***mčlekianiа***" [4, p.10]

2) before z (in personages' speech as well as in author's words):

"*... mašac unda ċaeqvana* ***samzγvars*** *gareta*" [4, p.61].

3) in front of uvular *k* and *γ*:

"*ganaxlda msaxureba* ***mγvtisa***" [14, p.27];

"*xviṭia aris cudi sakmeebis* ***momkmedi***" [2, p.154].

r appears:

1) before *d* and *s* consonants (in the author's speech):

"*amastan es* ***šeardgenda*** *ubralo peškašsac*" [2, p.75].

"*mtasa vakeši udgia tavis* ***persvi*** *da ǯiria*" [11, p.44].

2) before the sonorous consonant *m* (in the authors words):

"*ikidam amogvakvs amati uḳetesi* ***šermadgeneli*** *naċilebi*" [5, p.18].

3) before *t* and *c* (in personages' as well as author's words):

"*daṭrialda xalxši azri bunebis gareše mqops* ***samγvrto*** *ǯalazeđ*" [3, p.18].

"*čven* ***gvrċams*** *nabukodonosor...*" [14, p.34].

Gori Economical-Humanitarian Institute

REFERENCES

1. *V. Sergia.* Kartvel khalkhosan mtseralta enis taviseburebani. Tbilisi, 1970 (Georgian).
2. *A. Purtseladze.* Rcheuli natserebi. Tbilisi, 1963 (Georgian).
3. *A. Purtseladze.* Vai martalta. Tbilisi, 1881 (Georgian).
4. *A. Purtseladze.* Samis tavgadasavali. Tbilisi, 1889 (Georgian).
5. *A. Purtseladze.* Leksebi. Tbilisi, 1897 (Georgian).
6. *A. Purtseladze.* Avazakni. Tfilisi, 1891 (Georgian).
7. *A. Purtseladze.* Rcheuli tkhzulebani. Tbilisi, 1940 (Georgian).
8. *A. Purtseladze.* Tamar Gazneli. Tbilisi, 1901 (Georgian).
9. *A. Purtseladze.* Tsiskara. Tfilisi, 1899 (Georgian).
10. *A. Purtseladze.* Davit Aslanishvili-Dzhandieri. Tfilisi, 1888 (Georgian).
11. *A. Purtseladze.* Tskaloba. Axalsenaki, 1894 (Georgian).
12. *Iv. Kavtaradze.* Kartuli enis istoriisatvis, XII-XVIII ss. Tbilisi, 1954 (Georgian).
13. *Ar. Martirosovi, Gr.Imnaishvili.* Kartuli enis kakhuri dialekti. Tbilisi, 1956 (Georgian).
14. *A. Purtseladze.* Asuli israelisa. Tfilisi, 1900 (Georgian).

საქართველოს მეცნიერებათა აკადემიის მოამბე, 159, №2, 1999
BULLETIN OF THE GEORGIAN ACADEMY OF SCIENCES, 159, №2, 1999

PHILOLOGY

N. Ratiani

The Function of the Tree in the Ritual of Blood Sacrifice

Presented by Corr. Member of the Academy R. Gordeziani, April 27, 1999

ABSTRACT. **All lives belong to God. It comes from him and to him it returns, and when he wants it he takes it. But it differs otherwise from true sacrifice where man makes an offer of his own accord. Since in most sacrifices men eat the carcass of the victim, what is God supposed to receive? We hypothesize that burning of the victim was an important and necessary part in the rituals of blood sacrifice.**

Key words: blood sacrifice, burning of the victim, sacrificial barrel, tree of life.

The act of burning of the victim during the ritual of blood sacrifice should be payed special attention. In our opinion one of the intentions of this act may be connected with smoke. Smoke would reach Him whom the victim is aimed for. The idea about smoke that reaches God in the heaven, as met in some African legends, where God breaths in the smoke of the burnt victim with pleasure.

Smoke of the burnt victim is often mentioned in Homer's poems (A, 315-317).

We think that the barrel of smoke of the burnt victim is the analogy of the tree of life. It represents one of the modifications of the axis of the world, which connects and unites three zones of the mythological world. The tree of life itself reflects all the main elements and parametres of the cosmic construction. It is symbolic image of the world with its three parts and its construction on the vertical. The parts of the tree: the roots, the trunk and the top fit the underworld, the middle and the upper worlds. Many mythological systems display the relations between these three worlds by the tree. From the old times the world structure is reflected in several parts: the surface of the earth is the middle part, there is the lower world in the depth of the earth with permanent darkness, and the sky with its stars and luminary is the upper world. All these three parts in spite of the distance and incompatibility are given in a complex way. Shaman has connection with all the three parts, but lives, multiplies only in the middle world. But can he reach contact with the other worlds?

Often a tree is represented in the role of the way. Sternberg L. notices that in Tungusian the name of the Shaman tree is Turu, what means the way by which Shaman and his prayers reach the sky. Close to this opinion stands the Sintoistic gate of Japanese. Koreans practised a rule of building gates in front of which Shaman was praying for deads. In the Korean language the word *Toro* also means "a way". So in the role of the way we have a gate or a tree by which a man comes in contact with the other worlds. Sometimes this world is the upper world, sometimes it is the lower world.

In the role of the way besides the tree we also have other elements. For example, in Georgian dancing ballads "Goddess Dali Labours in the Rocks", "Betkili", "Hunter Chorla", "White Manguri" with their variations declare in one voice, that goddess Dali

living among inaccessible rocks has golden hair. She often lowers down her tail of hair and picks up her son Amirani. The rock is near the sky; Amirani is taken from the earth, so in the role of the way we have a tail of hair.

As we have already noticed, the barrel of smoke of the burnt victim is analogy of the tree, so it may be met in the role of the way. For example, this function of the smoke is given in the Old Testament. Also smoke of the fire of Agni and even Agni is compared with the sacrificial barrel and all the marks of the victim pass on the barrel. Localization of the victim is in the centre of the world, in the place, where the humans world is united with the God's world. A victim as a sacrificial barrel unites the parts of the world. It is considerable that the invocation to the sacrificial barrel is the same as to the tree, its mythological analogy: "Oh, tree, you know the names (nature) of the Gods, you lead victim..." (V, 5-10, Rigveda) or invocation to Agni as a connector of the worlds: "I want to praise Agni, which connected two worlds passing the space..." (X, 88-3); "Here he goes to finish his work, knowing his way as well".

So, Agni is a victim, barrel, tree – the center of the world. This important mythological complex was noticed by Ogibenin B. in his "Structure of the mythological texts of Rigveda". It is interesting to compare Agni with an altar, as localization of the altar in the cosmogonic scheme is identical of the localization of the victim. Often sacrificial fire and tree can replace themselves. In the scientific literature there is a hypotheses that (according to Homer`s hymn) Apollo while changing his cows with Lire of Hermes, takes the function of Hermes (owning the sacrificial altar) on himself. The Greek words Herm and Hermes, according to Hocart A., have the same ethymology. So In Delphi the tree becomes the center instead of the fire. Oracle is sitting in the center of the world and she has a leaf of laurel in her mouth. Laurel is a tree of Apollo; otherwise laurel is a tree of life. The leaf in the mouth of Pythia is a sign of belonging of oracle`s to the vertical of the world. Also she is Apollo's oracle, Apollo typologically is identical to Odin with his functions in the mythological world. Odin reaches the highest wisdom after assimilating with the sacred axis of the world. This axis is the carrier of the wisdom. He becomes the God of the center of the world and takes his place in the pantheon undertaking the sacral function. As known, the burning of the victim was not aimed only for the heavenly god but for deads` world too. Thus the idea that sacrificial smoke`s barrel is an analogy of the tree is proved. A tree has a root, which connects the under world with two other worlds. But smoke (as a barrel) is not the only thing, that can reach the under world. The act of burning of the victim should imply something else, what would please Him to whom it is done more (there is no difference who he is: god or soul; where he lives: in the heaven or anywhere else). We should mention the following: before burning, the victim is to be skinned. Skin was not edible, but it had many other uses in living habits . From Iliad we know that skin replaced money. Skin was used to make dresses. Skin was used as a cover on the chairs and beds for honourable guests. Therefore, we hypothesize, that skinning was a necessary moment in the ritual of sacrifice, as the skin has fur, hair or feather , which according to the ancient peoples` beliefs had power. After burning of a victim he for whom the sacrifice is made acquires the living force.

We conclude that burning of the victim was important and necessary act for the following moments:

1) it gave the possibility to the liberation of power;
2) it gave the vertical, which connected three parts of the world, symbolizing the center of the world.

Tbilisi I. Javakhishvili State University

REFERENCES

1. Bible, Tbilisi, 1989.
2. *M. Chikovani.* Identical Structural Components, Georgian 'Folklore, XIV, Tbilisi, 1984.
3. *Ch. A., Clark.* Religions of Old Korea, N. Y., 1932.
4. *E. E. Evans-Pritchard.* Nuer Religion Oxford University Press, 1956.
5. *Y. V. Ionova.* The Cult of the Trees In Korea, Moscow, 1986.
6. Homer, Iliad, Oxford University Press, 1960.
7. *E. S. Kotliar.* Myth and Tale of Africa, Moscow, 1975.
8. *B. L. Ogibenin.* Structure of mythological texts of Rigveda, Moscow, 1968.
9. Pausaniae Graeciae Descriptio, VII, 1 vol. II, Leipzig, 1973.
10. *E. G. Rabinovich.* The Lira of Hermes, Folklore and Ethnography, Leningrad, 1974.

საქართველოს მეცნიერებათა აკადემიის მოამბე, 159, №2, 1999
BULLETIN OF THE GEORGIAN ACADEMY OF SCIENCES, 159, №2, 1999

M.Kapanadze, R.Chagunava

Old Georgian Names of Glass and Glassware

Presented by Member of the Academy T.Andronikashvili, November 23, 1998

ABSTRACT. **The names of glass and glass products are studied on the basis of analysis of old Georgian literary sources.**

Key words: glass, glass products.

The word glass is mentioned in ancient Georgian literary sources of different types and date with various interpretations. Detailed study of these monuments makes possible to get acquainted with terminological changes which took place in the course of centuries.

Generally, the oldest name of glass as a substance is considered the word "čika". According to I.Javakhishvili "čika" denoted material and later it became the drinking vessel [1,53]. One of the earliest Georgian monuments, The Martyrdom of St.Shushanik, (Vc.) proves the above mentioned argument [2,13]. Glass (čika) here is used as a drinking vessel. At the same time, the author uses the word "šelecva" indicating to the material from which it is done. This word doesn't denote such unbreakable articles of dishes which are manufactured from woody, clay or some metals. Transparent, easily broken substance is meant here which according to the archaeological data had already been widely spread in Georgia in everyday life of upper society.

The fact that in "The Martyrdom of St. Shushanik" the word "čika" (glass) is mentioned as a drinking vessel proves that "čika" was known earlier with the meaning of substance and the production of vessel was such a common phenomenon that it transformed into the notion of a drinking vessel in the 5th century.

Unfortunately the glass (čika) itself as a term denoting the substance was not fixed in that time due to the scarcity of sources and also anaccessibility of the monuments having terminological character up to now.

In the 10-11th century from Georgian written sources it becomes evident that the word glass (čika) along with the meaning of drinking vessel preserves its primary meaning too. In the literary monument of the X century "Limonari" by I.Moskhi [3] we found such word combination as "čikis mokmedi" which denotes profession. There existed a term "mečike" i.e. glass maker which is also found in I.Abuladze's Dictionary [4]. T.Gabashvili implies substance under the word glass [5].

The interpretation of the word glass by Sulkhan-Saba Orbeliani is of interest. In earlier edition (before 1715-1716) "čika" is explained as substance from which it is possible to manufacture various articles. But in later edition Sulkhan-Saba Orbeliani explains "čika" as glass vessel and at the same time the word glass (mina) is used with the meaning of substance i.e. as "čika" [6].

King Vakhtang VI in his works uses the term "čika" both for substance and denotation of vessel [7, 117, 188-196]. Together with Georgian "čika" in OG literary language

there appeared borrowed words too which denoted both vessel and substance. The most interesting is the word "šuša".

The earliest reference to "šuša" appeared in Adisha Gospel dated 897 from Matthew and Mark and also the Gospel Dzrucha (936) and Parkhli (973). In these Gospels there is mentioned alabaster with the meaning of dish. The translator of Adishi Gospel used the word "šiš" for alabaster [8, 692]. This term is seems to be used in Persian form [9,10].

It is interesting that if "čika" in its transformation to drinking term generally denoted vessel made of any substance the word "šuša" still remained in Georgian as a notion denoting dishes made of glass. It should be noted that Sulkhan-Saba didn't use the term "shusha' at all. This word is identified by him with distorted term "daman" and in both cases means metal molded in a special form. But King Vakhtang VI used this term very often in the meaning of glass vessel [7,160].

Since X-XI centuries we often found the term "mina" borrowed from Persian [9,10]. In Georgia on early stage as it is seen the term was used mainly for denotation of articles made of stained glass or enamel.

According to Petritsi (XI century) "mina" denotes green glass vessel [11,245]. In literary monuments of XI-XVI centuries "mina" is often found denoting enamel. It is evidenced from the last will of Ivane Liparit's son (XI century) [2,214] and from the Gospel of the 15-16 centuries [12,213].

The word "mina" as well as "čika" was used for denotation of articles and substance. The mentioned term is used by Sulkhan-Saba with these two meanings. In one case the word "mina" is determined as a drinking vessel and in another case it means enamel [6].

King Vakhtang VI used the word "mina" to denote dishes [7,154]. Very often he used simultaneously "mina" and "glass" for denoting the dishes [7,160]. While describing Mt. Athos monastery T. Gabashvili used the word "mina" meaning stained glass [5,468] and "čika" as it was above mentioned was used as substance.

Beginning from XI century the term "broli" (crystal) is found in Georgian literary monuments and very often it is associated with the notion of glass.

In the last will of David the Builder [1,54] and in "Visramiani" the word "broli" is often found [13,53]. It is evident that these dishes were not made of mountaineous crystal because it required technically hard work. Generally very few cases are known from literature when wares are made of mountain crystal [14,175; 15,44-45].

In old Rome glass-ware was usually made of stained glass because it didn't need a special pure raw material. But transparent glass-ware which production was technically rather difficult and looked like mountain crystal was the most expensive. Therefore it was denoted by this term.

According to Ar-Razi (IX c.) "mina" is of different types. Sirian white (colorless) transparent glass which looked like crystal was considered to be the best by its properties [16,153]. By the way in the translation of Ar-Razi fragment made by Vakhtang VI it is mentioned that the glass is of various sorts but the black one is better and it should be as transparent as crystal [7,145].

The identity of crystal and glass is marked by Biruni (X c.) who stated that crystal is a natural glass but glass "mina" (ordinary) is an artificial product [15,174].

According to Sulkhan-Saba's determination crystal is a natural white stone and is made of glass [6].

We consider that crystal dishes mentioned in old Georgian monuments were made of white colorless glass wares of high quality. If we remember "Petritsoni" [11,245] here stained glass (green) is opposed to crystal which perceived only as colorless glass.

Georgian Academy of Sciences
R. Agladze Institute of Inorganic Chemistry and
Electrochemistry

REFERENCES

1. *I. Javakhishvili*. Materials to the History of Georgian Material Culture. Tbilisi, 1965 (Georgian).
2. *I. Khutsesi*. The Martyrdom of St. Shushanik. Tbilisi, 1982 (Georgian).
3. *I. Moskhi*. Limonari. Tbilisi, 1960 (Georgian).
4. *I. Abuladze*. Dictionary of Old Georgian Language. Tbilisi, 1973 (Georgian).
5. *T. Gabashvili*. Mimosvla. Tbilisi, 1983 (Georgian).
6. *S-S. Orbeliani*. Georgian Dictionary, v.1-2. Tbilisi, 1991 (Georgian).
7. *King Vakhtang VI*. Tsigni zebis šezavebisa da kimiis kmnis. Tbilisi, 1981.
8. *I. Imnaishvili*. Kartuli otxtavis simponia-leksikoni. Tbilisi, 1986.
9. *B. V. Miller*. Persian-Russian Dictionary, v.1,2, M., 1970.
10. *Y. A. Rubinchik*. Persian-Russian Dictionary, 1,2. M., 1970.
11. *S. Kaukhchishvili*. Georgika, 5. Tbilisi, 1963.
12. Description of Monuments of Kutaisi State Historical Museum, v.1-2, Tbilisi, 1973-1986 (Georgian).
13. Vis-Ramiani. Ed. A.Gvakharia and M.Todua. Tbilisi, 1964.
14. *Abu-r-Raikhan Mukhamed Ibn Akhmed al-Biruni*. Mineralogiya. M., 1963 (Russian).
15. *E. Chizhov*. Steklo. St.-Petersburg, 1912.
16. *U. I. Karimov*. Neizvestnoe sochinenie Ar-Razi. Tashkent, 1957 (Russian).

Subscription Information

Bulletin of the Georgian Academy of Sciences
is published bimonthly

Correspondence regarding subscriptions, back issues should be sent to:

Georgian Academy of Sciences,
52, Rustaveli Avenue, Tbilisi, 380008, Georgia
Phone : + 995-32 99-75-93;
Fax/Phone : + 995-32 99-88-23
E-mail : BULLETIN@PRESID.ACNET.GE

Annual subscription rate for 1999 is US $ 400

გადაეცა წარმოებას 20.02.1999 ხელმოწერილია დასაბეჭდად 2.06.1999.
ფორმატი 70×108 $^{1}/_{16}$. აწყობილია კომპიუტერზე. ოფსეტური ბეჭდვა.
პირობითი ნაბ. თ. 12. სააღრიცხვო-საგამომცემლო თაბახი 11.
ტირაჟი 250. შეკვ. 143 ფასი სახელშეკრულებო.

რედაქციის მისამართი: 380008, თბილისი-8, რუსთაველის პრ. 52, ტელ. 99-75-93.
საქართველოს მეცნიერებათა აკადემიის საწარმოო-საგამომცემლო გაერთიანება „მეცნიერება",
380060, თბილისი, დ. გამრეკელის ქ. 19, ტელ. 37-22-97.